2005

Development of enhanced multiport network analyzer calibrations using non-ideal standards

John Edward Daniel
University of South Florida

Development Of Enhanced Multiport Network Analyzer Calibrations

Using Non-Ideal Standards

by

John Edward Daniel

A thesis submitted in partial fulfillment
of the requirements for the degree of
Master of Science in Electrical Engineering
Department of Electrical Engineering
College of Engineering
University of South Florida

Major Professor: Lawrence Dunleavy, Ph.D.
Thomas Weller, Ph.D.
Stephen Saddow, Ph.D.

Date of Approval:
November 4, 2005

Keywords: rf, models, loads, vna, 4-port, solr,

DEDICATION

This thesis is dedicated to my parents, Richard and Susie Daniel, as well as my grandparents, Arnold and Julia Bowers and Eddie and Pinky Daniel. Thank you for the love and support you have given me, so that I may achieve my goals.

ACKNOWLEDGEMENTS

I would like to thank Dr. Lawrence Dunleavy for giving me the opportunity to work within his research group. I would also like to thank my committee members, Dr. Thomas Weller and Dr. Stephen Saddow for their participation and thoughtful insights into my work.

I would like to thank M/A Com, Anritsu, and Insyte for directly funding my research work. Also I would like to thanks GGB and Gore for their contributions in the way of discounts and donations of the multiport probes, calibration substrates, and cables used in the multiport measurement setups.

To Alberto Rodriguez, thanks for our numerous technical as well as non-technical conversations and for helping stack the house of cards so carefully. Thanks to Sathya Padmanabhan for helping me get started in lab and taking the time to show me the ropes. Thanks to Rick Connick of USF/Modelithics for always being there to lend a helping hand or a piece of equipment and for joining me in wave propagation studies. Thank you to the rest of my friends and colleagues in ENB 412 for their help and support

I would like to thank my closest friends: Scott, Tim and Tiffany Hughes, Jason and Jenifer Ingram, and Shawn and Dana Ingram for being there as I we grew up and continuing to be there now. Finally I would like to thank my girlfriend and future fiancé Elizabeth Chandler for always be there to support me through the long nights and times of doubt

TABLE OF CONTENTS

LIST OF TABLES

LIST OF FIGURES

DEVELOPMENT OF ENHANCED MULTIPORT NETWORK ANALYZER CALIBRATIONS USING NON-IDEAL STANDARDS

John Edward Daniel

ABSTRACT

An Improved Short-Open-Load-Reciprocal (SOLR) Vector Network Analyzer (VNA) calibration is developed and validated. Through the use of a more complex load model the usable frequency range of the SOLR calibration algorithm is expanded. Comparisons are made between this new calibration and existing calibration techniques that are known to be accurate at high frequencies. The Anritsu 37xxx Lightning series 65GHz VNA is used as the principle measurement tool for calibration comparison and verification. This work is built off of previous work done at USF in which it is shown that the Short-Open-Load-Thru (SOLT) calibration's accuracy improves through the implementation of more complex load and thru models.

One of the most significant advantages of the SOLR calibration algorithm is that it does not require an ideal well behaved thru standard. This is extremely useful in multiport probing environments where it is often necessary for speed and space conservation purposes to use loopback thrus or other non-ideal transmission structures during calibration. Multiport test equipment and measurement techniques are highlighted and discussed. A general n-port expansion of a two-port calibration algorithm is presented and used to adapt the improved two-port SOLR algorithm to a four-port

calibration. In doing so a theoretical development that addresses error model treatment, and switch term corrections is presented that includes an improved set of the redundancy equations that enable the multiport SOLR algorithm.

The algorithm uses a four-port SOL calibration at each port and then determines the remaining error terms by measuring a minimal set of reciprocal passive standards. The four-port SOLR algorithm developed was illustrated through the use of a four-port test set that consists of a two-port VNA input multiplexed to four-ports through an RF switch array. Verification of the four-port SOLR calibration is made by comparing it to available four-port calibration techniques using available on-wafer test structures. As another promising advance of the work the possibility of using of a multiport reciprocal standard is shown to have potential for reducing the number of standard connections needed to accomplish multiport SOLR calibration. Differential measurements are facilitated through mixed-mode calculations of single ended S-parameter measurements made with the four-port SOLR calibrations improved with this work.

CHAPTER 1

INTRODUCTION

1.1 Overview and Problem Statement

In the past few years, there has been a significant rise in the use of differential devices in radio frequency integrated circuit (RFIC) design and multiport measurements have become increasingly popular to address this as well as other multi-port device characterization needs. Characterization of differential and multi-port devices is a major concern for engineers in order to provide accurate models and precision device data for design work as well as evaluation of their completed designs. In a differential signal environment, rather than a signal and ground conductor, a signal is supported by a two signal lines that are each 180 degrees out of phase with each other. This is advantageous in Silicon-based RFIC designs because of the noise suppression and reduced power consumption of differential circuits [1].

One of the most critical measurements of any RF device is its S-parameters. In order to achieve accurate scattering parameter (S-parameter) measurements of a device, an accurate calibration of the vector network analyzer (VNA) must be made. Calibrations are necessary to remove the measurement errors associated with the network analyzer as well as external hardware used in connecting the device under test (DUT). Once the calibration procedure is performed, and the systematic errors known, these errors can be

mathematically de-embedded from the raw, uncorrected S-parameter measurements of the device-under-test (DUT). Finding a broadband calibration solution for a two-port network analyzer is not a trivial task. The problem is compounded when it is done on-wafer or in a custom board environment and more measurement ports are added. Many of the problems that arise can be attributed to an insufficient calibration algorithm and/or the quality and suitability of the associated calibration set.

The goal of this work is to find a broadband multiport on-wafer calibration procedure that can utilize non-ideal standards on commercially available substrates. Different two-port calibration techniques and theories are studied and compared. Once a suitable two-port solution is found the algorithm will be adapted to a 4-port algorithm to be used with existing multiport measurement equipment available at the University of South Florida (USF).

1.2 Multiport On-Wafer Probing

Some specific challenges occur when making multiport measurements and calibrations on-wafer. One of the most obvious of these challenges is the probe configuration used. In a 4-port on-wafer S-parameter measurement setup ground-signal-ground (GSG) probes can be positioned in a north south east west configuration as shown in Figure 1.1 or a pair of ground-signal-ground-signal-ground (GSGSG) or ground-signal-signal-ground (GSSG) probes Figure 1.2. may be used. Any combination of probes and configurations may be used to accommodate the pad footprint of the DUT; however, most configurations do not lend themselves for making precise on-wafer calibrations. These setups are particularly problematic with calibrations that require well behaved

uniform transmission line standards. A transmission line that is bent to achieve connectivity or ran closely to another transmission line does not meet this requirement. This is especially true when GSGSG and GSSG probes are used because the transmission lines are ran within 300 microns of each other and loopback or U thrus may be used in the calibration. GSGSG and GSSG probes are favored in differential measurements because many designers run balanced transmission lines in parallel to preserve symmetry. Also it is common and spatially efficient in RFIC chip design to include GSSG or GSGSG probe pads on the device layout to facilitate differential measurements. There are many calibration techniques available; however, not all are suitable for this kind of application.

1.3 Available Calibration Techniques

Many calibration techniques exist and they can be divided into many different categories. Most commercial VNAs utilize the 12-term error model [2] that will be discussed in more detail in Chapter 2. There are direct calibration techniques, such as short, open, load, thru (SOLT). SOLT uses modeled calibration standards to identify the 12 error terms [2]. There are self-calibration techniques [3] such as line, reflect, match (LRM) [4] and thru, reflect line (TRL) [5] that utilize a reduced 8-term error model that can be converted to 12-term error models. Finally there are hybrid calibrations such as short-open-load-reciprocal or (SOLR) [6,7] that combine modeled based techniques along with measurement redundancy to provide and 8-term error model. It is generally accepted that multiline TRL [8] developed at the National Institute of Standards and Technology (NIST) is the most accurate two-port on-wafer calibration available. It

utilizes multiple transmission line standards of varying length that allows it to maintain optimal accuracy over a wide bandwidth.

However, because the standards are based on quarter wavelength center frequencies the lower in frequency desired for calibration the longer the line needed. At some point, around 2 GHz, this begins to become highly impractical. Wafer real estate is very valuable and many companies can not afford to give up 20mm or more for a low frequency delay line. Another problem that arises at low frequencies is that due to finite conductor film thickness limitations of practical circuit processing, the characteristic impedance (Z_0) that defines the reference impedance of the calibration can become complex (or have a significant imaginary component) at low frequencies. This effect, as described by Williams [9] can be difficult to correct for and, in combination with the limit on the length of the longest delay line that can be built, ultimately limits how low in frequency an accurate Z_0 corrected (usually corrections are made to reference S-parameters to 50 ohms) TRL measurement can be made.

Recently USF has developed an SOLT based algorithm using more complex load and thru models (than available in conventional algorithms) to achieve multiline TRL accuracy up to 110 GHz without TRL's low frequency loss of precision. This technique detailed in [10,11] is called complex SOLT (cSOLT). cSOLT uses a compact set of calibration standards of equal footprint in order to conserve wafer space and facilitate fast calibration times with semi-automated probing systems.

Both multiline TRL and cSOLT have proven to be accurate two-port calibration techniques and LRRM [12] is a widely used compromise that achieves better accuracy that LRM but is still not as accurate as multiline TRL because it still relies on a resistance

inductance load model. These methods multiport applications are limited due to their use of ideal transmission standards. NIST has developed a 4-port calibration software NISTcal that allows a 4-port calibration to be obtained through a pair of two-port calibrations, either LRM or TRL, between the north south and east west probes. LRM requires a very good broadband match standard to be accurate. An ideal match is usually not available over extremely broadband conditions such as 40 MHz to 65 GHz. Both the LRM and the TRL calibrations require well behaved transmission line standard to produce a valid calibration. Such line standards are more difficult to obtain in a GSGSG or GSSG probing environment where lines are closely coupled. In a coax multiport setup it is difficult to achieve good 4-port results when the cables must be moved around to make multiple connections unless those cables are extremely phase stable at the frequencies of interest. TRL requires many connections of standards with various lengths and one must still have a good broadband load to perform LRM. SOLT and cSOLT also require a well behaved or modeled thru standard that makes them less useful in a multiport on-wafer calibration.

In contrast, SOLR has a unique property that lends itself perfectly to on-wafer calibrations. SOLR is similar to SOLT in that it uses a model based extraction to determine the reflectometer error terms, however it does not require a well known/well behaved thru standard. The only requirement of the transmission line standard is that it be reciprocal ($S_{21} = S_{12}$). A rough knowledge of its phase is also needed in order to make a proper root choice. Therefore, in the same way that TRL precision was achieved with cSOLT through the implementation of a complex load model cSOLR (complex model based SOLR) can be created. With cSOLR adapted to a 4-port algorithm, no matter what

the probing situation as long as reciprocity of the thru standard is held, the calibration can be accurately performed. Using mixed mode analysis of single ended 4-port measurements, differential measurements can be performed as well.

1.4 Summary of Contributions

The contributions of this work may be summarized as follows:

1. An improved SOLR algorithm, referred to herein as cSOLR has been implemented and verified to 65 GHz for two-port (Chapter 5) and to 26 GHz for multiport (Chapter 8) calibrations. cSOLR is enabled by the development of a complex load model that has been verified to 110 GHz. This model was co-developed with another USF student who first presented the model in her (cSOLT) calibration improvement work [11].

2. The redundancy equations that enable the SOLR algorithm for multiport calibrations have been improved with consistent notation carried through a thorough treatment of the calibration mathematics for two-port and multi-port mathematics. (see 7.3.3).

3. The potential for using a 4-port reciprocal device in place of a series of two-port thru devices has been positively demonstrated (Chapter 9) as a means to significantly reduce the number of calibration standard connections (or probe contacts) to be made during a multi-port SOLR calibration.

1.5 Thesis Organization

This thesis has been something with its conventions to provide the reader a seamless transition between the different two-port error models as well as give a fluid progression to multiport error models.

The thesis starts out with a review of vector network analyzer principles and theory in Chapter 2. The reader is given a background in calibration fundamentals such as error models and correction in Chapter 3 which follows closely to Doug Rytting's work [13] but uses a slightly different convention that allows a better transition from the 12-term to 8-term error model. Then in Chapter 4 various two-port calibration techniques are discussed and compared in more detail. In Chapter 5 the development of cSOLR is shown and verified through on-wafer measurements of structures on commercial calibration substrates as well as those designed by a former USF Student and fabricated by M/A-Com (formerly ITT GaAstek) are presented in Chapter 5.

As an introduction to multiport and differential measurements, an overview of the different types of systems and techniques that are used to make these measurements is given in Chapter 6. Chapter 7 covers multiport calibration techniques including the adaptation of two-port cSOLR to 4-port cSOLR, and the correcting for imperfect auxiliary terminations (internal to the switch box or VNA). Extensive verification measurements of the multiport cSOLR algorithm are presented in Chapter 8. Chapter 9 contains measurement results using a reciprocal 4-port device as the transmission standard for multiport cSOLR. Finally conclusions from the work are presented in Chapter 10 along with recommendations for future work.

CHAPTER 2

VECTOR NETWORK ANALYZER THEORY AND ARCHITECTURE

2.1 Introduction

A vector network analyzer (VNA) is an instrument which provides network S-parameters by making measurements of transmitted and reflected voltage ratios. When an incident voltage wave is presented at the input of a device some of this signal will transmit through the device and some will be reflected due to a variation of impedances between the device and the connecting network as shown in Figure 2.1. S-parameters are simply ratio measurements of the incident wave voltage to the transmitted and reflected wave voltages. Formally, a single element of the S-parameter matrix can be determined as, $S_{ij} = \left.\frac{b_i}{a_j}\right|_{a_k = 0 \ for \, k \neq j}$. This means that S_{ij} is measured by driving port j with an RF source to produce an incident wave a_j, and measuring the wave b_i that enters port i. simultaneously the incident waves on all other ports except the jth port should be set to 0, therefore, all other ports should be terminated in matched loads to avoid reflections [14].

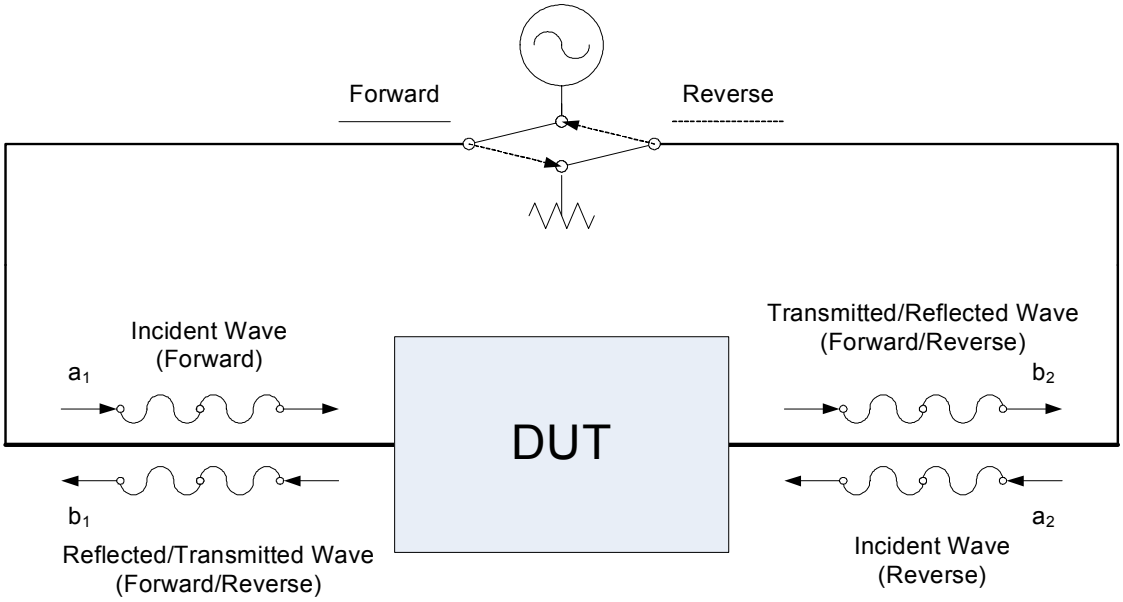

Figure 2.1 - Signal Diagram of an S-parameter Measurement.

A device with two ports is characterized by four S-parameters: two reflection coefficients, $S_{11} = \frac{b_1}{a_1}$ $S_{22} = \frac{b_2}{a_2}$ and two transmission coefficients, $S_{21} = \frac{b_2}{a_1}$ $S_{12} = \frac{b_1}{a_2}$.

The parameters S_{11} and S_{22} are called reflection coefficients; because they are the ratio of the incident wave amplitude to the amplitude of the resultant wave reflected back to the incident port. S_{12} and S_{21} are called transmission coefficients; because they are the ratio of the incident wave amplitude at one port to the amplitude of the resultant wave transmitted to the opposite port. It can be seen in Figure 2.1 that a two port, full S-parameter, VNA uses a single RF source that is switched between port 1 and port 2. This single source is used to create the incident "a" waves, which are used as the reference signals in determining the S-parameters. Because there is only one source, and because S-parameters are defined as having only one port driven at a time, a two port VNA is said to have a forward and reverse state. In the forward state, port 1 is driven by the RF

source, and an incident wave is produced at this port while port 2 is terminated; during this state S_{11} and S_{21} are measured. In the reverse state, port 2 is driven by the source and an incident wave is produced at port 2 while port 1 is terminated during this S_{22} and S_{12} are measured.

A VNA is designed to measure these signals; however, at higher frequencies, measurement of these discrete waves becomes very difficult. Therefore a VNA does not measure voltages directly but rather measures sampled waves. The signals that make up the S-parameters are actually measured within the VNA. Shown in Figure 2.2, there is a large amount of error between what the VNA measures and the signals that are incident to and resultant from the DUT. It is similar to making a voltage measurement with a multimeter using a very long cable; there will be a large difference between what the meter measures and what the voltage actually is at the device. For this reason, calibration routines are used to characterize this error and mathematically remove it from the measurements.

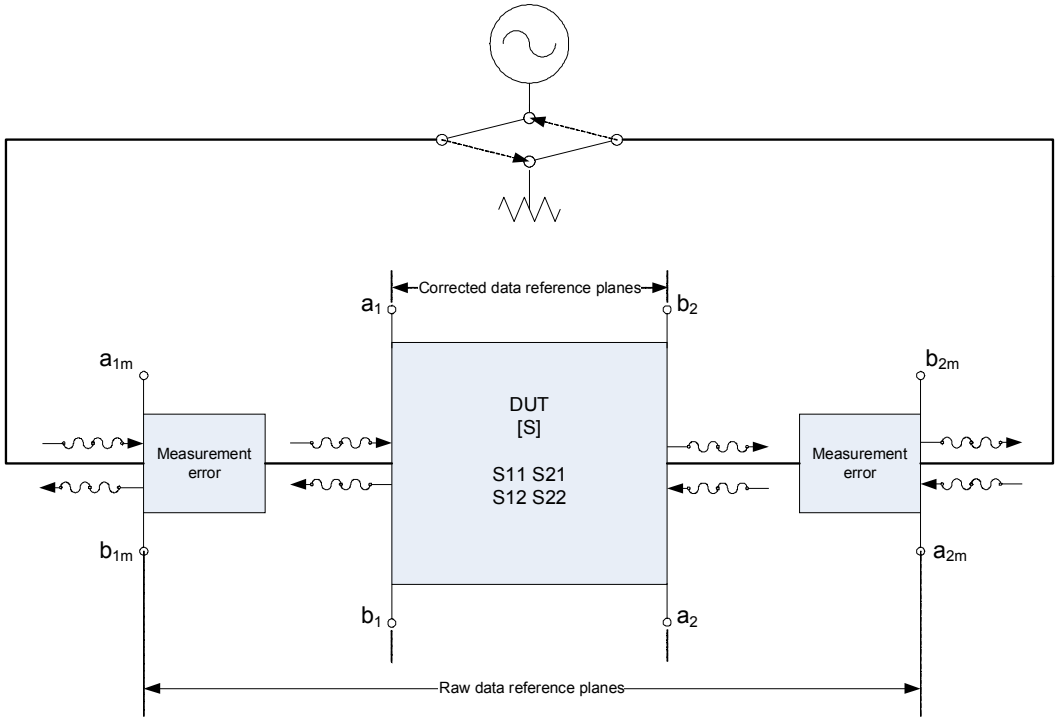

Figure 2.2 - Measurement Diagram Showing the Measured vs. DUT Reference Planes.

When a VNA is showing "raw" uncalibrated data is showing what the VNA is physically measuring at that instance. The points up to which unwanted measurement error has been characterized and corrected for is known as the reference planes. Once a proper calibration is applied the VNA is still measuring the same raw data with all the errors present, however, the data that is displayed has had unwanted errors mathematically removed, and it represents the S-parameters of the DUT up to the reference planes.

2.2 VNA Theory of Operation

In the late 1960s Hewlett Packard revolutionized network analysis with the invention of the first automatic network analyzer, the 8410 [15,16]. The purpose of a

VNA is to measure the S-parameters which are simply signal ratios. For this reason, it is not necessary to directly measure the discrete signals that make up these ratios it is only necessary to measure a representative portion of these signals that will give the same ratios. There are many different ways VNAs measure the signals. The operational analog subsystem of a VNA can be separated in three main areas: the RF source, the test set, and the receivers. The RF source generates the stimulus for the network. The incident and resultant waves are coupled off and sampled in the test set. The sampled signals are then down converted and detected in the receiver and finally digitized and processed by the VNA's processor. Each path by which an individual signal is coupled off and sampled is called a measurement channel. The process performed by each measurement channel is called sampling. The measured representative waves a_{1m}, a_{2m}, b_{1m} and b_{2m} obtained through their individual measurement channel are said to be sampled waves.

Often the term measurement channel will be used interchangeably with the term sampler because the number of measurement channels and the number of samplers are generally the same. S-parameter VNAs can be separated into two categories: three channel and four channel analyzers. Three channel VNAs include, Transmission reflection only (T/R) analyzers, and full S-parameter three channel analyzers that are capable of measuring both forward and reverse responses. The most common four channel VNAs available are 4/3 channel hybrids. These hybrids are simply four channel VNAs which operate in a three channel mode, with the option of measuring the fourth channel by customizing the parameter definitions. A few manufacturers and some metrology labs have custom full 4 channel VNAs. A simple block diagram of (T/R) analyzer is shown in Figure 2.3 to illustrate basic VNA functionality.

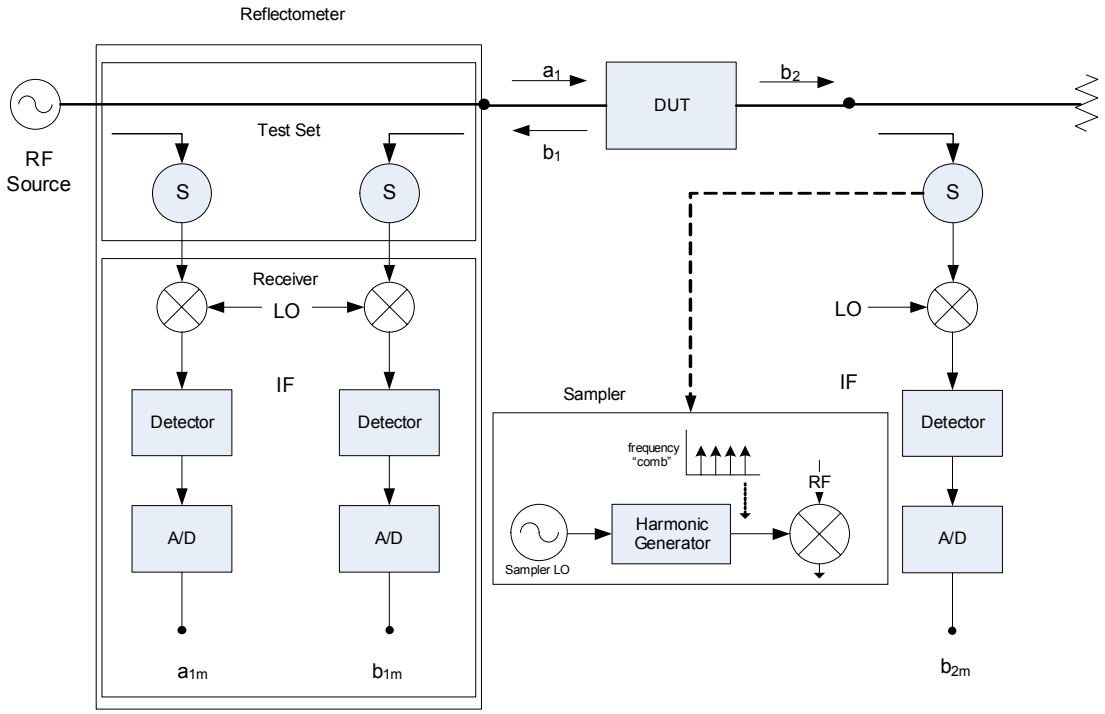

Figure 2.3 – Transmission/Reflection Only (T/R) VNA Internal Block Diagram.

2.2.1 RF Source

In most all VNAs a single RF source is used to produce the incident wave stimulus to be used as the reference signal. On transmission/reflection (T/R) only analyzers, like that of Figure 2.3, the source is only incident on port one and only forward reflection and transmission can be measured (S_{11} and S_{21}). In order to measure the reverse transmission and reflection parameters (S_{22} and S_{12}) the DUT has to be manually turned around and re-measured. In order to speed the measurement process full S-parameter test sets were developed, similar to those presented later in Figures 2.4-2.6, in which a switch is added to the RF source so that either port 1 could be sourced or port 2 allowing both forward and reverse S-parameters to be measured.

2.2.2 VNA Test Sets

The number of signals that can be independently separated and sampled is known as the number of measurement channels in a VNA. The role of a test set is to separate these channels. A representative portion a_{1m} of the incident signal is separated from the incident wave through a directional coupler or divider. Ideally a directional coupler would be used to extract the sample because it can distinguish between incident and reflected signal by its directional nature. However, because of cost many network analyzers use a power divider to sample off the incident wave. The reflected signal b_{1m} will also have a portion of the signal removed from it by means of a directional coupler in order to compare it to the reference incident signal. Once the scaled portions of the signals are extracted they are then sampled. Because RF and Microwave frequencies are so high the measurement of the discrete waves is usually not possible. Therefore the high frequency signals are down converted to more manageable frequencies, this is the job of the sampler.

The sampler performs the first stage of this down conversion process. A mixer could also be used for this task; however, a broadband mixer that will function to mm-wave frequencies is not cheap and requires a complementary local oscillator (LO) [17]. A sampler uses diodes to sample very short time sections of the incoming RF signal. A sampler can be thought of as a mixer with an internal pulse generator driven by the LO signal. The LO is fed to the samplers harmonic generator to create a broadband frequency spectrum, consisting of a comb of spectral lines. The RF signal mixes with the appropriate spectral line to produce a desired “intermediate” frequency (IF). A major

advantage of operating with the harmonics is that the LO does not need to produce a broadband high frequency signal.

2.2.3 Receiver Down Conversion and Detection

Most VNAs utilize a tuned receiver approach to detection. An RF signal in a VNA may be down converted two or even three times. As mentioned earlier, the first down conversion occurs in the test set with the samplers. The remaining down conversions are made in the receiver portion of the network analyzer. Tuned receivers use a local oscillator (LO) to mix the RF down to a lower IF. The LO is locked to either the RF or IF so that the receivers are always tuned to the RF signal at the input. Once the RF signal is down converted to the IF it is filtered. This helps to improve sensitivity and dynamic range by reducing the noise floor it also removes harmonic and spurious responses [17].

Once it is filtered most modern analyzers use an analog to digital converter and digital signal processing (DSP) to extract magnitude and phase information from the IF signal. The analog to digital converter (A/D) creates a digital representation of the detected IF signal, from which magnitude and phase can be calculated. In modern VNAs, the A/D is pushed up the chain and the IF signal is digitized before it is detected. Once it is digitized it can mathematically manipulated and systematic measurement errors can be removed.

2.3 VNA Architectures

This section will discuss the various architectures of Vector Network Analyzers. The architectures will be divided into two sub categories: three channel and four channel VNAs.

2.3.1 Three Channel Network Analyzers

In the block diagram of a T/R only VNA, shown in Figure 2.3, the first portion of the analyzer, which measures the incident and reflected waves, is historically known as the reflectometer, because it measures the reflection coefficient of the DUT. This simple network analyzer consists of three samplers, two of which make up the reflectometer, where the incident and reflected wave is coupled off and sampled, and the third measures the transmitted wave directly without coupling. Full S-parameter test sets like that shown in Figure 2.4 incorporate a switch for the RF source, and allow all of the S-parameters to be measured.

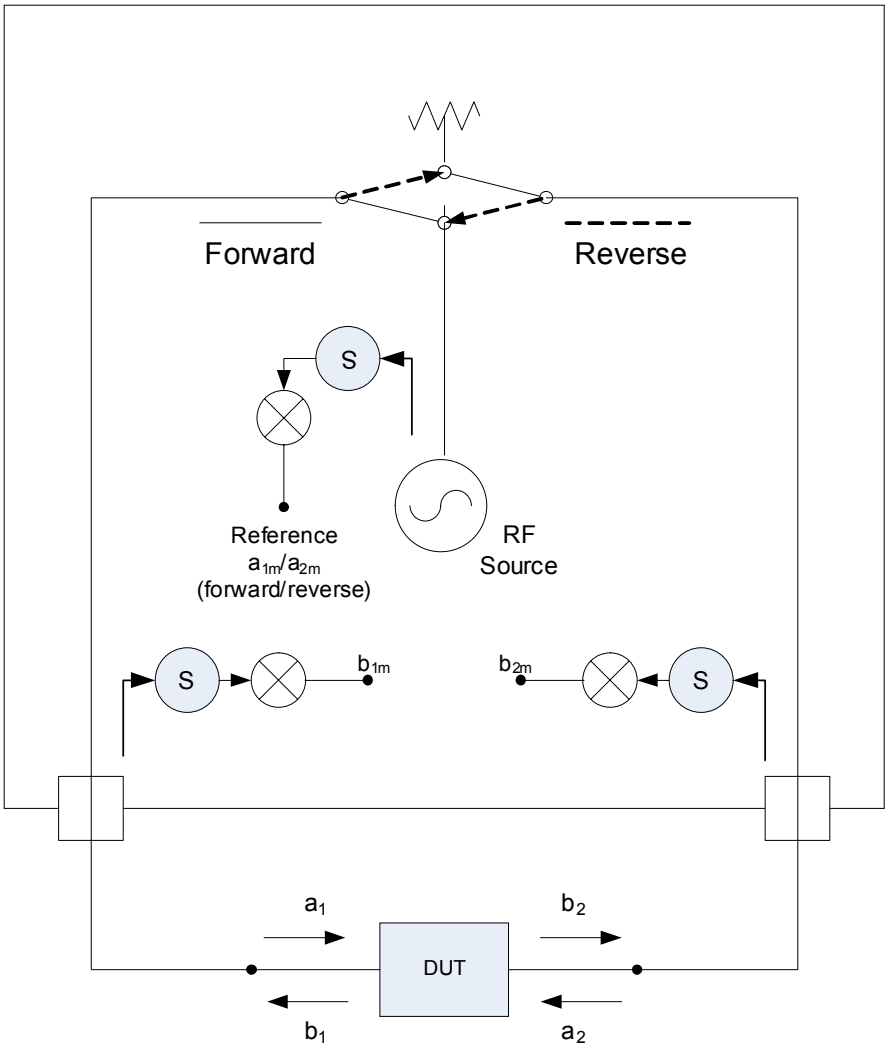

Figure 2.4 – Switched Three Channel Full S-parameter VNA Block Diagram.

These three sampler three coupler network analyzers have two dedicated samplers which measure the resultant waves, b_{1m} at ports 1 and b_{2m} at port 2, while one sampler is located on the source side of the switch so as to always measure the incident wave. New calibration algorithms were developed in the mid 70s based on a custom network analyzer known as the dual six-port analyzer [18]. These algorithms, detailed in Chapter 4, make use of the 4 measurement channels of the dual six-port VNA and have revolutionized network analyzer calibration.

2.3.2 Four Channel Network Analyzers

Motivated by the dual six-port calibration techniques, 4 channel network analyzers like that shown in Figure 2.5 were developed in order to utilize the new algorithms and expand measurement flexibility.

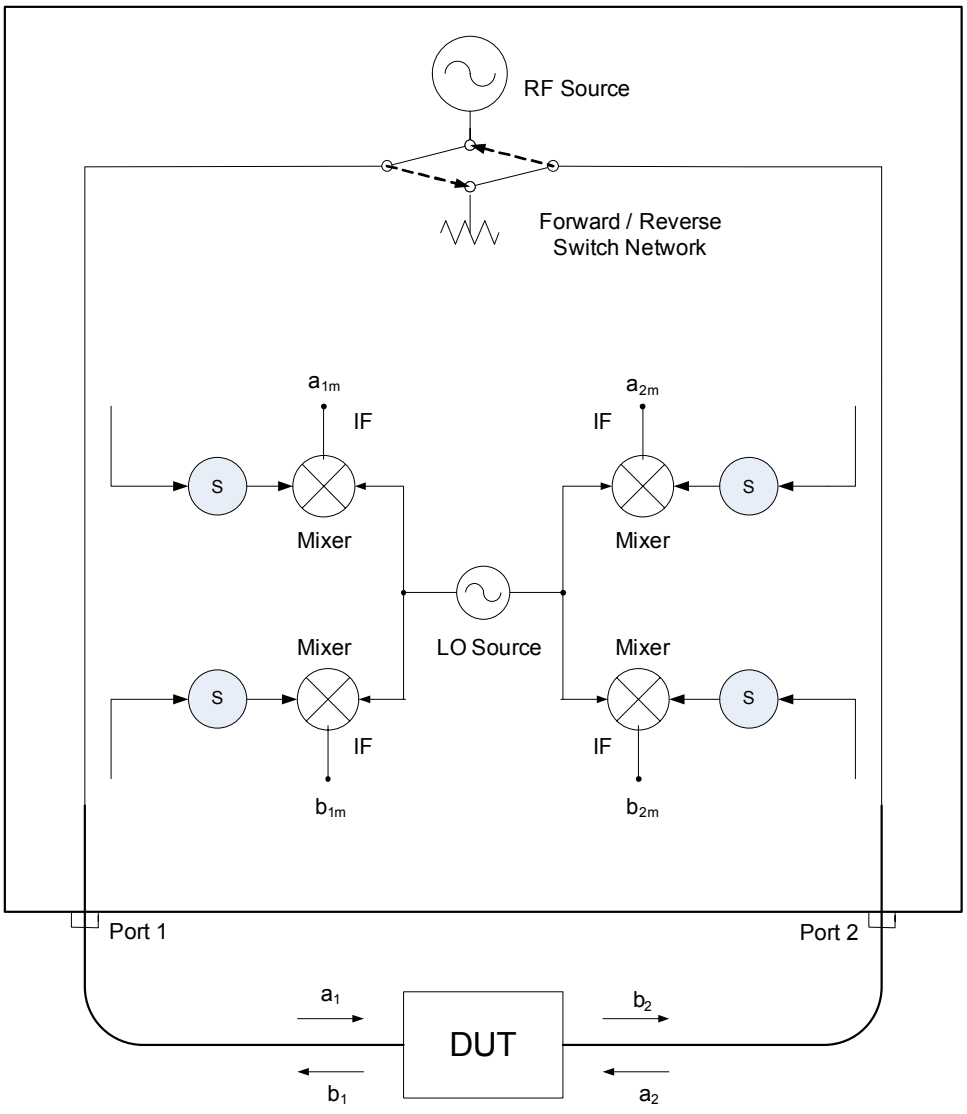

Figure 2.5 – Four Channel Network Analyzer with Four Receivers.

A four channel network analyzer takes data from all of its four samplers, a_{1m}, a_{2m}, b_{1m}, and b_{2m}, in both the forward and reverse directions. Although the data from only three of the four samplers are required in each direction to fully characterize the S-parameters, the information provided from making the 4^{th} sampler measurement gives a great advantage in terms of error calculation and calibration standard requirements by providing measurement redundancy. A four channel VNA has 4 samplers all on the DUT side of the switch; two pairs of directional couplers on each port separately couple off incident and resultant waves where they are sampled.

The measurement of this fourth channel allows the complete DUT measurement transmission matrix to be characterized, detailed in Section 3.5**,** through which the imperfections of the switch are effectively removed through the forward and reverse measurement ratios. It is also shown that this matrix can be developed by measuring the DUT S-parameters and also measuring the imperfect switch. Because the switch error is highly repeatable it only needs to be measured once during a measurement session and not with every standard or DUT. Because of this it is not necessary to obtain information from all 4 samplers during every measurement a process which slows measurement speed and often is only used in standards laboratories. Therefore, in an effort to conserve cost manufactures created a hybrid VNA like that shown in Figure 2.6.

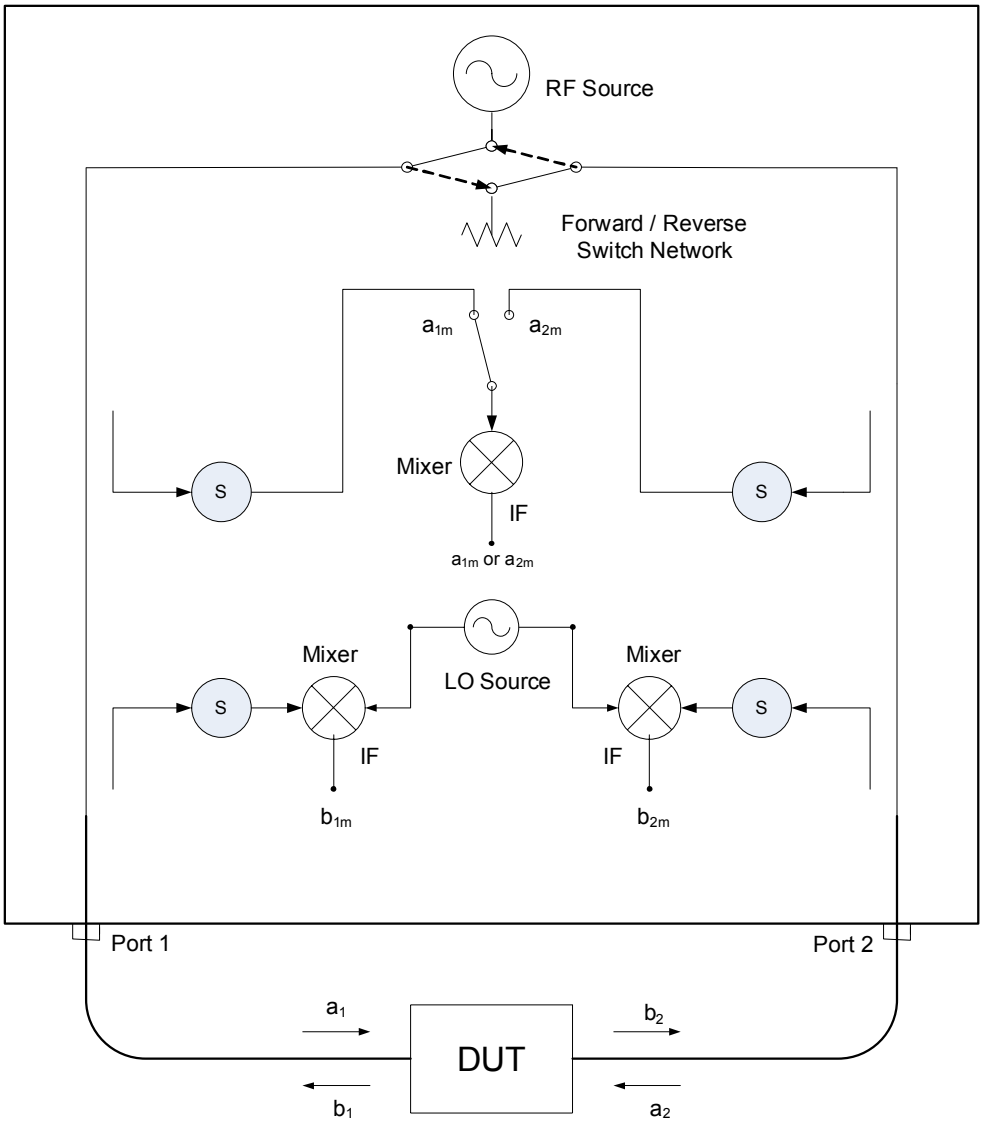

Figure 2.6 – The Four Sampler Three Receiver Four Channel VNA.

The four sampler three receiver VNAs are the most common commercially available four channel VNAs. The two resultant waves are always measured however only one of the incident waves are measured at a time. These VNAs are capable of measuring the 4th channel but do not do so under normal operating conditions.

2.4 Chapter Summary

The basic principles behind the theory of operation as well as the various architectures of vector network analyzers have been presented. The defining characteristics of a VNA that will be used in the proceeding chapters to determine both error model and calibration type are the number of measurement channels. Much of the terminology used in describing VNA S-parameter measurements and calibrations have been discussed so that in the upcoming chapters one can easily understand what is being presented. To summarize a VNA provides a stimulus to a DUT through and RF source which is switched between a forward and reverse state the incident and resultant voltage waves are separated and sampled in order to form the measurement ratios known as S-parameters. This raw measured data is corrected by mathematically removing systematic errors from the raw data through calibration thereby resulting in corrected DUT S-parameter data.

CHAPTER 3

VECTOR NETWORK ANALYZER NON-IDEALITIES AND ERROR MODELS

3.1 VNA Non-Idealities

The forward measurement path of the three channel network analyzer shown in Figure 3.1 will be used to illustrate the network analyzers measurement errors. These errors are similar for the forward measurement path of all full S-parameter network analyzers and duality applies for the reverse measurement condition.

Imperfections internal to the VNA lead to issues such as mismatch, leakage and loss. These imperfections cause significant measurement errors that must be accounted for during calibration. Figure 3.1 shows the VNA block diagram in the forward measurement direction and the detailed error flow graph, adapted from [13], that corresponds to this block diagram. Table 3.1 gives the error definitions to the detailed error flow graph presented in Figure 3.1. In Figure 3.1 the system errors are related to the VNA architecture. The RF source has some mismatch (M_s) associated with its impedance and connection interface. Ideally, when the incident wave from the source a_s reaches the incident coupler, the VNA would be able to measure that signal directly. However, there are losses associated with the signal being coupled off and down converted before it is measured ($L_{S\text{-}a1m}$). Because it is assumed that the incident wave measured at a_{1m} is the same as that incident at port 1 there is an error from the loss incurred from the source to

the incident port (L_{S-1}). The reflected signal also suffers losses due to the reflected wave coupler and down conversion (L_{1-b1m}). The imperfect directivity of the coupler used to sample off the reflected wave causes some of the incident wave to be sampled at b_{1m} (L_{S-b1m}). Similarly, the imperfect directivity of the incident wave coupler allows some of the reflected wave to be coupled to the a_{1m} sampler (L_{1-a1m}).

When the incident signal reaches port 1 there is also a mismatch associated with the port (M1). Outside the VNA there are many errors attributed to the connection of the DUT. Loss and mismatch of cable and probe connections are present on both sides of the DUT (Mc and Lc). Similar to port 1, there is a match error at port 2 (M2) and losses associated with the sampling of the transmitted wave at port 2 (L_{2-b2m}).

Table 3.1 - Detailed Error Model Definitions for Figure 3.1 from [13].

a1 = Incident Signal at DUT Port-1
b1 = Reflected Signal at DUT Port-1
a2 = Incident Signal at DUT Port-2
b2 = Transmitted signal at DUT Port-2
aS = Source Port
a1m = Measured Incident Port
b1m = Measured Reflected Port
b2m = Measured Transmitted Port
LS-1 = Loss from Source to Port-1
L1-S = Loss from Port-1 to Source
LS-a1m = Loss from Source to a 0
LS-b1m = Loss from Source to b 0 (Directivity)
L1-a1m = Loss from Port-1 to a 0 (Directivity)
L1-b1m = Loss from Port-1 to b 0
L2-b2m = Loss from Port-2 to b 3
La1m-b2m = Loss from a 0 to b3 (Leakage)
LC = Loss of Cables
S11 = Refl. Coef. of DUT at Port-1
S21 = Forward Trans. Coef. of DUT
S12 = Reverse Trans Coef. of DUT
S22 = Refl. Coef. of DUT at Port-2
M1 = Match at Port-1
M2 = Match at Port-2
MS = Match of Source
MC = Match of Cables
NLa1m = Low Level Noise at a 0
NLb1m = Low Level Noise at b 0
NLb2m = Low Level Noise at b 3
NHa1m = High Level Noise at a 0
NHb1m = High Level Noise at b 0
NHb2m = High Level Noise at b 3
Aa1m = Dynamic Accuracy at a 0 (Linearity)
Ab1m = Dynamic Accuracy at b 0 (Linearity)
Ab2m = Dynamic Accuracy at b 3 (Linearity)

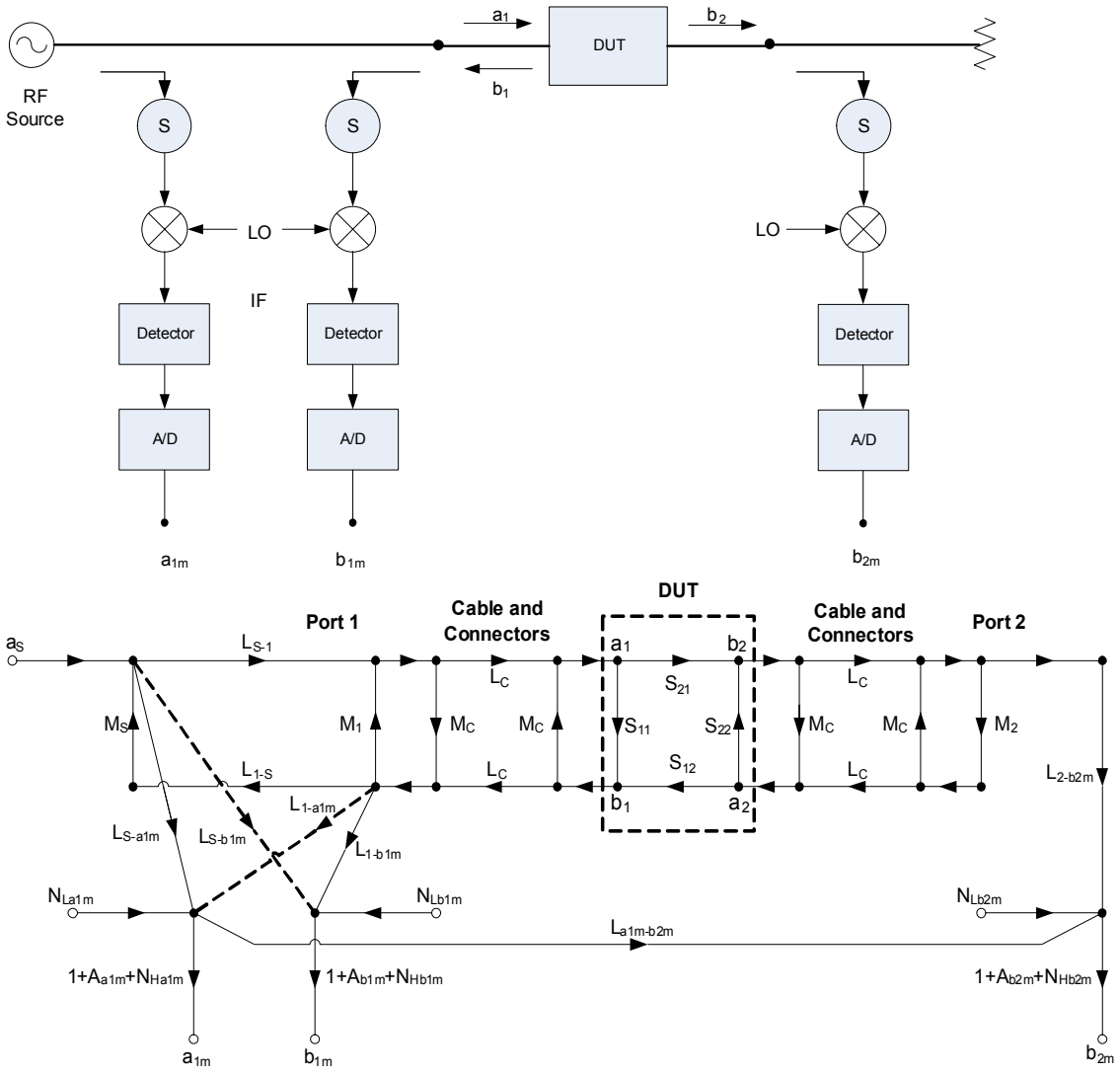

Figure 3.1 – Block Diagram of a Three Channel VNA in the Forward Measurement Direction and the Corresponding Detailed Error Flow Graph Adapted from Rytting [13].

The leakage or crosstalk term ($L_{a1m\text{-}b2m}$) is due to internal isolation imperfections and isolation problems with DUT interconnection especially through the substrate when measurements are performed on-wafer. This isolation error is generally small and mostly is ignored in calibration.

Errors that cannot be corrected for are high and low level noise present at the samplers. This noise is causes the light fuzz observed on measurement data. Because the noise is random it cannot be corrected for, however, using a higher averaging factor of 16 or greater will usually alleviate the problem. The ability of the VNA to produce the exact same measurement repeatedly under the same conditions is known as dynamic accuracy this is another error that calibration cannot correct but, like noise the problem is usually reduced by the use of averaging.

The model can be simplified by mathematically reducing the flow graph without suffering any losses in accuracy. This simplified flow graph shown in Figure 3.2 is what the two port error models, which will be explained in more detail in Section 3.3, are derived from. The prime (') on certain error terms indicates that the value of the error term in the forward direction is different from the similar reverse error term, because of the termination reflection difference due to the imperfect RF switch.

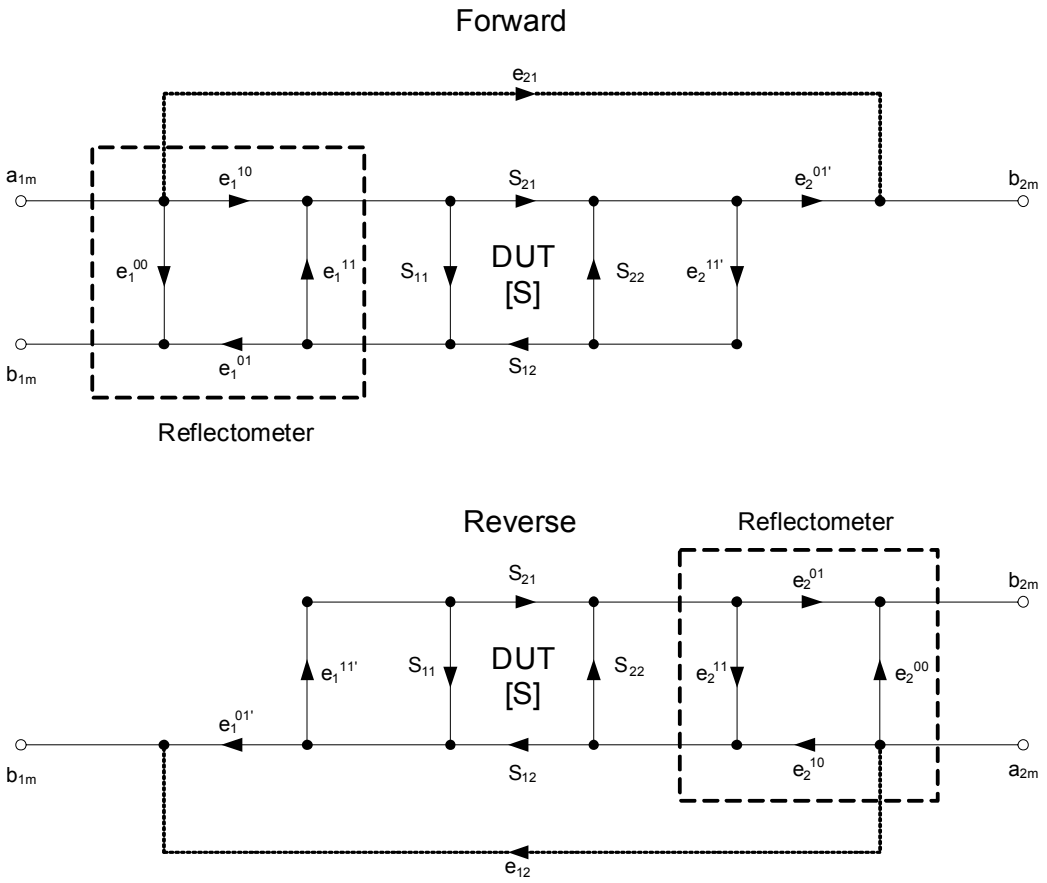

Figure 3.2 - Simplified VNA Error Flow Graph of the Forward and Reverse Measurement Direction.

3.2 One-Port Error Model and Reflectometer Error Term Definitions

The errors associated with a single port or reflectometer of the VNA can be represented by a two port S-parameter block also referred to as an error box. Because S-parameters are ratio measurements the 4 error terms of this portion of the VNA error flow graph can be normalized thereby reducing the 1-port error model to three terms, as shown in Figure 3.3. These three terms, often named: directivity, source match, and reflection frequency tracking, are known as the reflectometer terms.

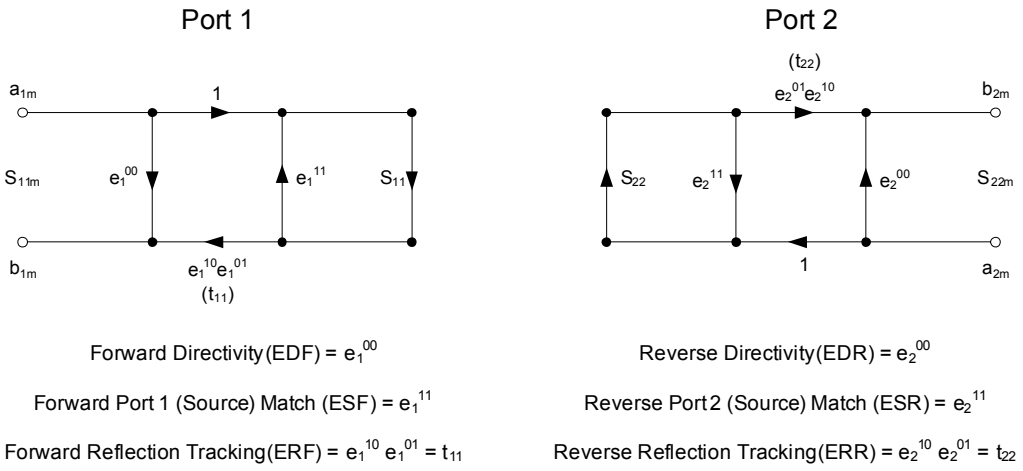

Figure 3.3 – One-Port Error Model and the Three Associated Error Terms.

Directivity is a parameter that pertains to the measurement couplers. The directivity is the difference in the power output at a coupled port, when power is transmitted in a desired direction to the power output at the same coupled port when the same amount of power is transmitted in the opposite direction [17]. Ideally the directional couplers in the analyzer would only sample the power of the intended measurement signal, for example, the incident wave a_1 would only be coupled off and sampled by the incident sampler (a_{1m}). Te directivity error term is used to reduce errors associated with unwanted leakage in the couplers.

The port match or source match is defined as the vector sum of the signals present at the output of the network analyzer due to its inability to maintain a constant power at the input of the test device [17]. In the forward model, the port 1 match is the source match; conversely, in the reverse model the port 2 match is the source match. Uncertainty is caused when the impedance of the source does not match the impedance of the port that connects the input of the DUT and the impedance of the analyzer's port does not

match the impedance of the DUT input connections. The purpose of the source match term is to reduce this uncertainty

The reflection frequency tracking is the vector sum of measurement variations in magnitude and phase of the frequency response of the reflected signal [17]. Basically these are the errors, due to the fact that: the RF source, the incident sampler and the reflected sampler are not physically in the same place and are not at the input of the DUT. Therefore, there are losses and phase deviations due to cables and signal flow though the VNA that the reflection tracking term corrects for.

3.3 Two-Port Error Models and Transmission Error Term Definitions

When transmission measurements are made additional errors are introduced. There are two main errors models used to describe this complete two port measurement. The first is the twelve term error model described in 3.3.1, which is actually two six term error models one for the forward direction and the other the reverse direction. The second is the 8-term error model, also known as the error box model, which is detailed in 3.3.2. The 8-term error model is a simplified version of the 12-term error model which assumes no isolation and a perfect RF switch which removes the need for a separate forward and reverse model and in effect creates a cascaded, port 1 and port 2, error box model.

3.3.1 The 12-Term Error Model

The twelve term error model is actually two six-term error models one for the forward measurement direction and one for the reverse. As stated earlier the 7 error terms of the VNA error flow graph can be reduced to six which characterizes a single

measurement direction. The forward and reverse error models which make up the 12-term error model are shown in Figure 3.4 below which has been adapted from [13].

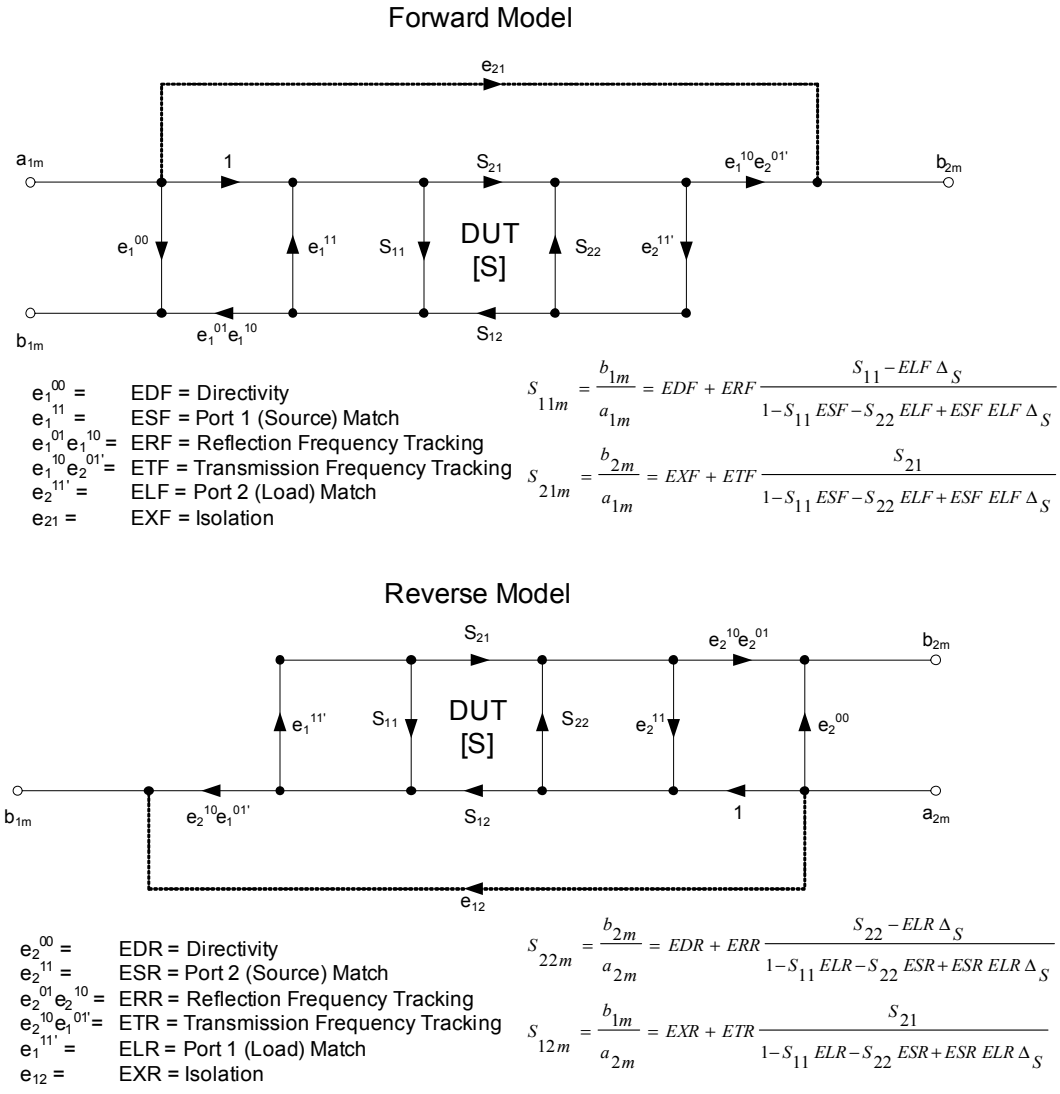

$$where: \quad \Delta_S = S_{11}S_{22} - S_{21}S_{12}$$

Figure 3.4 – 12-Term Error Model Forward and Reverse Direction.

In addition to the 3 reflectometer terms, 3 additional error terms are present in the forward and reverse directions. The transmission tracking, load match and isolation terms are all associated with the transmission measurement.

Similar to the reflection frequency tracking term, the transmission frequency tracking term accounts for the magnitude and phase error of the signal transmitting from the output of the analyzer at the incident port to the terminated input of the analyzer.

The load match term in the 12-term error model accounts for the match error between the output of the DUT and the input of the VNA [17]. These errors become more significant when a device is highly reflective, because there is a lower amount of transmitted power and any mismatches will further reduce the dynamic range of the measurement. The load match term is unique to the 12-term error model because not only does it represent the associated port match but also the match of the switch termination in a particular direction.

The isolation term, also referred to as leakage or crosstalk, is the measurement error caused from by the signal transmitting through unwanted paths from the source to the samplers [17]. This could include unwanted transmission through the substrate or a test fixture, as well as, leakage between the RF and IF sections. Usually the isolation error is small enough that it can be ignored; because, in order for an isolation error correction to be accurate the vector quantity representing the leakage must not change when the DUT is connected. In an on-wafer measurement this translates to not changing the probe contact footprint between calibration and measurement which is difficult to achieve.

The reason for the forward and reverse models is that in the twelve term error model the load match term contains information about the error due to the imperfect switch. If we assume that we have a perfect switch then the forward load match term ELF will be equal to the reverse source match term ESR.

If isolation is also ignored, or assumed to be perfect, the model is then reduced to what is known as the 8-term error model.

3.3.2 The 8-Term Error Model

The main assumption in the 8-term error model is the presence of a perfect switch [13]. If a perfect RF switch is assumed than there is no difference in the errors associated with ports of the VNA whether measuring the in the forward or reverse direction. Essentially the error model is comprised of a port 1 error box (E_1) and a port 2 error box (E_2) identical to those shown in Section 3.2. The 8-term error model is shown in Figure 3.5. The simplicity of the two 2-port error boxes, and the elimination of a separate forward and reverse model, makes finding a calibration solution easier because there are fewer error terms to calculate. The error associated with the perfect switch assumption is easy to remove through the techniques discussed in Section 3.5.

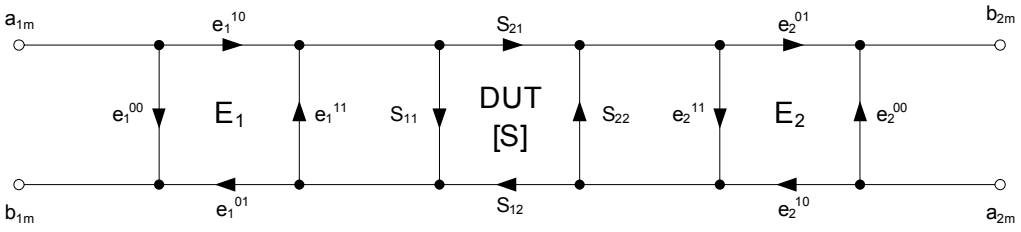

Figure 3.5 - The 8-Term Error Model.

Another powerful feature of the 8-term error model's simplicity is that is makes mathematical calculation of the error terms and manipulation of the error model much easier because the system can be represented as cascaded transmission parameter matrices. The bold parameters in the equations below indicate those that have had the switch error removed from them through one of the techniques in Section 3.5. Although

the removal of the switch error to calculate the 8-term error model is not necessary, the accuracy will be severely degraded if a perfect switch is assumed and the switch error is not removed from the measurements. Therefore, for all 8-term calibration techniques presented within this thesis, the switch error will be accounted for. The associated math for relating the raw measurements to the error model terms is most easily developed using the transmission matrix parameters. The cascaded error box nature of the 8-term error model is developed through the following relationships.

$$\boldsymbol{T_m} = T_1 T T_2$$

$$T = \frac{1}{S_{21}}\begin{bmatrix} -\Delta_S & S_{11} \\ -S_{22} & 1 \end{bmatrix} \quad \boldsymbol{T_m} = \frac{1}{\mathbf{S_{21m}}}\begin{bmatrix} -\mathbf{\Delta_{Sm}} & \mathbf{S_{11m}} \\ -\mathbf{S_{22m}} & 1 \end{bmatrix}$$

$$\Delta_S = S_{11}S_{22} - S_{21}S_{12} \quad \mathbf{\Delta_{Sm}} = \mathbf{S_{11m}S_{22m}} - \mathbf{S_{21m}S_{12m}}$$

$$T_1 = \frac{1}{e_1^{10}}\begin{bmatrix} -\Delta_{e1} & e_1^{00} \\ -e_1^{11} & 1 \end{bmatrix} \quad T_2 = \frac{1}{e_2^{01}}\begin{bmatrix} -\Delta_{e2} & e_2^{11} \\ -e_2^{00} & 1 \end{bmatrix}$$

$$\Delta_{e1} = e_1^{00}e_1^{11} - (e_1^{10}e_1^{01}) \quad \Delta_{e2} = e_2^{00}e_2^{11} - (e_2^{10}e_2^{01})$$

$$t_{11} = e_1^{10}e_1^{01} \qquad t_{22} = e_2^{10}e_2^{01}$$

$$\boldsymbol{T_m} = \frac{1}{(e_1^{10}e_2^{01})}\begin{bmatrix} -\Delta_{e1} & e_1^{00} \\ -e_1^{11} & 1 \end{bmatrix} T \begin{bmatrix} -\Delta_{e2} & e_2^{11} \\ -e_2^{00} & 1 \end{bmatrix} = \frac{1}{(e_1^{10}e_2^{01})} ATB$$

$$t_{21} = e_1^{10}e_2^{01} \quad t_{12} = e_2^{10}e_1^{01}$$

Where, T_1 and T_2 are the transmission parameters from left to right of the port 1 and port 2 error boxes respectively and T and $\mathbf{T_m}$ are the transmission parameters of the corrected

and raw DUT S-parameters. Similar to the 12-term model, the 8-term error model can be reduced to 7 terms. From the equations above the 7 error terms are easily identified. There are 3 terms at port 1: e_1^{00}, e_1^{11}, and t_{11} three terms at port 2: e_2^{00}, e_2^{11}, and t_{22} and a forward transmission term $e_1^{10}e_2^{01}$ (t_{21}). It is only necessary to solve for 7 of the 8 terms during the calibration routine. The other transmission term t_{12} can be solved through the following relation.

$$(e_1^{10}e_1^{01})(e_2^{10}e_2^{01}) = (e_1^{10}e_2^{01})(e_1^{01}e_2^{10}) \quad \text{or} \quad t_{11}t_{22} = t_{21}t_{12}$$

3.4 Error Correction

For the 12-term error model once the 12 terms are calculated through a calibration procedure the DUT raw S-parameter data can be corrected using the following equations.

12-term

$$S_{11} = \frac{\left(\frac{S_{11m} - EDF}{ERF}\right)\left[1 + \left(\frac{S_{22m} - EDR}{ERR}\right)ESR\right] - ELF\left(\frac{S_{21m} - EXF}{ETF}\right)\left(\frac{S_{12m} - EXR}{ETR}\right)}{D}$$

$$S_{21} = \frac{\left(\frac{S_{21m} - EXF}{ETF}\right)\left[1 + \left(\frac{S_{22m} - EDR}{ERR}\right)(ESR - ELF)\right]}{D}$$

$$S_{12} = \frac{\left(\frac{S_{12m} - EXR}{ETR}\right)\left[1 + \left(\frac{S_{11m} - EDF}{ERF}\right)(ESF - ELR)\right]}{D}$$

$$S_{22} = \frac{\left(\frac{S_{22m} - EDR}{ERR}\right)\left[1 + \left(\frac{S_{11m} - EDF}{ERF}\right)ESF\right] - ELR\left(\frac{S_{21m} - EXF}{ETF}\right)\left(\frac{S_{12m} - EXR}{ETR}\right)}{D}$$

$$D = \left[1 + \left(\frac{S_{11m} - EDF}{ERF}\right)ESF\right]\left[1 + \left(\frac{S_{22m} - EDR}{ERR}\right)ESR\right] - \left(\frac{S_{21m} - EXF}{ETF}\right)\left(\frac{S_{12m} - EXR}{ETR}\right)ELF\ ELR$$

It can be seen from the equations that if isolation is ignored the EXF and EXR terms will be zero and the equations simplify slightly.

If the perfect switch assumption is also made as it is with the 8-term error model than the equations for the corrected S-parameters also simplify. If a perfect switch is assumed then ELF = ESR and ESF = ELR, or equivalently, e211'= e_2^{11} and $e_1^{11} = e_1^{11'}$. Therefore, for the 8-term error model the corrected S-parameters are found through the following equations.

8-Term

$$S_{11} = \frac{\left(\frac{\mathbf{S_{11m}} - e_1^{00}}{t_{11}}\right)\left[1 + \left(\frac{\mathbf{S_{22m}} - e_2^{00}}{t_{22}}\right)e_2^{11}\right] - e_2^{11}\left(\frac{\mathbf{S_{21m}}}{t_{21}}\right)\left(\frac{\mathbf{S_{12m}}}{t_{12}}\right)}{D}$$

$$S_{21} = \frac{\left(\frac{\mathbf{S_{21m}}}{t_{21}}\right)}{D}$$

$$S_{12} = \frac{\left(\frac{\mathbf{S_{12m}}}{t_{12}}\right)}{D}$$

$$S_{22} = \frac{\left(\frac{\mathbf{S_{22m}} - e_2^{00}}{t_{22}}\right)\left[1 + \left(\frac{\mathbf{S_{11m}} - e_1^{00}}{t_{11}}\right)e_1^{11}\right] - e_1^{11}\left(\frac{\mathbf{S_{21m}}}{t_{21}}\right)\left(\frac{\mathbf{S_{12m}}}{t_{12}}\right)}{D}$$

$$D = \left[1 + \left(\frac{\mathbf{S_{11m}} - e_1^{00}}{t_{11}}\right)e_1^{11}\right]\left[1 + \left(\frac{\mathbf{S_{22m}} - e_2^{00}}{t_{22}}\right)e_2^{11}\right] - \left(\frac{\mathbf{S_{21m}}}{t_{21}}\right)\left(\frac{\mathbf{S_{12m}}}{t_{12}}\right)e_1^{11}e_2^{11}$$

As mentioned before the bold measured S-parameters indicate raw measured data which has had the switch error removed.

Another useful method of obtaining corrected data with the 8-term error model is to perform the correction with the t-parameters. As shown earlier the raw measured transmission matrix data $\mathbf{T_m}$ is a result of a cascaded series of the port 1 error box t-parameters T_1 the actual DUT t-parameters T and the port 2 error box t-parameters T_2. The actual T-parameters of the DUT can be easily solved from this relation using the following equation.

$$T = T_1^{-1} \boldsymbol{T_m} T_2^{-1}$$

3.5 Removing the Effects of an Imperfect Switch

Much has been said about the 8-term error model and the assumption of a perfect switch. To assume that a network analyzers switch is perfect and that the terminations of the forward and reverse directions are equivalent is very inaccurate, this will be shown in Chapter 5. Therefore, in order to make this assumption valid, the error caused by this forward and reverse difference must be characterized, and somehow removed from the raw measurement data. This can only be done if there are four measurement channels (four samplers) that are all on the DUT side of the switch. There has been many publication related to this issue most notably are [13,19]. When raw measured data ($[S_m]$) has had the switch errors removed ($\mathbf{[S_m]}$) it is said to have been "switch corrected" [19]. Once the raw measured data has been switch corrected, it is then representative of that which would be obtained, if measured on a network analyzer with a perfect switch.

In a true 4 sampler 4 receiver VNA when measurement data is taken it is collected from all 4 samplers in both the forward and reverse state. These four-sampler measurements are shown in [3] and presented below as m_1 and m_2 where the primed (')

terms are those measured in the reverse direction. When originally working with the dual six-port reflectometer system engineers wanted to create an error model which could be represented as a two port error box for port 1 and port 2 that did not change when the source was switched from forward to reverse. This resulted in,

$$\begin{bmatrix} b_{m1} \\ a_{m1} \end{bmatrix} = \begin{bmatrix} X_{11} & X_{12} \\ X_{21} & X_{22} \end{bmatrix} \begin{bmatrix} T_{11} & T_{12} \\ T_{21} & T_{22} \end{bmatrix} \begin{bmatrix} Y_{11} & Y_{12} \\ Y_{21} & Y_{22} \end{bmatrix}^{-1} \begin{bmatrix} a_{m2} \\ b_{m2} \end{bmatrix}$$

for the forward case; however, there is not enough information. Therefore, by including the reverse measurements the full relationship is formed between the measured data and the unchanging error boxes ([X], [Y]) and the constant actual DUT T-parameters [T]

$$\begin{bmatrix} b_{m1} & b'_{m1} \\ a_{m1} & a'_{m1} \end{bmatrix} = \begin{bmatrix} X_{11} & X_{12} \\ X_{21} & X_{22} \end{bmatrix} \begin{bmatrix} T_{11} & T_{12} \\ T_{21} & T_{22} \end{bmatrix} \begin{bmatrix} Y_{11} & Y_{12} \\ Y_{21} & Y_{22} \end{bmatrix}^{-1} \begin{bmatrix} a_{m2} & a'_{m2} \\ b_{m2} & b'_{m2} \end{bmatrix}.$$

Then by solving for the measured data

$$T_m = XTY^{-1}$$

Where,

$$m_1 = \begin{bmatrix} b_{m1} & b'_{m1} \\ a_{m1} & a'_{m1} \end{bmatrix} \qquad m_2 = \begin{bmatrix} b_{m2} & b'_{m2} \\ a_{m2} & a'_{m2} \end{bmatrix}.$$

The transmission parameter matrix of the raw measured DUT data can be formed by cascading the two measurement boxes

$\boldsymbol{T_m} = m_1 m_2^{-1}$. By forcing the error boxes X and Y to remain the same in the forward and reverse measurements the resulting formulation for the measured transmission parameter matrix must contain the information about the difference between the forward and reverse measurement states. Therefore, when the transmission matrix is formed this way, the

ratios formed from the additional sampler measurements effectively remove the switch error. And thus the 8-term error model can assume a perfect switch if and only if the switch error is removed from the raw measurements.

If a four channel VNA is being operated in a 3 receiver mode, as are most commercial 4 channel VNAs, than the needed ratios must be separately measured.

The switch terms are nothing more than supplementary ratios which are used to de-embed the switch error from raw measured data. These ratios have been well defined in [13,19] The ratios can be obtained from four channel three receiver network analyzer by changing the S-parameter definitions, to measure the desired ratios, using the VNA's front panel controls to setup the measurement.

There are two sets of ratios that can be used to remove the switch error from raw measurement data. The first set was derived from the above equations from the four receiver operation. The two ratios that must be measured are: with power incident at port 1 (forward) $\frac{a_{2m}}{a_{1m}}$ and with power incident at port 2 (reverse) $\frac{a'_{1m}}{a'_{2m}}$. These are simply the fourth typically unmeasured samplers measured with respect to the incident signal in a given direction. Once these ratios have been measured they can be used to calculate switch corrected raw measured S-parameters through the following equations.

$$\boldsymbol{S_{11m}} = \frac{\frac{b_{1m}}{a_{1m}} - \frac{b'_{1m}}{a'_{2m}}\frac{a_{2m}}{a_{1m}}}{d} \qquad \boldsymbol{S_{12m}} = \frac{\frac{b'_{1m}}{a'_{2m}} - \frac{b_{1m}}{a_{1m}}\frac{a'_{1m}}{a'_{2m}}}{d}$$

$$\boldsymbol{S_{21m}} = \frac{\frac{b_{2m}}{a_{1m}} - \frac{b'_{2m}}{a'_{2m}}\frac{a_{2m}}{a_{1m}}}{d} \qquad \boldsymbol{S_{22m}} = \frac{\frac{b'_{2m}}{a'_{2m}} - \frac{b_{2m}}{a_{1m}}\frac{a'_{1m}}{a'_{2m}}}{d}$$

$$d = 1 - \frac{a_{2m}}{a_{1m}}\frac{a'_{1m}}{a'_{2m}}$$

By substituting in the raw measured S-parameter ratios [S_m] the switch corrected raw measurement (**[S_m]**) equations can be re-written as follows.

$$\boldsymbol{S_{11m}} = \frac{S_{11m} - S_{12m}\frac{a_{2m}}{a_{1m}}}{d} \qquad \boldsymbol{S_{12m}} = \frac{S_{12m} - S_{11m}\frac{a'_{1m}}{a'_{2m}}}{d}$$

$$\boldsymbol{S_{21m}} = \frac{S_{21m} - S_{22m}\frac{a_{2m}}{a_{1m}}}{d} \qquad \boldsymbol{S_{22m}} = \frac{S_{22m} - S_{21m}\frac{a'_{1m}}{a'_{2m}}}{d}$$

$$d = 1 - \frac{a_{2m}}{a_{1m}}\frac{a'_{1m}}{a'_{2m}}$$

The switch corrected raw S-parameters can be inserted into the equations found in Section 3.3.2 to calculate the $\mathbf{T_m}$ matrix or the switch corrected raw transmission parameters can be calculated directly through the following identities.

$$\boldsymbol{T_{11m}} = \frac{\frac{b_{2m}}{a_{1m}}\frac{b'_{1m}}{a'_{2m}} - \frac{b_{1m}}{a_{1m}}\frac{b'_{2m}}{a'_{2m}}}{d} \qquad \boldsymbol{T_{12m}} = \frac{\frac{b_{1m}}{a_{1m}} - \frac{a_{2m}}{a_{1m}}\frac{b'_{1m}}{a'_{2m}}}{d}$$

$$\boldsymbol{T_{21m}} = \frac{-\frac{b'_{2m}}{a'_{2m}} + \frac{b_{2m}}{a_{1m}}\frac{a'_{1m}}{a'_{2m}}}{d} \qquad \boldsymbol{T_{22m}} = \frac{1 - \frac{a_{2m}}{a_{1m}}\frac{a'_{1m}}{a'_{2m}}}{d}$$

$$d = \frac{b_{2m}}{a_{1m}} - \frac{a_{2m}}{a_{1m}}\frac{b'_{2m}}{a'_{2m}} \qquad \boldsymbol{T_m} = \begin{bmatrix} \boldsymbol{T_{11m}} & \boldsymbol{T_{12m}} \\ \boldsymbol{T_{21m}} & \boldsymbol{T_{22m}} \end{bmatrix}$$

Substituting for the raw S-parameter ratios gives:

$$\boldsymbol{T_{11m}} = \frac{S_{21m}S_{12m} - S_{11m}S_{22m}}{d} \qquad \boldsymbol{T_{12m}} = \frac{S_{11m} - \frac{a_{2m}}{a_{1m}}S_{12m}}{d}$$

$$\boldsymbol{T_{21m}} = \frac{-S_{22m} + S_{21m}\frac{a'_{1m}}{a'_{2m}}}{d} \qquad \boldsymbol{T_{22m}} = \frac{1 - \frac{a_{2m}}{a_{1m}}\frac{a'_{1m}}{a'_{2m}}}{d}$$

$$d = S_{21m} - \frac{a_{2m}}{a_{1m}}S_{22m}$$

The calculation presented above for the switch corrected measured transmission parameters, whether calculated directly or thru the switch corrected S-parameters and the relationships of 2.4.2, are identical to those measured through a true full time 4-sampler measurement system. One of the main problems with this method of switch correction is that the measured switch ratios $\frac{a_{2m}}{a_{1m}}$ and $\frac{a'_{1m}}{a'_{2m}}$ are dependent on the S-parameters of the DUT. This means that the supplementary ratio measurements must be made for every

DUT that is measured. This is very time consuming much like if data was being taken from all four samplers, thus another method of switch correction was developed.

This second method also employs two auxiliary ratio measurements; however, the emphasis is on characterizing the actual switch termination itself and thereby removing the error from the measured data. The RF switch termination, though different in the forward and reverse state, is highly repeatable. Therefore, it is only necessary to measure it once during a measurement session.

The two measured ratios that represent the forward and reverse switch termination reflection coefficients are respectively: with signal incident on port 1 $\frac{a_{2m}}{b_{2m}}$ and with signal incident on port 2 $\frac{a'_{1m}}{b'_{1m}}$. These ratios are generally measured with the thru standard connected during calibration; however, any transmission standard that will deliver enough power to the opposite port can be used to make the two measurements which form the ratio. Because these ratios are not dependent on the DUT they can be measured once during a measurement session and used to correct all of the raw measured S-parameter data by the following equations.

$$\Gamma_F = \frac{a_{2m}}{b_{2m}} \qquad \Gamma_R = \frac{a'_{1m}}{b'_{1m}}$$

$$\boldsymbol{S_{11m}} = \frac{\frac{b_{1m}}{a_{1m}} - \frac{b'_{1m}}{a'_{2m}}\frac{b_{2m}}{a_{1m}}\Gamma_F}{d} \qquad \boldsymbol{S_{12m}} = \frac{\frac{b'_{1m}}{a'_{2m}} - \frac{b_{1m}}{a_{1m}}\frac{b'_{1m}}{a'_{2m}}\Gamma_R}{d}$$

$$\boldsymbol{S_{21m}} = \frac{\frac{b_{2m}}{a_{1m}} - \frac{b'_{2m}}{a'_{2m}}\frac{b_{2m}}{a_{1m}}\Gamma_F}{d} \qquad \boldsymbol{S_{22m}} = \frac{\frac{b'_{2m}}{a'_{2m}} - \frac{b_{2m}}{a_{1m}}\frac{b'_{1m}}{a'_{2m}}\Gamma_R}{d}$$

$$d = 1 - \frac{b_{2m}}{a_{1m}}\frac{b'_{1m}}{a'_{2m}}\Gamma_F\Gamma_R$$

Substituting for raw measured S-parameters gives:

$$\Gamma_F = \frac{a_{2m}}{b_{2m}} \qquad \Gamma_R = \frac{a'_{1m}}{b'_{1m}}$$

$$\boldsymbol{S_{11m}} = \frac{S_{11m} - S_{12m}S_{21m}\Gamma_F}{d} \qquad \boldsymbol{S_{12m}} = \frac{S_{12m} - S_{11m}S_{12m}\Gamma_R}{d}$$

$$\boldsymbol{S_{21m}} = \frac{S_{21m} - S_{22m}S_{21m}\Gamma_F}{d} \qquad \boldsymbol{S_{22m}} = \frac{S_{22m} - S_{21m}S_{12m}\Gamma_R}{d}$$

$$d = 1 - S_{21m}S_{12m}\Gamma_F\Gamma_R$$

The two ratios Γ_F and Γ_R are known as the forward and reverse switch terms, respectively. This method of switch term measurement is the most widely used in terms of four-channel, three-receiver network analyzers. The $\frac{a_{2m}}{a_{1m}}$ and $\frac{a'_{1m}}{a'_{2m}}$ method, when implemented correctly, is the most accurate method of switch correction because there is no switch repeatability error however, this error is usually very small making the added

measurement time usually not a sufficient trade-off. The $\frac{a_{2m}}{b_{2m}}$ and $\frac{a'_{1m}}{b'_{1m}}$ ratios can be determined from the $\frac{a_{2m}}{a_{1m}}$ and $\frac{a'_{1m}}{a'_{2m}}$ ratios through the following relationships.

$$\frac{a_{2m}}{b_{2m}} = \frac{\frac{a_{2m}}{a_{1m}}}{S_{21m}} \qquad \frac{a'_{1m}}{b'_{1m}} = \frac{\frac{a'_{1m}}{a'_{2m}}}{S_{12m}}$$

Therefore, if converted to the $\frac{a_{2m}}{b_{2m}}$ and $\frac{a'_{1m}}{b'_{1m}}$ ratios, the $\frac{a_{2m}}{a_{1m}}$ and $\frac{a'_{1m}}{a'_{2m}}$ ratios only need to be measured once. However, it takes an extra calculation step which can compound any measurement errors thus, $\frac{a_{2m}}{b_{2m}}$ and $\frac{a'_{1m}}{b'_{1m}}$ are better determined by direct measurement.

3.6 8-Term to 12-Term Error Model Conversion

The switch terms are the link between the 12 and the 8-term error model [13,19]. The 8-term model is essentially the 12-term model with the switch error removed from the error terms and no isolation terms. Therefore, in order to derive the 12-term error model the switch error must be re added to the error terms. The primary reason for doing this conversion is that most VNAs only support a 12-term error correction which means that when an 8-term error model calibration is performed it must be converted to a 12-term error model before it can be loaded to the VNA.

Figure 3.6, which has been adapted from [13], illustrates the process of conversion in the forward direction. First the switch reflection coefficient Γ_F and the isolation term e_{21} are added to the 8-term model. Then the model can be reduced using

flow graph reduction techniques. The reduction gives rise to two values $e_2^{11'}$ which is the forward load match term (ELF) and $e_2^{01'}$ that is used to form the value for the forward transmission term (ETF) $e_1^{10}e_2^{01'}$.

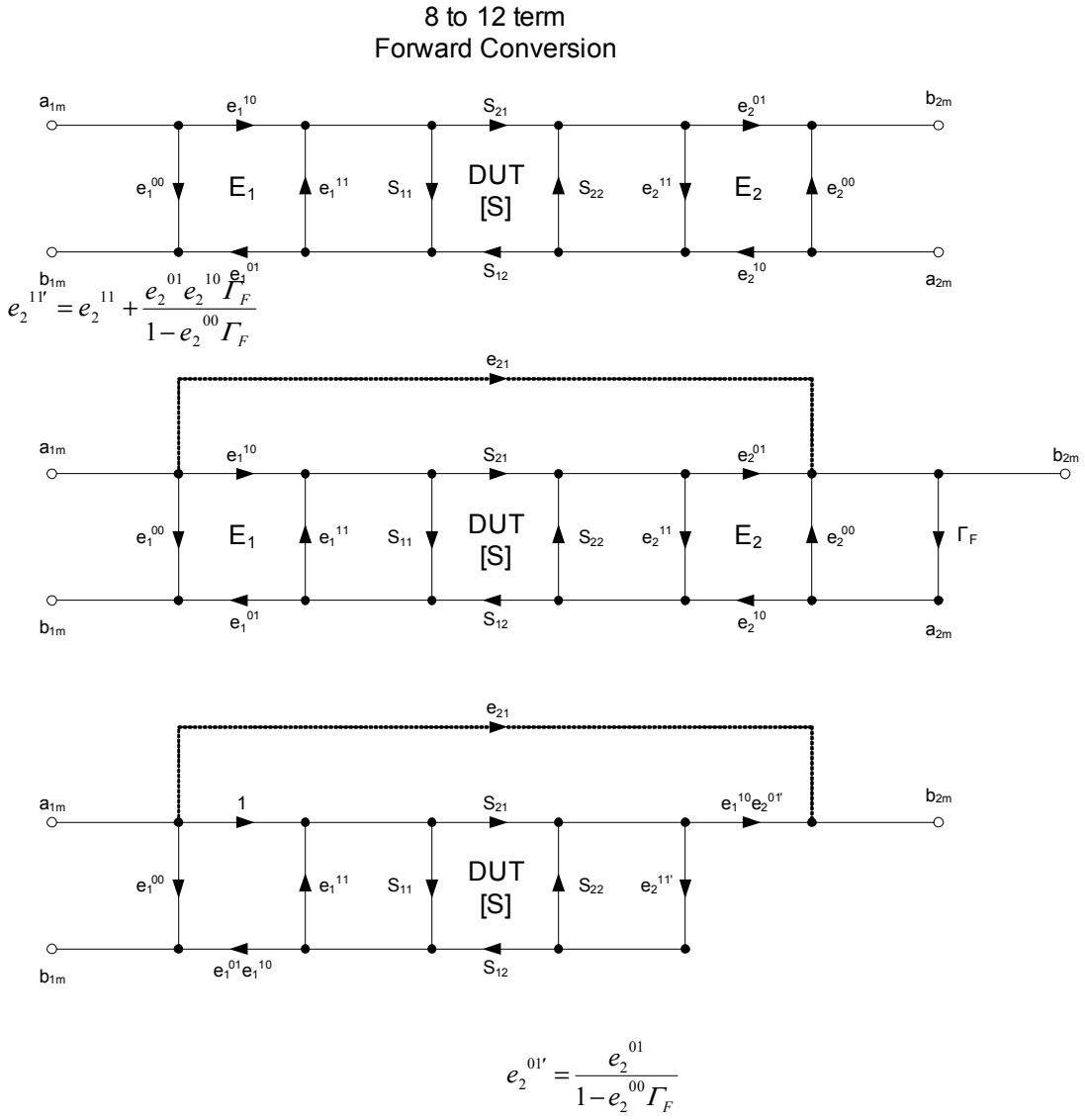

Figure 3.6 – The 8 to 12-Term Error Model Conversion in the Forward Direction [13].

A similar process is used to convert the 8-term error model to the 12-term error model in the reverse direction and is shown in Figure 3.7 that was also adapted from [13].

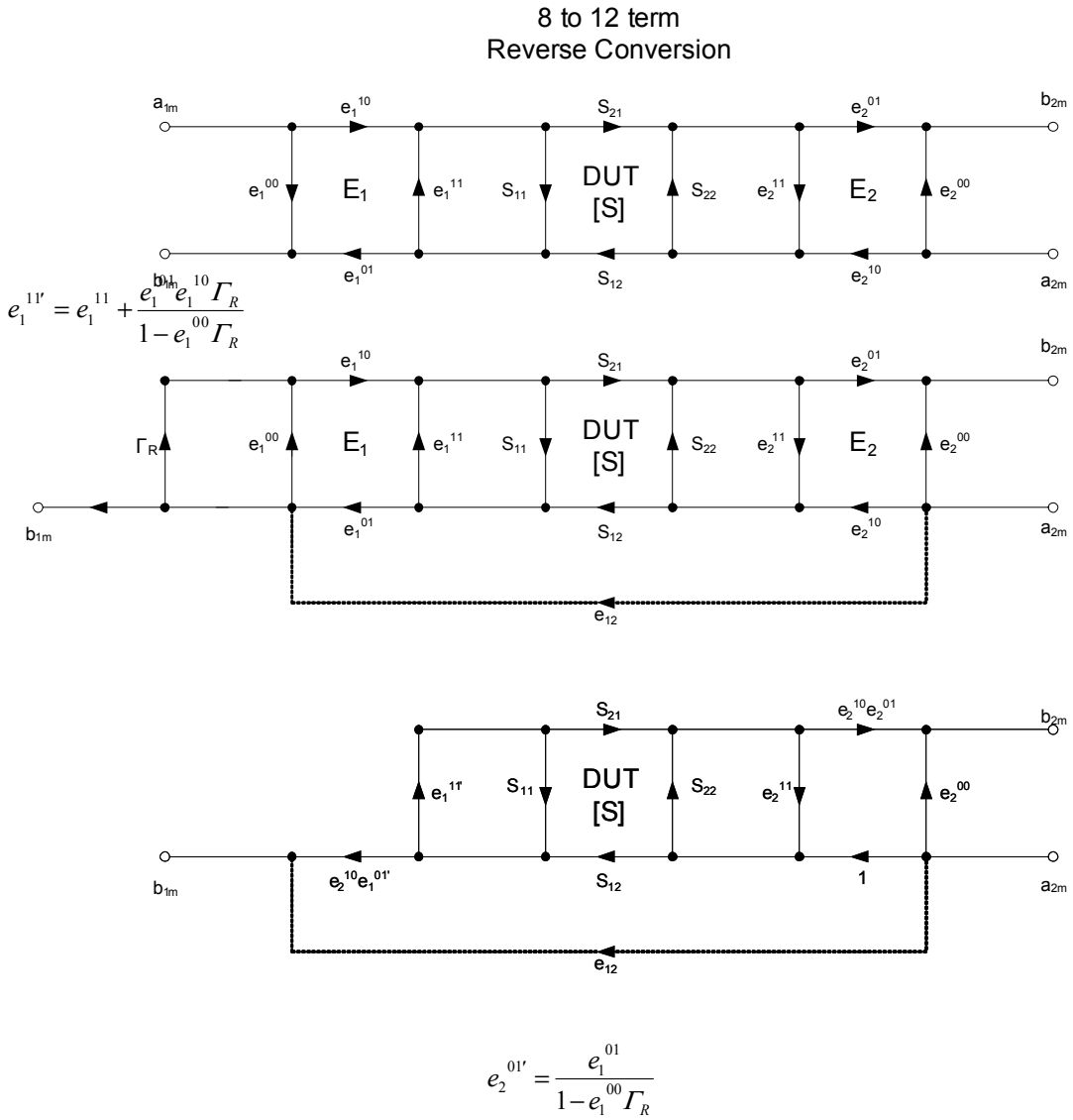

Figure 3.7 - The 8 to 12-Term Error Model Conversion in the Reverse Direction [13].

Now that is has been shown how to convert between the two models table 3.2 is presented to show the relationships between the 12-term and the 8-term models error terms. *note- the isolation terms for the 8-term error model can either be set to 0 or measured and removed from the raw data.

Table 3.2 – 8-Term and 12-Term Error Model Relationships.

12-Term Model Error Terms		8-Term Model Error Terms
EDF = e_1^{00}	=	e_1^{00}
EDR = e_2^{00}	=	e_2^{00}
ESF = e_1^{11}	=	e_1^{11}
ESR = e_2^{11}	=	e_2^{11}
ERF = $e_1^{01}e_1^{10}$	=	$t_{11} = e_1^{01}e_1^{10}$
ERR = $e_2^{01}e_2^{10}$	=	$t_{22} = e_2^{01}e_2^{10}$
ELF = $e_2^{11'}$	= (≠)	$e_2^{11} + \frac{e_2^{01}e_2^{10}\Gamma_F}{1-e_2^{00}\Gamma_F}$ (e_2^{11})
ELR = $e_1^{11'}$	= (≠)	$e_1^{11} + \frac{e_1^{01}e_1^{10}\Gamma_R}{1-e_1^{00}\Gamma_R}$ (e_1^{11})
ETF = $e_1^{10}e_2^{01'}$	= (≠)	$e_1^{10}\frac{e_2^{01}}{1-e_2^{00}\Gamma_F}$ ($t_{21} = e_1^{10}e_2^{01}$)
ETR = $e_2^{10}e_1^{01'}$	= (≠)	$e_2^{10}\frac{e_1^{01}}{1-e_1^{00}\Gamma_R}$ ($t_{12} = e_2^{10}e_1^{01}$)
EXF = e_{21}	=	e_{21}*see note
EXR = e_{12}	=	e_{12}*see note

3.7 Chapter Summary

The 12 and 8-term error models have been developed and the relationships between them discussed. A unique error term convention has been used to provide a seamless transition from the 12-term to the 8-term error model. The methods of applying switch term correction have been demonstrated and a bolding convention established that will carry throughout the thesis. The equations for applying error correction to raw two-port data have also been presented.

CHAPTER 4

VECTOR NETWORK ANALYZER CALIBRATION TECHNIQUES

4.1 Introduction

As shown in Chapter 3 there are main classifications of error models used the 8 and the 12-term. The 12-term error model calibration algorithms are referred to as direct calibration techniques because they incorporate the measurement of well known or well defined calibration standards. The 8-term error model calibration algorithms take advantage of the model's cascaded error box topography and utilize more advanced network solution techniques, which require less information about the calibration standards. These more advanced, and potentially more accurate algorithms are known as "self-calibration" techniques [3]. Though these calibrations are derived here as two-port calibrations the technique used for their adaptation to a multiport calibration algorithm can be found in Chapter 7.

4.2 12-Term Error Model Calibration Techniques

The 12-term error model calibration is traditionally achieved by measuring three well known or well characterized calibration standards on each port, an isolation measurement with a load on each port and a thru measurement. This direct calibration technique was the first calibration algorithm implemented on an automated network analyzer [2,13]. As seen in Chapter 3 the error model has 12 terms six forward and six

reverse. The direct 12-term calibration begins with a one port calibration on each port which will provide 6 of the 12 error terms. These six error terms, 3 forward (EDF,ESF and ERF) and 3 reverse (EDR,ESR and ERR), are known as the reflectometer error terms. Each one port calibration will provide the corresponding ports 3 reflectometer terms. A one port, or reflectometer, calibration is performed by connecting three well known unique terminations to the analyzers ports and measuring their respective reflection coefficients. As shown in Figure 4.1 the measured reflection coefficient is a function of the terminations reflection coefficient and the port's reflectometer error terms. For simplicity the one port calibration will be developed for port 1 however a dual procedure is used to calibrate port 2.

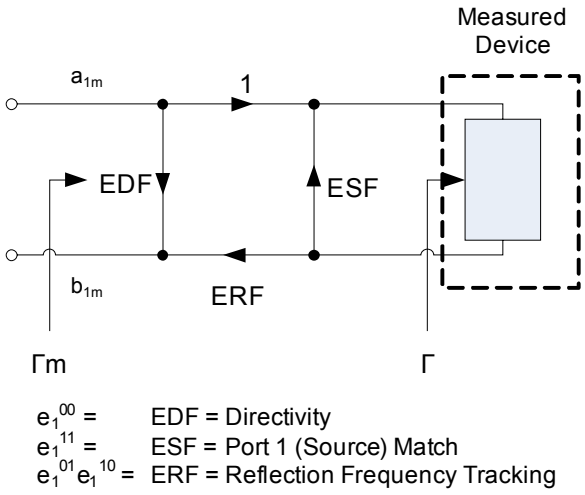

Figure 4.1 - Simple One-Port Termination Connection.

The raw measured reflection coefficient Γm can be represented through the following equation.

$$\Gamma_m = e_1^{00} + \frac{e_1^{10} e_1^{01} \Gamma}{1 - e_1^{11} \Gamma}$$

Rearranging in order to isolate error terms gives:

$$\Gamma_m = e_1^{\,00} + \Gamma e_1^{\,11}\Gamma_m - \Gamma\Delta^1{}_e \qquad \text{where, } \Delta^1{}_e = e_1^{\,00} e_1^{\,11} - e_1^{\,10} e_1^{\,01} = EDF\ ESF - ERF$$

The reflection coefficient of the termination connected to the port, Γ, is assumed to be known and Γm is known because it is measured. That leaves only three unknowns in order to characterize the reflectometer error terms. By making two additional measurements there will be a linear system of three equations by which a solution for the three unknown variables can be found.

$$\begin{bmatrix} 1 & \Gamma_{ma}\Gamma_a & \Gamma_a \\ 1 & \Gamma_{mb}\Gamma_b & \Gamma_b \\ 1 & \Gamma_{mc}\Gamma_c & \Gamma_c \end{bmatrix} \begin{bmatrix} e_1^{\,00} \\ e_1^{\,11} \\ \Delta^1{}_e \end{bmatrix} = \begin{bmatrix} \Gamma_{ma} \\ \Gamma_{mb} \\ \Gamma_{mc} \end{bmatrix}$$

In order to find a unique solution to the linear system it is necessary that the three known terminations (calibration standards) be unique at all frequency points. From this solution we obtain the directivity term EDF ($e_1^{\,00}$) and the port 1 source match term ESF ($e_1^{\,11}$) while the reflection tracking term ERF ($e_1^{\,10} e_1^{\,01}$) can be calculated from $\Delta^1{}_e$. Note: Γm is either $S11_m$ when calibrating on port 1 or $S22_m$ when calibrating on port 2. Once the two reflectometer calibrations are performed the remaining six error terms can be calculated. The isolation terms are directly found by terminating both ports with a matched load and measuring S21 which will be EXF and S12 which will be EXR. The development of the error correction procedures for the 12-term error model will include the isolation terms; however, in practice, isolation can be and most often is ignored.

Measurement of an ideal zero length thru will give the load match (ELF, ELR) and transmission tracking terms (ETF, ETR). The load match terms are found with the raw thru measurements using the following relationship.

$$ELF = \frac{S_{11m} - EDF}{S_{11m} ESF - \Delta^1_e} \qquad ELR = \frac{S_{22m} - EDR}{S_{22m} ESR - \Delta^2_e}$$

The transmission tracking terms are calculated as follows.

$$ETF = (S_{21m} - EXF)(1 - ESF\ ELF) \qquad ETR = (S_{12m} - EXR)(1 - ESR\ ELR)$$

It is very important to recognize the previous two equations are valid only for a zero length thru. What is meant by a zero length thru is that the reference planes of the direct 12-term calibration are set by the reference planes of the reflectometer calibrations. For instance if a calibration is performed on-wafer and the thru line has some length l and the reflectometer calibration standards each have a piece of transmission line of length l/2 preceding them than the reference planes are directly in the center of the thru. This is because the calibrations standards have been characterized without the half length of thru line, therefore when measuring; all that was not characterized as a part of the standard is removed as error. It is the same as performing the calibration with 7mm cables and standards and then connecting the cables directly together to give a perfect zero length thru.

If a non-zero length thru, with known S-parameters S_{11}, S_{12}, S_{21} and S_{22}, is inserted then a more generalized equation must be used.

$$ELF = \frac{S_{11}\Delta^1_e + S_{11m}(1 - S_{11} ESF) - EDF}{\Delta^1_e \Delta_s + S_{11m}(S_{22} - \Delta_s ESF) - S_{22} EDF} \qquad \text{where, } \Delta_s = S_{11}S_{22} - S_{12}S_{21}.$$

The transmission tracking term for a non-zero length thru can be calculated as:

$$ETF = \frac{(S_{21m} - EXF)(1 - S_{11} ESF - S_{22} ELF + ESF\ ELF\ \Delta_s)}{S_{21}}$$

The reverse load match and transmission tracking terms for a non-zero length thru can be calculated using the duality of the previous two equations.

Once the error terms have been calculated the raw measured S-parameters of the DUTs can be corrected using the equations presented in Chapter 3. There are many calibrations spun off from this basic procedure. The three types of direct 12-term calibration that are presented are SOLT, mSOLT and cSOLT. The main difference between these calibrations is the method used for characterizing and representing the calibration standards S-parameters for use in the error term calculations.

4.2.1 SOLT

The three standards used in the reflectometer portion of the direct calibration must be different in terms of their reflection coefficients at all frequency points. In order to ensure this it is a good idea to select standards whose reflection coefficients are as different as possible. The "Short Open Load Thru" or (SOLT) calibration provides three very different reflectometer standards, the short open and a 50Ω load [13, 20]. The SOLT method uses a model based method of characterizing the calibration standards. The calibration standards are measured and then represented through their simple equivalent circuit models shown below. During the reflectometer calibration Γa, Γb and Γc are derived from the reflection parameters of the equivalent circuit models. The model parameters are often called the standard definitions.

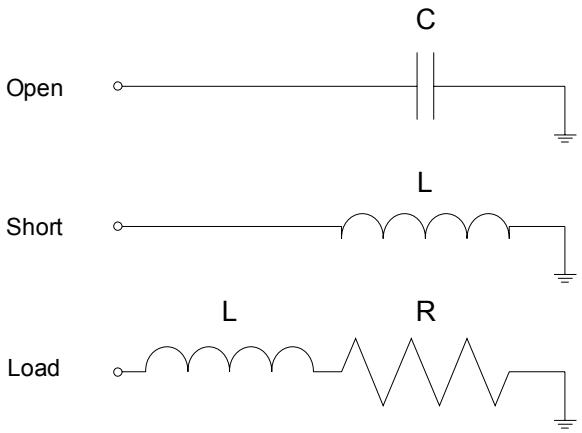

Figure 4.2 - SOL Calibration Standard Equivalent Circuit Models.

The open is modeled as a capacitance, the short as an inductance and the load as an inductance and a series resistance.

These are the standard models used in most VNAs. The problem, however, is with on-wafer measurements the load model is over simplified. As the measurement frequency increases and the measurement bandwidth widens simple models begin to break down and the calibration standard is no longer accurately represented by its model. This directly leads to errors in calculating the reflectometer terms, which carries the problem over into the calculation of the remaining terms as well.

For this reason SOLT's upper calibration frequency is limited by the accuracy of its models. However these models are very good at lower frequencies and gives SOLT excellent low frequency accuracy all the way to DC. Standard SOLT uses a zero length thru. Most VNAs allow the line length to be entered for a non-zero length thru this will allow it to calculate the phase offset however any loss within the thru will not be accounted for and will cause error in the calibration. This calibration error will not be visible in the thru measurement however because it has essentially "zeroed" out the thru.

The best way to verify an SOLT calibration is to use a verification DUT one whose S-parameters are known and was not used in the calibration.

4.2.2 mSOLT

Because the simple models of SOLT breakdown at higher frequencies it was thought that the useful upper frequency of SOLT could be expanded by foregoing the modeling process and using an actual measurement of the calibration standard's reflection coefficient to represent it in the SOLT algorithm. This idea is incorporated in measured SOLT or mSOLT [13,14]. Now, during the reflectometer calibration Γa, Γb and Γc are actual characterization measurements of the calibration standards made using a high frequency calibration technique like TRL which is explained in Section 4.3.

The problem with this is that the calibration must be performed over the exact frequencies used during the calibration standard characterization measurements. This is not convenient because the calibration standard must be characterized for every new frequency list as opposed to a model which can be used to calculate the calibration standards S-parameters over any range of frequencies. The mSOLT calibration has almost identical accuracy properties of TRL because the mSOLT calibration is directly linked to the TRL measurements of the calibration standards. However because of this TRL mirroring it also has the low frequency accuracy problems associated with TRL.

4.2.3 cSOLT

The answer to a flexible high frequency broadband SOLT calibration is cSOLT developed at USF [10,11]. The main inadequacy with SOLT at higher was found to be

the load model. On-wafer microstrip loads like those shown in Figure 4.3 parasitics cannot be fully represented through more simplified load models [10,11].

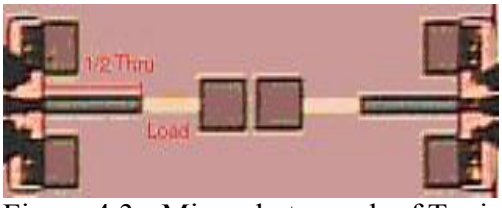

Figure 4.3 - Microphotograph of Typical GaAs Microstrip Load.

Complex SOLT or cSOLT uses a high frequency complex load model shown in Figure 4.4 which allows the SOLT calibration to achieve high frequency accuracy comparable to TRL and still maintain the low frequency accuracy of standard SOLT.

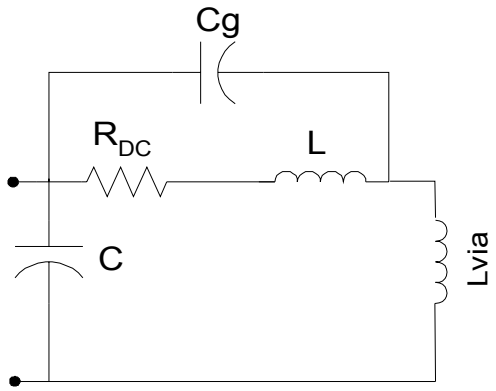

Figure 4.4 - Complex Load Model.

The present author contributed to development of this load model which provides an accurate characterization of most any load up to 110 GHz. The R_{DC} component of the load model is an actual measured DC resistance. It was found that, on a wafer with multiple calibration sets, once the substrate parasitics where modeled on one load sample the model was valid for similar loads on the wafer simply by measuring and changing the

DC resistance of the model [10,11]. The accuracy of the modeled versus TRL measured load data can be seen in Figure 4.5 and 4.6.

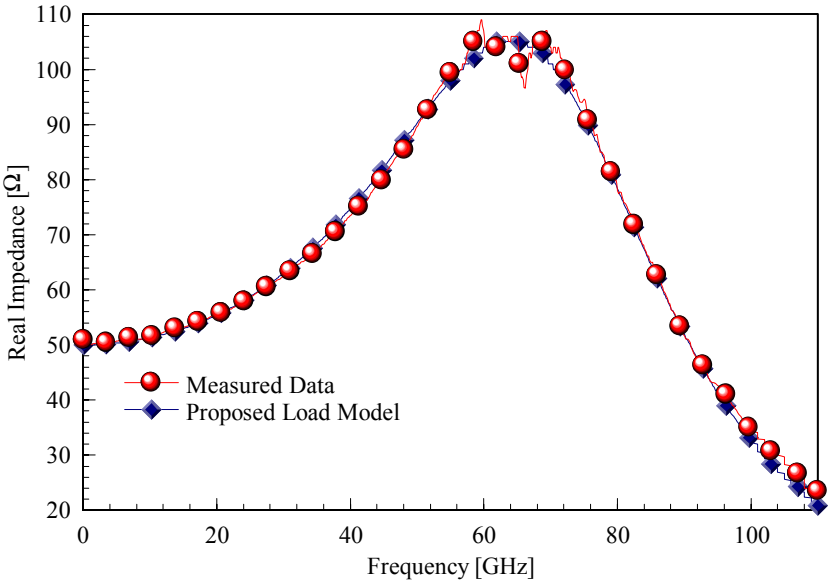

Figure 4.5 - Real Part of Load Impedance of "Center of Thru" Referenced GaAs Microstrip Load Measured (Rdc=49.9799) Versus Proposed Load Model Impedance.

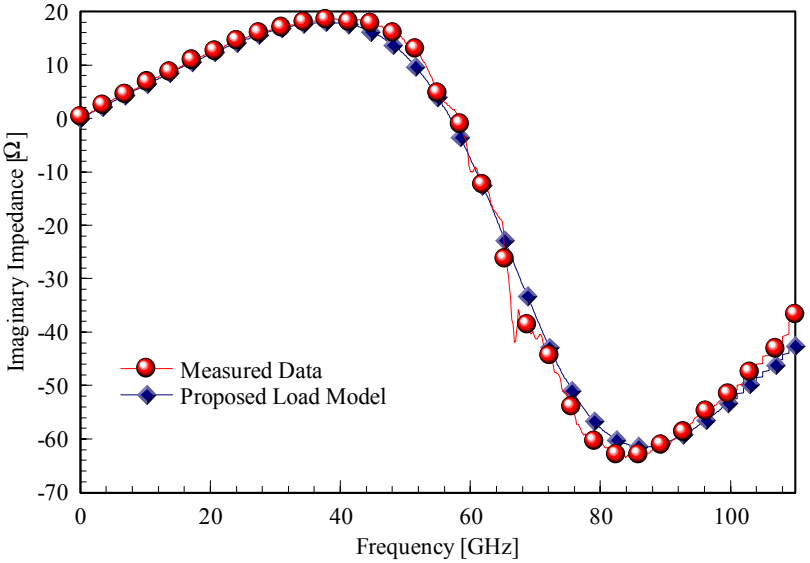

Figure 4.6 - Imaginary Part of Load Impedance of "Center of Thru" Referenced GaAs Microstrip Load Measured (Rdc=49.9799) Versus Proposed Model Load Impedance.

The broadband measurement data in Figures 4.5 and 4.6 was obtained by combing data taken from two separate VNAs; the Anritsu "Lightning" 37397C (40MHz – 65 GHz) and the Wiltron 360B (65 GHz to 110 GHz). The distortion of the measurement data from 50 GHz to 70 GHz is a result of the two VNAs nearing their upper/lower measurement frequency capabilities. The cSOLT calibration also uses a complex thru model described in [10] which can be used to represent the S-parameters of a line in a non-zero length thru situation or to shift the reference plane of an on-wafer calibration from the center of thru back to the probe tips. There are many advantages to the cSOLT calibration especially on-wafer. The main advantage is broadband calibration accuracy from DC-110GHz which is shown in Figures 4.7 and 4.8.

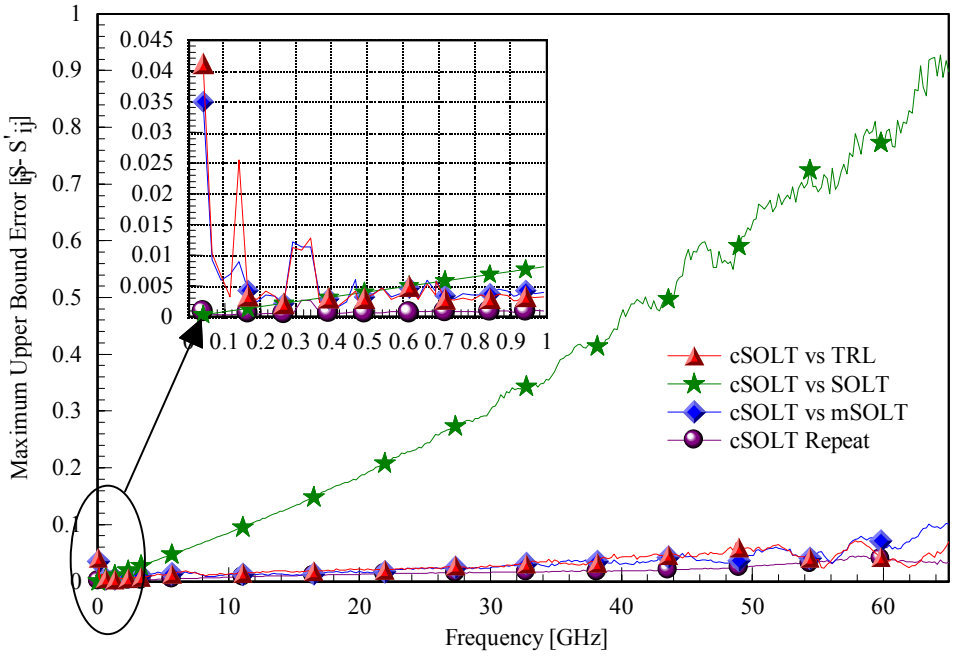

Figure 4.7 – Upper Bound Error Difference Between TRL, cSOLT, mSOLT and SOLT Calibrations with Respect to cSOLT for Reference (from [10]).

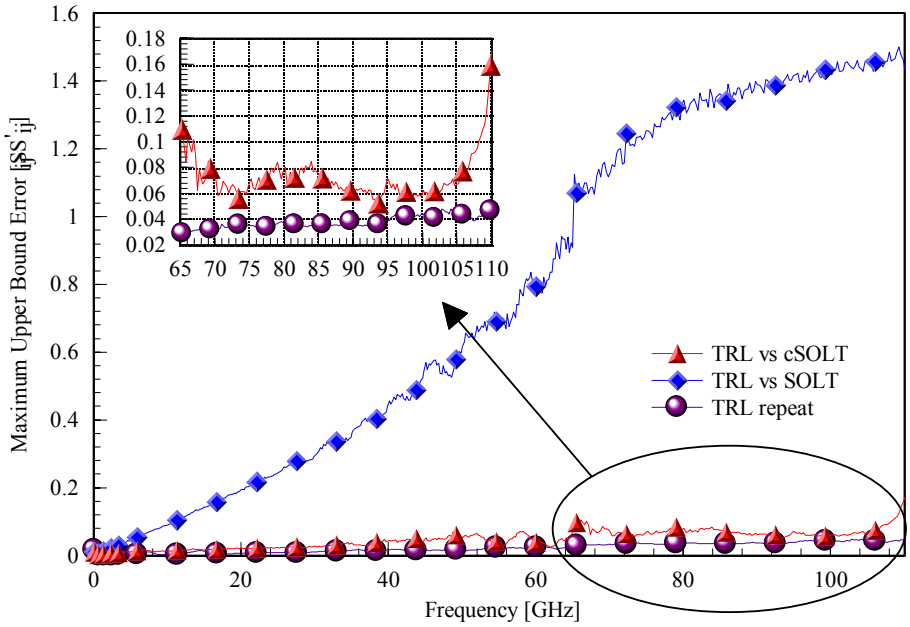

Figure 4.8 - Upper Bound Error Difference Between TRL, cSOLT, and SOLT Calibrations with Respect to TRL for Reference to 110 GHz.

Figure 4.8 shows that cSOLT retains TRL's accuracy to 110 GHz; while simultaneously, not suffering from low frequency degradation, as shown in Figure 4.7, like TRL and mSOLT. The calibration allows the use of equidistant calibration standard footprints to allow semi-automated probing. Semi-automated probing with equal footprint standards speeds up the calibration process by automatically moving to and connecting the different calibration standards.

Similar to mSOLT, the cSOLT calibration is based on TRL measurements of the calibration standards. However, unlike mSOLT, because the TRL measurements are used to fit models rather than directly represent the standards the models force the response towards the correct DC value at low frequency by incorporating a measured DC resistance thus being more accurate at low frequencies than the TRL data. Another advantage to cSOLT is the on-wafer calibration standards are compact which conserves

valuable on-wafer real-estate. Through the complex modeling the need for a well behaved precision broadband load is eliminated allowing calibration loads designed for normal lower frequency SOLT to be used at millimeter waves. The treatment also accommodates a more complex thru model for improved non-zero length thru standard conditions.

4.3 8-Term Error Model Calibration Techniques

As seen in Chapter 3 the 8-term error model can be represented as cascaded transmission matrix system composed of two error boxes. It was also shown that the model could be fully represented by characterizing 7 of the 8 error terms therefore only seven independent equations must be obtained in order to solve this system. Because of this, it is not required to have a complete set of fully characterized calibration standards as with SOLT. Only seven characteristics of the standards are required to be known. As presented by Doug Rytting [13], Table 4.1 shows a few possible 8-term calibration routines and their requirements that are used to satisfy the 7 needed conditions.

Table 4.1 – 8-Term Calibration Methods Which Satisfy the Need for 7 Known Conditions from Rytting [13].

TRL & LRL	Thru (T) or Line (L) with known S-parameters [4 conditions]	Unknown equal Reflect (R) on port-1 and port-2 [1 condition]	Line (L) with known S_{11} and S_{22} [2 conditions]
TRM & LRM	Thru (T) or Line (L) with known S-parameters [4 conditions]	Unknown equal Reflect (R) on port-1 and port-2 [1 condition]	Known Match (M) on port-1 and port-2 [2 conditions]
TXYZ & LXYZ (QSOLT)	Thru (T) or Line (L) with known S-parameters [4 conditions]	3 known Reflects (XYZ) on port-1 or port-2 [3 conditions]	
TXYX & LXYX	Thru (T) or Line (L) with known S-parameters [4 conditions]	2 known Reflects (XY) on port-1 [2 conditions]	One known Reflect (X) on port-2 [1 condition]
LRRM	Line (L) with known S-parameters [4 conditions]	2 unknown equal Reflect (RR) on port-1 and port-2 [2 conditions]	Known Match (M) on port-1 [1 condition]
UXYZ (SOLR)	Unknown Line (U) with $S_{12} = S_{21}$ [1 condition]	3 known Reflects (XYZ) on port-1 [3 conditions]	3 known Reflects (XYZ) on port-2 [3 conditions]

Those 8-term calibration methods which are derived from three calibration standards, such as TRL and LRM, use a procedure of error term calculation known as "self-calibration" [3].

Self calibration is performed by completely knowing the S-parameters of one standard such as the thru line (T) in TRL or TRM or the transmission line (L) in LRL or LRM. Knowing these four S-parameters gives four conditions however by measuring two other standards each, with four complex S-parameters, eight more equations can be formed and only 3 more conditions must be known. Therefore, the redundant measurements enable the calculation of the remaining unknowns. The following theory for the self-calibration technique is developed from [3,13]. Because the 8-term error model is used, the raw measured data can be represented simply as a cascaded error box equation, which was presented in Chapter 3. The three equations given by the switch corrected raw t-parameter data are shown below where $T_{m(i)}$ are the measured

transmission parameter data of the three standards and $T_{(i)}$ are the actual transmission parameters for the three standards i = (1,2,3).

$$\boldsymbol{T_{m1}} = A\,T_1\,B^{-1}$$

$$\boldsymbol{T_{m2}} = A\,T_2\,B^{-1}$$

$$\boldsymbol{T_{m3}} = A\,T_3\,B^{-1}$$

As with TRL, LRL, LRM, TRM one standard is completely known (T_1) one has two known conditions (T_2) and one has a single known condition (T_3). By exploiting the measurement redundancies we can determine the remaining t-parameters for the unknown standards. Assume for a moment that the parameters of all three standards are already known. From the three equations above, A can be determined by combining equations and eliminating B. Then, by knowing the 4 parameters of one standard, B can be determined as well by solving the T_{m1} equation. However, in order to carry out this process more of the standards unknown must be mathematically determined by the measurement redundancies. If T_2 has two known conditions, then there remain two unknown conditions that can still be determined. Therefore, T_2 can be described as a function of its two unknown parameters x_1, x_2 as presented in the equation below.

$$T_2(x_1, x_2) = \begin{bmatrix} T_{2,11}(\underline{x}) & T_{2,12}(\underline{x}) \\ T_{2,21}(\underline{x}) & T_{2,22}(\underline{x}) \end{bmatrix}$$

$$where: \quad \underline{x} = \begin{bmatrix} x_1 \\ x_2 \end{bmatrix}$$

$$Given: \quad P(\underline{x}) = [T_2(\underline{x})]T_1^{-1} \quad and \quad Q = T_{m2}T_{m1}^{-1}$$

Because T_2 is now a function of $\underline{x}$ so is P, and the values of $\underline{x}$ can be determined by solving the following equations for $\underline{x}$.

$$P_{11}(\underline{x}) + P_{22}(\underline{x}) = Q_{11} + Q_{22}$$

$$P_{11}(\underline{x})P_{22}(\underline{x}) - P_{12}(\underline{x})P_{21}(\underline{x}) = Q_{11}Q_{22} - Q_{12}Q_{21}$$

By solving for $\underline{x}$, T_2 has been fully characterized and we drop the "of x" functionality because we now have explicit values for T_2. The third standard T_3 is treated similarly it has three unknown free parameters characterized by (y_1, y2, and y_3). The relationship between T_1 the newly determined T_2 and T_3 can also be exploited to determine the three unknowns. First two relationships come from combining T_1 and T_3.

$$Given: \quad U(\underline{y}) = (T_3(\underline{y}))T_1^{-1} \quad and \quad V = T_{m3}T_{m1}^{-1}$$

$$U_{11}(\underline{y}) + U_{22}(\underline{y}) = V_{11} + V_{22}$$

$$U_{11}(\underline{y})U_{22}(\underline{y}) - U_{12}(\underline{y})U_{21}(\underline{y}) = V_{11}V_{22} - V_{12}V_{21}$$

$$where: \quad \underline{y} = \begin{bmatrix} y_1 \\ y_2 \\ y_3 \end{bmatrix}$$

The third relationship is between T_2 and T_3.

$$R_{11}(\underline{y}) + R_{22}(\underline{y}) = W_{11} + W_{22}$$

$$where: \quad R(\underline{y}) = N_3N_2^{-1} \quad W = M_3M_2^{-1}$$

Once this has been done T_1, T_2, and T_3 are completely known and can be used to determine the A transmission parameter error box. Any calibration with three standards,

one fully known one with 2 unknowns and one with three unknowns can use this self-calibrating procedure.

4.3.1 TRL and Multiline TRL

The Thru-Line-Reflect or TRL calibration is a very accurate calibration [5]. It incorporates a known thru line standard, a transmission line standard, which is longer than the thru often called a delay line, and a highly reflective standard either an open or a short. All four S-parameters must be known for the thru standard. The reflect standard is usually an open or a short. The one condition imposed by the algorithm on the reflect standard is that the port 1 and port 2 reflect standard be identical.

The delay standard is a matched transmission line that assumes a zero reflection. The length of the transmission line is designed for a quarter wavelength at some center frequency the performance of the calibration degrades as the phase of the delay line approaches 0 or 180 degrees because a difference between the zero reference thru and the delay line must be seen. A good rule of thumb is to use a delay with frequencies for which the line has between 60 and 120 degrees of phase [23]. For this reason, multiple delay lines are often used to calibrate broadband measurements, and a delay frequency range is inputted by the user to determine the start and stop of the error term calculation with a specific delay line. The problem of the accuracy degrading as the delay line approaches a 0 degree phase is one reason why TRL loses accuracy at low frequencies making a lower frequency calibration difficult without using an impractically long delay line this is one reason why cSOLT was developed.

Another TRL method that incorporates multiple delay lines, but does not use the start and stop frequency designation is multiline TRL [8]. Multiline TRL is the most robust and accurate two port calibration and is the benchmark by which all other broadband calibrations are compared. Because a long delay line will "wrap around" the 360 degree phase point several times as the frequency increases it has the potential to become usable again at other frequency bands.

The Multiline method utilizes an collection of uncorrected two-port S-parameter measurements collected from a set of calibration standards, plus a measurement of the switch terms in order to compute the two-port VNA correction coefficients[8]. The multiline TRL uses the same standards as regular TRL. However, multiline TRL estimates the propagation-constant of the standards frequency-by-frequency, and then computes the S-parameter correction coefficients in two parts, using the estimate of the propagation-constant [24]. The reference impedance of all TRL type calibrations is determine by the characteristic impedance of the transmission lines, because, the transmission lines are assumed to have zero reflection. For this reason multiline TRL is able to deal with the propagation-constant and correction coefficient problems without having to know the Z_o, of the standards.

If the Z_o, of the standards is known, the correction coefficients can be transformed to any desired reference impedance, such as $Zref = 50 + j0\ \Omega$ [9]**.** The multiline method applies the Gauss-Markov theorem to form a linear unbiased estimator for the propagation-constant and the error-box parameters [24]. Multiline TRL does not simply use the thru standard as the common line at all frequencies. Instead, it chooses a common line based on the resulting phase differences at each frequency point and chooses the best

line pairs with which to calculate the propagation constant and error parameters [24]. This explanation comes directly from the referenced papers [8,24] written by NIST engineers that developed the multiline TRL algorithm, it would benefit the reader greatly to read these papers; if they wish to gain a greater understanding of the multilane TRL method.

4.3.2 The LRM Calibration

Another self-calibration technique is the line-reflect-match or LRM technique [4]. Like the TRL calibration and other self-calibrations the LRM requires one standard (the transmission line "L") to be completely known, giving 4 of the seven required known conditions. One easy way to ensure this is known is to use a zero length transmission line (a thru) in which case the algorithm becomes known as thru-reflect-match or TRM.

The reflect standards are unknown except for having equal reflection on port one and two and knowing whether the impedance is greater than or less than Zo. Usually, a pair of opens or shorts are used as the reflect standards, this gives 1 more known parameter. A known match (conventionally assumed to have zero reflection) on port one and two gives the final two needed known parameters.

The match is where the robustness of the LRM calibration is weakest. Because a perfect match is required on both ports a high quality broadband load is required. Often this is not possible to obtain at higher broadband frequencies such as 50GHz. However, the use of techniques described in [25] can increase the upper frequency range of the calibration. One of the benefits of LRM is that the calibration standards are compact, they can have an equal footprint and there are only three standards. A good multiline TRL

calibration may have up to 3 or more lines depending on the frequency range and allowable λ/4 deviation. However, despite LRM's compact nature multiline TRL is generally more accurate and robust than standard LRM; because, it does not depend on a match standard to calculate the reference impedance [25].

4.3.3 The SOLR Calibration

There are several hybrid calibrations which use model based direct calibration techniques in conjunction with the 8-term error model's characteristic of only requiring 7 conditions. Quick SOLT or QSOLT, developed by Andrea Ferrero, was one of the first calibration techniques to combine model based direct calibration methods with the 8-term error model [26]. Essentially QSOLT allows a user to only perform one reflectometer calibration, which gives 3 of the seven conditions, and then measure a known thru standard that gives the remaining 4 conditions. This is very useful for coaxial calibrations in which standard connection is very time consuming.

An even more significant hybrid calibration development of Ferrero was the development of what is now known as the short-open-load-reciprocal calibration, or SOLR [6]. The SOLR calibration has a very useful and unique property in that it does not require a well known ideal transmission standard [7]. Two reflectometer calibrations are performed the same as with SOLT this gives six of the seven needed conditions for the 8-term calibration leaving only one condition to impose on the thru.

The only requirement for the transmission standard is that it be reciprocal ($S_{21} = S_{12}$) and a rough knowledge of the phase is needed in order to make a root choice later. This is a great benefit for on-wafer measurements particularly those which require the use

of a non-ideal transmission standard for calibration, such as a 90 degree probe setup for devices with right angle footprints. On a multi-signal probe a loop back or U thru is required which is far from ideal, in this case SOLR is highly beneficial. As a result of this property it will be shown in Chapter 7 to be a very useful multiport calibration technique.

The following development of the SOLR calibration will be done using 8-term error model notation presented in 3.3.2. It is noted at this time that this is an 8-term error model calibration and therefore all raw measured calibration data must be switch corrected in order to be accurate. Switch corrected raw data is designated by bold parameters. Then the user may choose to continue to switch correct the raw DUT data and use 8-term error correction techniques or perform an 8 to 12-term conversion in which the error terms include the switch error and regular raw DUT data may be used for 12-term correction. Both techniques are detailed in Chapter 3.

First two reflectometer calibrations must be performed by solving the linear system for each port using known modeled standards just like the SOLT calibration.

$$\begin{bmatrix} 1 & \Gamma_{m1a}\Gamma_a & \Gamma_a \\ 1 & \Gamma_{m1b}\Gamma_b & \Gamma_b \\ 1 & \Gamma_{m1c}\Gamma_c & \Gamma_c \end{bmatrix} \begin{bmatrix} e_1^{00} \\ e_1^{11} \\ \Delta^1_e \end{bmatrix} = \begin{bmatrix} \Gamma_{m1a} \\ \Gamma_{m1b} \\ \Gamma_{m1c} \end{bmatrix} \qquad \begin{bmatrix} 1 & \Gamma_{m2a}\Gamma_a & \Gamma_a \\ 1 & \Gamma_{m2b}\Gamma_b & \Gamma_b \\ 1 & \Gamma_{m2c}\Gamma_c & \Gamma_c \end{bmatrix} \begin{bmatrix} e_2^{00} \\ e_2^{11} \\ \Delta^2_e \end{bmatrix} = \begin{bmatrix} \Gamma_{m2a} \\ \Gamma_{m2b} \\ \Gamma_{m2c} \end{bmatrix}$$

$$where: \Delta^1_e = e_1^{00} e_1^{11} - t_{11} \quad and \quad \Delta^2_e = e_2^{00} e_2^{11} - t_{22}$$

From this all the reflectometer terms or 6 of the seven required terms for the 8-term error model are known (e_1^{00}, e_1^{11}, t_{11}, e_2^{00}, e_2^{11}, and t_{22}).

The only remaining term is the transmission term t_{21} which is now easily found by cascading the error box A and B transmission matrix and measuring the thru. It can be

recalled from Chapter 3 that the transmission matrices A and B of the 8-term error model are equal to:

$$A = \begin{bmatrix} -\Delta_{e1} & e_1^{00} \\ -e_1^{11} & 1 \end{bmatrix} \qquad B = \begin{bmatrix} -\Delta_{e2} & e_2^{11} \\ -e_2^{00} & 1 \end{bmatrix}$$

Recall that a raw switch corrected transmission parameter measurement $\mathbf{T_m}$ is represented as shown.

$$\boldsymbol{T_m} = \frac{1}{(t_{21})} ATB \qquad where: \boldsymbol{T_m} = \frac{1}{\mathbf{S_{21m}}} \begin{bmatrix} -\mathbf{\Delta_{Sm}} & \mathbf{S_{11m}} \\ -\mathbf{S_{22m}} & 1 \end{bmatrix} \quad and \quad t_{21} = e_1^{10} e_2^{01}$$

From the two reflectometer calibrations A and B are known. $\mathbf{T_m}$ is also known because it is the raw measured data of the thru standard. Therefore, all that is not known is the transmission parameter t_{21} and the actual S-parameters of the thru. However, the actual S-parameters of the thru do not need to be known. Because the thru must be reciprocal it follows that if the determinant of the actual thru parameters T is taken it will be equal to unity. If the determinants of both sides of the $\mathbf{T_m}$ equation are taken the result is as follows.

$$det(\boldsymbol{T_m}) = \frac{1}{(t_{21})^2} det(A) det(T) det(B) \qquad where: det(T) = 1$$

$$det(\boldsymbol{T_m}) = \frac{1}{(t_{21})^2} det(A) det(B)$$

Solving for the transmission parameter t_{21} gives.

$$t_{21} = \pm \sqrt{\frac{\det(A)\det(B)}{\det(\boldsymbol{T_m})}}$$

Now that the transmission parameter is solved for a root choice must be made because t_{21} can be either positive or negative. The way to determine whether it is positive or negative is by comparing the rough estimate of the thru phase to the corrected thru phase at every frequency point and determine whether a positive or negative t_{21} gives a closer response to the rough estimate. It can be seen by Figure 4.9 that with the corrected phase with a positive and negative transmission term only one is close to the estimate at any given point because they are 180 degrees out of phase. This demonstrates that an exact knowledge of the reciprocal thru phase is by no means necessary.

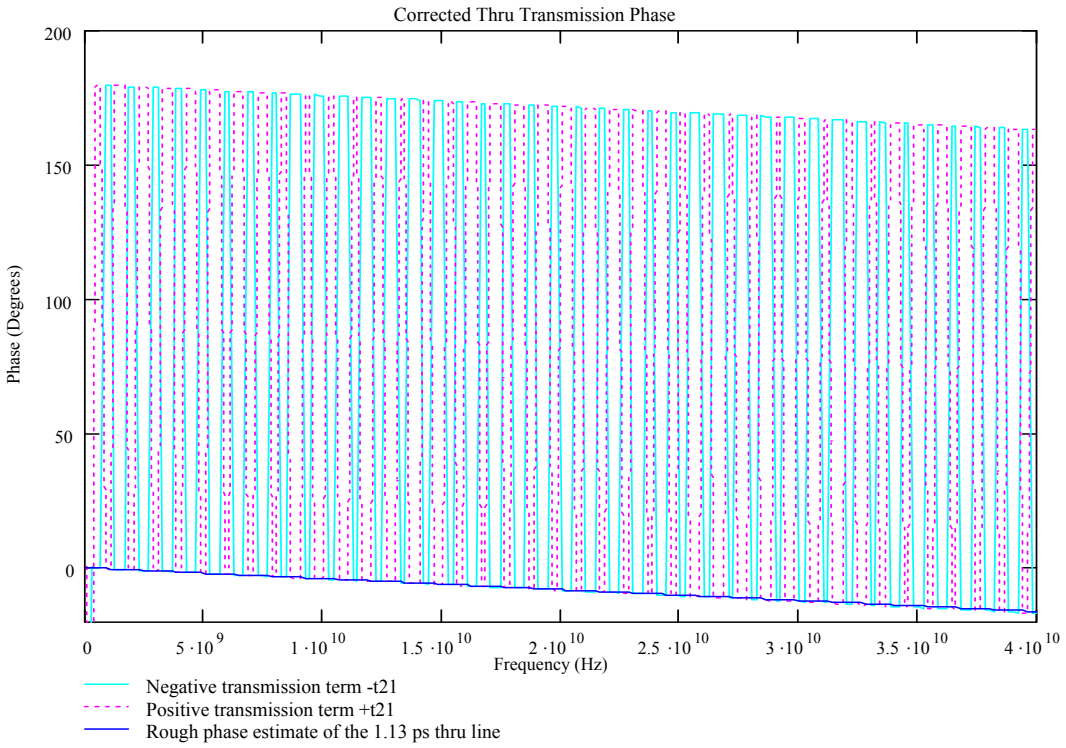

Figure 4.9 – The Corrected Reciprocal Transmission Phase Using Both the Positive and Negative Transmission Terms $\pm t_{21}$.

A simple if statement in the calibration algorithm will allow you to make the decision whether t_{21} should be positive or negative based on which corrected thru data, that which is calculated from $+t_{21}$ or $-t_{21}$, has the greatest phase difference from the rough estimate. Once t_{21} is calculated the final term of the 8-term error model the reverse transmission term t_{12} is easily calculated from the other 7 terms. Therefore, t_{12} can be found through the following relationship.

$$(e_1^{10}e_1^{01})(e_2^{10}e_2^{01}) = (e_1^{10}e_2^{01})(e_1^{01}e_2^{10}) \quad or \quad t_{11}t_{22} = t_{21}t_{12}$$

$$t_{12} = \frac{t_{11}t_{22}}{t_{21}}$$

Now that all 8-terms have been found error correction can be applied to DUT measurements.

Most passive devices are inherently reciprocal for this reason in some cases the actual DUT may be used a calibration standard. The benefits of SOLT are held with SOLR such as the equal footprint layout (when using a non-zero length thru) and the compactness of the calibration standards. However, it also has the drawbacks of SOLT in terms of the need for accurate broadband standard models. The need becomes more critical in SOLR because the transmission terms are highly dependent on all of the reflectometer terms. The use of accurate models like those presented in 3.2.4 will increase the accuracy of SOLR at high frequencies. The implementation of which is shown in Chapter 5.

4.4 StatistiCAL

StatistiCAL is a kind of mix and match calibration algorithm [27,28]. It was developed by NIST in order to create a flexible and highly robust calibration algorithm. It utilizes redundant calibration standards and an orthogonal distance regression algorithm [28]. This allows Statistical to calculate errors in measurements and standard definitions in order to find an optimal solution. Using this idea, the calibrations can be made up of any combination of standards. The more that is known about the standards and the more standards measured, the more optimal the calibration. Statistical can also reduce non-systematic errors such as connection repeatability by have multiple measurements of the same calibration standard or device. The calibration begins by entering an estimate for the error boxes which can be obtained from any previous Multical calibration for a particular system and then the standards are enter and defined and measured. Once everything is measured the algorithm goes to work and produces a 12-term error coefficient file by which raw data can be corrected.

4.5 Chapter Summary

Various 12 and 8-term calibration techniques have been discussed. The direct 12-term model based calibration has been developed in detail and a generalized procedure for performing self calibration techniques has been given. The various calibrations have been compared and their strengths and weaknesses discussed. It is generally accepted that Multiline TRL, despite its low frequency inadequacies, is the most robust broadband calibration algorithm. It has also been shown that through implementation of a complex load model direct calibration techniques such as SOLT, can achieve multiline TRL like

accuracy at higher frequencies and retain the low frequency accuracy of SOLT. The SOLR calibration algorithm has been developed in detail and it will be verified in the next chapter that the SOLR calibration technique can be improved by using a complex load model as well.

CHAPTER 5

COMPLEX SOLR (cSOLR) DEVELOPMENT AND VERIFICATION

5.1 Introduction

As with SOLT the reflectometer terms of the SOLR calibration are determined by finding a solution to a linear system of equations which relates raw measured data to calibration standard models. As was shown in Chapter 4 with SOLT, the standard load model is inadequate at higher frequencies and a more accurate model can be used in its place in order to achieve better broadband accuracy. This same method can be applied to the SOLR calibration to create what will be referred to as complex SOLR or cSOLR. The cSOLR calibration method will be discussed in this chapter and experimental results will be used to compare this calibration to other well-known calibrations and verify its accuracy.

5.2 cSOLR Development

The cSOLR algorithm was developed as a natural extension to the cSOLT algorithm. The SOLR algorithm is a unique and highly useful calibration that provides some significant advantages to SOLT and other calibrations in certain measurement conditions. Because SOLR suffers the same problems as SOLT at higher frequencies; it seemed relevant that the technique used to improve SOLT, be applied to SOLR. The high

frequency inaccuracies, caused by poor reflectometer term characterization, are more significant with SOLR because they are compounded by the fact that it uses an 8-term error model and the transmission terms are calculated in the SOLR algorithm, based directly on the reflectometer terms. As a result of this dependency, the need for a more accurate reflectometer characterization is essential in the SOLR calibration. This is the reason for developing cSOLR.

5.2.1 cSOLR Methodology

This is the basic procedure for performing the cSOLR calibration. There are two main parts to the cSOLR method, as with the cSOLT method: characterizing and modeling the standards and performing the calibration. The first part only needs to be performed one time as the same standard definitions can be used indefinitely for a given set of standards; unless the standards are somehow altered and then they must be re-characterized.

Characterizing and modeling the standards

1. Perform a Zo corrected multiline TRL calibration with the desired reference plane and measure the short, open and load standards.
2. Measure the DC resistance of the load standards and the short standards. Subtract the measured short resistances from the measured load resistance to obtain the actual load resistance.

3. Model the short, open and load standards in ADS using the appropriate complex model and optimization. Use the actual DC resistance of the load in the complex model; shown in Figure 4.4.

Performing the calibration

1. Connect and measure the short, open and load standards on ports 1 and 2.
2. Connect and measure the reciprocal standard (ideally some transmission line with length L)
3. While the reciprocal device is still attached, measure the VNA's switch terms.
4. Measure the raw data of any DUTs whose S-parameters are wanted.
5. Using raw measured standard and switch term data calculate the error coefficients using the procedures detailed in Section 4.3.3.
6. Correct the raw measured DUT data using procedures of Section 3.4

5.2.2 Eliminating the Need for a Complex Thru Model

Since cSOLR does not require any knowledge of the thru, other than a rough phase estimate, there is no need for a complex thru model, as is required in cSOLT when a non-zero length thru is used. The reference planes of cSOLR are set by the reflectometer portion of the calibration. Figure 5.1 illustrates this point with a generic set of microstrip SOLR calibration standards and Figure 5.2 shows a generic 90 degree standard layout.

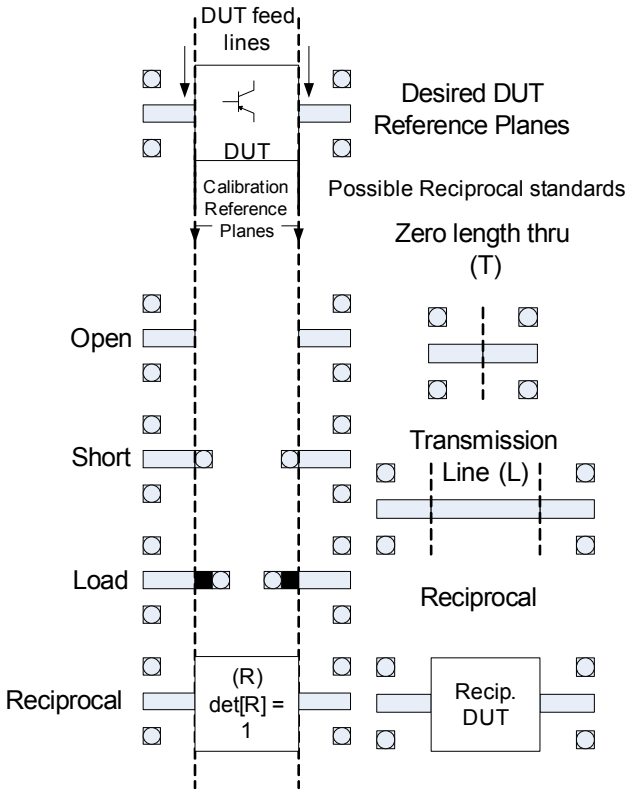

Figure 5.1 – A Generic Set of SOLR On-Wafer Calibration Standards.

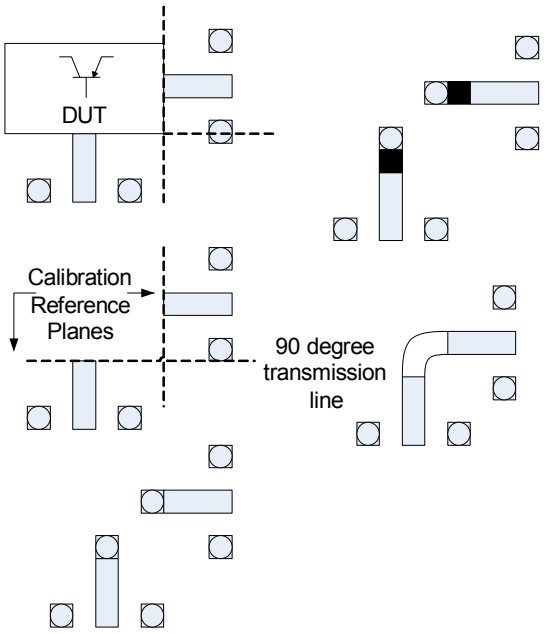

Figure 5.2 – A Generic Set of 90 Degree SOLR Calibration Standards.

All SOLR calibrations produce “center of thru” reference planes regardless of the reciprocal standard used providing that the reciprocal path contains the same transmission paths which preceded the SOL standards. This statement is clarified as follows. The phrase “center of thru” comes from on-wafer calibrations. Recall that a thru connection by definition is one in which port 1 is assumed to be directly connected to port 2. Therefore a thru is not a physical device because it has zero phase and zero loss thus there is no physical center. In a 7mm calibration for example a perfect thru can be realize by mating one 7mm adapter to another therefore the thru has no physical length and therefore has no center.

The term, as it applies to on-wafer measurements, implies the same condition. What is not often understood is that when measuring on-wafer the connection from VNA to DUT is a pair coax cables transitioned on-wafer to a pair of transmission lines and the thru standard, though it appears to have a physical length is simply the two transmission line’s sexless ends joined seamlessly together. Therefore, for on-wafer terminology a thru a standard is a transmission standard which provides a zero length connection with respect to the reference planes. If the transmission standard is non-zero length with respect to the reference planes, than it is not a thru standard it is a line standard.

What is typically meant in on-wafer calibrations by the term “center-of-thru” calibration is that the reference planes are directly at the DUT; it is incorrect to say center of thru. Therefore, if a calibration whose reference planes are at the DUT is needed the transmission line which precedes the SOL standards must be equal to that which precedes the DUT on the test board. It can be seen in Figure 5.1 that the desired reference planes are established by the SOL standards. In this case the calibrations standards are designed

based on the footprint of the DUT's feed lines in which case Figure 5.1 and 5.2 a 90 degree calibration layout would illustrate an appropriate layout. Note that for the 90 degree layout the SOL standards maintain a consistent reference plane which is carried over to the 90 degree transmission line standard.

Unfortunately, however, a custom set of calibration standards is not always available and commercial substrates must be used and a probe tip referenced calibration performed. Because, SOLR's reference planes are set by the SOL standards this makes it ideal when performing probe tip calibrations as the typically non-zero transmission line that is used for the transmission measurements is removed automatically as though it were a zero length thru line.

5.3 cSOLR Accuracy Verification Techniques

During the development of cSOLR the first step was to understand the SOLR algorithm. DUT S-parameter measurement results using SOLR, and ultimately the cSOLR algorithm, were initially compared to the SOLR algorithm implemented in Cascade Microtech's Wincal software [29]. By achieving very similar results to Wincal it was concluded that the algorithm was on track. Then it was compared to StatistiCAL [27], an algorithm which uses an entirely different method of solving and the results were identical. This gave good verification that our algorithm was at very least performing the basic error correction of the network analyzer. After the algorithms functionality was verified, its accuracy was verified as well. To verify cSOLR's accuracy, a USF developed software called Cal Compare [10], was used to compare cSOLR to TRL, SOLR and

cSOLT in the same manner that cSOLT was in Chapter 4. Cal Compare is USF's implementation of NIST's calibration comparison methods [30].

5.4 cSOLR Accuracy Verification Using Ideal Transmission Standards

It was important to first establish the cSOLR algorithm as an effective two port calibration with high accuracy using ideal thru standards, since introducing non-ideal thru standards could only degrade accuracy. Therefore, in order to initially test the calibration method, two very different sets of on-wafer calibration standards were used. The first is a commercially available substrate from GGB [31], the CS-5. The CS-5 is an alumina substrate with co-planar wave guide (CPW) based TRL and SOLT/R calibration structures including 90 degree SOL and transmission line standards.

The loads on these standards are very well behaved at higher frequencies and therefore do not necessarily require the complex load model's benefits. The second set of standards are microstrip structures on a GaAs substrate designed by Mike Imparato of USF [32] and fabricated by M/A-com [33] formerly ITT GaAsTek. These MMIC based standards are fabricated on a 75um substrate. The MMIC loads on this substrate require the use of the complex load model to be accurately represented at frequencies above 5GHz.

5.4.1 GGB CS-5 Calibration Substrate

Initially in order to verify the cSOLR calibrations functionality it was compared to Cascade Microtech's, Wincal based, SOLR and NIST's StatistiCAL calibration. Comparisons were made by comparing corrected DUT data of cSOLR to each algorithm.

It should be noted that in these two measurement cases the cSOLR algorithm is using a simplified RL load model because the CS-5 loads are well behaved at higher frequencies. These comparisons were only to verify that the basic USF SOLR algorithm was developed correctly. The following measurements were performed using the Wiltron 360B 65 GHz VNA and the Karl Suss semiautomatic probe station. Measurements and calibrations were made on a GGB CS-5 calibration substrate.

An SOLR calibration was performed using the WinCal software from Cascade. The calibration and measurements were made over a frequency range of 40MHz to 40 GHz using 201 points and an averaging factor of 64. The calibration standards were probed manually using the west and east probe configuration.

In order to obtain an unbiased calibration comparison, raw measured data was taken for the calibration standards directly after each calibration standard was measured for use Wincal's SOLR algorithm, thereby introducing only sweep repeatability into the potential difference error. During the thru measurements the switch terms are measured by manually setting up the VNA and taking the measurements.

The 200 um CPW line used as the calibration transmission standard is measured for a verification of the calibration, Figures 5.3-5.5. Also shown are the measurements of a 500um CPW line for a non calibration DUT, Figures 5.6-5.8. It can be seen from Figures 5.3-5.5 and 5.6-5.8 that the cSOLR calibration has a slightly better performance in the magnitude of the transmission coefficient S_{21} as well as a significant performance increase in the reflection coefficient S_{11}. The transmission phases measured with the two calibrations are almost identical to each other.

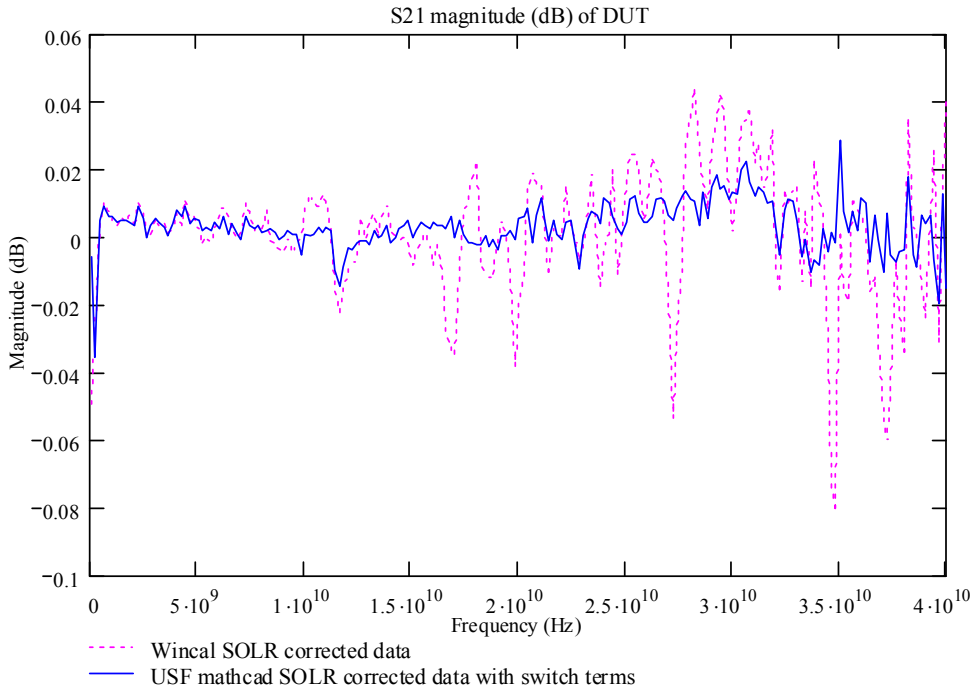

Figure 5.3 - Magnitude S_{21} (dB) of 200 um CPW Line On GGB CS-5 Substrate.

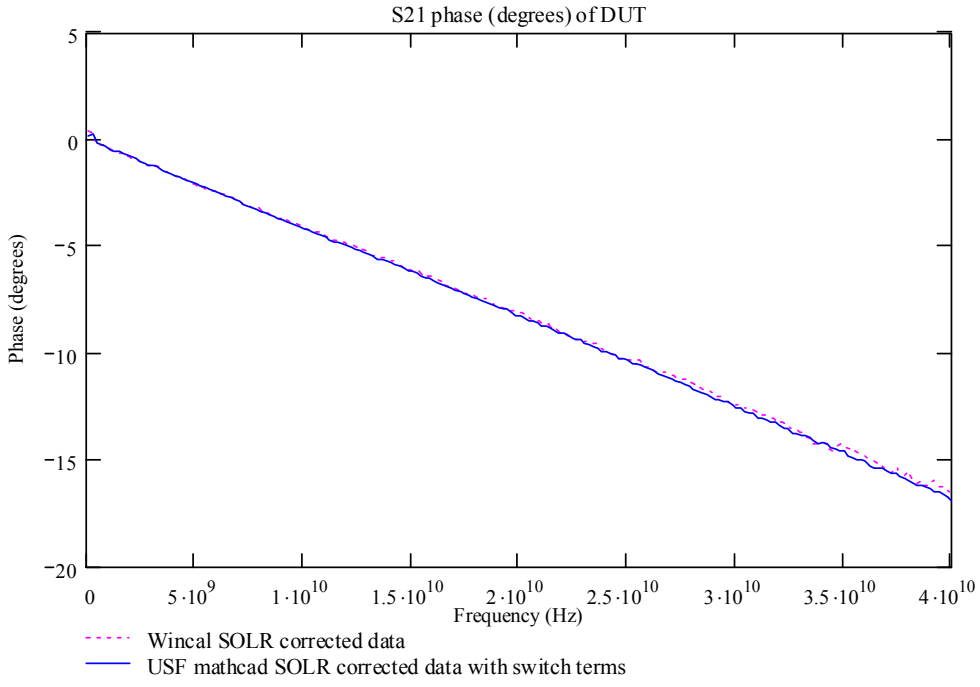

Figure 5.4 - Angle S_{21} (Degrees) of 200 um CPW Line On GGB CS-5 Substrate.

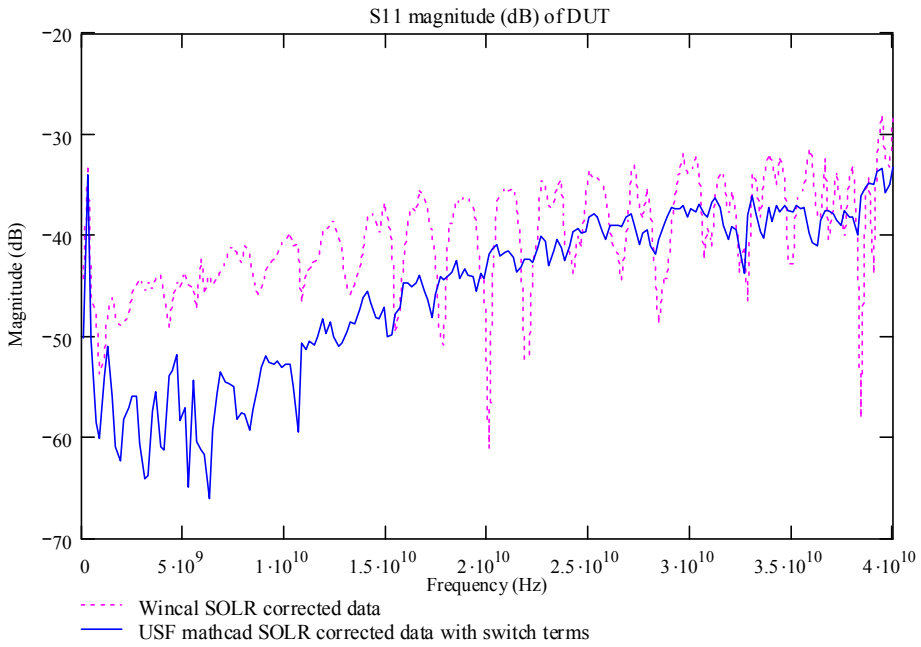

Figure 5.5 - Magnitude S_{11} (dB) of 200 um CPW Line On GGB CS-5 Substrate.

The reason for the performance difference between the two calibrations may be the result of the manner in which the switch term correction is handled. In Wincal's SOLR algorithm the switch ratios are measured as $\frac{a_{2m}}{a_{1m}}$ and $\frac{a'_{1m}}{a'_{2m}}$. These two ratios change based on the DUT S-parameters and must be measured with every raw DUT measurement unless they are converted to the $\frac{a_{2m}}{b_{2m}}$ and $\frac{a'_{1m}}{b'_{1m}}$ switch terms.

Wincal only measures the $\frac{a_{2m}}{a_{1m}}$ and $\frac{a'_{1m}}{a'_{2m}}$ ratios once during the thru measurement and because their algorithm is unpublished it is uncertain whether they make the conversion to the $\frac{a_{2m}}{b_{2m}}$ and $\frac{a'_{1m}}{b'_{1m}}$ ratios. Therefore Wincal's switch term

implementation may be what is introducing the added error into the measurements. The cSOLR algorithm uses the measurements of the switch reflection coefficients $\frac{a_{2m}}{b_{2m}}$ and $\frac{a'_{1m}}{b'_{1m}}$. These ratios, which need to be only measured once, only the switch repeatability error is introduced, which is generally very small as discussed in Chapter 3.

In Figure 5.6, the performance difference of the 500 um line S_{21} magnitude measurements, is not as pronounced; however, the Wincal measurement is slightly noisier.

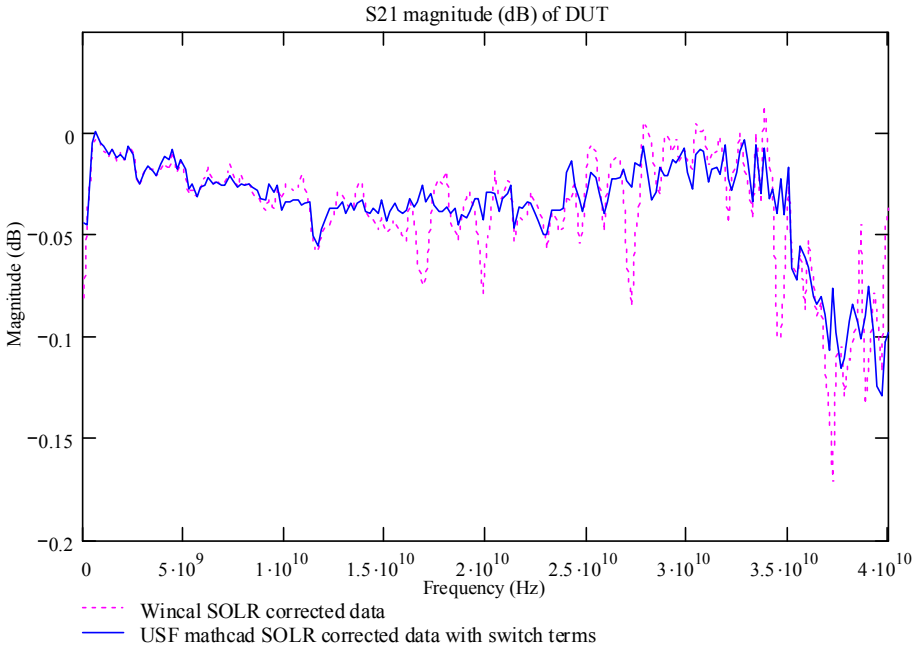

Figure 5.6 - Magnitude S_{21} (dB) of 500 um CPW Delay Line On GGB CS-5 Substrate.

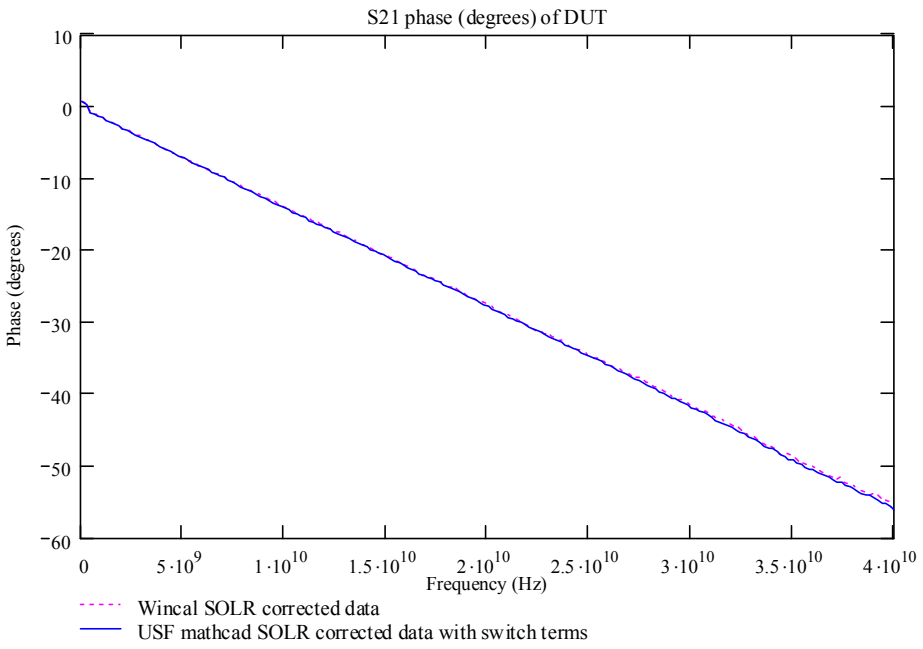

Figure 5.7 - Angle S_{21} (Degrees) of 500 um CPW Delay Line On GGB CS-5 Substrate.

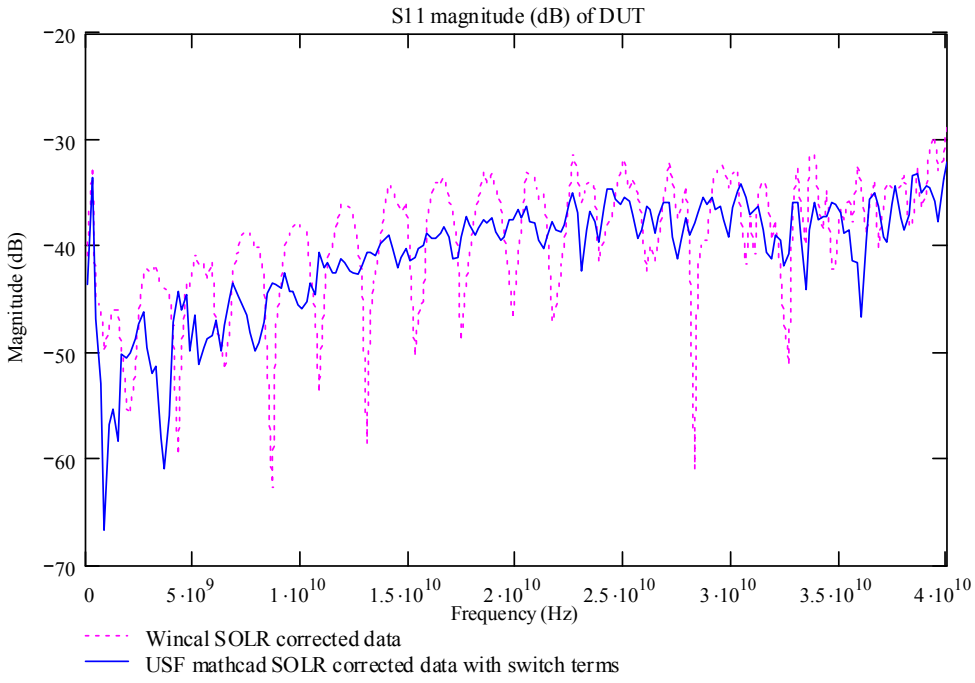

Figure 5.8 - Magnitude S_{11} (dB) of 500 um CPW Delay Line On GGB CS-5 Substrate.

The switch term correction when using an 8-term error model calibration is crucial. It can be seen from Figures 5.9-5.11 that by assuming the switch to be perfect, and not performing switch term correction on the measurements, severely degrades the measurement accuracy. It is obvious that the accuracy of the measurements is highly sensitive to the switch term characterization or the lack thereof. It is seen in Figure 5.10 that even the phase of the measurements is affected. Figure 5.11 shows almost a 25 dB difference in the S_{11} response between measurements with and without switch term correction.

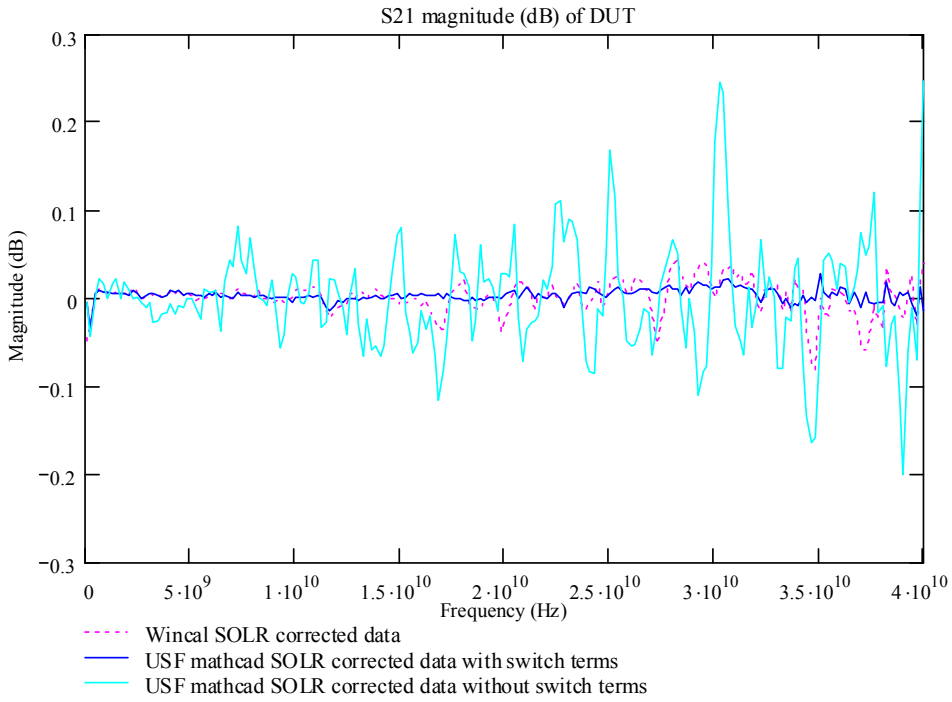

Figure 5.9 – Comparison of S_{21} Magnitude Data Corrected With and Without Switch Terms.

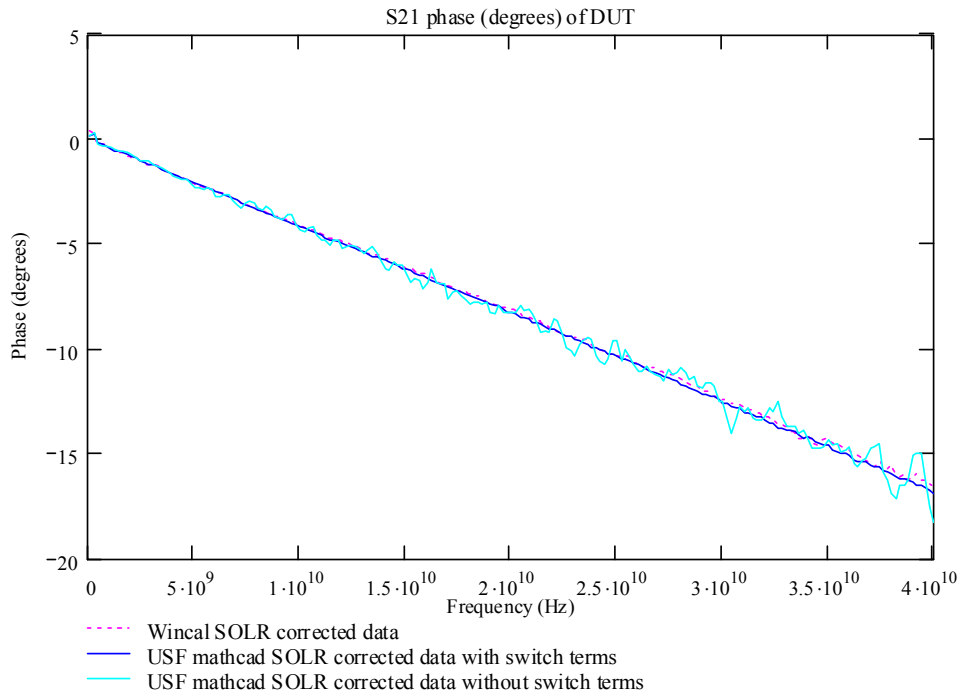

Figure 5.10 - Comparison of S_{21} Phase Data Corrected With and Without Switch Terms.

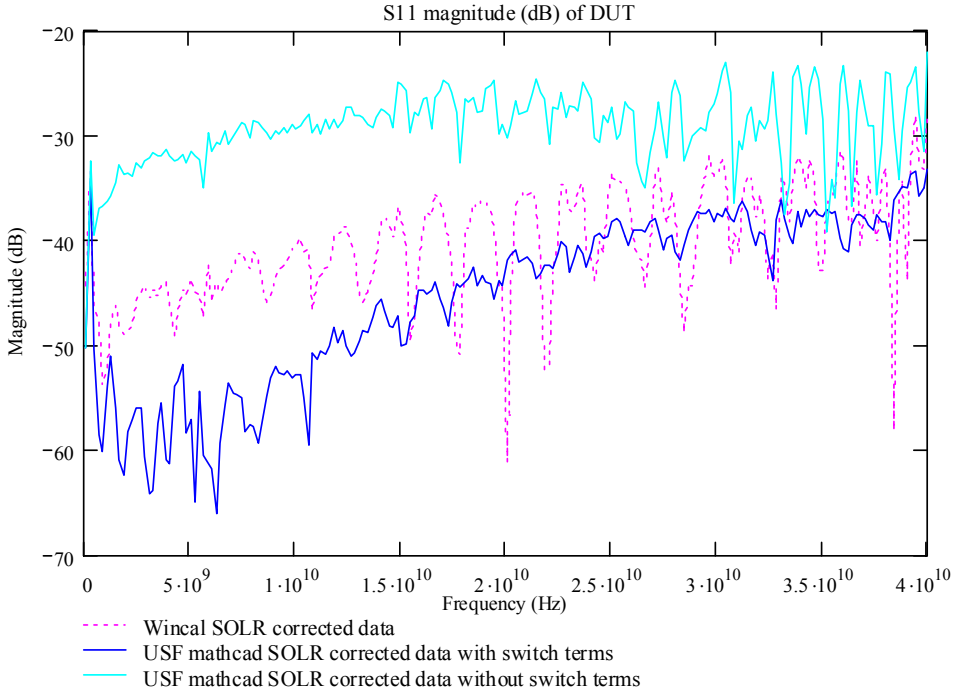

Figure 5.11 - Comparison of S_{11} Magnitude Data Corrected With and Without Switch Terms.

Once the calibration functionality had been verified it was necessary to benchmark its accuracy. This was done by using USF's Cal Compare software to compare cSOLR to multiline TRL, cSOLT and standard SOLR.

5.4.2 ITT GaAs Microstrip Substrate

The aforementioned ITT GaAs microstrip substrate will be used to evaluate the accuracy of cSOLR and demonstrate the additional performance provided by the complex load model. Measurements were made using the Anritsu 37xxxC series VNA from 40 MHz to 65 GHz. A TRL calibration is performed and then subsequent calibrations were performed for comparison to TRL followed by another TRL to establish a calibration repeatability level. These calibrations are compared to the initial multiline TRL calibration using the Cal Compare software developed by USF. It has been previously shown that an improved load model can improve an SOL based calibration's accuracy at high frequencies therefore only the upper error bound plot is presented rather than DUT data.

The high frequency accuracy of cSOLR can be seen in Figure 5.12 where it is compared to TRL along with standard SOLR and cSOLT. As with cSOLT the addition of a complex load model enables the usable frequency range of SOLR to be expanded. The cSOLR calibration has the high frequency accuracy of multiline TRL and the low frequency accuracy of SOLT as shown in Figure 5.13. The calibration is very similar to cSOLT in terms of accuracy; however, it does not require an ideal thru or a thru model.

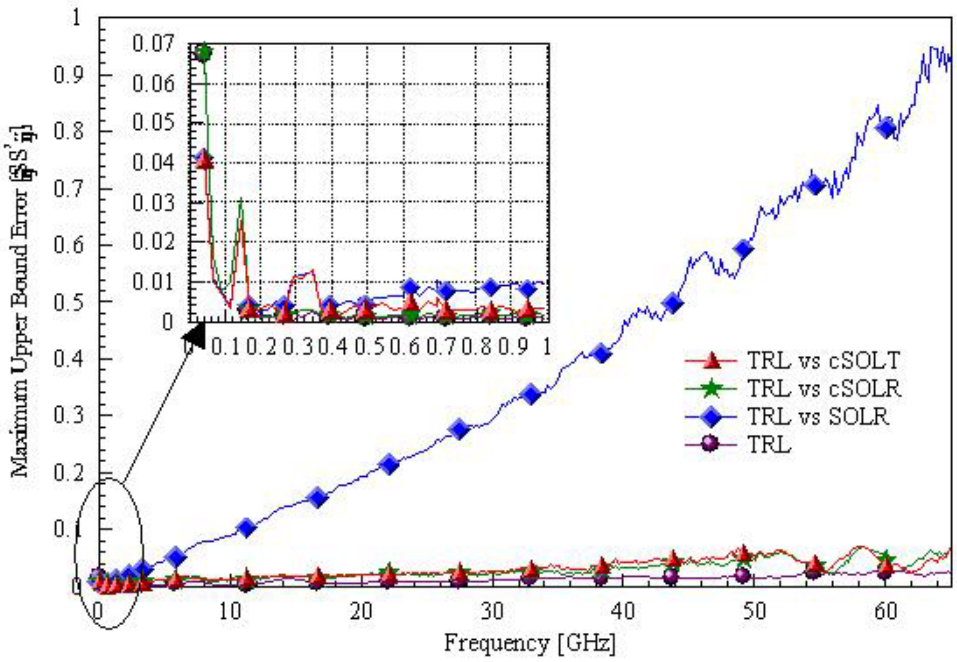

Figure 5.12 – Upper Error Bound of Calibrations Comparisons to Multiline TRL Performed on ITT GaAs Substrate.

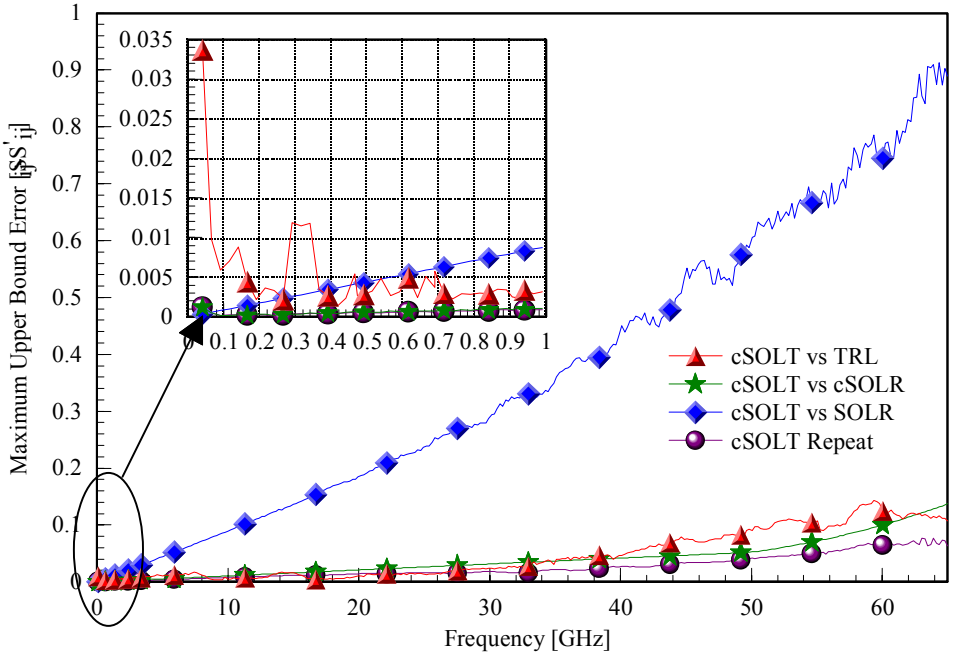

Figure 5.13 – Upper Error Bound of Calibrations Comparisons to cSOLT Performed on ITT GaAs Substrate.

5.5 cSOLR Using Non-Ideal Transmission Standards Characterization

Now that the accuracy of cSOLR has been established the calibration will be used to perform corrections in instances where an ideal thru is not available. The following measurements where made using the Anritsu 37xxxC series 65 GHz VNA. The measurements were made over a frequency range from 40 MHz to 26 GHz. It has been shown previously that calibrations such as TRL, LRM, and SOLT, which require a fully known transmission standard, breakdown when non-ideal standards are used [7]. Calibrations that require an ideal transmission standard when faced with a non-ideal standard will lure an inexperienced user into a false sense of security by showing the corrected thru measurement as an ideal thru standard which based on the reference planes of the previous standards is incorrect and is merely a testament to probe placement repeatability. This is documented in Basu's paper [7], and it shows quite clearly that other calibrations performed on non-ideal standards are incorrect.

It was concluded in [7] that other two port calibration methods were not able to perform an accurate calibration on orthogonal structures by performing in-line calibrations and then moving the probes to measure the orthogonal structures and then performing the reverse procedure. The only algorithm that provided consistent data whether calibrated in-line or orthogonally was SOLR. Therefore, comparisons of cSOLR to other calibrations will not be made where a non-ideal transmission standard is used as the calibration transmission standard.

5.5.1 GGB CS-5 Using Orthogonal Calibration Structures

The GGB CS-5 calibration substrate has orthogonal structures similar to those in Figure 5.2 with the exception that the CS-5's structures are CPW. These structures were probed using an orthogonal south/east probe setup on the Cascade Summit 12000 series semi-automatic probe station. The measurements were made on the Anritsu lightning VNA from 40 MHz to 40 GHz. The cSOLR calibration was used and reference planes of the measurements are at the probe tips. Measurements of similar structures were presented in [7]. The orthogonal CPW transmission line, with a 3.95ps electrical length, is measured as a test structure as shown in Figure 5.14 – 5.16.

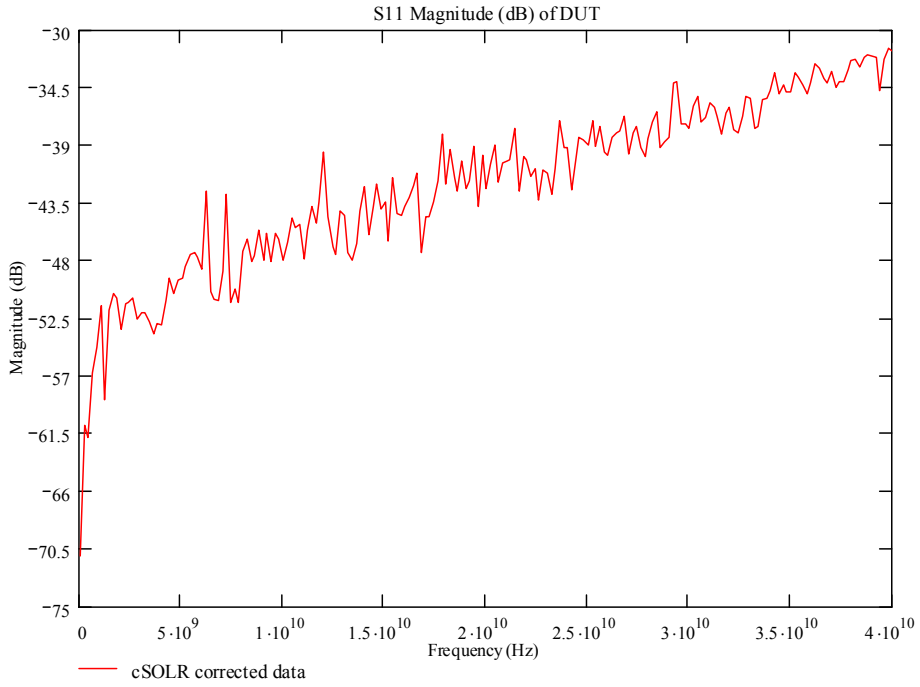

Figure 5.14 – S_{11} Magnitude of Orthogonal CPW Transmission Line.

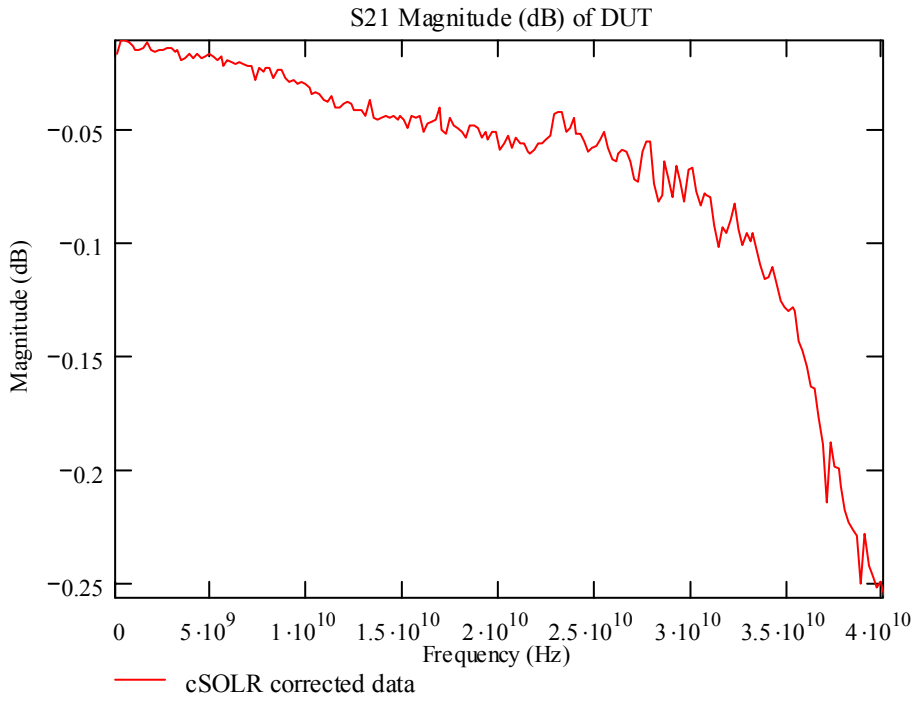

Figure 5.15 – S_{21} Magnitude of Orthogonal CPW Transmission Line.

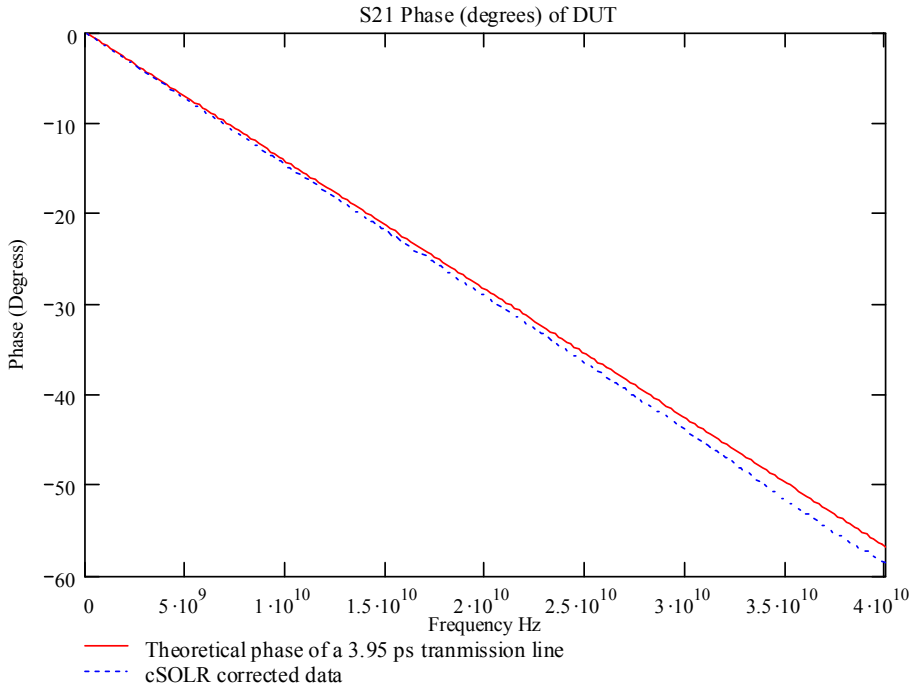

Figure 5.16 – S_{21} Phase of Orthogonal CPW Transmission Line.

5.5.2 GGB CS-2-150 Substrate Using a Loopback Transmission Structure

The GGB CS-2-150 substrate is an alumina calibration substrate designed for multiport GSGSG probes. One of the structures is a U shaped transmission standard which connects one signal line of the multiport probe to the other. This is a very non-ideal transmission standard. The 180 degree transmission line has an electrical length of 4.0ps. The measurements were made from 40 MHz to 26 GHz using the Anritsu 37xxx series VNA. It can be seen in Figure 5.17 that the match of the loopback transmission line is not as ideal as a straight CPW standard. This indicates that algorithms which assume a Z_o reference impedance line is used, such as TRL, will not be valid using this structure. However this is not a problem for cSOLR.

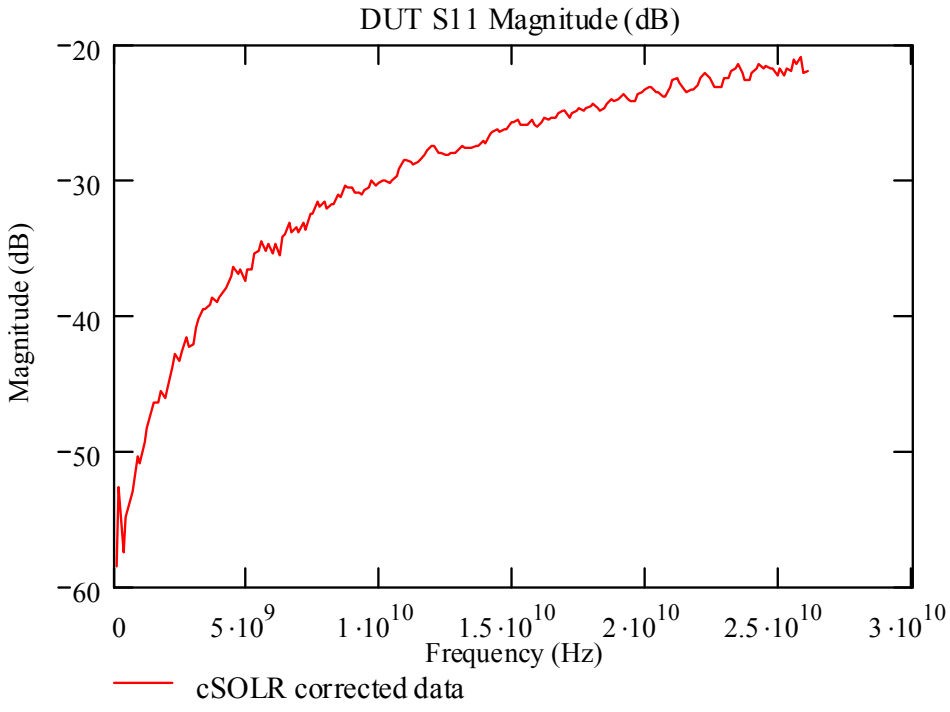

Figure 5.17 – S_{11} Magnitude (dB) of 4.0ps Loopback CPW Transmission Standard.

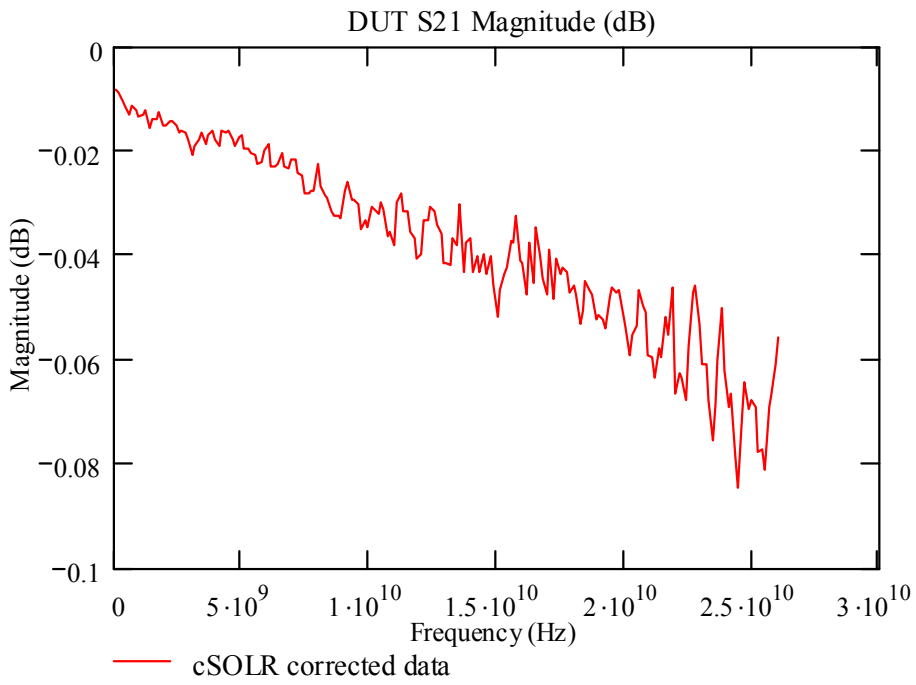

Figure 5.18 – S_{21} Magnitude (dB) of 4.0ps Loopback CPW Transmission Standard.

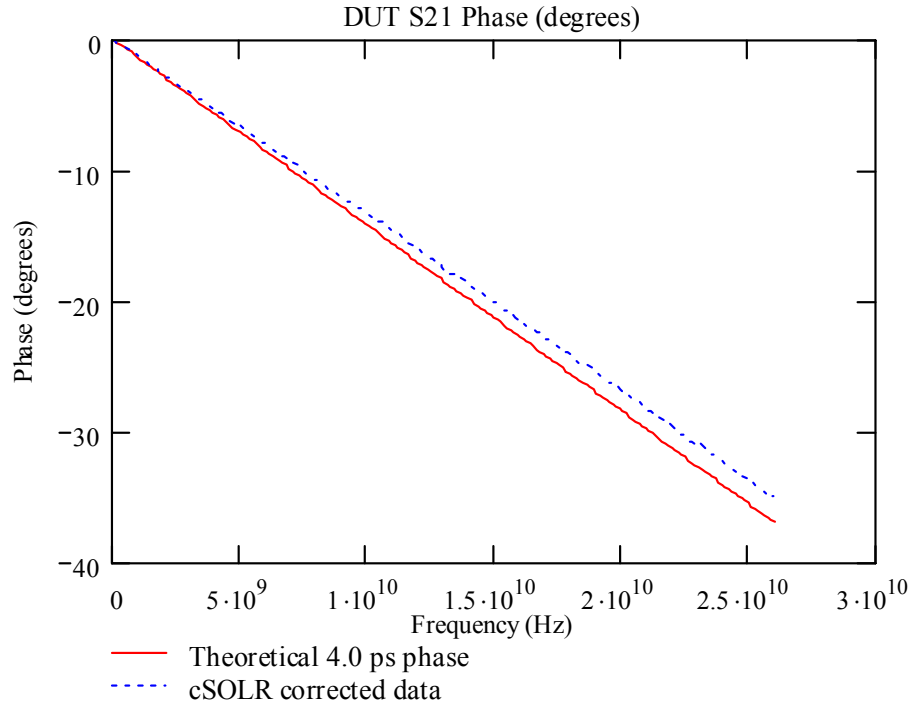

Figure 5.19 - S_{21} Phase (degrees) of 4.0ps Loopback CPW Transmission Standard.

5.6 Chapter Summary

In this chapter cSOLR methodology has been developed and verified as an accurate broadband calibration. The error calculation algorithm is the same as standard SOLR; however, the methodology for how to achieve a higher level of accuracy by using a more complex load model has been shown in this chapter. As with cSOLT the implementation of a complex load model enables SOLR to achieve greater accuracy at high frequencies similar to multiline TRL while still maintaining low frequency accuracy. It has also been shown that the switch terms are crucial to 8-term calibration and without them calibration accuracy suffers dramatically. The potential usefulness of cSOLR to multiport applications has been demonstrated and will be fully realized in Chapter 7.

CHAPTER 6

MULTIPORT AND DIFFERENTIAL MEASUREMENT SYSTEMS

6.1 Introduction

This chapter documents the methods and details of most common different multiport and differential measurement solutions, as well as the benefits and drawbacks of each. The solutions listed are from the simplest method of manually measuring multiport devices on a two port analyzer to multiport network analyzers that can measure S-parameters of the multiport devices with just one connection to the device ports. The main focus of this chapter is towards solutions that facilitate measurement of linear multiport and differential devices.

6.2 Multiport Measurement Solutions

The available multiport measurement solutions can be categorized into three groups 2xN methods, custom multiport analyzer and commercial multiport systems. The 2xN solutions use a two port network analyzer and make measurements of a 4-port two ports at a time. Commercial multiport VNAs are stand alone systems which have N reflectometers that allow all of the S-parameters to be measured for a given port incidence. Custom systems perform like true multiport VNAs, but, are usually using a

two port VNA to perform some function of the system. Most often contain forward couplers and may use port terminations that are separate from the VNA.

6.2.1 Manual Single-Ended Method Using Two-Port VNA

The simplest method to measure multiport devices is to measure the DUT as a with a two-port VNA [34,35]. Measurements of a multiport device are performed on a two-port VNA by terminating each of the unused ports with matched 50ohm loads. The method discussed is an extension of the single-ended method. The main advantage to this method is that it only requires a single two port calibration using any well known method. However, the disadvantage is that the DUT must be manually rotated and reconnected to all possible transmission paths; which can become very cumbersome as the number of ports increases. Also, the terminations are often imperfect and the error associated with them must be accounted for through renormalization, which will be discussed in Chapter 7.

6.2.2 Two-Port VNA with an External Switch Matrix

An alternative to the tedious single ended method suggested above is to use an external switch matrix that helps measure each port of the multiport device by multiplexing the ports of a two port VNA to N ports. An external power supply and computer controlled logic is required to coordinate the switching and measurements.

The NIST multiport solution [36] uses this concept for multiport measurements. An external switch matrix is used to multiplex the VNA's 2-port output to four ports. The switch matrix is controlled by a program ran from an external computer. NIST provides

TRL and LRM calibration routines for calibration and measurement of devices (SOLT calibration method is not supported in the NIST software). Figure 6.1 shows the switch matrix designed by NIST in the (2,1) switch configuration (port 2 of matrix connected to port 1 of VNA and port 1 of the matrix connected to port 2 of the VNA). The associated switch setting for Figure 6.1 are: S1=off S2=off S3=on S4=on S9=off S0=on.

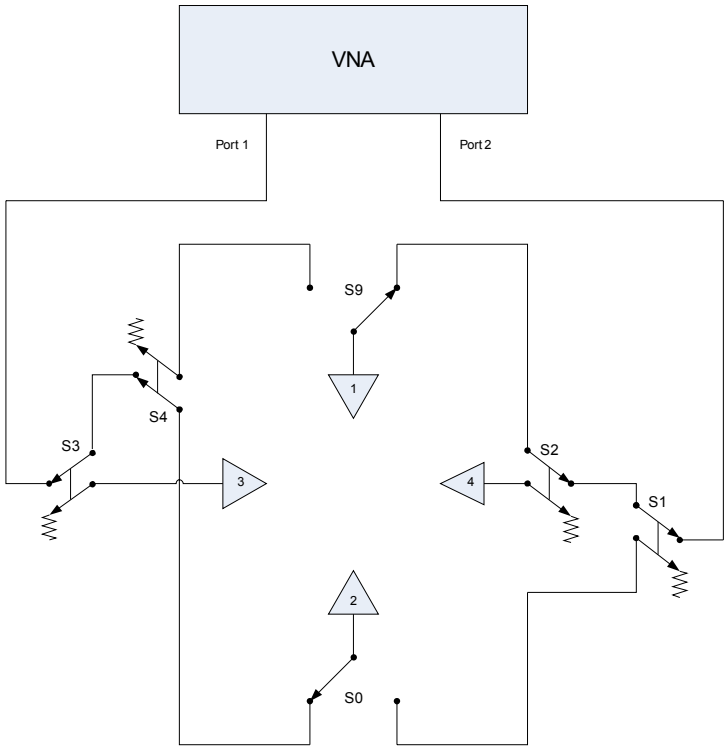

Figure 6.1 - NIST Designed 4-Port Switch Matrix in the (2,1) Switch Configuration [36].

It is also noted that this is one of the most cost effective solutions for a multiport measurement system. The main drawback to this type of system is that the four-port calibration routine can be more complicated and time consuming than when performed on a true multiport system. This will be discussed more in Chapter 7.

Anritsu's manufactures a basic multiport measurement system which consists of a 37347C 20 GHz Lightning Vector Network Analyzer (VNA), an SM5962 4-port test set, and the Multiport Navigator™ software. The SM5962 [37] test set is a 2x4 switch matrix that allows either port on the VNA to connect with any of the 4 ports on the test set. Multiport Navigator software provides full step-by-step direction, simplifying calibration, and speeding measurement throughput. Existing 20 GHz Lightning VNA's can be upgraded to add the new multiport test set and software.

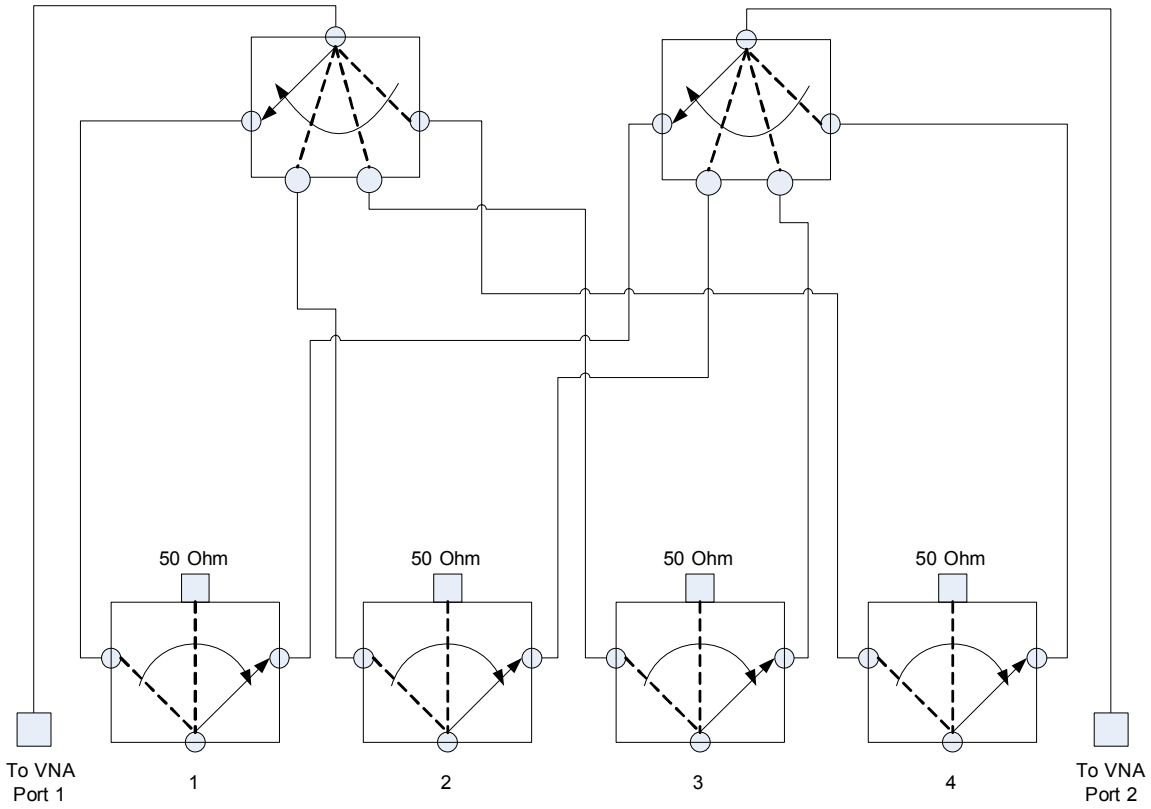

Figure 6.2 - SM5962 Test Set Block Diagram [37].

6.2.3 Single Sampler Solution (RF Switched)

In this method [38] the source signal is routed to the different DUT ports though a switching matrix for the different single-ended measurements of the device.

One channel of the microwave transition analyzer (MTA) is used as the reference signal and the second channel receives the incident and reflected signals sampled from the N 10dB bi-directional couplers that are routed via the source switching network. The MTA is used as a broadband sampling oscilloscope for the frequency range DC – 40GHz. This method can be easily extended to n-ports by adding more couplers and channels to the switching networks. The system can also be used to carry out time domain measurements by replacing the RF source with a pulse generator. The two main advantages of this method are that the system can measure both linear and non-linear multiport RF and digital circuits and since it can process the signals at a high speed, they can be used to characterize high speed digital interconnects. However, the frequency bandwidth of the measurement system is limited by the n bi-directional couplers and switches used.

6.2.4 Multi-Sampler Solution (IF Switched)

This method, developed by Ferrero and Kerwin [39], uses two different frequency converters to sample the ratio of single-ended voltage waves. One channel in each frequency converter is used as a reference channel for the NWA phase locking. An IF switch connects the appropriate signal pairs to the network analyzer IF converter for further down conversion and signal processing. By increasing the number of switches and four channel converters, the method can be extended to n-port measurements. Though

this method is highly accurate and fast, it is very expensive as it needs more than one sampler to measure the devices. Figure 6.3 was presented in [39] and copied here for ease of explanation.

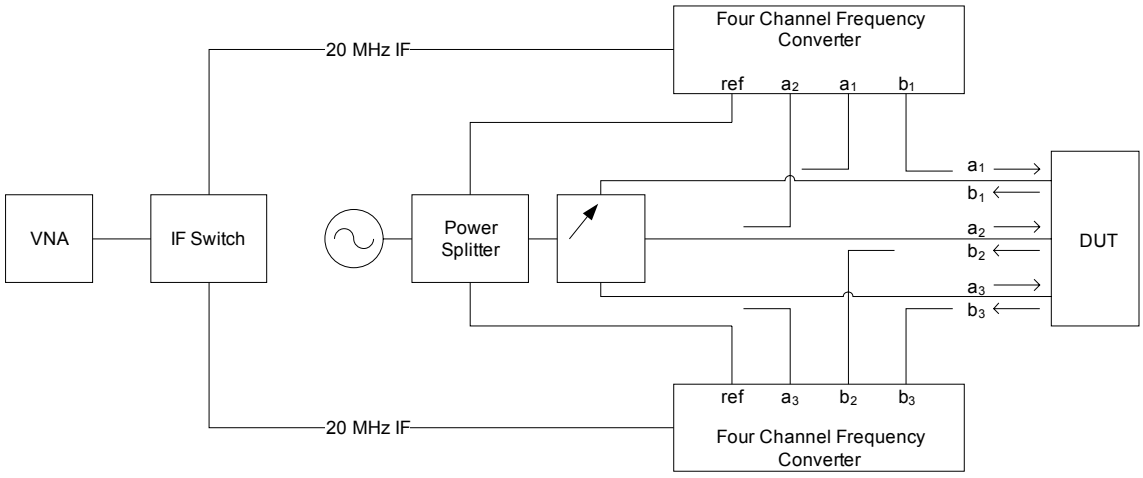

Figure 6.3 - Multi-Sampler (IF Switched) Solution for 3-Port Device Measurement from [39].

6.2.5 Commercial True Multiport Vector Network Analyzers

Agilent Technologies has different Physical Layer Test System [40] solutions that have frequency domain, time domain reflectometry and time domain transmission analysis. The software suite can operate with a Time Domain Reflectometer (TDR) or VNA. The systems can characterize single ended, differential mode, common mode and mode conversion behavior of the device under test. The accuracy of these systems are enhanced with low-noise RF source, phase locked receiver and systematic error correction. For a full four-port correction, a total of 72 error terms are measured during calibration. They can also re-normalize test data for non-50ohm devices.

For example, the N1957A (PLTS) consists of E8364B PNA series vector network analyzer, a test set, and software. The system can be used to characterize passive linear differential devices up to 50GHz. It has a high dynamic range, which makes the measurement of small mode-conversion signals possible. The only apparent drawback to the PLTS system is the relative high cost when compared to the other solutions.

The PNA series can be used for measurements between the range 300 KHz – 50 GHz. Agilent makes a 4-port PNA and a multiport test set (E5091A) [41] for multiport measurements up to 9 ports. The advantage of the four-port PNA system, Figure 6.5, is that multiple transmission measurements can be performed simultaneously, thereby reducing the number of sweeps required to measure all the S-parameters. The reference receiver at each port helps in optimizing high speed multiport measurements. Multiport measurements for devices up to nine ports can be done with the addition of a E5091A test-set.

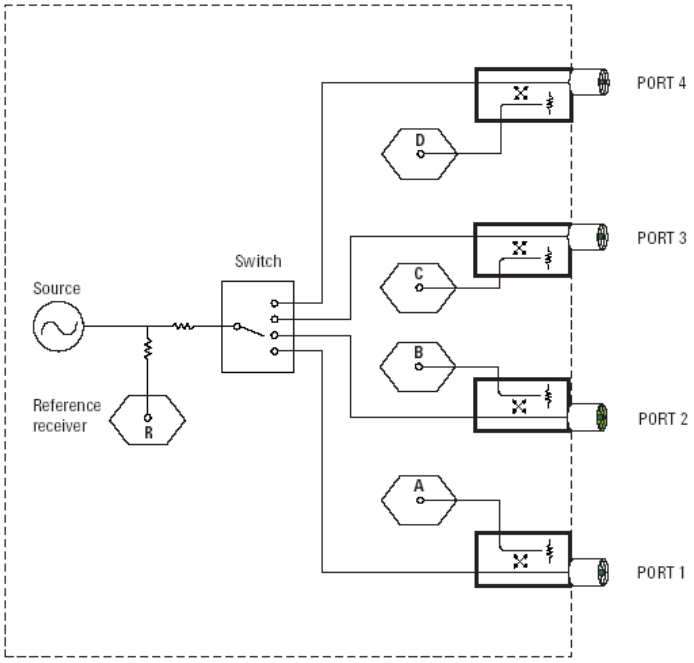

Figure 6.4 – Basic 4-Port PNA Block Diagram [41].

6.3 Differential Measurement Solutions

There is increasing interest in integrating wireless communications and electronic circuits to reduce cost, weight, power consumption to a single substrate. Thus the end product has multiple RF paths and terminal connections that are considered as one single device. When an analog circuit has to be integrated with a digital circuit which is the case in most of applications presently, it results in issues with continuity of ground plane. Since the digital circuits do not have an analog RF ground reference (as they use logic states to turn on and off), there are problems with plane discontinuities between the two circuits. Also, the digital circuits are also high speed circuits requiring that the analog circuits work at the same speed when combined. The solution was to give differential input/output for analog devices.

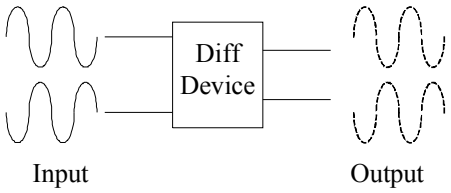

Figure 6.5 - General Diagram of a Differential Device.

Differential devices are devices that have two signal inputs that are ideally equal amplitude and 180° out of phase with each other. Each signal is referenced to its own compliment and thus forms a differential pair. Since an ideal differential device responds only to signals out of phase by 180°, these signals are called the differential mode signals. These differential devices ideally do not respond to or generate in-phase signals

called the common mode signals. This is why differential circuits are used for low noise applications.

Though in theory, differential devices do not produce amplify or produce any common mode signals, this is not the reality.

Differential devices like most things are not perfect, variations in device process and other factors cause some common mode signal to occur at the output. This is due to mode conversion that takes place in any differential device operation. Common to differential mode conversion occurs when a device converts some of its incoming differential signal to common mode on its output. This may be due to some variation in the transistors which make up the differential device causing a common signal to appear differential. This same problem can result in other forms of mode conversion including differential to common mode. In short, though the desired mode of operation is differential to differential mode, the mixed mode S-parameter matrix [42] of a differential device is defined by –

$$\begin{pmatrix} b_{d1} \\ b_{d2} \\ b_{c1} \\ b_{c2} \end{pmatrix} = \begin{pmatrix} S_{dd11} & S_{dd12} & S_{dc11} & S_{dc12} \\ S_{dd21} & S_{dd22} & S_{dc21} & S_{dc22} \\ S_{cd11} & S_{cd12} & S_{cc11} & S_{cc12} \\ S_{cd21} & S_{cd22} & S_{cc21} & S_{cc22} \end{pmatrix} \cdot \begin{pmatrix} a_{d1} \\ a_{d2} \\ a_{c1} \\ a_{c2} \end{pmatrix}$$

Where the S_{dd} parameters in the matrix represent the differential S-parameters, S_{cc} represent the common mode parameters, S_{dc} are the mode conversion that occurs when the device is excited with common mode signal and differential is measured and the S_{cd}

are the mode conversion parameters that occur when the device is excited with differential mode signal and common mode response is measured [43].

The S parameter notation used is defined by

$S_{abcd} = S_{(output\text{-}mode)\ (input\text{-}mode)\ (output\text{-}port)\ (input\text{-}port).}$

The advantages [44] to using differential input output are:

1. Since it is easy to control the shifts in logic states for a signal pair when compared to signal referenced to some other reference (i.e., ground), timing is well defined. With the use of differential techniques common mode noise issues are also reduced.
2. Using differential RF devices allows integration with high speed digital circuits. This is because the signals are referenced to its signal pair, not requiring RF ground to be the reference for the signals.
3. Differential signals have greater signal to noise ratios since the signals respond to the difference between the signal pair. This implies that a differential device has double the dynamic range with less noise with the same voltage given to a single ended device.
4. Differential circuits are less sensitive to ground interference, as the input signal is referenced to its own compliment. Also, since the differential device does not respond to the in-phase signals and the noise introduced in the input (which appears equally on the both inputs) are cancelled at the output; it results in less noise and EMI at the output.

Since the differential device requires two input signals with a phase difference of 180°, it becomes necessary that a network analyzer generating such an RF output is required. Due to the fact that the phase stability at 0 and 180° cannot be maintained to high precision, a pure broadband differential network analyzer is not yet available. Hence different methods that help measure S-parameters of differential devices have been suggested.

6.3.1 Balun Method

The traditional method of measuring a differential device was to combine each balanced pair to a single port using baluns. The baluns [34] are used to convert the single ended signals from the VNA to differential signals to the DUT. It also transforms the impedance of the differential device to the impedance of the analyzer. The method provides some degree of accuracy about the differential characteristics but no information about the common mode performance. The accuracy is also highly dependent on the calibration reference plane and characteristics of the balun.

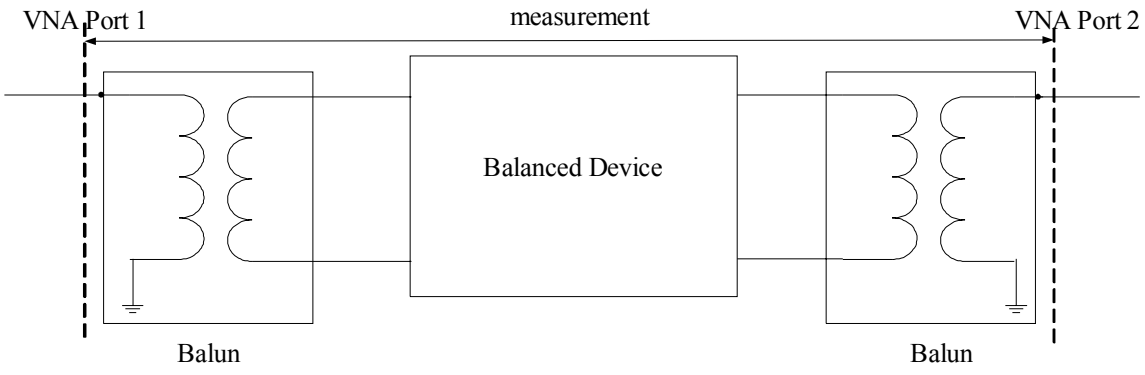

Figure 6.6 - Measurement Setup With Baluns from [34].

Additional drawbacks of this type of differential measurement are:

1. The balun has finite return loss, insertion loss, amplitude and phase balance that can lead to measurement errors. Furthermore, the accuracy of the method is highly dependent on the calibration and location of the reference plane.
2. Baluns convert the single ended signal from the network analyzer to differential signal for the device. Since there were no calibration standards for the differential mode measurements, it becomes necessary that the reference plane is always at the input of the balun (Cascade Microtech has differential calibration standards that addresses the calibration issues).
3. There is no way to measure mode conversion from differential to common-mode. Only the differential quadrant of the mixed-mode S-parameter matrix can be measured, since baluns exhibit high isolation to common mode signals.
4. One of the most limiting characteristics of baluns is that they have a narrow bandwidth. Therefore, another method must be used if the device is to be measured over a wide frequency range.

6.3.2 Mixed Mode S-parameters from Single-Ended Data

Bockelman and Eisenstad developed a method [42] to convert single ended data to mixed mode using mathematical algorithms (NIST method uses this algorithm as one its methods to calculate the mixed mode S-parameters). The equations relate the nodal waves from a standard two port vector network analyzer and the associated common and differential waves that result in the mixed mode S-parameters. This method thus accurately predicts the differential behavior of the device. It is a simple and quick method

of calculating the mode conversion parameters. They also suggested that a pure mode network analyzer (PMVNA) has the best accuracy when measuring a differential device and implemented a system based on 8510C-modular network analyzer system.

6.3.3 Pure Mode VNAs

The system employs two 8517A test sets (with minor control hardware modifications) for simultaneous operation. The RF inputs to the test sets are obtained from the 85651 RF source routed via a 0°/180° 3dB hybrid coupler. An RF switch selects the phase difference inputs to the test sets. The measurement frequency range is limited by the hybrid coupler between 1GHz – 12GHz though it has been extended from 0.1GHz to 20GHz by the authors [45] with calibration. The output ports of the two test-sets 1 and 2 forms the mixed mode port 1 and ports 3 and 4 form the mixed mode port 2 for the differential measurement system. With the nodal waves measured for the 0 and 180° positions, the mixed-mode S-parameters are calculated.

1. It requires two RF test sets to provide a differential input to the device. Hence the system can become more complex and expensive.
2. With the use of a 3dB coupler, the system is limited in terms of bandwidth of measurements.
3. It is important that the any imbalance in the PMVNA with respect to the coupler and RF signal paths is accurately calibrated. It could otherwise trigger some unintended signal or mode generation.

4. It is important the phase stability is maintained well with less than one degree deviation at the calibration plane.

6.3.4 Pure Mode VNA with Two Source Signals

This method suggested by Joel Dunsmore (Agilent Technologies) [46] overcomes the difficulties of creating differential or common mode drive signals with signal-source architecture that can provide arbitrary amplitude and phase control. It utilizes three electronic signal generators (ESG) (Agilent E4438B) which has arbitrary amplitude and phase control between the source signal outputs.

Two of the ESG's are modified to provide an input of the signal before the vector modulator, bypassing the internal source. The ESG (without any modifications) provides a part of the signal to the rear panel as a coherent carrier. This is given as an input to one of the ESG that is modified. This input is phase controlled and shifted in phase by 180° which is then sent to the third ESG. The output of this setup is coherent vector signal of the same amplitude with a phase difference of 180°. To measure a differential device, a VNA is used in tuned receiver mode. This method provides is accurate in terms of providing the differential input since the ESG can provide less than 0.1° phase control. Since this has a true differential input, the non-linear characteristics of active differential devices can be measured.

6.3.5 Multimode Technique

A more resent technique in differential device measurement involves the use of multimode structures [47]. A single-ended to multimode transitiona are used to convert a

single-ended excitation into it even and odd mode components.. Results up to 40 GHz are shown in [48] using a TRL calibration method that incorporates these multimode structures. The idea behind this is to simultaneously generate a common and differential excitation by transitioning a single ended signal to a multimode signal which can then be separated by applying a specific algorithm to the measured signals. This will allow the measurement of mode conversion and gain similar to a pure mode VNA. The advantage of this technique over pure mode analysis it that single ended excitation can be used, which reduces system complexity and cost because it only requires a standard multiport VNA. However, the method is still developed and further research will increase the calibration algorithm's robustness.

6.4 Multiport Probing Environments

When multiport measurements are made on-wafer the probing setups can become very complex. The most basic setups involve N ground-signal-ground (GSG) probes to connect the N ports. A four-port setup is shown in Figure 6.8. The probes are positioned at right angles to one another, because of this it is often referred to as a, (north south west east) setup. This method provides good performance in terms of isolation but, can be bulky in terms of probe positioners and has a more difficult cable connection solution.

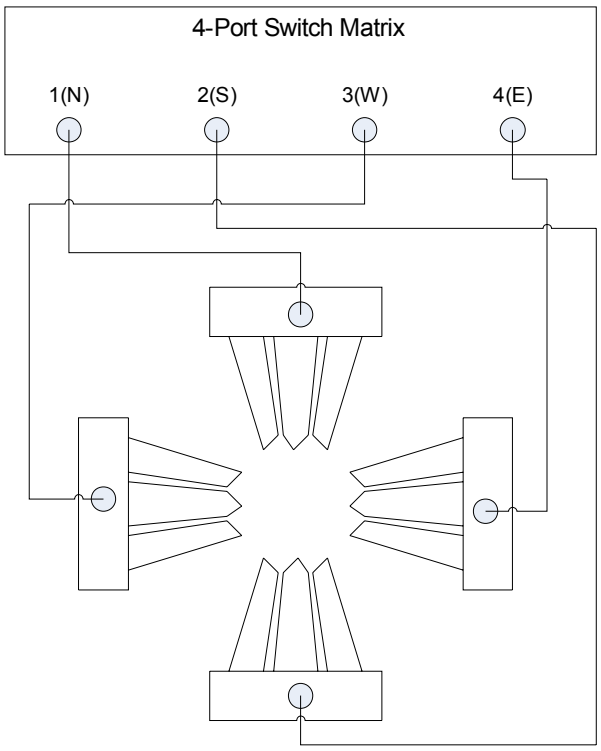

Figure 6.7 – North, South, West and East 4-Port On-Wafer Probe Setup.

With the use of more differential on-wafer devices the probing solutions have expanded to accommodate devices with dual signal inputs and outputs by making multi-signal probes. The first of these, shown in Figure 6.9, are the ground-signal-ground-signal-ground or (GSGSG) probes. These probes are essentially two GSG probes placed side by side and allow the probing of balanced signal lines which can be located in close proximity of each other. The main advantage of these probes which is also its main disadvantage is the compact nature of the probes which causes degradation in isolation. This is a small tradeoff for the ability to probe differential inputs and outputs.

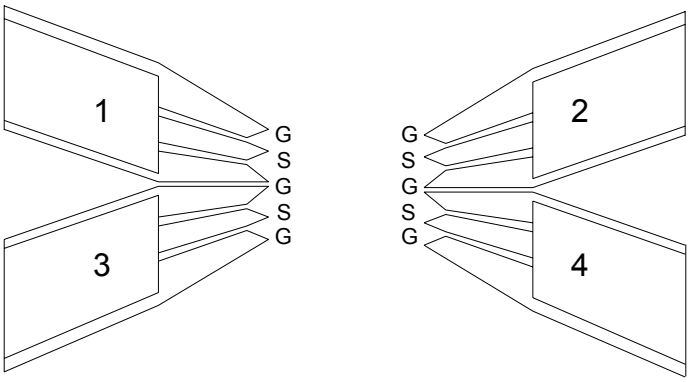

Figure 6.8 – GSGSG Multiport Probe Setup.

The last on-wafer multiport probe setup is also a multi-signal probe application similar to the GSGSG probes, except that is has to common center ground connection. Ground-signal-signal-ground probes, shown in Figure 6.10, are used in differential applications and like GSGSG have the advantage of compactness which saves on-wafer real-estate and allows a less complex probe positioner and cabling setup. However, these probes have the worse isolation of all the multiport probes.

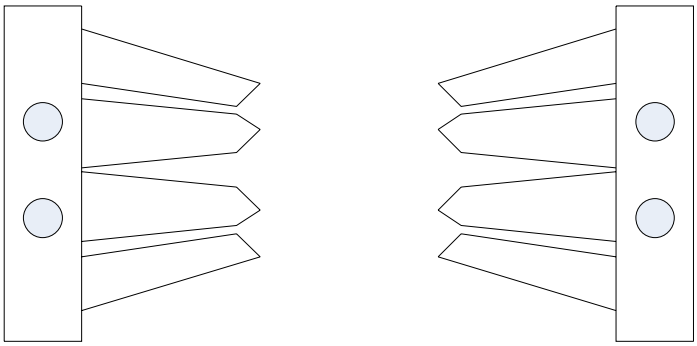

Figure 6.9 – GSSG Multiport Probe Setup.

All of these on-wafer multiport solutions have the potential for needing a non-ideal transmission connection between certain port combinations during calibration. For this reason a multiport calibration is needed which can handle these standards, which will be shown in Chapter 7.

6.5 Chapter Summary

Several methods that can be used to measure differential S-parameters of multiport devices were discussed. The advantages and drawbacks of the systems were also discussed. The manual measurement of a multiport device on a two port VNA is not practical when N is greater than 3 or when multiple DUTs must be measured. The commercial solutions for multiport device measurement are very expensive and have a limited upper frequency range. The custom multiport hybrid VNAs provide are lower cost than the commercial solutions but, are very complex and still fairly expensive when designing for broadband measurements. The multiport switch matrix solutions are fairly simple and inexpensive and allow a good operating frequency range. However, there are some issues that limit the calibration flexibility of these systems. These issues will be discussed in Chapter 7.

CHAPTER 7

MULTIPORT CALIBRATION

7.1 Introduction

Multiport measurements and calibrations can be very difficult especially if they are made on wafer where probe setups do not always allow an ideal transmission connection. Such is the case with multi-signal probes. The cSOLR algorithm which was developed in the previous chapter is ideal in this situation as well as other multiport measurement scenarios. This chapter will detail the adaptation of cSOLR from a two-port calibration routine to a multiport. It will be shown that the method used for the multiport calibration can be done with any two port calibration. The developmental portion of the chapter is divided into two sections. First, multiport calibration models and procedures for use with an ideal 4-port VNA will be discussed. Then the models and procedures for performing a multiport calibration with a two port VNA will be developed. The details for the 4-port implementation of the cSOLR algorithm with the USF 4-port switch matrix will be given after the initial more general development.

7.2 Calibrations Using True Multiport Network Analyzers

In a true four-port VNA, like that discussed in Chapter 6, there are four reflectometers each with two samplers. Many times a single switched RF source is used to excite one of the ports and measurement data is collected from all of the samplers. By collecting data from all samplers any switch error can be effectively removed as was shown in Chapter 3. By removing the switch error the error box model can be used. In the 8-term error model there are two error boxes E_1 and E_2 which represent the errors of the ports 1 and 2.

7.2.1 True Multiport VNA Error Models

With the addition of extra ports, as shown in Figure 7.1, there are now N error boxes; one for each port. The diagram of the error box model is shown in Figure 7.1.

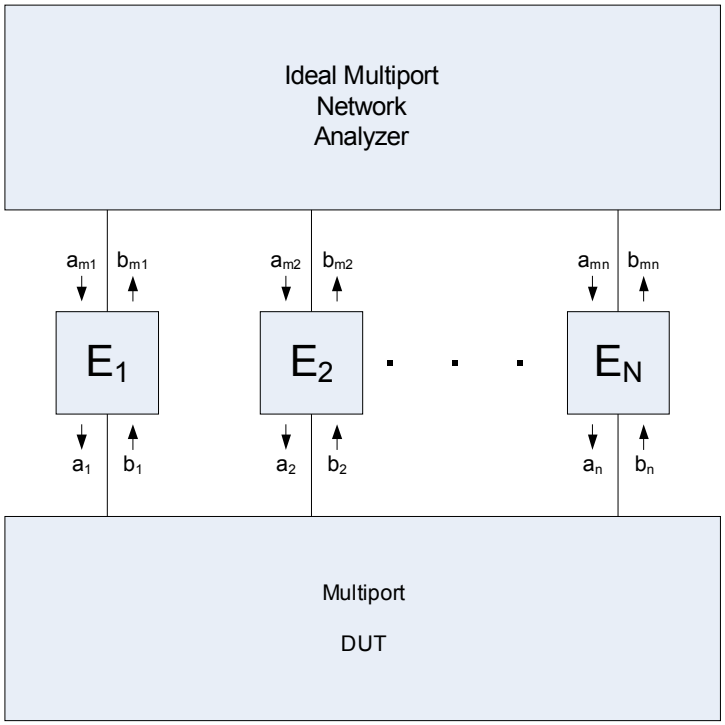

Figure 7.1 – Block Diagram of Ideal Multiport Network Analyzer Error Model.

The S-parameter definition for a multiport network analyzer remains the same. Excitation occurs only on one port except now there is more than one port that must be terminated in a matched condition. The four error boxes can be described as follows:

$E_n = \begin{bmatrix} e_n^{00} & e_n^{01} \\ e_n^{10} & e_n^{11} \end{bmatrix}$. Where, n = 1,2…N and N is the number of ports.

The following relationships of the error coefficients and the multiport S-parameters have been detailed in [39]. These N error boxes can be extended to a multiport situation by letting:

$$E^{00} = \begin{bmatrix} e_1^{00} & 0 & 0 & 0 \\ 0 & e_2^{00} & 0 & 0 \\ 0 & 0 & \ddots & 0 \\ 0 & 0 & 0 & e_n^{00} \end{bmatrix} \qquad E^{01} = \begin{bmatrix} e_1^{01} & 0 & 0 & 0 \\ 0 & e_2^{01} & 0 & 0 \\ 0 & 0 & \ddots & 0 \\ 0 & 0 & 0 & e_n^{01} \end{bmatrix}$$

$$E^{10} = \begin{bmatrix} e_1^{10} & 0 & 0 & 0 \\ 0 & e_2^{10} & 0 & 0 \\ 0 & 0 & \ddots & 0 \\ 0 & 0 & 0 & e_n^{10} \end{bmatrix} \qquad E^{11} = \begin{bmatrix} e_1^{11} & 0 & 0 & 0 \\ 0 & e_2^{11} & 0 & 0 \\ 0 & 0 & \ddots & 0 \\ 0 & 0 & 0 & e_n^{11} \end{bmatrix}$$

Then the raw measured multiport S-parameters [$\mathbf{S_m}$] are related to the corrected multiport S-parameters [S] by the following equations [39]

$\boldsymbol{S_m} = E^{00} + E^{01}\left[I - S\,E^{11}\right]^{-1} S\,E^{10}$, where I is an N dimensional identity matrix.

Note the representation of **Sm** indicates that it has been switch corrected and therefore the switch can be assumed to be perfect.

By letting $A = \left(E^{01}\right)^{-1}\left[\boldsymbol{S_m} - E^{00}\right]\left(E^{10}\right)^{-1}$

$$A = \begin{bmatrix} \frac{\left(\boldsymbol{S}_{m11} - e_1^{00}\right)}{t_{11}} & \frac{\boldsymbol{S}_{m12}}{t_{12}} & \cdots & \frac{\boldsymbol{S}_{m1n}}{t_{1n}} \\ \frac{\boldsymbol{S}_{m21}}{t_{21}} & \frac{\left(\boldsymbol{S}_{m22} - e_2^{00}\right)}{t_{22}} & \cdots & \frac{\boldsymbol{S}_{m2n}}{t_{2n}} \\ \vdots & \vdots & \ddots & \vdots \\ \frac{\boldsymbol{S}_{mn1}}{t_{n1}} & \frac{\boldsymbol{S}_{mn2}}{t_{n2}} & \cdots & \frac{\left(\boldsymbol{S}_{mnn} - e_n^{00}\right)}{t_{nn}} \end{bmatrix} \quad \text{where, } t_{ij} = e_i^{01} e_j^{10}$$

Then the corrected multiport S-parameters are equal to,

$$S = A\left(I + E^{11} A\right)^{-1}.$$

It is seen from the equations above that the needed relationships are similar to those calculated for the 8-term two-port case. It is shown in [49] that with this generalized method any standard calibration method available may be used to characterize these terms.

7.2.2 Calculation of the Transmission Terms on a True Multiport System

For an N port device there are $\frac{N(N-1)}{2}$ possible transmission paths and it is shown that N-1 two-port transmission standards are required for a calibration providing that all ports are connected at least once in a transmission measurement [39, 49]. Therefore it is not necessary to measure all the possible thru standards in order to calculate the transmission terms. The (N-1)*2 transmission terms are found through measurement of the two port transmission standards using any desired two-port calibration method which will allow you to calculate these terms and the remaining terms can be calculated by the redundant measurements through the following relationship

$$t_{ij} = \frac{t_{in} t_{nj}}{t_{nn}} \qquad \text{for, any n} \neq \text{i} \neq \text{j}.$$

For example, if an SOLR or TRL calibration was performed between ports (1,2) and (1,4) then t_{11}, t_{22}, t_{44}, t_{21}, t_{12}, t_{14} and t_{41} are directly known from the calibrations, and t_{24} and t_{42} can be found by

$$t_{24} = \frac{t_{21}t_{14}}{t_{11}} = \frac{e_2^{01}e_1^{10}e_1^{01}e_4^{10}}{e_1^{01}e_1^{10}} = e_2^{01}e_4^{10} \qquad t_{42} = \frac{t_{41}t_{12}}{t_{11}} = \frac{e_4^{01}e_1^{10}e_1^{01}e_2^{10}}{e_1^{01}e_1^{10}} = e_4^{01}e_2^{10}.$$

This is important because using this potentially allows the use of equal foot print calibration standards which can be performed with a semi-automatic probing system.

7.3 Multiport Calibrations with a Two-Port Network Analyzer

The method presented in 7.2 is only valid for actual multiport systems where a single error box is dedicated to a single port. It has been shown in Chapter 6 that a multiport measurement can be carried out using a two port network analyzer and terminating the auxiliary N-2 ports with matched terminations [35]. It was further shown that, in order to expedite the process, a 2xN port multiplexing switch matrix could be used to automatically perform this task.

This section will develop the calibration and error correction of a multiport system using this method in general and give examples for the equation in the four-port case. A diagram of a multiplexed two port analyzer with a 4-port switch matrix, or a 2x4 network analyzer, is shown in Figure 7.2.

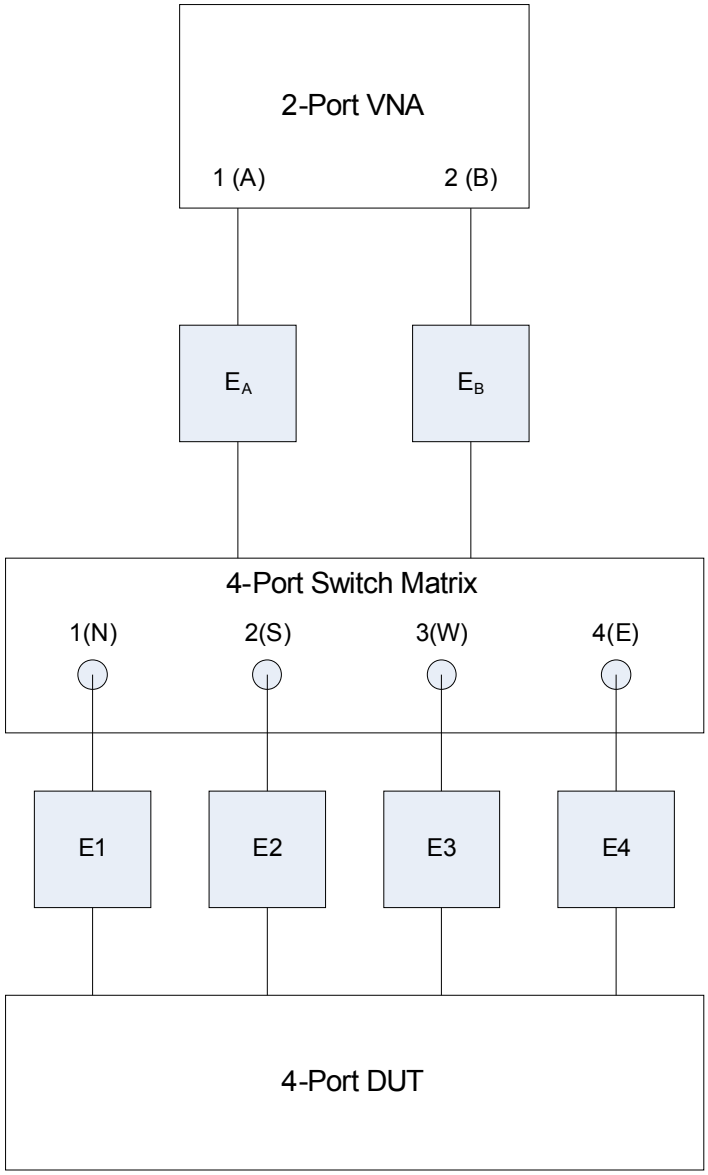

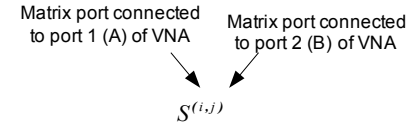

$$S^{(i,j)} = \begin{bmatrix} S_{11}^{(i,j)} & S_{12}^{(i,j)} \\ S_{21}^{(i,j)} & S_{22}^{(i,j)} \end{bmatrix}$$

Figure 7.2 – Block Diagram of 2x4 4-Port Measurement System and Conceptual Error Model.

7.3.1 Two-Port Measurement Paths of a Multiport Switch Matrix

When measuring a multiport device with a two-port network analyzer a series of $\frac{N(N-1)}{2}$ two port measurements are made. The internal single-pole double-throw (SPDT) terminated switches of the matrix are controlled via the switch settings to give the $\frac{N(N-1)}{2}$ two-port measurement combinations. For example the four-port system shown in Figure 7.2 has six possible switch settings to give the $\frac{4(4-1)}{2}$, or six, possible two-port combinations.

The (N)orth (S)outh (W)est and (E)ast port designation is presented in Figure 7.2 in order to conform with NIST's port naming convention in their multiport software NISTcal [45]. The 6 measurement combinations that are used by the USF switch matrix are: (1,2) NS, (3,4) WE, (1,4) NE, (3,2) WS, (3,1) WN and (2,4) SE.

For measurements paths (i,j), i indicates the matrix port connected to port A of the VNA and j is the matrix port connected to analyzer port B

For example, the switch setting (3,1) is port 3 of the switch matrix connected to port A of the VNA and port 1 of the matrix connected to VNA port B. The two port S-parameters measured by the VNA under each unique setting will be designated as

$$S^{(i,j)} = \begin{bmatrix} S_{11}^{(i,j)} & S_{12}^{(i,j)} \\ S_{21}^{(i,j)} & S_{22}^{(i,j)} \end{bmatrix}.$$

When measuring a four-port system with a two port analyzer it stands to reason that the port 1 error box of the switch matrix when connected to port 1(A) of the analyzer as in

the (1,2) measurement is different than when port 1 of the switch matrix connected to port 2(B) of the analyzer as in the (3,1) measurement. Therefore separate error boxes must be used to identify these differences.

7.3.2 2xN Port Error Box Conventions

As shown in Figure 7.2 the error box of each port can be conceptually thought of as a cascaded error box of the errors between the VNA samplers and the external switch matrix and the errors associated with the switch matrix to the DUT reference planes. The naming convention that will be used to reflect this dependency on analyzer port connection is

$$E_n^k = \begin{bmatrix} e_{nk}^{00} & e_{nk}^{01} \\ e_{nk}^{10} & e_{nk}^{11} \end{bmatrix},$$

where, n designates the switch matrix port that is connected to analyzer port k.

Notice that the error box model is the same as it was for the two port case because measurements are still only being made two ports at a time. In the case of the four-port, by characterizing two of the switch matrix port's reflectometer terms on port A and B of the VNA, it will allow correction to be applied to all possible measurement paths; as shown in Figure 7.3. Figure 7.3 is a four-port example where ports (1 and 2) and ports (3 and 4) have been characterized using the (1,2) and (3,4) measurement settings respectively. Consequently, the error boxes for ports 1 and 3 have been characterized on port A of the VNA (E_1^A, E_3^A). The error boxes for ports 2 and 4 have been characterized on VNA port B (E_2^B, E_4^B).

Resulting problems occur when measuring the (3,1) and (2,4) paths because each pair of ports have been characterized on the same VNA port.

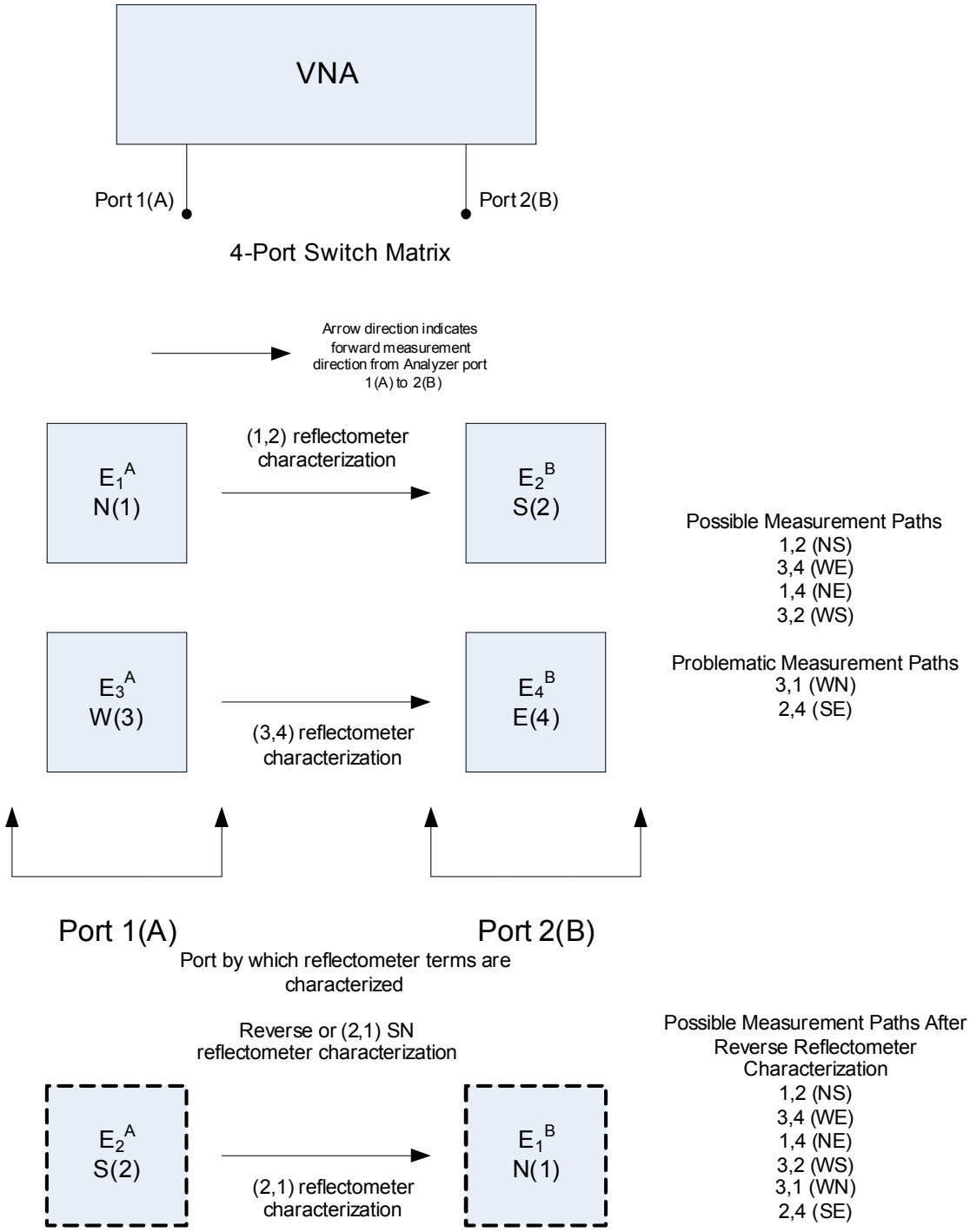

Figure 7.3 – Reverse Reflectometer Characterization.

The solution to this problem is to additionally characterize the error boxes for ports 1 and 2 when connected to the opposite VNA ports. In other words, characterize the port 1 and 2 errors boxes for the (2,1) measurement path (E_2^A, E_1^B). The (2,1) or SN switch setting is present specifically for this purpose, as it is not a device characterization measurement and only needs to be measured during calibration. Now that the six needed error boxes have been calculated all six possible measurement paths may be corrected. This has a profound effect when attempting to calculate the transmission tracking terms using the redundancy equations.

7.3.3 Calculating Transmission Coefficients for a 2xN System

Calculating the transmission tracking terms for a 2xN system is not a trivial solution. The well known measurement relationship for calculating the terms using redundant measurements which was shown in Section 7.2.1 will not work for a 2xN system because the N port's reflectometers are not independent. Therefore, the redundancies available for calculating the transmission tracking terms are reduced and the classic redundancy equations shown in Section 7.2.2 will not work.

Because, of this a modified redundancy equation,

$$t_{ij} = e_{iA}^{01} e_{jB}^{10} = \frac{(e_{iA}^{01} e_{xB}^{10})(e_{yA}^{01} e_{jB}^{10})}{(e_{yA}^{01} e_{xB}^{10})}$$; where, x, y, i and j are matrix port numbers

and $x \neq y \neq i \neq j$ has been developed. Now a minimum of four transmission standards must be measured. However, because of the requirement that the transmission standards ports be mutually independent $x \neq y \neq i \neq j$, the flexibility of transmission connection

combinations is limited. The six available transmission connections can be put into three groups that contain mutually independent port pairs.

Table 7.1 – Transmission Connection Groups with Mutually Independent Port Pairs.

Group 1	Group 2	Group 3
(1,2)/(2,1)	(3,1)	(1,4)
(3,4)	(2,4)	(3,2)

In order for the modified redundancy relationship to work one entire group must be measured and one from each of the remaining groups must be measured. It is required that one of the choices be the (1,2)/(2,1) path. Making intelligent choices for the other paths on wafer will be discussed in Section 7.4.1.

7.3.4 Switch Term Correction on a 2xN System

The switch term correction on a 2xN system is the same as it is for a two port system. Any of the methods detailed in Chapter 3 can be used for simplicity the switch reflection measurement method will be detailed for the 2xN case. Given the two switch reflection coefficients: $\Gamma_{B,}$ when power is incident at VNA port 1(A), and Γ_A when power is incident at port 2(B) the switch corrected two-port S-parameters of any selected measurement path are given by the following general equation.

$$\Gamma_B = \frac{a_{2m}}{b_{2m}} \qquad \Gamma_A = \frac{a'_{1m}}{b'_{1m}}$$

$$\boldsymbol{S}_{\boldsymbol{11m}}^{\boldsymbol{(i,j)}} = \frac{S_{11m}^{(i,j)} - S_{12m}^{(i,j)} S_{21m}^{(i,j)} \Gamma_B}{d} \qquad \boldsymbol{S}_{\boldsymbol{12m}}^{\boldsymbol{(i,j)}} = \frac{S_{12m}^{(i,j)} - S_{11m}^{(i,j)} S_{12m}^{(i,j)} \Gamma_A}{d}$$

$$\boldsymbol{S}_{\boldsymbol{21m}}^{\boldsymbol{(i,j)}} = \frac{S_{21m}^{(i,j)} - S_{22m}^{(i,j)} S_{21m}^{(i,j)} \Gamma_B}{d} \qquad \boldsymbol{S}_{\boldsymbol{22m}}^{\boldsymbol{(i,j)}} = \frac{S_{22m}^{(i,j)} - S_{21m}^{(i,j)} S_{12m}^{(i,j)} \Gamma_A}{d}$$

$$d = 1 - S_{21m}^{(i,j)} S_{12m}^{(i,j)} \Gamma_B \Gamma_A$$

Since the measurements that are made by the VNA are still only two port measurements the termination of the RF switch of the analyzer is the only termination which changes in the forward and reverse measurement directions. Therefore the switch terms are the same for the two port case and may be measured only once using any two ports of the switch matrix provided the ports are connected through a transmission DUT such as a thru or the most ideal available transmission DUT.

7.3.5 Error Correction of a 2xN System

Once all the error terms, the six sets of reflectometer terms and the 12 transmission terms, have been calculated, each of the six sets of raw measured two-port data for the 4-port DUT may be corrected as any other two port measurements using the same techniques shown in Chapter 3. The 8-term error model coefficients may be transformed to 12-term error model coefficients and thus switch correction does not need to be applied to raw DUT measurements. Table 7.2 shows the relationship between the 2xN error terms of the 12-term error model to the 8-term error model for the (i,j) measurement path.

Table 7.2 – 12-Term vs. 8-Term Model Parameters for the (i,j) Measurement Path of a 2xN System.

12-Term Model Error Terms		8-Term Model Error Terms
$ED_i^A = e_{iA}^{00}$	=	e_{iA}^{00}
$ED_j^B = e_{jB}^{00}$	=	e_{jB}^{00}
$ES_i^A = e_{iA}^{11}$	=	e_{iA}^{11}
$ES_j^B = e_{jB}^{11}$	=	e_{jB}^{11}
$ER_i^A = e_{iA}^{01} e_{iA}^{10}$	=	$t_{ii} = e_{iA}^{01} e_{iA}^{10}$
$ER_j^B = e_{jB}^{01} e_{jB}^{10}$	=	$t_{jj} = e_{jB}^{01} e_{jB}^{10}$
$EL_i^A = e_{jB}^{11'}$	= (≠)	$e_{jB}^{11} + \frac{e_{jB}^{01} e_{jB}^{10} \Gamma_B}{1 - e_{jB}^{00} \Gamma_B}$ (e_{jB}^{11})
$EL_j^B = e_{iA}^{11'}$	= (≠)	$e_{iA}^{11} + \frac{e_{iA}^{01} e_{iA}^{10} \Gamma_A}{1 - e_{iA}^{00} \Gamma_A}$ (e_{iA}^{11})
$ET_i^A = e_{iA}^{10} e_{jB}^{01'}$	= (≠)	$e_{iA}^{10} \frac{e_{jB}^{01}}{1 - e_{jB}^{00} \Gamma_B}$ ($t_{ij} = e_{iA}^{10} e_{jB}^{01}$)
$ET_j^B = e_{jB}^{10} e_{iA}^{01'}$	= (≠)	$e_{jB}^{10} \frac{e_{iA}^{01}}{1 - e_{iA}^{00} \Gamma_A}$ ($t_{ji} = e_{jB}^{10} e_{iA}^{01}$)

In performing the error correction of the six two-port measurements, if a 12-term error model is used to correct each of the two port data sets, correction can be applied through the following equations,

$$S_{11}^{(i,j)} = \frac{\left(\frac{S_{11m}^{(i,j)} - ED_i^A}{ER_i^A}\right)\left[1 + \left(\frac{S_{22m}^{(i,j)} - ED_j^B}{ER_j^B}\right)ES_j^B\right] - EL_i^A\left(\frac{S_{21m}^{(i,j)}}{ET_i^A}\right)\left(\frac{S_{12m}^{(i,j)}}{ET_j^B}\right)}{D^{(i,j)}}$$

$$S_{21}^{(i,j)} = \frac{\left(\frac{S_{21m}^{(i,j)}}{ETF}\right)\left[1 + \left(\frac{S_{22m}^{(i,j)} - ED_j^B}{ER_j^B}\right)\left(ES_j^B - EL_i^A\right)\right]}{D^{(i,j)}}$$

$$S_{12}^{(i,j)} = \frac{\left(\frac{S_{12m}^{(i,j)}}{ETR}\right)\left[1 + \left(\frac{S_{11m}^{(i,j)} - ED_i^A}{ER_i^A}\right)\left(ES_i^A - EL_j^B\right)\right]}{D^{(i,j)}}$$

$$S_{22}^{(i,j)} = \frac{\left(\frac{S_{22m}^{(i,j)} - ED_j^B}{ER_j^B}\right)\left[1 + \left(\frac{S_{11m}^{(i,j)} - ED_i^A}{ER_i^A}\right)ES_i^A\right] - EL_j^B\left(\frac{S_{21m}^{(i,j)}}{ET_i^A}\right)\left(\frac{S_{12m}^{(i,j)}}{ET_j^B}\right)}{D^{(i,j)}}$$

$$D^{(i,j)} = \left[1 + \left(\frac{S_{11m}^{(i,j)} - ED_i^A}{ER_i^A}\right)ES_i^A\right]\left[1 + \left(\frac{S_{22m}^{(i,j)} - ED_j^B}{ER_j^B}\right)ES_j^B\right] - \left(\frac{S_{21m}^{(i,j)}}{ET_i^A}\right)\left(\frac{S_{12m}^{(i,j)}}{ET_j^B}\right)EL_i^A\ EL_j^B .$$

The isolation terms have been ignored in the 12-term correction equations.

If the 8-term model is preferred and raw switch-corrected DUT data is being used the corrected S-parameters are calculated by the relationships on the following page.

$$S_{11}^{(i,j)} = \frac{\left(\frac{\mathbf{S}_{\mathbf{11m}}^{(i,j)} - e_{iA}^{\ 00}}{t_{ii}}\right)\left[1+\left(\frac{\mathbf{S}_{\mathbf{22m}}^{(i,j)} - e_{jB}^{\ 00}}{t_{jj}}\right)e_{jB}^{\ 11}\right] - e_{jB}^{\ 11}\left(\frac{\mathbf{S}_{\mathbf{21m}}^{(i,j)}}{t_{ji}}\right)\left(\frac{\mathbf{S}_{\mathbf{12m}}^{(i,j)}}{t_{ij}}\right)}{D^{(i,j)}}$$

$$S_{21}^{(i,j)} = \frac{\left(\frac{\mathbf{S}_{\mathbf{21m}}}{t_{ji}}\right)}{D^{(i,j)}}$$

$$S_{12}^{(i,j)} = \frac{\left(\frac{\mathbf{S}_{\mathbf{12m}}}{t_{ij}}\right)}{D^{(i,j)}}$$

$$S_{22}^{(i,j)} = \frac{\left(\frac{\mathbf{S}_{\mathbf{22m}} - e_{jB}^{\ 00}}{t_{jj}}\right)\left[1+\left(\frac{\mathbf{S}_{\mathbf{11m}} - e_{iA}^{\ 00}}{t_{ii}}\right)e_{iA}^{\ 11}\right] - e_{iA}^{\ 11}\left(\frac{\mathbf{S}_{\mathbf{21m}}}{t_{ji}}\right)\left(\frac{\mathbf{S}_{\mathbf{12m}}}{t_{ij}}\right)}{D^{(i,j)}}$$

$$D^{(i,j)} = \left[1+\left(\frac{\mathbf{S}_{\mathbf{11m}} - e_{iA}^{\ 00}}{t_{ii}}\right)e_1^{\ 11}\right]\left[1+\left(\frac{\mathbf{S}_{\mathbf{22m}} - e_{jB}^{\ 00}}{t_{jj}}\right)e_{jB}^{\ 11}\right] - \left(\frac{\mathbf{S}_{\mathbf{21m}}}{t_{ji}}\right)\left(\frac{\mathbf{S}_{\mathbf{12m}}}{t_{ij}}\right)e_{iA}^{\ 11}e_{jB}^{\ 11}$$

Once all six two-port measurements have been corrected the final step of the measurement process is to renormalize the two-port S-parameter data to create a complete four-port measurement S-parameter matrix.

7.3.6 Correcting for Imperfect Auxiliary Terminations (Renormalization)

When multiport S-parameters are made on a two port VNA the ports which are not connected to the VNA are terminated with matched loads. In a 2xN system this is done automatically. These loads are assumed to be perfect; however, they often are far from ideal. Because of this, the measurements must be renormalized in order to correct for any reflections associated with the imperfect auxiliary terminations [35].

The two ports that are connected to the VNA are also terminated; however, any imperfections of the VNA's termination have been removed by the two-port error correction for that measurement state. This is why a true four-port VNA does not need renormalization, because the error model that is applied during DUT measurements is applied for all N ports and thereby the terminations on the ports can be assumed perfect.

A four-port device is characterized by a 2x4 system by making one two-port measurement for all six two port combinations. These two port measurements populate the four-port S-parameter matrix. It should be obvious however, that because each individual port is connected three times there are 3 separate measurements for each reflection coefficient. For example S_{22} of the DUT is measured as $S_{22}^{(1,2)}$, $S_{11}^{(2,4)}$, and $S_{22}^{(3,2)}$. This concept is visually represented by Figure 7.4 which was originally shown in [35]. The corners of the boxes contain the S-parameters of the two-port submatrices and the circled overlaps represent multiple measurements

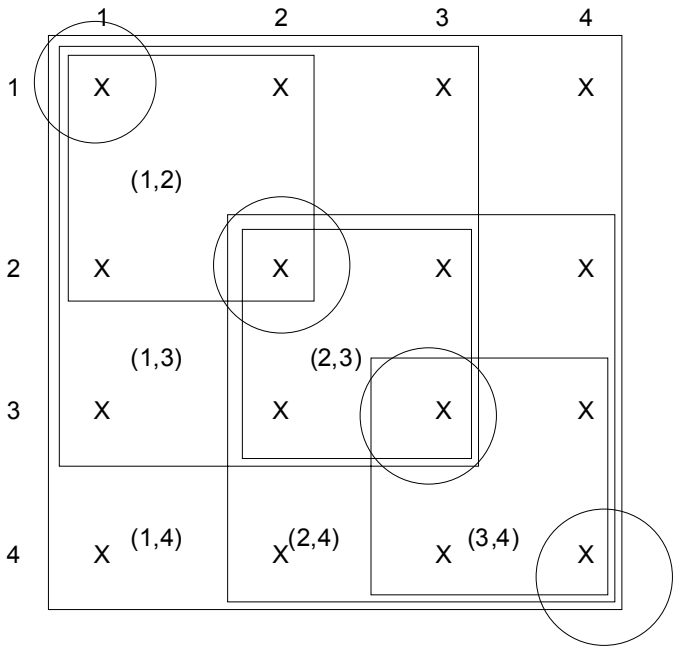

Figure 7.4 – Populated 4-Port S-parameter Matrix from Two-Port Characterization Measurements.

By measuring auxiliary port terminations for the switch matrix, the effects of the termination reflection coefficient can be removed through renormalization. The renormalization equation [35], $S' = (I - S)^{-1}(S - \Gamma)(I - S\,\Gamma)^{-1}(I - S)$, where I is an N dimensional identity matrix and Γ is the N dimensional diagonal matrix of the reflection coefficient of the new impedances referenced to the old impedances.

$\Gamma_n = \dfrac{Z_n - z_n}{Z_n + z_n}$ where, n = 1,2…N.

The renormalization equation renormalizes a given S-parameter matrix S from impedance z_n to impedance Z_n to create a new S-parameter matrix S'. The $S^{(i,j)}$ matrices which represent the 2x2 submatrices of a complete 4x4 matrix. The $S^{(1,2)}$ and $S^{(3,4)}$ matrix for examples are submatrices of a four-port matrix whose ports are normalized to (50, 50, Z_3, and Z_4) and (Z_1, Z_2, 50, and 50) respectively. This is a very inconsistent normalization because the port impedances changes from one two-port submatrix to another. Therefore, it is necessary to renormalize all the two-port submatrices to have a consistent set of port impedances $Z_i = Z_1, Z_2, Z_3$, and Z_4 which are the impedances of the corresponding ports auxiliary loads.

This first step is performed by renormalizing each two port sub matrix from it's (z_i, z_j = 50,50) ohm impedance to the impedance of the corresponding ports auxiliary impedance Z_i, Z_j. For instance the (1,2) measurement will be renormalized from 50,50 to Z_1, Z_2.

$$S^{(i,j)'} = \left(I - S^{(i,j)}\right)^{-1}\left(S^{(i,j)} - \begin{bmatrix} \Gamma_i & 0 \\ 0 & \Gamma_j \end{bmatrix}\right)\left(I - S^{(i,j)}\begin{bmatrix} \Gamma_i & 0 \\ 0 & \Gamma_j \end{bmatrix}\right)^{-1}\left(I - S^{(i,j)}\right)$$

Where: $\Gamma^{(i,j)} = \begin{bmatrix} \Gamma_i & 0 \\ 0 & \Gamma_j \end{bmatrix} = \begin{bmatrix} \frac{Z_i - z_i}{Z_i + z_i} & 0 \\ 0 & \frac{Z_j - z_j}{Z_j + z_j} \end{bmatrix} = \begin{bmatrix} \frac{Z_i - 50}{Z_i + 50} & 0 \\ 0 & \frac{Z_j - 50}{Z_j + 50} \end{bmatrix}$

After this is done to each of the six two port sub matrices the four-port S-parameter matrix can be formed and the three measurements of each reflection coefficient can be averaged to give a single value for each reflection coefficient.

$$S' = \begin{bmatrix} \frac{\left(S_{11}^{(1,2)\prime} + S_{11}^{(1,4)\prime} + S_{22}^{(3,1)\prime}\right)}{3} & S_{12}^{(1,2)\prime} & S_{21}^{(3,1)\prime} & S_{12}^{(1,4)\prime} \\ S_{21}^{(1,2)\prime} & \frac{\left(S_{22}^{(1,2)\prime} + S_{11}^{(2,4)\prime} + S_{22}^{(3,2)\prime}\right)}{3} & S_{21}^{(3,2)\prime} & S_{12}^{(2,4)\prime} \\ S_{12}^{(3,1)\prime} & S_{12}^{(3,2)\prime} & \frac{\left(S_{11}^{(3,4)\prime} + S_{11}^{(3,2)\prime} + S_{11}^{(3,1)\prime}\right)}{3} & S_{12}^{(3,4)\prime} \\ S_{21}^{(1,4)\prime} & S_{21}^{(2,4)\prime} & S_{21}^{(3,4)\prime} & \frac{\left(S_{22}^{(3,4)\prime} + S_{22}^{(1,4)\prime} + S_{22}^{(2,4)\prime}\right)}{3} \end{bmatrix}$$

Now that the 4-port S-parameter matrix normalized to Z_n has been formulated it is necessary to renormalize it back to a consistent $z_n = 50$ ohms. Now

$$S = \left(I - S'\right)^{-1}\left(S' - \Gamma_{50}\right)\left(I - S'\,\Gamma_{50}\right)^{-1}\left(I - S'\right)$$

$$\Gamma_{50} = \begin{bmatrix} \frac{50 - Z_1}{50 + Z_1} & 0 & 0 & 0 \\ 0 & \frac{50 - Z_2}{50 + Z_2} & 0 & 0 \\ 0 & 0 & \frac{50 - Z_3}{50 + Z_3} & 0 \\ 0 & 0 & 0 & \frac{50 - Z_4}{50 + Z_4} \end{bmatrix}$$

This is the final four-port S-parameter matrix. Figures 7.5 through 7.7 show the results of the renormalization process using measurements made of a parallel CPW delay line using GSGSG probes. Figure 7.5 shows an example of the three measurements of S_{11}

prior to renormalization. It can be seen in Figure 7.5 that only one of the measurements, the one measured during the (1,2) configuration, looks correct.

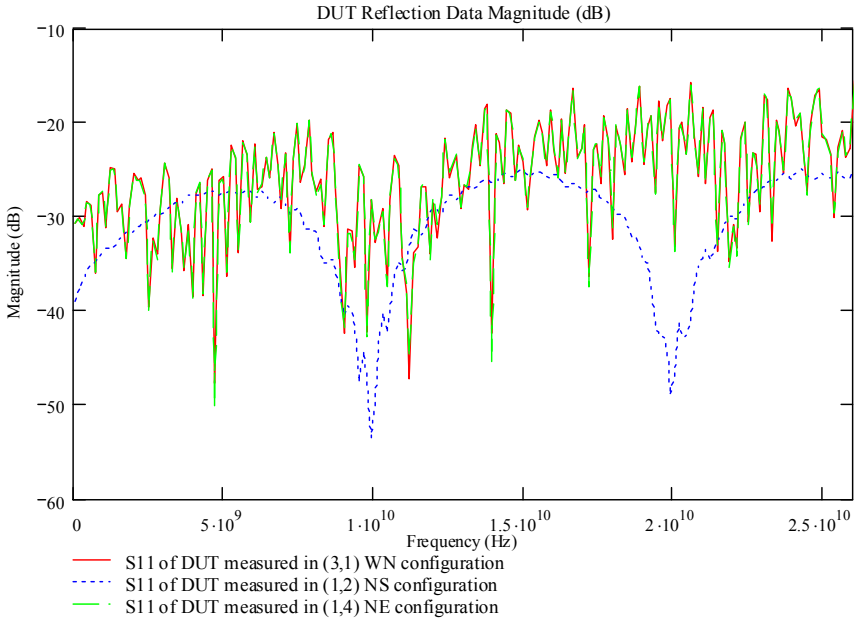

Figure 7.5 – Three S_{11} Measurements of GSGSG Delay Line Prior to Renormalization.

Figure 7.6 shows the same three measurements after renormalization. Notice that the three measurements now look almost identical hence averaging can be used to obtain a single S_{11} parameter value. Because the measurements in Figure 7.6 are not normalized to 50 ohms they do not appear as expected. Once they are finally renormalized back to 50 ohms the single measurement appears ideal as shown in Figure 7.7

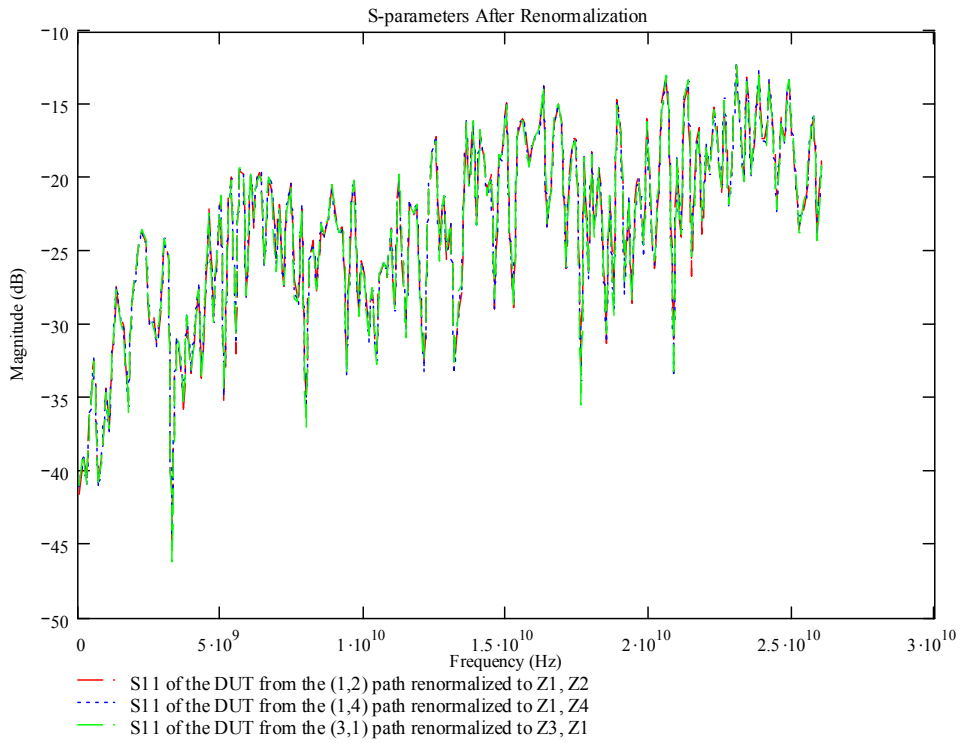

Figure 7.6 – S_{11} Parameters of a Parallel CPW Delay Line After Initial Renormalization to Auxiliary Termination Impedances $Z_1..Z_4$.

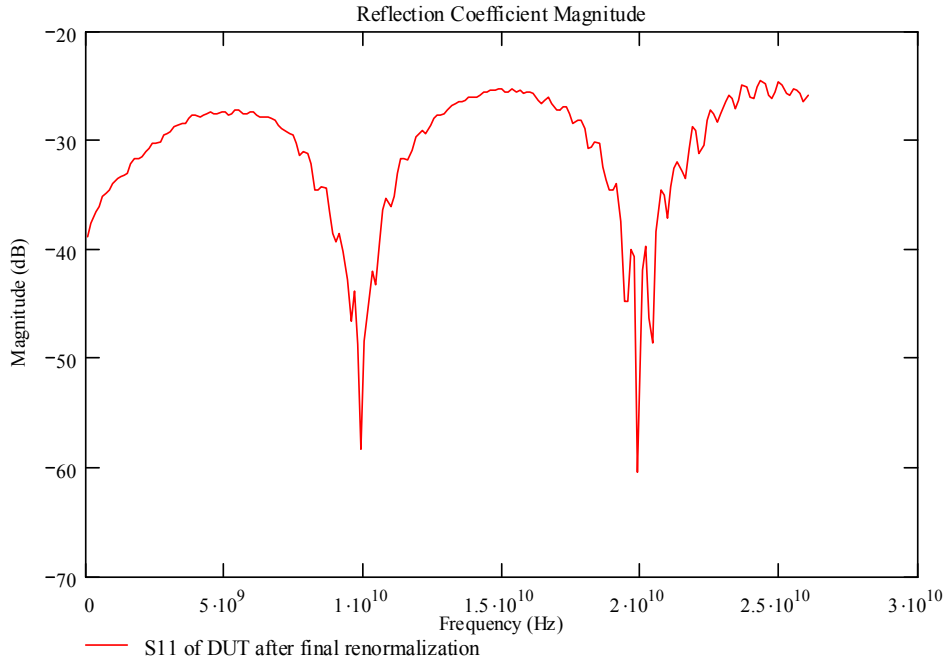

Figure 7.7 - S_{11} of a Parallel CPW Delay Line After Final Renormalization to 50 ohms.

The renormalization of the two port data to create a single multiport S-parameter matrix is what makes this method of multiport measurement correct. By renormalizing the measurements are the same as the results that would have been obtained if they were made on a true four-port analyzer.

7.4 Multiport cSOLR Calibration

With the general adaptation of a two port calibration to a multiport calibration shown in Section 7.3 the details involved in the adaptation and procedure for performing the multiport cSOLR algorithm will be detailed in this section. The adaptation of the SOLR algorithm to a multiport algorithm has been previously demonstrated in [51,52] Multiport cSOLR is essentially six two-port cSOLR calibrations. The only difference is that only four of the six sets of tracking terms will be calculated via the cSOLR algorithm the other will be calculated through redundancies. Therefore, a generalized representation of the cSOLR equations will be shown for any two port i and j. Where iA is the i_{th} matrix port connected to port A of the VNA and jB is the j_{th} matrix port connected to port B. Using the same method as shown in Section 4.3.3, the following equations can be used to calculate the error terms for multiport cSOLR.

$$\begin{bmatrix} 1 & \Gamma_{ma}^{iA}\Gamma_a & \Gamma_a \\ 1 & \Gamma_{mb}^{iA}\Gamma_b & \Gamma_b \\ 1 & \Gamma_{mc}^{iA}\Gamma_c & \Gamma_c \end{bmatrix} \begin{bmatrix} e_{iA}{}^{00} \\ e_{iA}{}^{11} \\ \Delta^{iA}{}_e \end{bmatrix} = \begin{bmatrix} \Gamma_{ma}^{iA} \\ \Gamma_{mb}^{iA} \\ \Gamma_{mc}^{iA} \end{bmatrix} \qquad \begin{bmatrix} 1 & \Gamma_{ma}^{jB}\Gamma_a & \Gamma_a \\ 1 & \Gamma_{mb}^{jB}\Gamma_b & \Gamma_b \\ 1 & \Gamma_{mc}^{jB}\Gamma_c & \Gamma_c \end{bmatrix} \begin{bmatrix} e_{jB}{}^{00} \\ e_{jB}{}^{11} \\ \Delta^{jB}{}_e \end{bmatrix} = \begin{bmatrix} \Gamma_{ma}^{jB} \\ \Gamma_{mb}^{jB} \\ \Gamma_{mc}^{jB} \end{bmatrix}$$

$$where: \Delta^{iA}{}_e = e_{iA}{}^{00} e_{iA}{}^{11} - t_{ii} \quad and \quad \Delta^{jB}{}_e = e_{jB}{}^{00} e_{jB}{}^{11} - t_{jj}$$

$$\boldsymbol{T_m^{(i,j)}} = \frac{1}{(t_{ji})} E_i^A \, T^{(i,j)} \left(E_j^B\right)^{Transpose} \qquad where: \boldsymbol{T_m^{(i,j)}} = \frac{1}{\mathbf{S_{21m}^{(i,j)}}} \begin{bmatrix} -\boldsymbol{\Delta}_{\mathbf{sm}}^{\mathbf{(i,j)}} & \mathbf{S_{11m}^{(i,j)}} \\ -\mathbf{S_{22m}^{(i,j)}} & 1 \end{bmatrix} \quad and \quad t_{ji} = e_{jB}{}^{10} e_{iA}{}^{01}$$

$$det\left(\boldsymbol{T_m^{(i,j)}}\right) = \frac{1}{(t_{ji})^2} det\left(E_i^A\right) det\left(T^{(i,j)}\right) det\left(\left(E_j^B\right)^{Transpose}\right) \qquad where: det\left(T^{(i,j)}\right) = 1$$

$$det\left(\boldsymbol{T_m^{(i,j)}}\right) = \frac{1}{(t_{ji})^2} det\left(E_i^A\right) det\left(\left(E_j^B\right)^{Transpose}\right)$$

Solving for the transmission parameter t_{21} gives,

$$t_{ji} = \pm \sqrt{\frac{\det\left(E_i^A\right) \det\left(\left(E_j^B\right)^{Transpose}\right)}{\det\left(\boldsymbol{T_m^{(i,j)}}\right)}} \, .$$

Using the same method as shown in Section 4.3.3, the above equations can be used to calculate the error terms for multiport cSOLR.

The generalized procedure for performing a four-port cSOLR calibration on a 2x4 system is made up of the following steps. A flow chart can be found in Appendix A.

Characterize Standard Definitions

1. Measure and model the standards using complex models (*only done initially when using a new calibration standard see 4.2.1).*

SOL Reflectometer Characterization

2. Measure raw data for the short, open, and load standards on ports 1 and 2 using the (1,2) NS and (2,1) SN measurement switch settings.
3. Measure raw data for the short, open, and load standards on ports 3 and 4 using the (3,4) WE measurement switch setting.

Transmission Measurements

4. Connect and measure raw data of the four required reciprocal two port transmission standards (*see 7.3.3).* If a true four-port VNA is used measure any three of the six available measurement paths making sure that all ports are connected at least once (*see 7.2.2*).
5. Measure the network analyzer's switch terms (*see 7.3.4).*
6. Measure the auxiliary terminations (*see 7.4.3).*

Measure DUTs

7. Measure raw two port S-parameters for all six available measurement paths of any DUTs (*see 7.3.1).*

Error Term Calculation and Data Correction

8. Switch correct all raw measured calibration standard data (*see 7.3.4).*
9. Use raw measured switch corrected SOL data to generate reflectometer terms (*see 4.3.3).*
10. Use raw measured switch corrected reciprocal transmission data to calculate transmission terms for the transmission paths measured *(see 7.4 and 4.3.3).*
11. Use redundancy equation to calculate any remaining transmission terms *(see 7.3.3).*
12. Apply two port corrections to all raw two port measurements of DUT data *(see 7.3.5).*
13. Renormalize two port DUT data to give corrected four-port DUT S-parameter matrix. *(see 7.3.6).*

7.4.1 Choosing On-Wafer Transmission Standards Using a True 4-Port System

Because cSOLR was designed with the intent of on-wafer calibrations using multiport probes, the transmission connections have been selected logically to reduce calibration time by reducing the number of probe connections or they can be optimized such that only the best transmission standards are used in order to reduce coupling. Recall from Section 7.2.2 that a true 4-port network analyzer only requires any three of the available six transmission standard connections provided that each port is connected at least once.

Because of this, there is a good deal of flexibility in choosing which standards to use. If the goal is to optimize time then the equal footprint standards such as a U thru and a parallel thru should be chosen. Since a pair of standards are connected each time a semi-automatic probe station makes contact on these standards it make since to measure both pairs. By measuring the (1,2) (3,4) parallel standards and the (3,1) (2,4) loopback standards it will only cost the time of one additional sweep and an extra measured set of transmission standards will be gained reducing the emphasis on redundancy and therefore any error that that may result from using it.

However, if coupling is a concern it may be better to use the offset standards. Even though only one transmission standard can be connected with both probes down the isolation is generally better in these standards. Thus, it would be best to measure the (1,4) and (3,2) standard as well as any of the in-line standards (1,2) or (3,4). There are several iterations and it is up to the users to choose what best suits their needs. These have been presented as suggested examples but, the calibration is not limited to them.

7.4.2 Choosing On-Wafer Transmission Standards When Using a 2xN System

When it comes time to measure the reciprocal transmission DUTs a decision must be made as to which port combinations should be measured. This decision is limited by the fact that the port error terms depend on which analyzer port they are connected to as was discussed in Section 7.3.3. Therefore since it is required to measure the (1,2) an (2,1) path, based on the measurement convention of Figure 7.3, it makes sense to measure the (3,4) path since it is simultaneously connected. Then either the (3,1) and (1,4) or the (3,2) and (2,4) transmission paths must be chosen this is personal preference. It should be noted that the port numbering convention shown here is flexible so long as the procedure is followed such that the physical port connections remain the same. As long as the equations are applied to the same physical ports of the switch matrix whose measurement paths are determined by the switch settings and remain fixed the equations will hold.

For measurement presented in this thesis in which redundancies are used the (1,2)/(2,1), (3,4), (3,1), and (1,4) transmission standards are measured. Note that only four standards are needed and that (1,2) and (2,1) use the same standard and connection. The transmission tracking terms for these measured paths can be calculated directly using the two port calibration technique and are shown in Table 7.2

Table 7.3 – Transmission Tracking Terms Found from Transmission DUT Measurements.

Transmission Path Measured	Calculated Transmission Tracking Terms
(1,2)	$t_{21} = e_{2B}^{01} e_{1A}^{10}$ $t_{12} = e_{1A}^{01} e_{2B}^{10}$
(2,1)	$t'_{21} = e_{2A}^{01} e_{1B}^{10}$ $t'_{12} = e_{1B}^{01} e_{2A}^{10}$
(3,4)	$t_{43} = e_{4B}^{01} e_{3A}^{10}$ $t_{34} = e_{3A}^{01} e_{4B}^{10}$
(3,1)	$t_{31} = e_{3A}^{01} e_{1B}^{10}$ $t_{13} = e_{1B}^{01} e_{3A}^{10}$
(1,4)	$t_{41} = e_{4B}^{01} e_{1A}^{10}$ $t_{14} = e_{1A}^{01} e_{4B}^{10}$

7.4.3 Measuring the Auxiliary Terminations

During the reciprocal transmission DUT measurements after the raw S-parameters of the standard have been taken, with the appropriate switch setting, it is necessary to change the switch setting to another that still leaves one of the ports connected to the transmission DUT. This is done in order to measure the reflection coefficient of the auxiliary termination of the port which is connected to the transmission DUT but not to the VNA. In general the solution for solving for the reflection coefficients of the auxiliary termination while connected to the (i,j) transmission standard which has S-parameter $S^{(i,j)}$ is:

$$\Gamma_j = \frac{S_{11}^{(i,j)} - S_{11}^{(i,n)}}{\Delta_S^{(i,j)} - S_{22}^{(i,j)} S_{11}^{(i,n)}}$$

where, $n \neq j$ and $\Delta_S^{(i,j)} = S_{11}^{(i,j)} S_{22}^{(i,j)} - S_{12}^{(i,j)} S_{21}^{(i,j)}$.

$$\Gamma_i = \frac{S_{22}^{(i,j)} - S_{22}^{(n,j)}}{\Delta_S^{(i,j)} - S_{11}^{(i,j)} S_{22}^{(n,j)}}$$

Note: this must only be done when the S-parameters of the transmission standard connecting the auxiliary termination must be removed.

Figure 7.8 illustrates this measurement by showing the necessary switch setting and connections to measure the port 2 and port 3 auxiliary terminations.

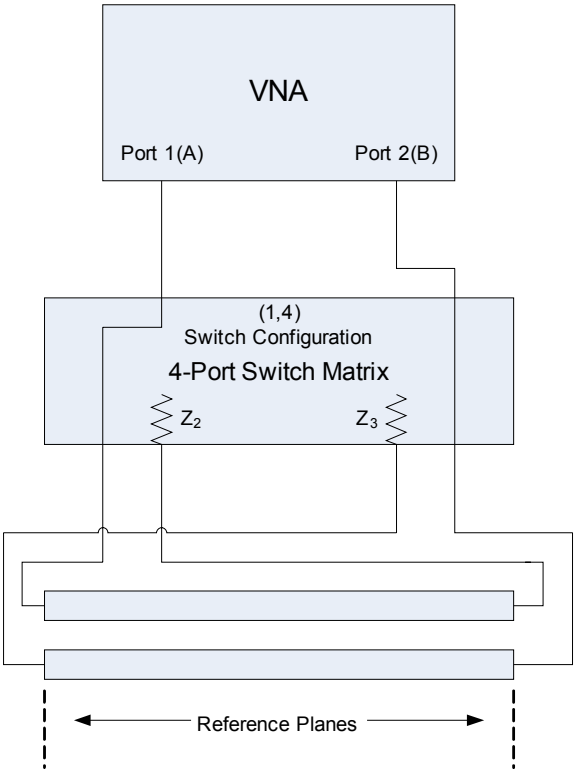

Figure 7.8 – Auxiliary Termination (Z_2 and Z_3) Measurement Setup.

For Figure 7.8 with the reference planes at the ends of the lines the port 2 and 3 auxiliary load reflection coefficients Γ_2 and Γ_3 can be found by measuring and correcting the (1,4) measurement data that gives $S^{(1,4)}{}_{11}$ and $S^{(1,4)}{}_{22}$ and knowing the S-parameters of the transmission standard. The S-parameters of the transmission standard are found by correcting the raw measured data for the (1,2) and (3,4) measurements of the parallel line DUT. The calculated coefficients Γ_2 and Γ_3 are:

$$\Gamma_2 = \frac{S_{11}^{(1,2)} - S_{11}^{(1,4)}}{\Delta_S^{(1,2)} - S_{22}^{(1,2)} S_{11}^{(1,4)}}$$

$$\Gamma_3 = \frac{S_{22}^{(3,4)} - S_{22}^{(1,4)}}{\Delta_S^{(3,4)} - S_{11}^{(3,4)} S_{22}^{(1,4)}}$$

When a zero length thru is used as the (i,j) transmission DUT the auxiliary loads are simply measured as

$$\Gamma_j = S_{11}^{(i,n)}$$

where n ≠ j.

$$\Gamma_i = S_{22}^{(n,j)}$$

Once the termination reflection coefficients have been determined they can be used to renormalize the multiport S-parameters.

7.5 Chapter Summary

Multiport calibration error models for both a true multiport system as well as 2xN systems have been presented. The techniques and methodology for performing measurements and calibrations on a 2xN system have been developed and discussed in detail. A solution has been presented for the problem of calculating the transmission tracking terms via redundancy on a 2xN system. Unique generalized solutions for the correction and renormalization of four-port S-parameters on a 2xN system are presented in detail.

CHAPTER 8

MULTIPORT CSOLR VERIFICATION

8.1 Introduction

The measurement results using the multiport cSOLR calibration will first be shown in Section 8.2.1 on the GGB CS-2-150 commercial GSGSG calibration substrate [31]. The multiport cSOLR calibration will be performed using all 6 possible thru measurements to establish a reference as the most accurate multiport adapted cSOLR calibration achievable. Essentially 6 separate 2-port calibrations, one for each measurement path, are performed to correct 6 separate sets of 2-port measurements. This method will be called the 6/2 multiport cSOLR calibration.

At the end of Section 8.2.1 it will be shown that the 4/2 multiport cSOLR calibration, which uses the equations shown in Chapter 7, to exploit the measurement redundancies and calculate all the transmission tracking terms from four thru connections provides virtually identical results to the 6/2 multiport cSOLR calibration. Because the two are equivalent, the N/2 notation will be dropped as only the 4/2 method will be used in the subsequent measurements and the calibration will simply be referred to as multiport cSOLR.

Multiport cSOLR will then be compared to the NIST 4-port TRL calibration method in Section 8.2.2. In Section 8.3 the multiport cSOLR method will be compared to the NIST 4-port LRM calibration in a coaxial environment with the corresponding data being shown in Appendix C. The characterization of the GGB GSSG calibration substrate will be presented in Section 8.4.

8.2 GGB CS-2-150 Calibration Substrate (GSGSG)

The GGB CS-2-150 was designed for calibrations using GSGSG probes. The substrate is alumina and the calibration structures are co-planar. The measurements were made using the Anritsu 37xxx series 65 GHz network analyzer and the 26.5 GHz external 4-port multiplexing switch matrix USF constructed based on NIST information [36]. This equipment is shown Figure 8.1. The Cascade [53] summit 12000 series semi-automatic probing station is used as the measurement platform. The overall measurement setup shown in Figure 8.2 provides a stable and highly reliable measurement platform. As seen in Figure 8.3, GGB [31] 150um pitch GSGSG probes and Gore [54] phase flex cables were used for interconnection. The 4-port 26.5 GHz switch matrix is used to multiplex the 2-port network analyzer to 4-ports. Measurements were made over a frequency range of 40 MHz to 26 GHz. The raw data was measured using the Multical software and then converted to tab delimited text files for use with the Mathcad based multiport cSOLR calibration. The probe setup and port designation is shown in Figure 8.4.

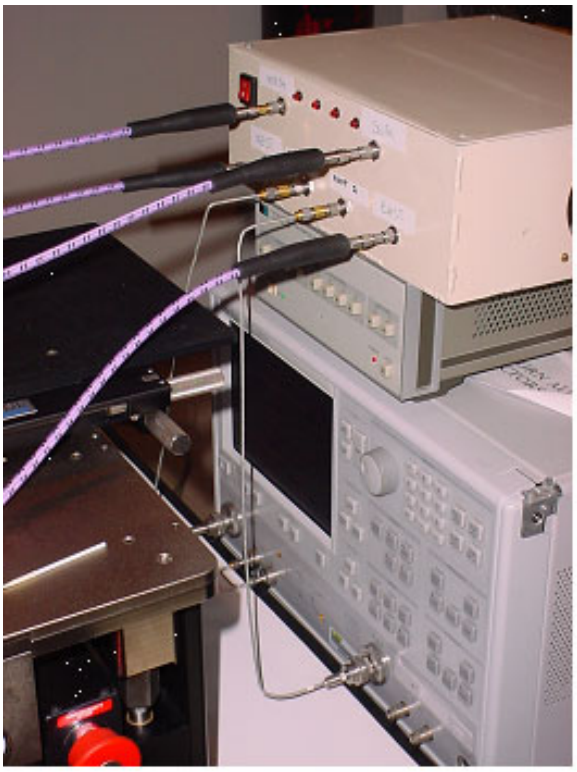

Figure 8.1 - Anritsu 37xxx Series 65 GHz Network Analyzer and the USF Built 26.5 GHz External 2x4 Multiplexing Switch Matrix.

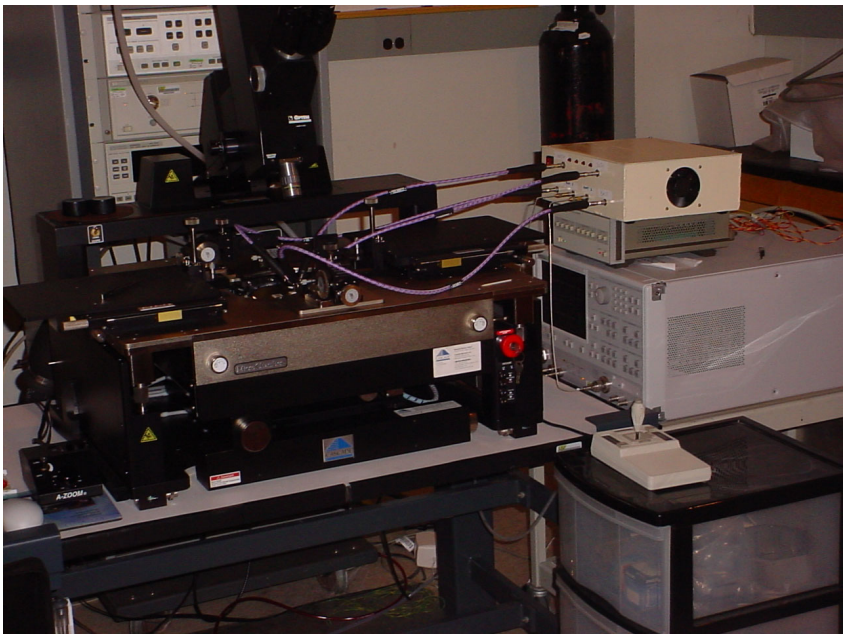

Figure 8.2 – 4-Port On-Wafer Measurement Setup Including a Cascade Summit 12000 Series Semi-Automatic Probe Station Combined with the Equipment from Fig. 8.1.

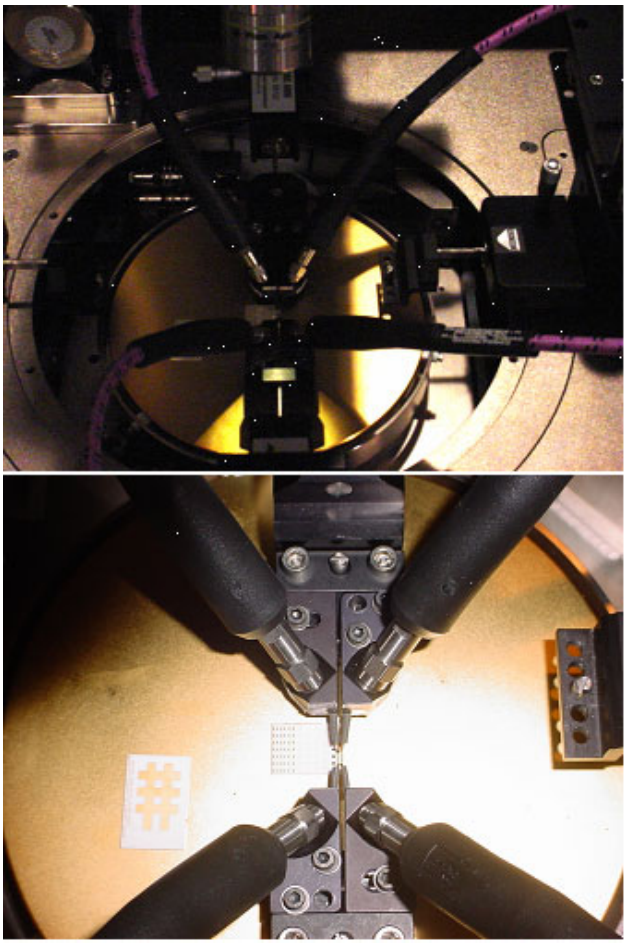

Figure 8.3 - GGB 150um Pitch GSGSG Probes and Gore Phase Flex Cables Used for Interconnection Between Instruments and Substrate.

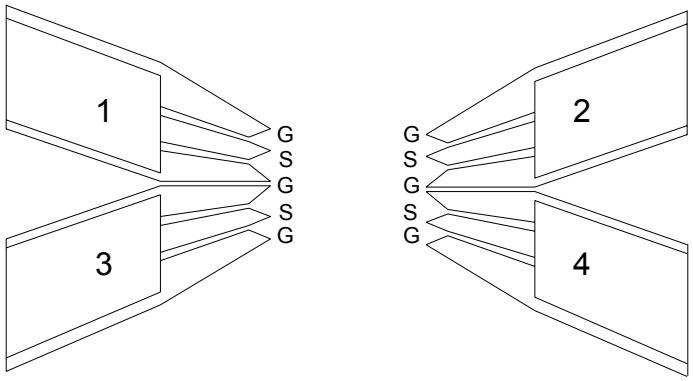

Figure 8.4 – Probe Setup and Port Designation for the GGB GSGSG 150 Pitch Probes.

The GGB CS-2-150 Substrate layout is provided in Figure 8.5 and will be useful in interpreting the data. Section 8.2.1 will give the characterization of some of the structures found on the substrate. First all six corrected thru measurements are shown and then a measurement of each port connected to a 50 ohm load is shown for calibration verification. Then one of each type of transmission standard will be shown as a characterized DUT, including: a parallel line structure, a loopback or "U" thru structure and an offset single thru structure.

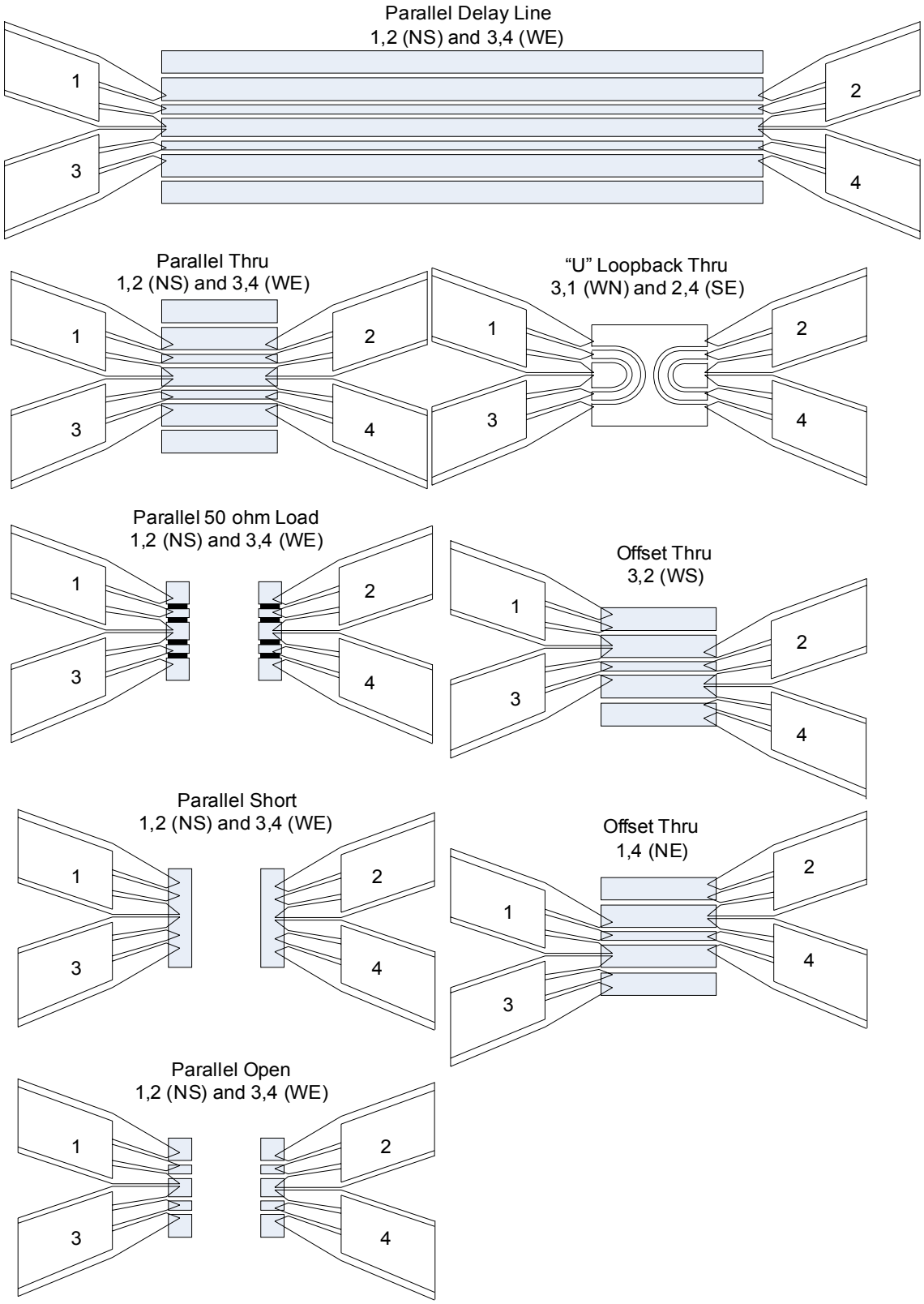

Figure 8.5 – GGB CS-2-150 Calibration Substrate Layout and Standard Connectivity Diagram.

8.2.1 GGB CS-2-150 Characterization

Figures 8.6 through 8.8 show the corrected measurement data for all six transmission standards used in the 6/2 multiport cSOLR calibration procedure. All of the thrus are said by GGB to have a 4.0ps length. Figures 8.7 and 8.8 respectively show that the loopback transmission standard seem to deviate from the 4.0ps specification, and has a less ideal match response like that of the straight transmission standards. The non-ideal nature of this standard is why other calibration algorithms that require well behaved transmission line standards cannot be implemented when a loopback standard is used. It is also seen (Figure 8.6) that the data becomes more somewhat more unstable as frequency increases above 17 GHz. However this instability is not linear to the data magnitude in that it does not increase as the loss or gain increases.

Transmission Standards

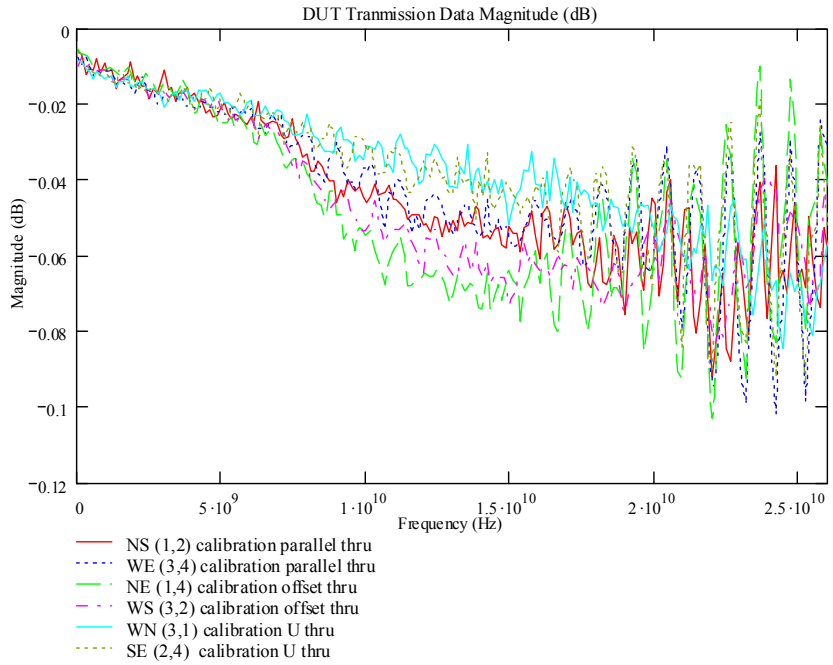

Figure 8.6 – Transmission Magnitude Data of Transmission Standards Using 6/2 Multiport cSOLR Calibration.

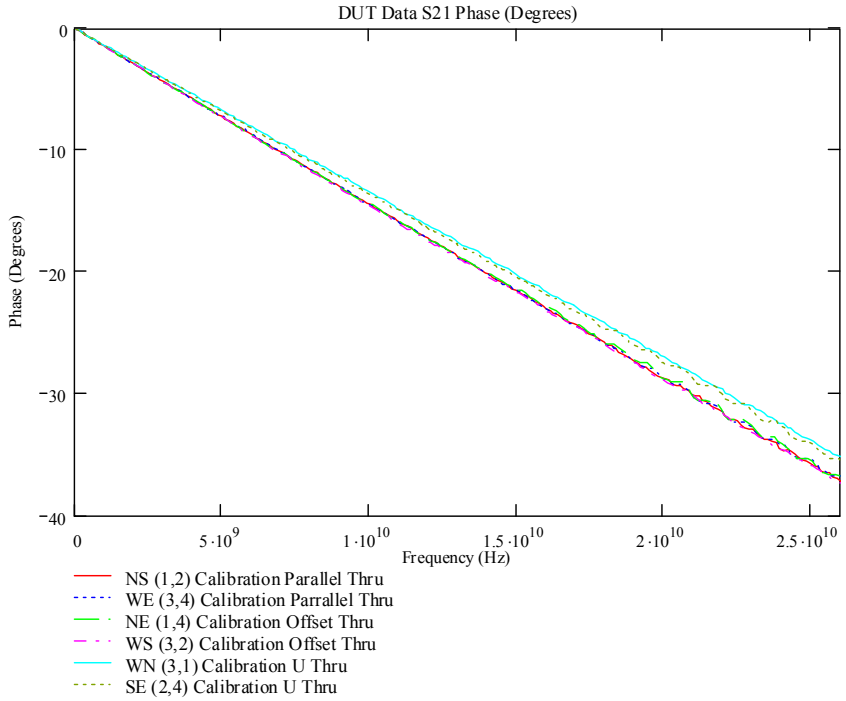

Figure 8.7 - Transmission Phase Data of Transmission Standards Using the 6/2 Multiport cSOLR Calibration.

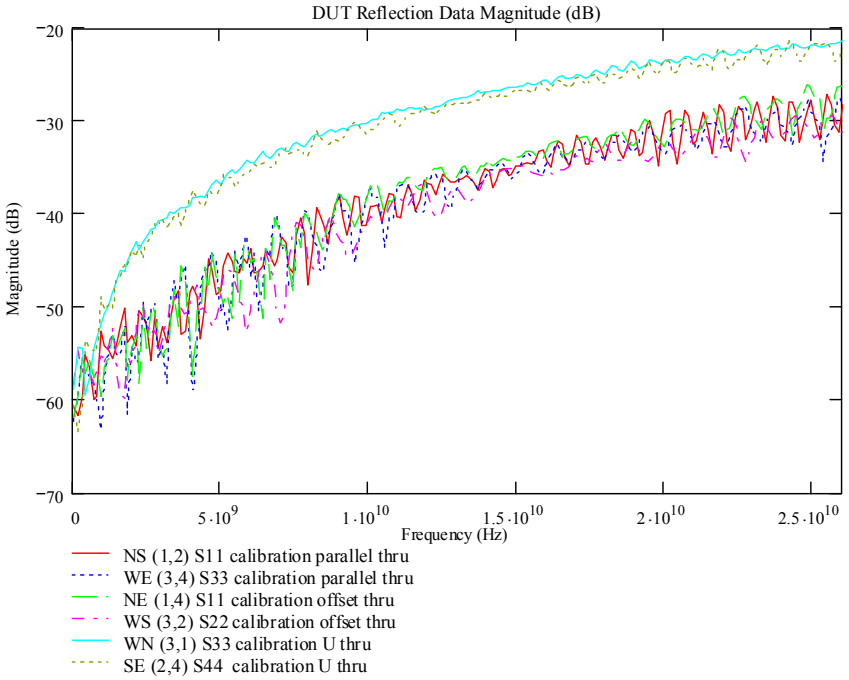

Figure 8.8 - Calibrated Transmission Standard Match Data Using 6/2 Multiport cSOLR Calibration.

Loads

The 50 ohm load reflection data after calibration are shown in Figure 8.9 to present a good response. However, this does not give verification as to the absolute accuracy of the calibration only to the probe placement repeatability, as any SOL calibration forces the reflection devices it measures to look like the models that represent them. Figure 8.10 shows the isolation between the signal lines of a multiport GSGSG probe. The reduced isolation with increasing frequency may be the reason why the measurement data degrades slightly above 17 GHz. The characterization measurements of the other standards used in the calibration, the open and short, are shown in Appendix B.

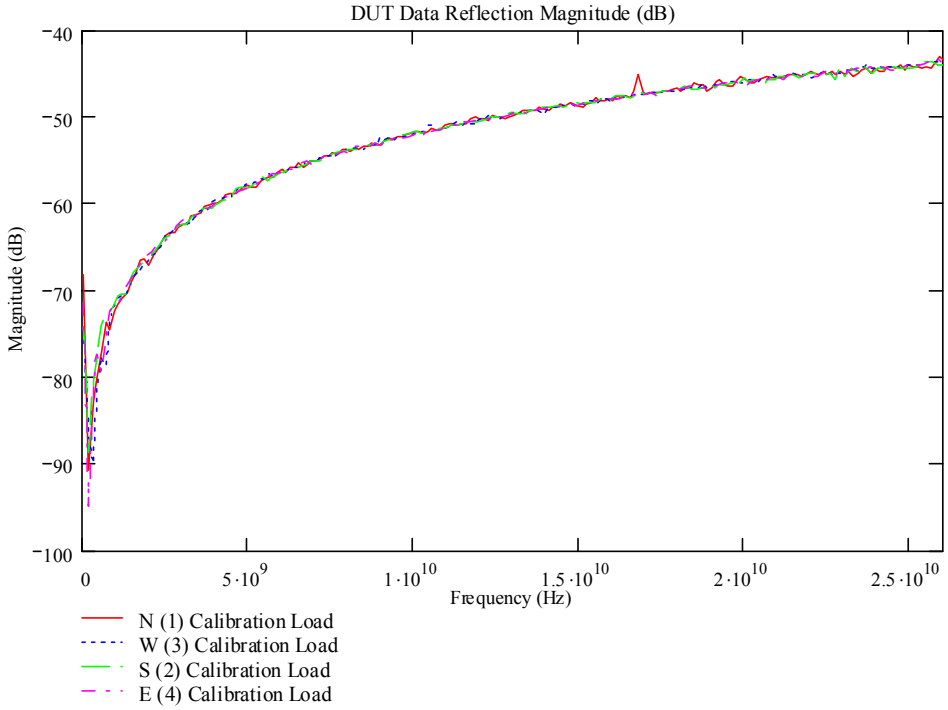

Figure 8.9 - Calibrated Load Reflection Data Using the 6/2 Multiport cSOLR Calibration.

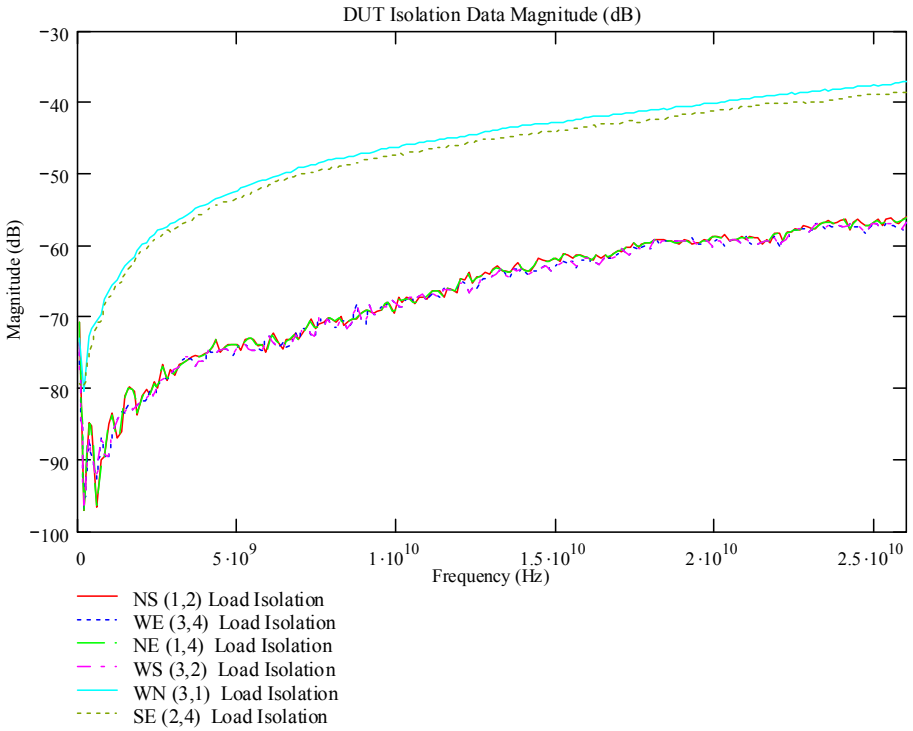

Figure 8.10 - Load Isolation Data Using the 6/2 Multiport cSOLR Calibration.

Delay 1

Figures 8.12 through 8.13 indicate that the parallel transmission line has a fairly ideal response for its direct transmission paths. The 6600 um parallel CPW line measurements using multiport cSOLR will be shown here. The other measured standards on the substrate are shown in Appendix B.

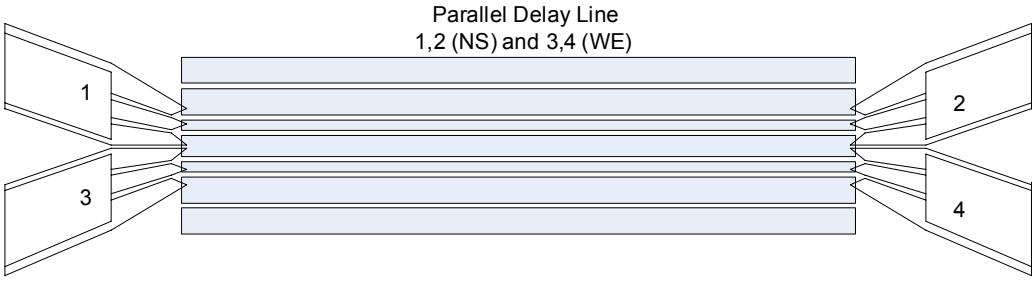

Figure 8.11 – GSGSG Layout of the 6600 um Parallel CPW Transmission Structure.

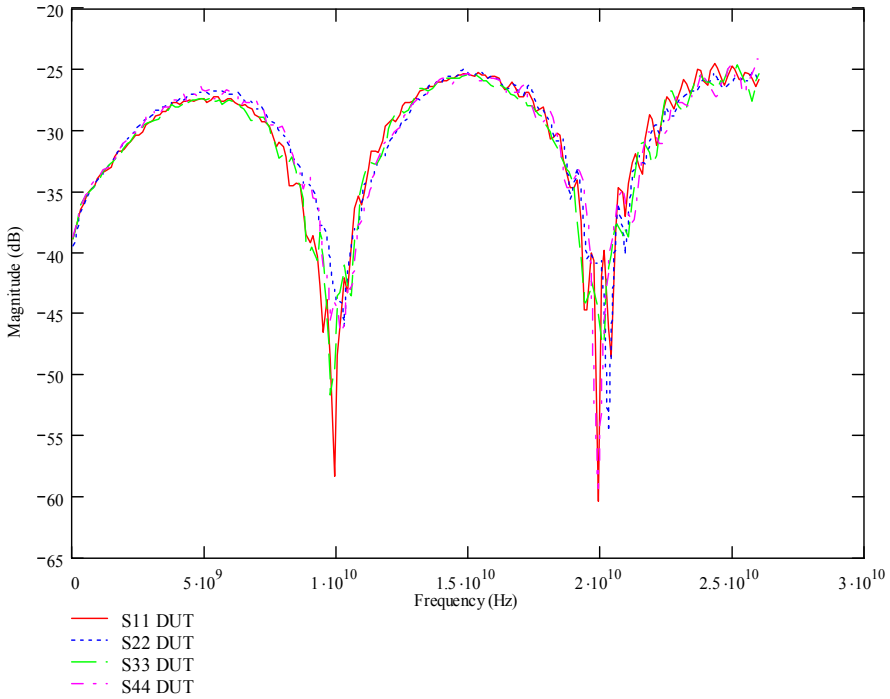

Figure 8.12 - Reflection Magnitude Data of 6600 um CPW Parallel Transmission Line Using the 6/2 Multiport cSOLR Calibration Routine.

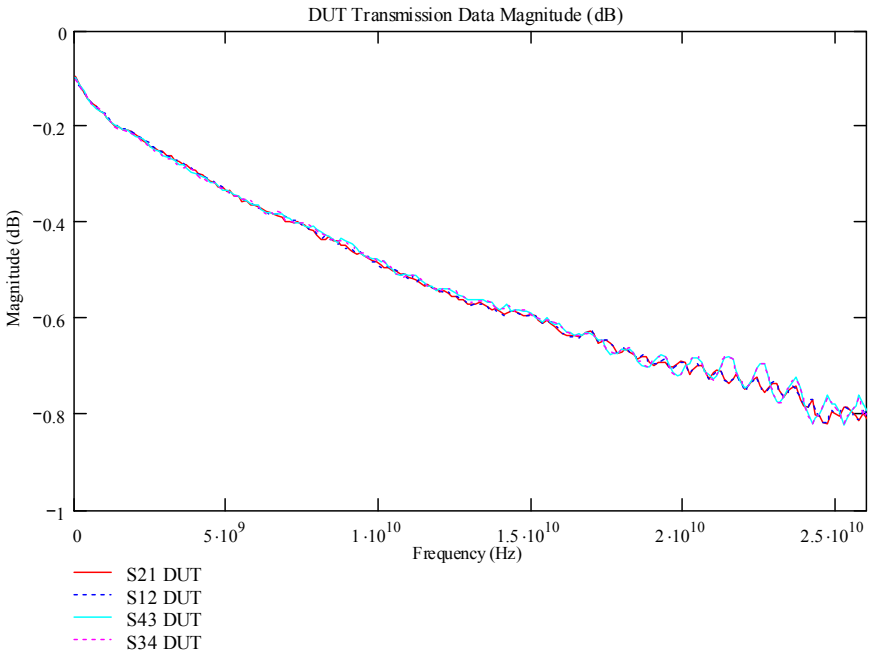

Figure 8.13 - Transmission Magnitude Data of 6600 um Parallel CPW Transmission Line Using the 6/2 Multiport cSOLR Calibration Routine.

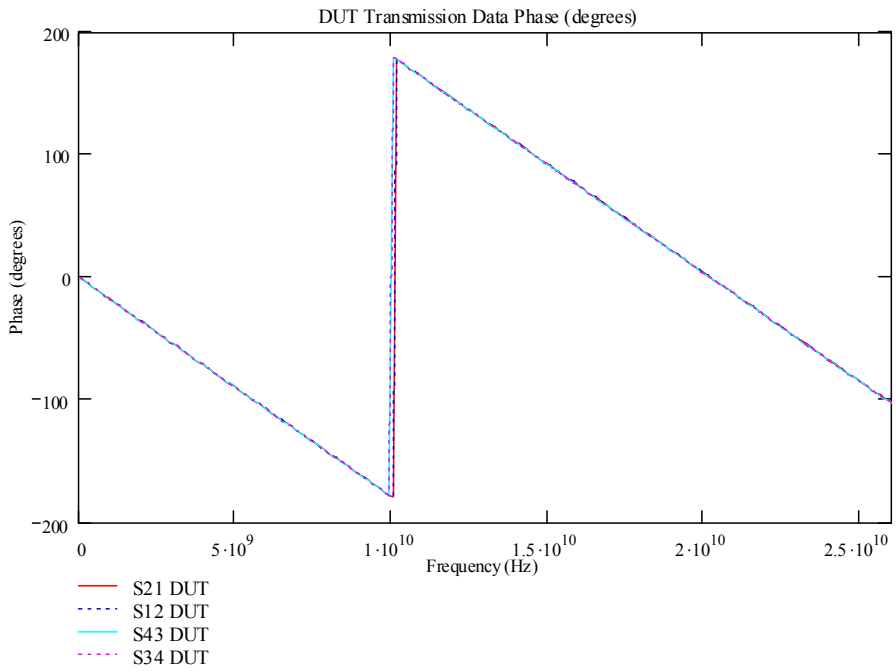

Figure 8.14 - Transmission Phase Data of 6600 um CPW Parallel Transmission Line Using the 6/2 Multiport cSOLR Calibration Routine.

When comparing the isolation of the parallel delay, shown in Figure 8.15, to the isolation of the parallel thru, Figure 8.16, the isolation of the parallel delay is less. This indicates some possible coupling or alternate transmission mode. This is a non-ideality that may limit other calibration algorithms such as TRL in their ability to provide an accurate error model solution; when using this device as one of the standards. It should be noted from Figure 8.14 that this non-ideal behavior is highly reciprocal.

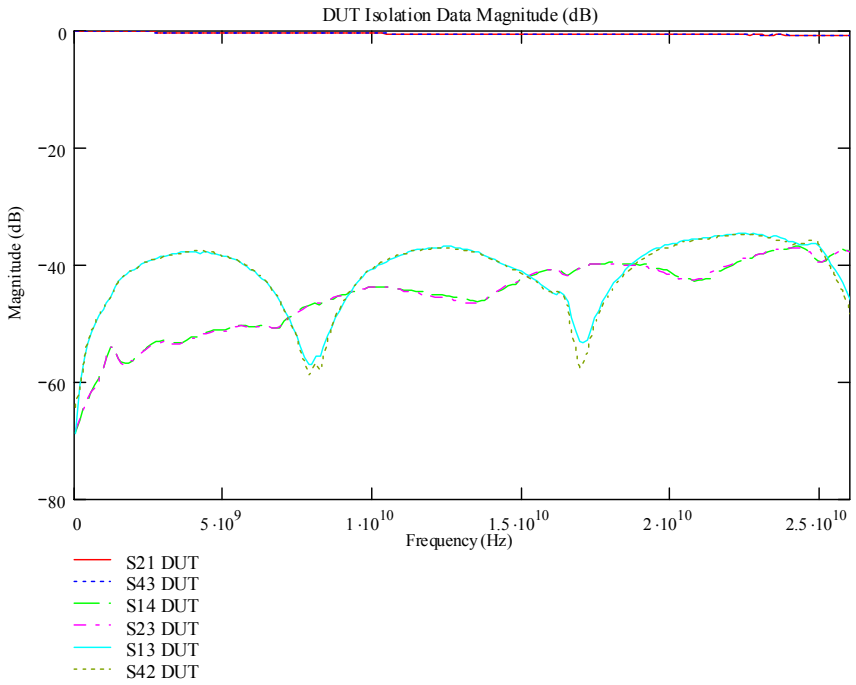

Figure 8.15 - Isolation Data of 6600 um CPW Parallel Transmission Line Using the 6/2 Multiport cSOLR Calibration Routine.

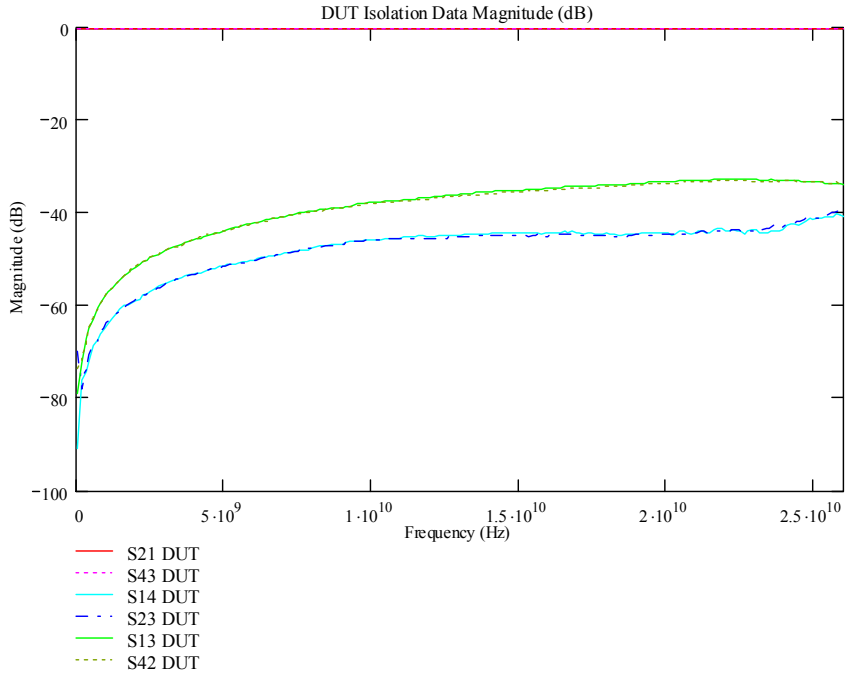

Figure 8.16 - Isolation Data of the 580 um CPW Parallel Transmission Line Using the 6/2 Multiport cSOLR Calibration Routine.

Using the identical raw calibration data, a calibration was performed using the four of the 6 available transmission standards (4/2 method). Using the redundancies discussed in Chapter 7, the unmeasured transmission tracking terms are calculated. Figure 8.17 shows the magnitude vector difference of a reflection and transmission measurement made on the 6600 um parallel delay line that was not used in the calibration.

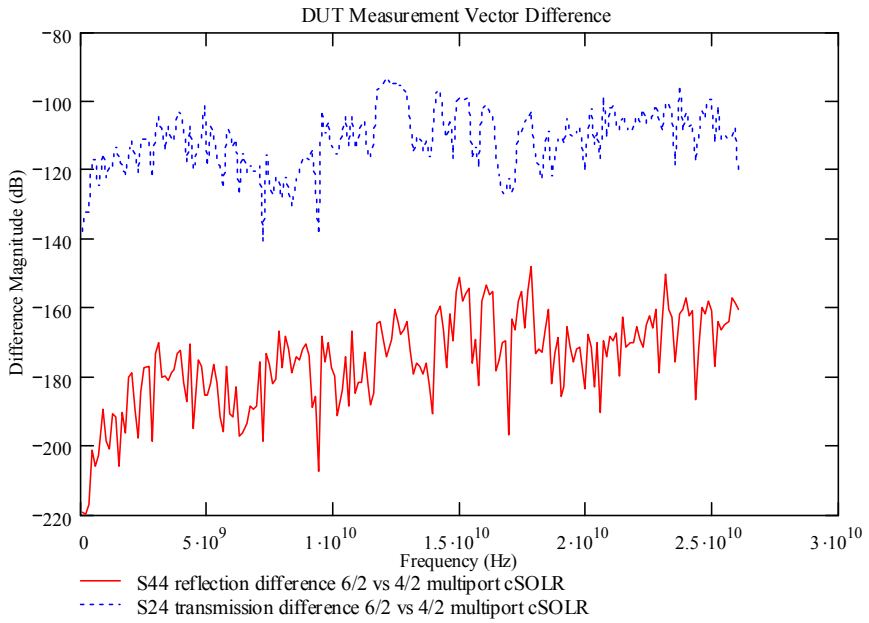

Figure 8.17 – 6600 um Parallel Delay Line Measurement Vector Difference Between Data Corrected Using the 6/2 Multiport cSOLR Method and the 4/2 Multiport cSOLR Method.

The subsequent measurements presented have been made using the 4/2 multiport cSOLR technique. Since the same raw uncorrected data was used in both the 6/2 and 4/2 technique, and Figure 8.17 shows the 6/2 and 4/2 results to be virtually identical, it can be concluded that the error term solutions of both calibrations are identical. Therefore,

only the 4/2 technique will be used, and will simply be referred to as multiport cSOLR from here forward.

8.2.2 Multiport cSOLR Measurement Comparison to NIST 4-port TRL

The measurements in this section are the same as those used to perform the multiport cSOLR calibrations of the previous section. The NIST 4-port TRL calibration was performed using the GGB CS-5 substrate and the GSGSG probes. The CS-5 substrate is the same material and thickness as the CS-2-150 the only difference is that the CS-5 was designed for 2-port calibrations using GSG probes. Both utilize CPW transmission structures however there are no parallel structures on the CS-5. The GSGSG probes are simply two GSG probes side by side therefore it was thought that because the NIST 4-port TRL method requires ideal transmission standards to perform a pair of in-line 2-port TRL calibrations the CS-5 could be used to provide these more ideal standards. Thus the GSGSG probes were used to probe the GSG standards between the (1,2) and (3,4) port pairs in order to perform the NIST 4-port TRL calibration. Two DUTS were used to compare the calibrations the 6600 um parallel CPW delay line (delay 1) and the U thru. The 1880 um parallel CPW delay line (delay 2) and the 580um parallel CPW thru are shown in appendix B.

6600 um Parallel CPW Transmission Line

It is observed in Figure 8.19 that the transmission magnitude of the delay 1 structure is very similar between the two calibrations. However, in Figure 8.20 the transmission phase of delay 1 measured with the NIST algorithm indicates some error

beginning at around 17 GHz. This appears to be due to some root choice error in the software's algorithm that caused the phase to flip 180 degrees. Also, it should be noted that the (1,2) port calibration for the NIST algorithm is achieved through the second tier of a two tier method which may make it more prone to cascading errors.

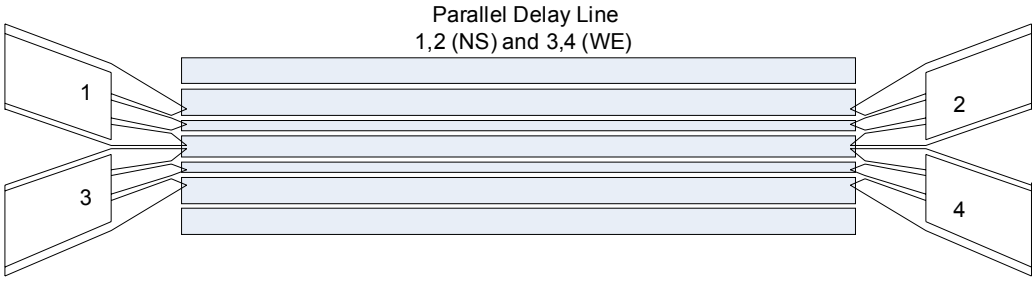

Figure 8.18 – GSGSG Layout of the 6600 um Parallel CPW Transmission Structure.

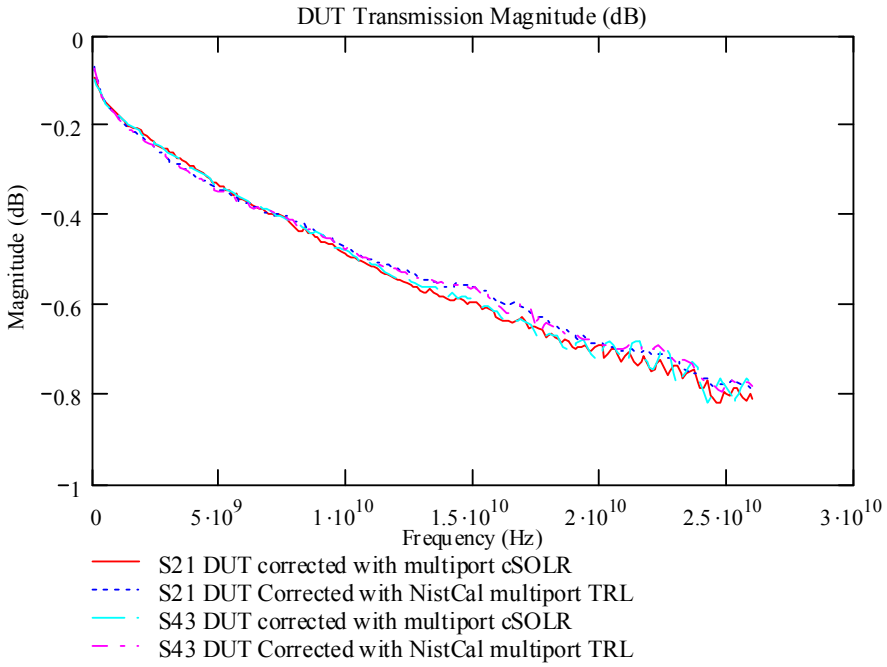

Figure 8.19 – Transmission Magnitude Measurements of 6600 um Parallel CPW Transmission Line Corrected with NIST 4-port TRL vs. Multiport cSOLR.

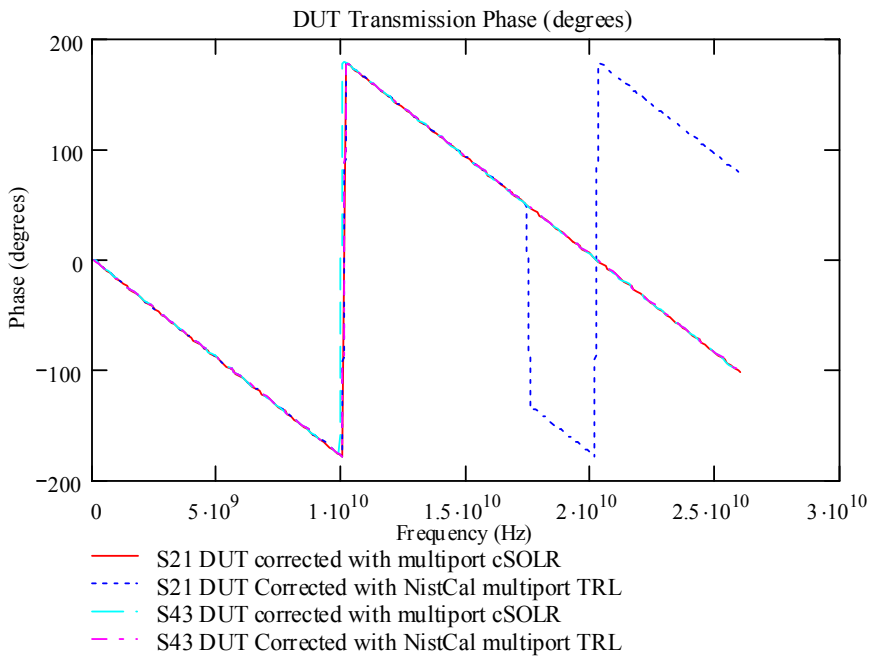

Figure 8.20 – Transmission Phase Measurements of 6600 um Parallel CPW Transmission Line Corrected with NIST 4-port TRL vs. Multiport cSOLR.

Figure 8.21 relates an apparent increase in match performance in the TRL measurement of the delay 1 structure. However; because, TRL assumes the input match of its delay line to be perfect, if there was coupling present between the unused signal pin and the signal pin measuring the delay line on the CS-5 substrate the algorithm would have zeroed this out and the true nature of the device would not be seen. This trend was not seen in the U thru, Figures 24 through 27, or other parallel CPW devices which are shown in Appendix B. Also the directivity error, the humps in the reflection data of Figure 8.21, in the TRL calibrations seems inconsistent between ports and because this is a symmetrical device it probably should be more similar.

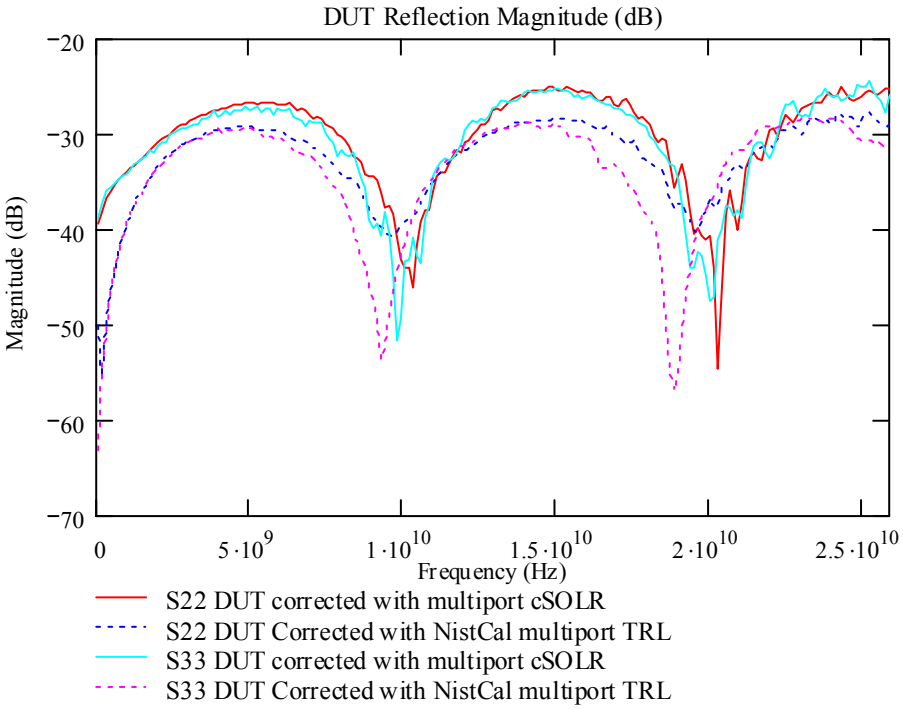

Figure 8.21 – Reflection Magnitude Measurements of 6600 um Parallel CPW Transmission Line Corrected with NIST 4-port TRL vs. Multiport cSOLR.

The isolation data, shown in Figure 8.22, presents good agreement between NIST TRL and multiport cSOLR, however, the TRL data does becomes slightly erratic after about 17 GHz which is where the phase shift problem also occurred.

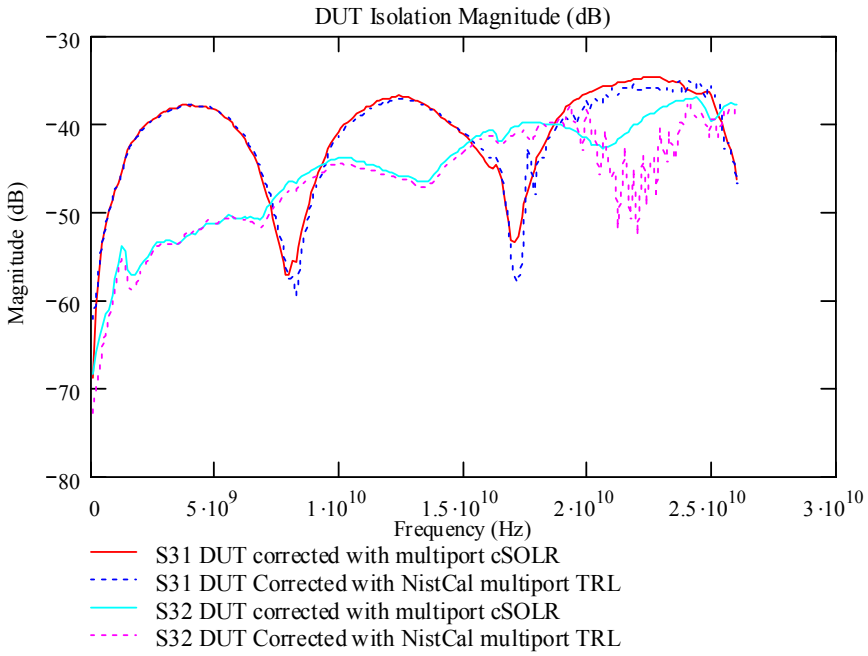

Figure 8.22 – Isolation Measurements of 6600 um Parallel CPW Transmission Line Corrected with NIST 4-port TRL vs. Multiport cSOLR.

Looback "U" Thru

As illustrated in Figure 8.24 the transmission magnitude data measured with the 4-port TRL calibration is more erratic and unstable than the cSOLR. Also, once again a discrepancy in the transmission phase data measured with the 4-port TRL can be seen in Figure 8.25.

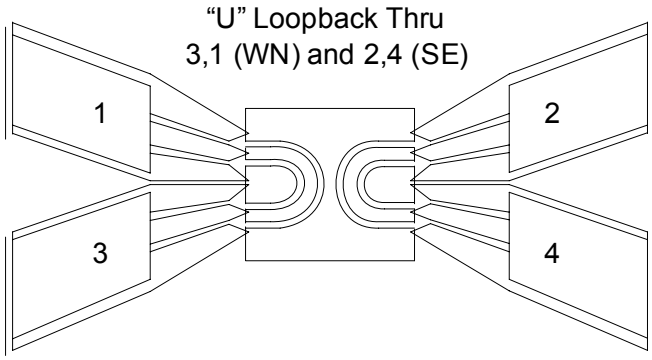

Figure 8.23 – GSGSG Layout of the Loopback Transmission Standard.

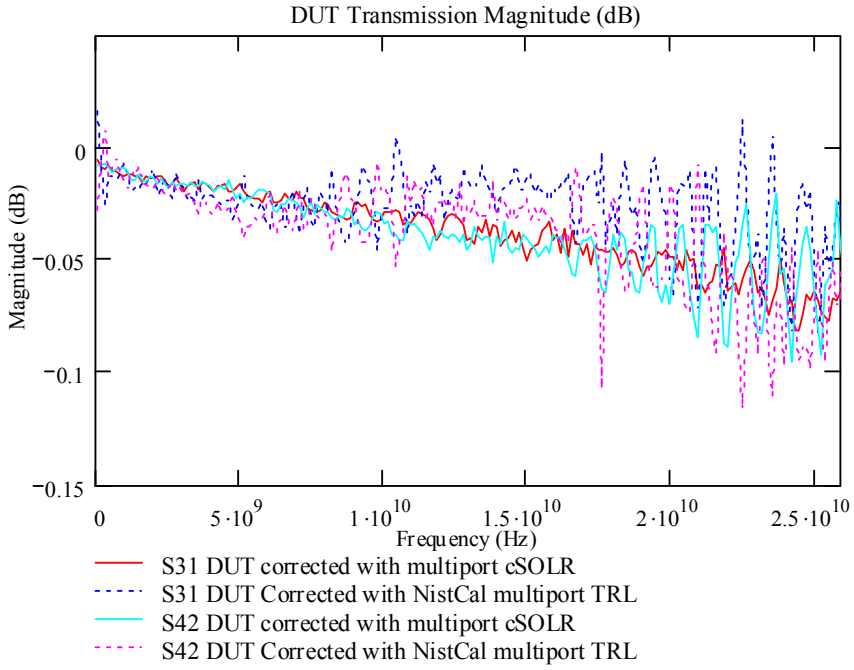

Figure 8.24 – Transmission Magnitude Measurements of 4.0 ps Loopback "U" Transmission Line Corrected with NIST 4-port TRL vs. Multiport cSOLR.

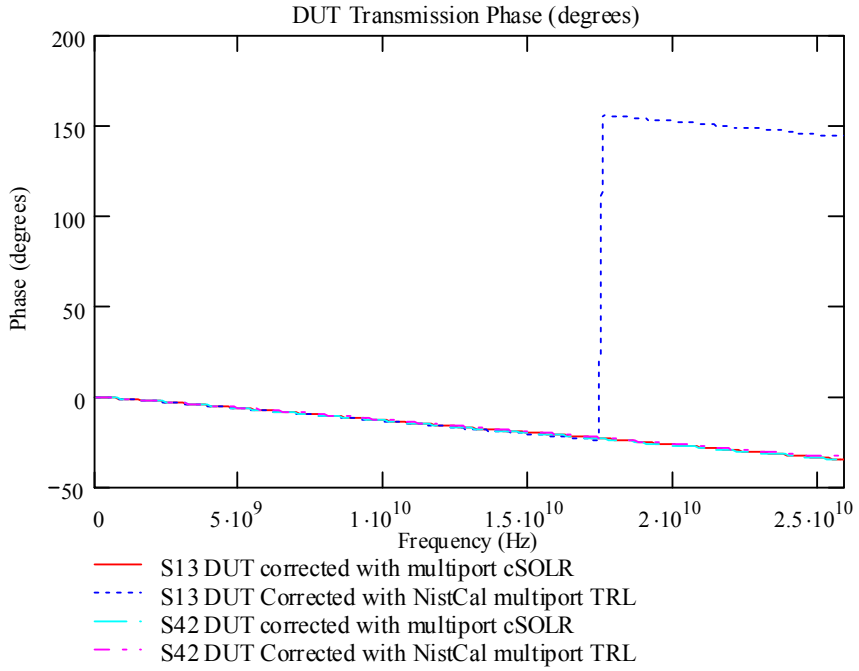

Figure 8.25 – Transmission Phase Measurements of 4.0 ps Loopback "U" Transmission Line Corrected with NIST 4-port TRL vs. Multiport cSOLR.

Figure 8.26 shows that as with the delay line there is a discrepancy between the reflection coefficients measured at port 2 and port 3 of the symmetrical device using the 4-port TRL method. The port 3 reflection measurement using 4-port TRL does agree with the multiport cSOLR measurements of ports 2 and 3 reflection.

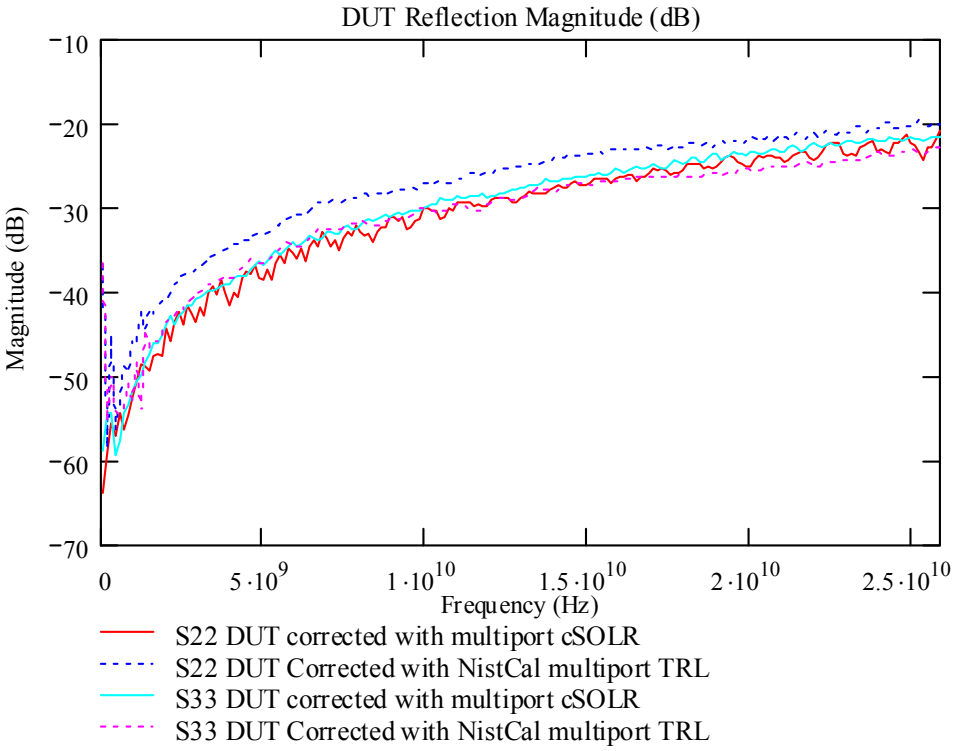

Figure 8.26 – Reflection Magnitude Measurements of 4.0 ps Loopback "U" Transmission Line Corrected with NIST 4-port TRL vs. Multiport cSOLR.

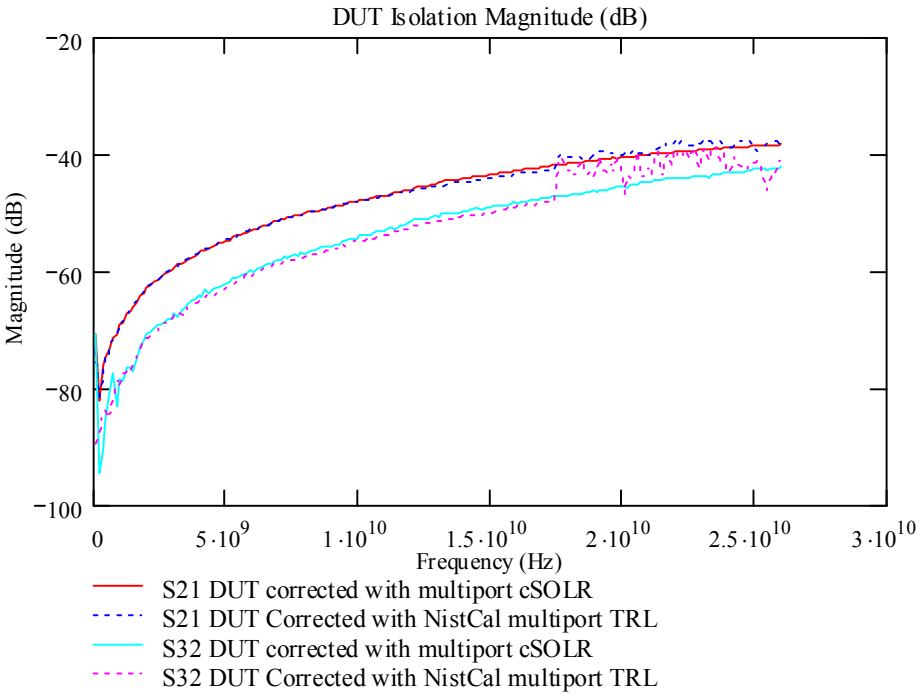

Figure 8.27 – Isolation Measurements of 4.0 ps Loopback "U" Transmission Line Corrected with NIST 4-port TRL vs. Multiport cSOLR.

8.3 Coaxial Measurement Verification of Multiport cSOLR

The coaxial measurement verification of multiport cSOLR will be done by comparing the measurements, of a 5.25 GHz triplexer made using multiport cSOLR to those made using other calibrations. Comparisons were made between multiport cSOLR and NISTcal 4-port LRM as well as a manual 4-port SOLT calibration. The manual 4-port SOLT was done by performing a two-port front panel calibration is performed and device's 6 paths are manually connected and unmeasured ports are manually terminated. The three calibrations showed good agreement and thus multiport cSOLR's functionality can be verified. The results of these measurements can be seen in Appendix C.

8.4 GGB CS-13-4109 Calibration Substrate (GSSG)

These measurements were made using the same system as Section 8.2. The GGB CS-13-4109 calibration substrate is designed for use with GSSG probes. As shown in Figure 8.28, the structures used as thru connection are the same and only the rotation changes. A thru path calibration standard characterization will be presented in Section 8.4.1 by showing the four thru standards used for the multiport cSOLR calibration. Measurements of two unique devices are presented in 8.4.2: a 6600um coupled line structure and a set of 100 ohm series loads between each probes signal lines. The remaining calibration standard and DUT measurements are shown in Appendix D.

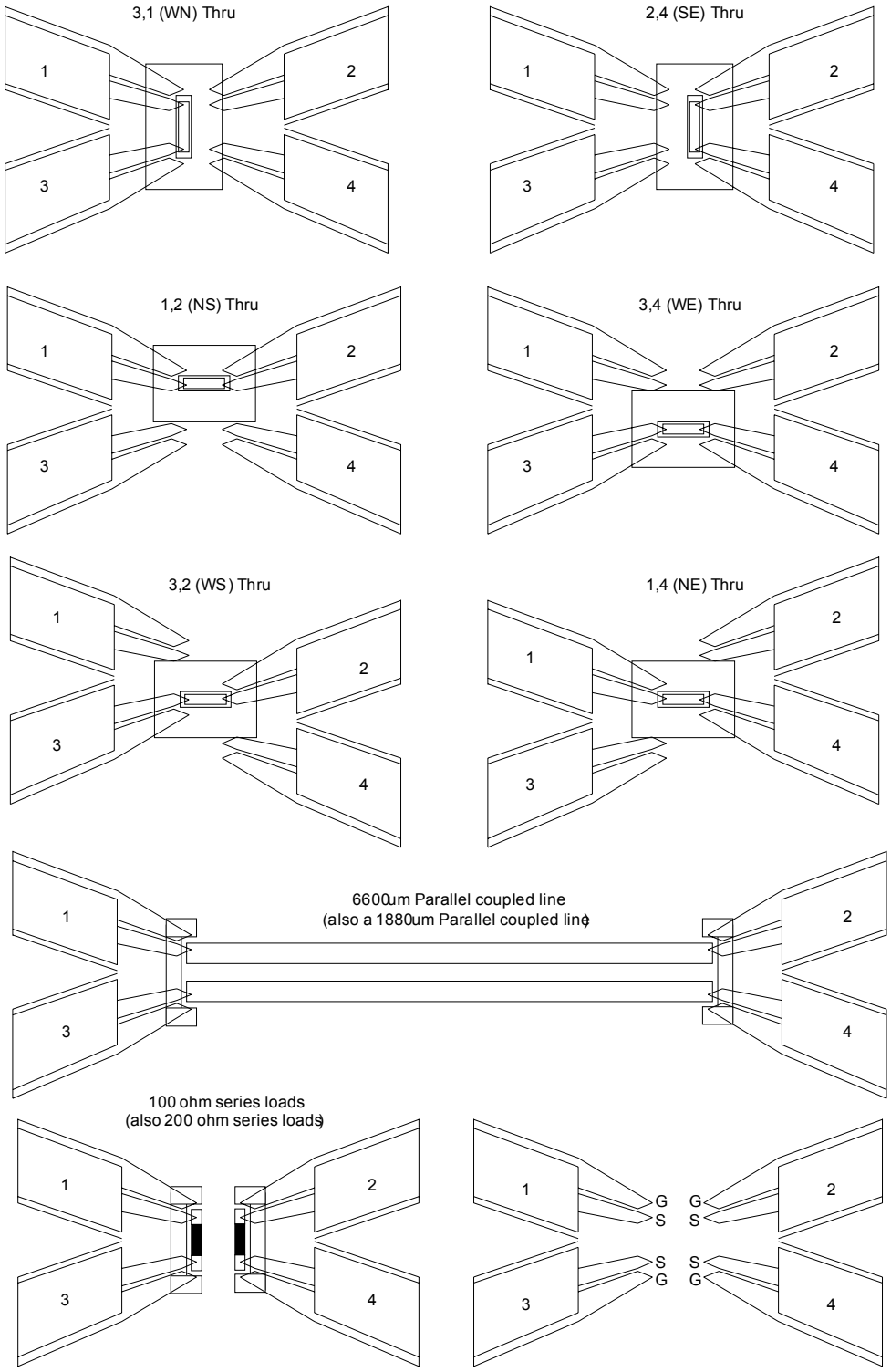

Figure 8.28 - GGB CS-13-4109 GSSG Calibration Substrate Conceptual Layout and Port Identification.

8.4.1 GGB CS-13-4109 Calibration Standard Characterization

The transmission and reflection measurements of the four transmission standards used in the multiport cSOLR calibration are presented in Figures 8.29 through 8.32. The four corresponding isolations plots , that represent where the highest amount of leakage is occurring for each thru are shown in Figure 8.32. The reflection measurement of the 50 ohm loads used during the calibration is displayed in Figure 8.33 and the isolation measurements associated with the loads are shown in Figure 8.34. The remaining characterization measurements of the substrate's standards can be found in Appendix D.

Transmission Standards

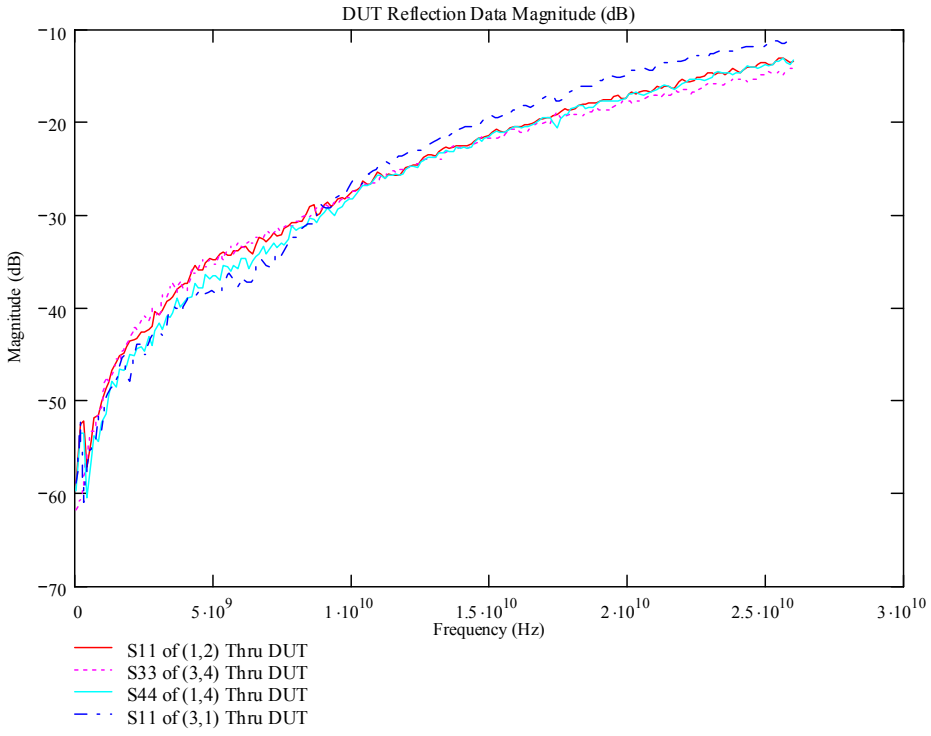

Figure 8.29 – Reflection Magnitude of the GGB CS-13-4130 Calibration Transmission Standards Used in the Multiport cSOLR Calibration.

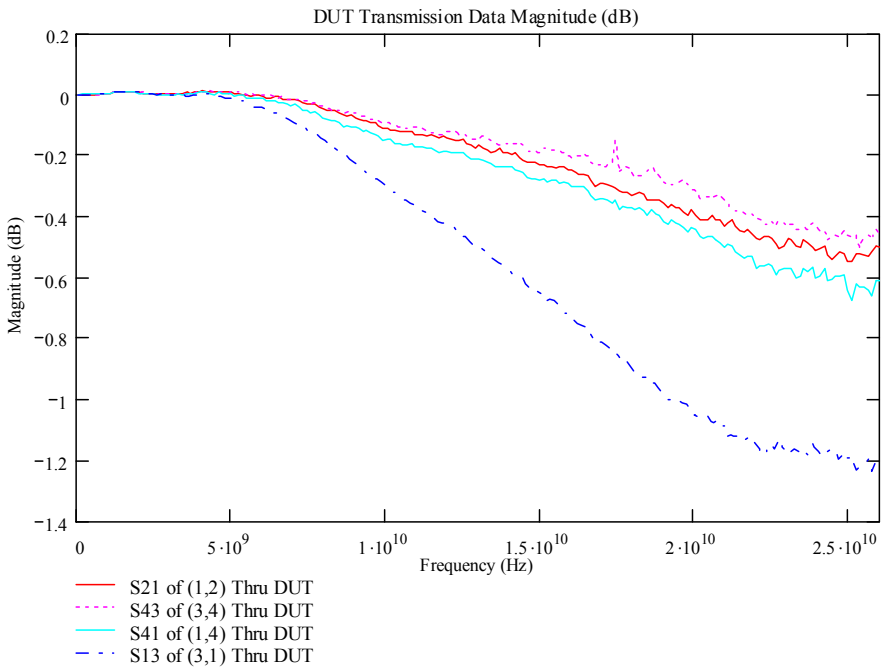

Figure 8.30 – Transmission Magnitude of the Calibration Transmission Standards Used in the Multiport cSOLR Calibration.

It can be seen from Figure 8.30 that the (3,1) transmission standard has the most loss with it. However, all the standards are the same length and therefore should all have similar loss. It would be reasonable to conclude that the signal must be coupling somewhere, but according to Figure 8.32 the (3,1) transmission standard remains very well isolated from ports 2 and 4. By examining Figure 8.34 it can be seen that when a 50 match is applied to each port, which is what our calibration transmission standards characteristic impedances should roughly look like, the (3,1) and (2,4) ports have the worse isolation. Therefore, it could be concluded that the reason for the high transmission loss in the (3,1) transmission standard is because some of the signal is bypassing the transmission line and directly coupling from port 1 to 3; also, the device could be radiating power. Another indicator of this is the transmission phase of the (3,1) standard.

It can be seen from Figure 8.31 that phase begins to increase at the same point as the transmission loss begins to dramatically decrease.

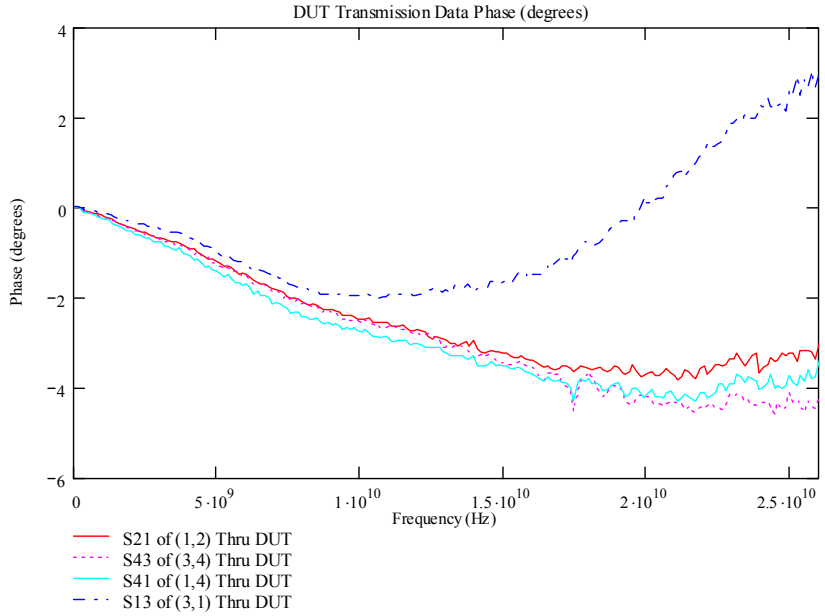

Figure 8.31 – Transmission Phase of the Calibration Transmission Standards Used in the Multiport cSOLR Calibration.

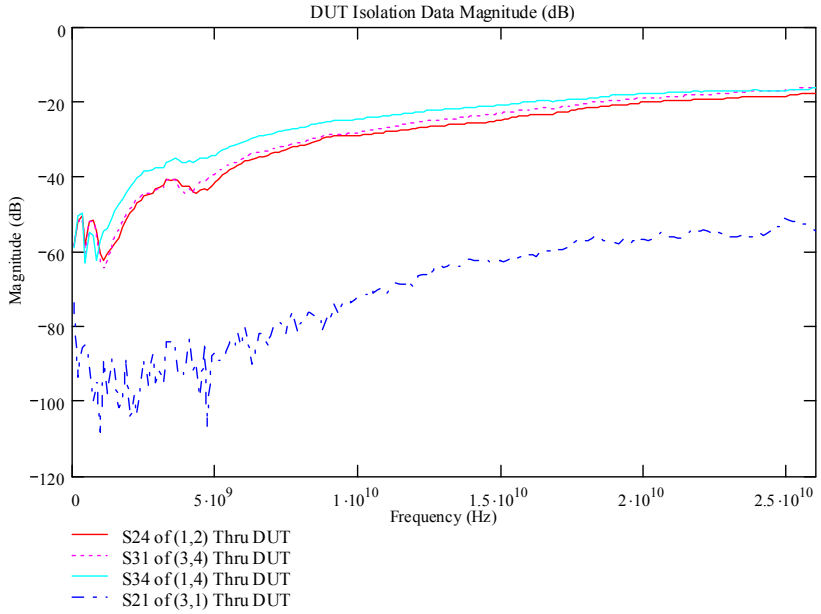

Figure 8.32 – Isolation Magnitude of the Highest Leakage Path of Each of the Calibration Transmission Standards Used in the Multiport cSOLR Calibration.

Loads

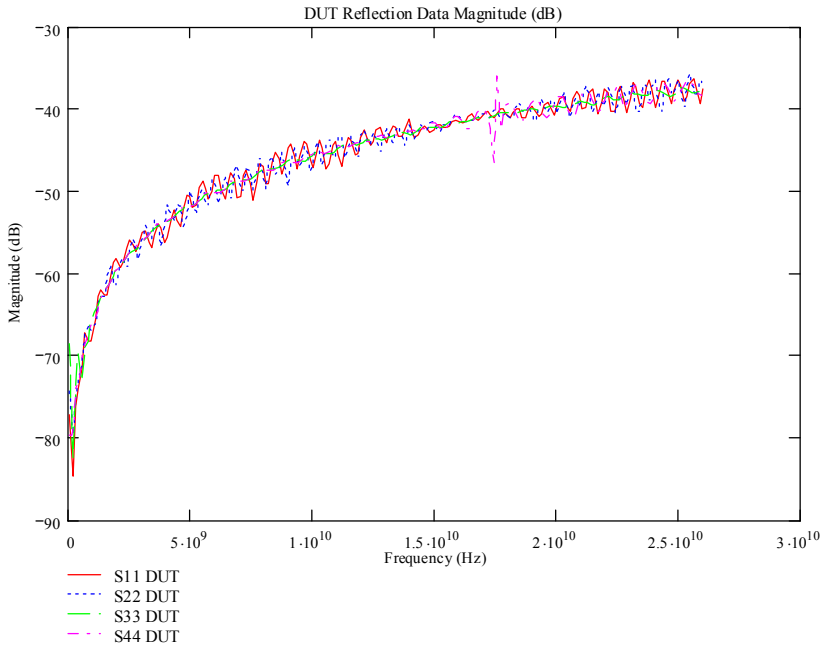

Figure 8.33 – Reflection Magnitude of the 50 Ohm Load Standards Used in the Multiport cSOLR Calibration.

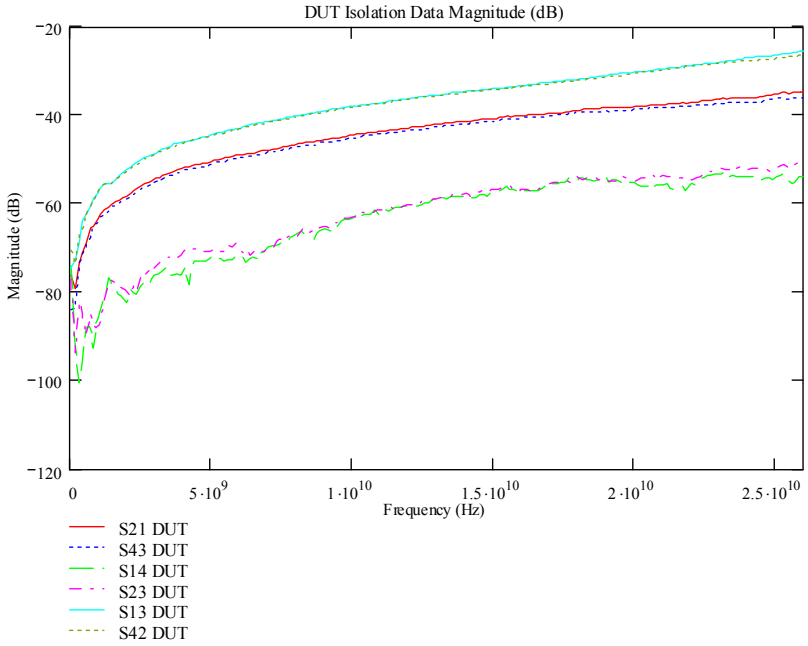

Figure 8.34 – Isolation Magnitude of the 50 Ohm Load Standards Used in the Multiport cSOLR Calibration.

8.4.2 GGB CS-13-4130 DUTS

The DUTs presented here are a 6600 um coupled line structure and a set of 100 ohm series loads located between the (1 and 3) and (2 and 4) probe tips. The remaining structure's measurements can be found in Appendix D.

6600 um Coupled Line Structure

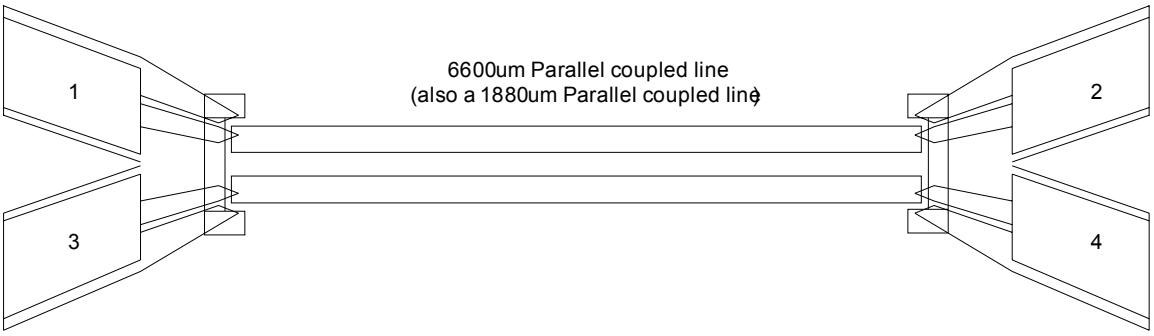

Figure 8.35 – GSSG Layout of 6600 um Parallel Line Structure.

The coupling associated with the parallel lines is evident in Figure 8.36. The phase of the direct transmission port (1,2) and the coupled transmission port are 180 degrees out of phase from one another as shown in Figure 8.37. The reflection coefficient at the input ports, Figure 8.38, represents the reflection which results from the entire network's characteristics and therefore is not highly matched as frequency increases.

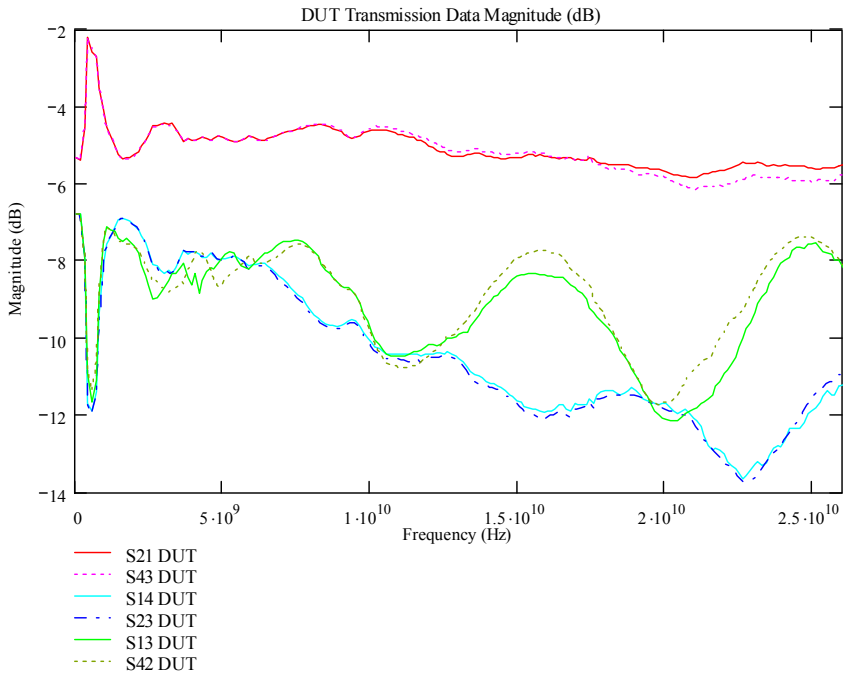

Figure 8.36 – Transmission Magnitude of the 6600 um Coupled Line Measured with the Multiport cSOLR Calibration.

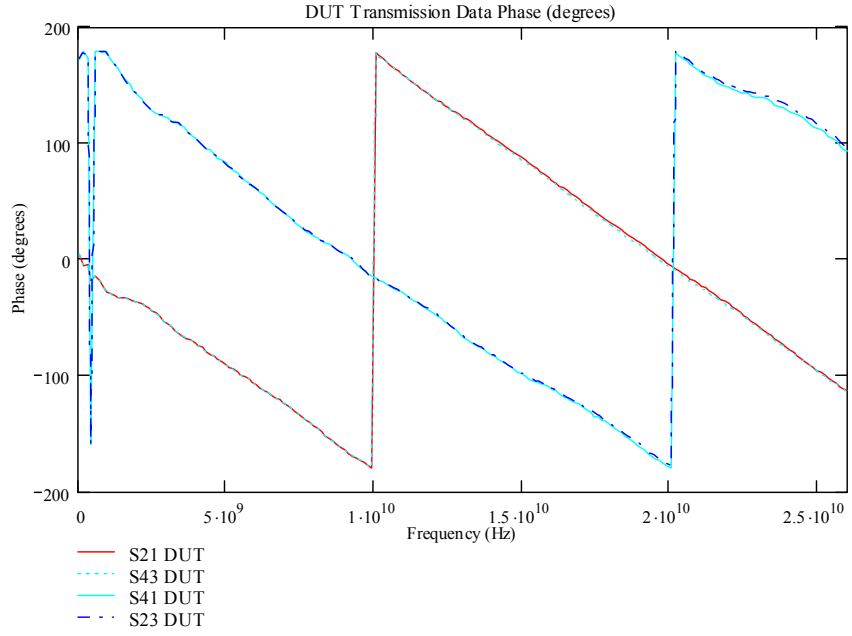

Figure 8.37 – Transmission Phase of the 6600 um Coupled Line Measured with the Multiport cSOLR Calibration.

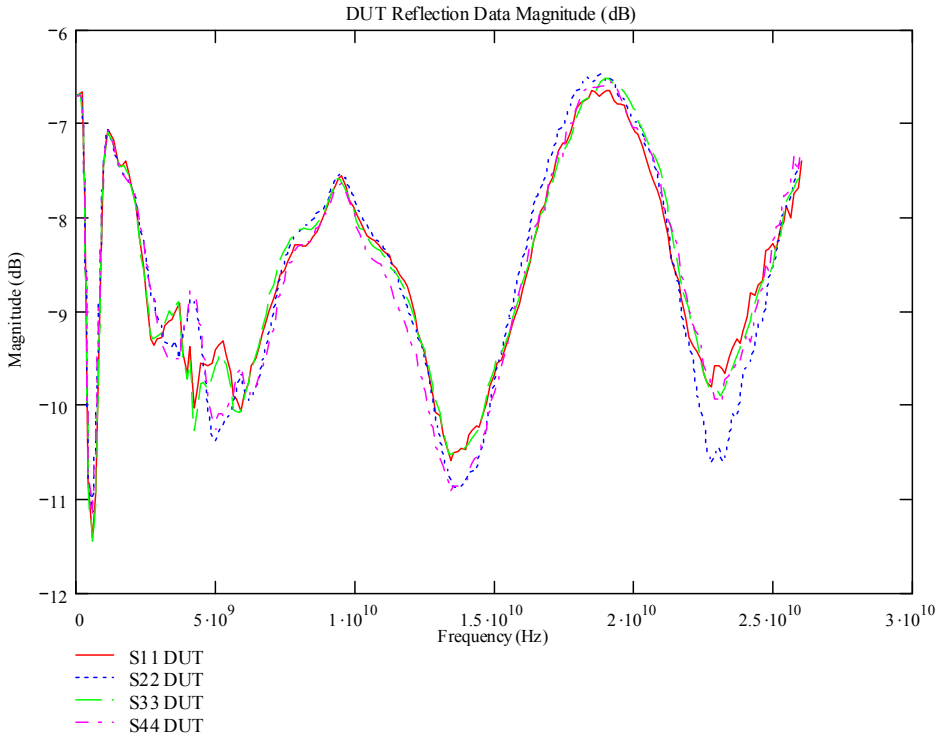

Figure 8.38 – Transmission Magnitude of the 6600 um Coupled Line Measured with the Multiport cSOLR Calibration.

100 Ohm Series Load

The 100 ohm load structure is a very interesting DUT. Ideally the 100 ohm series load would create split the reflection and transmission in half. This is evident in the low frequency portion of the measurements shown in Figures 8.40 and 8.41.

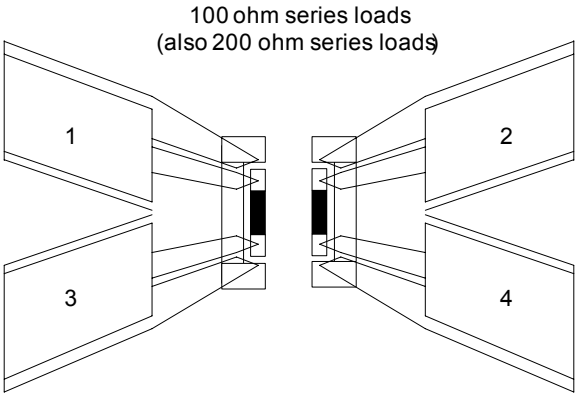

Figure 8.39 – GSSG Layout of 100 Ohm Series Load Pair.

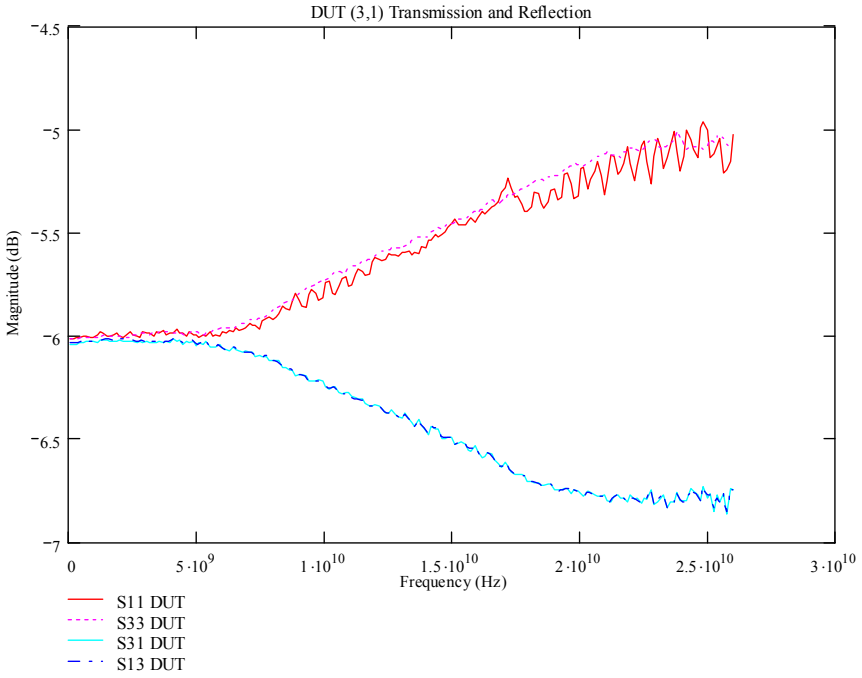

Figure 8.40 – (3,1) Transmission and Reflection Magnitude of the 100 Ohm Series Load Measured with the Multiport cSOLR Calibration.

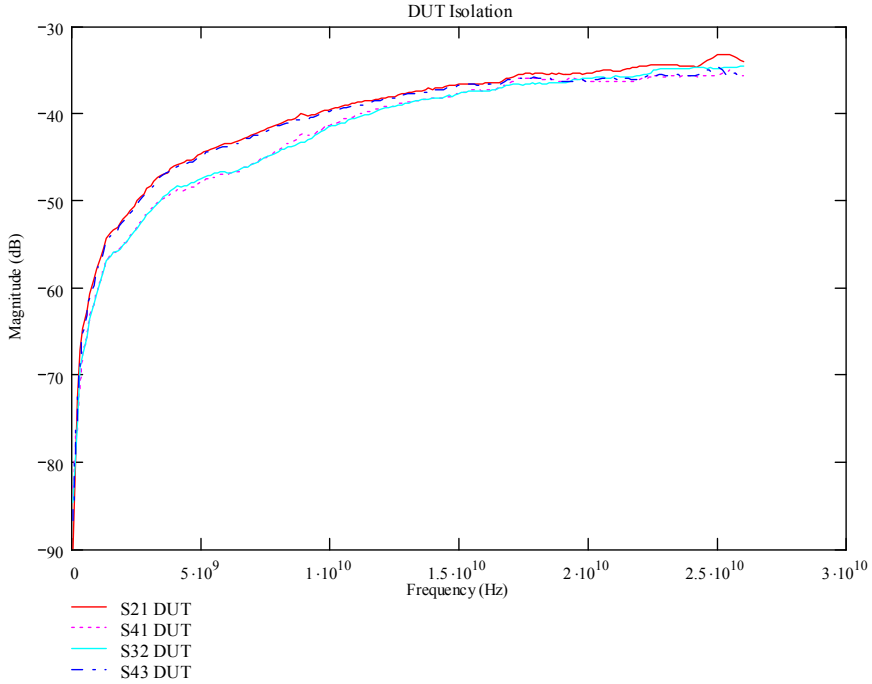

Figure 8.41 – Isolation Magnitude of the 100 Ohm Series Load Measured with the Multiport cSOLR Calibration.

8.5 Chapter Summary

It has been shown in this chapter that multiport cSOLR is a useful multiport calibration method. Multiport cSOLR has been demonstrated by comparing it to other multiport calibrations including NIST 4-port TRL and LRM. The use of multiport cSOLR to perform on-wafer calibrations using GSGSG and GSSG probe setups in which non-ideal transmission standards has been presented. Good agreement is seen between the various calibration methods.

The non-ideal structures found on the GGB CS-2-150 and CS-13-4130 has been characterized using the multiport cSOLR algorithm. It is obvious from looking at the transmission standard measurements that the delay line and loopback transmission standards are far from ideal. Therefore TRL and LRM calibration would not be able to calibrate using these structures. The use of the modified redundancy equations, Section 7.3.3, to calculate the transmission tracking terms, causes very little change in terms of measurement results, versus using all six possible thru measurements.

CHAPTER 9

MULTIPORT CSOLR WITH RECIPROCAL 4-PORT TRANSMISSION STANDARD

The 6600 um coupled line structure on the GGB CS-13-4109, shown in Figure 9.1, allows the exploitation of cSOLR's unique reciprocal properties; because the amount of coupling between the lines provides sufficient transmission to allow calibration [51]. Therefore, rather than measure several transmission structures the 6600 um coupled line will be used for the four needed calibration transmission standards. This is very helpful when performing multiport calibrations, because it will reduce calibration time by reducing the total number of required calibration standard connections.

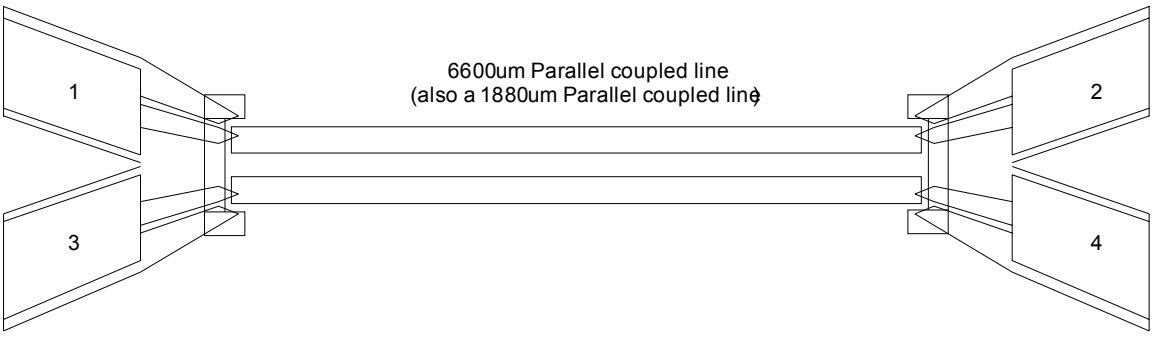

Figure 9.1 – Parallel Line Structure on GGB CS-13-4130 Calibration Substrate.

The measurement data taken using the 4-port structure as the transmission standard will be compared to measurements made with the same multiport cSOLR calibration using the normal 2-port transmission standards that were shown in Section

8.4. Three DUTs will be compared: The 50 ohms loads used in both calibrations, the (1,2) thru, the 6600 um coupled transmission line (Delay 1). The remaining DUT comparison measurements can be found in Appendix D. Because all of the measured DUTs are symmetrical only, one of the redundant isolation and reflection measurement paths will be compared.

9.1 One and Two Port Standards

As an initial verification the reflection magnitude and isolation of the 50 ohm loads, which are used in both calibrations, are shown in Figures 9.2 and 9.3 respectively.

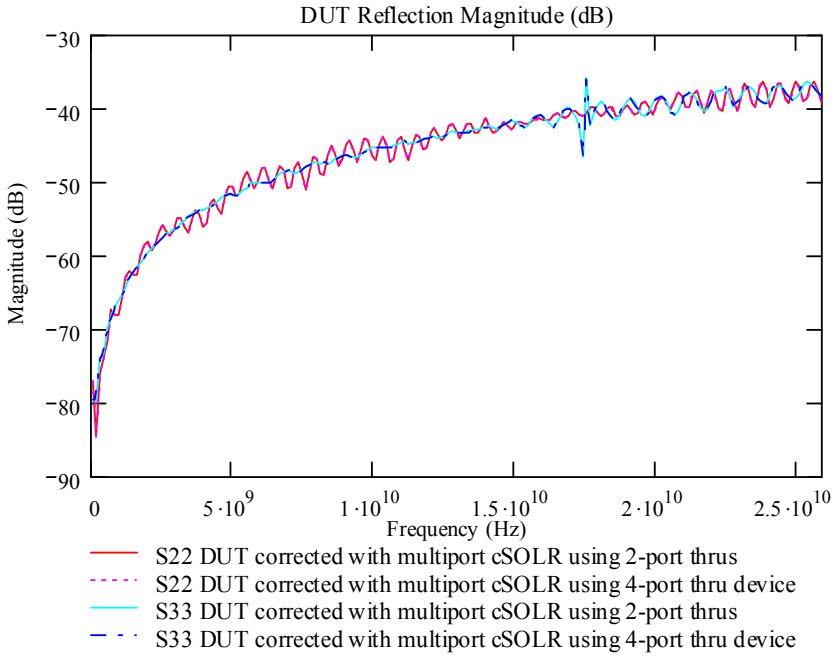

Figure 9.2 – 50 Ohm Loads, Reflection Magnitude Measurements Using a 4-Port Transmission Standard in the Multiport cSOLR Calibration.

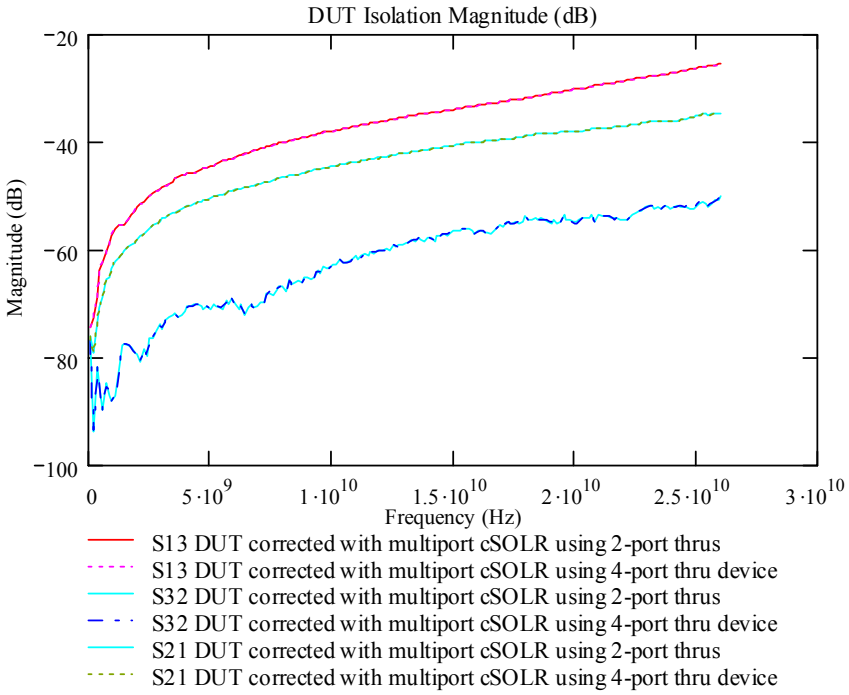

Figure 9.3 – 50 Ohm Loads, Isolation Magnitude Measurements Using a 4-Port Transmission Standard in the Multiport cSOLR Calibration.

It can be seen from Figures 9.2 and 9.3 that there is very good agreement between reflection and isolation measurements made with the two calibrations. This shows that the use of a reciprocal 4-port device for the transmission standards in multiport cSOLR is a viable solution to the problem of having a longer calibration time caused by needing an extra redundant measurement as discussed in Chapter 7. However the match standard represents an ideal case because the isolation is very high. For purposes of the discussion within this section the multiport cSOLR calibration that uses the 4-port reciprocal DUT will be called multiport cSOLmR or complex (Short, Open, Load, multiport Reciprocal multiport).

(1,2) Two-Port Transmission Standard

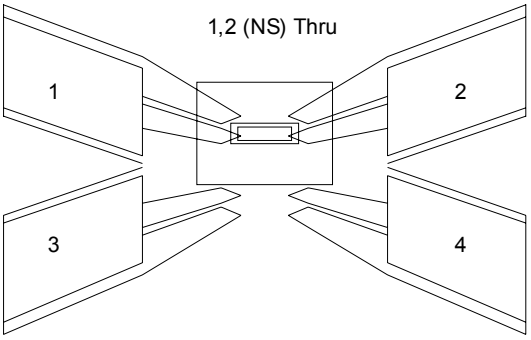

Figure 9.4 – GSSG (1,2) Two-Port Transmission Standard.

It is observed in Figure 9.5 that the reflection magnitude of the (1,2) transmission standard measured using the multiport cSOLmR calibration is slightly degraded compared to the standard multiport cSOLR.

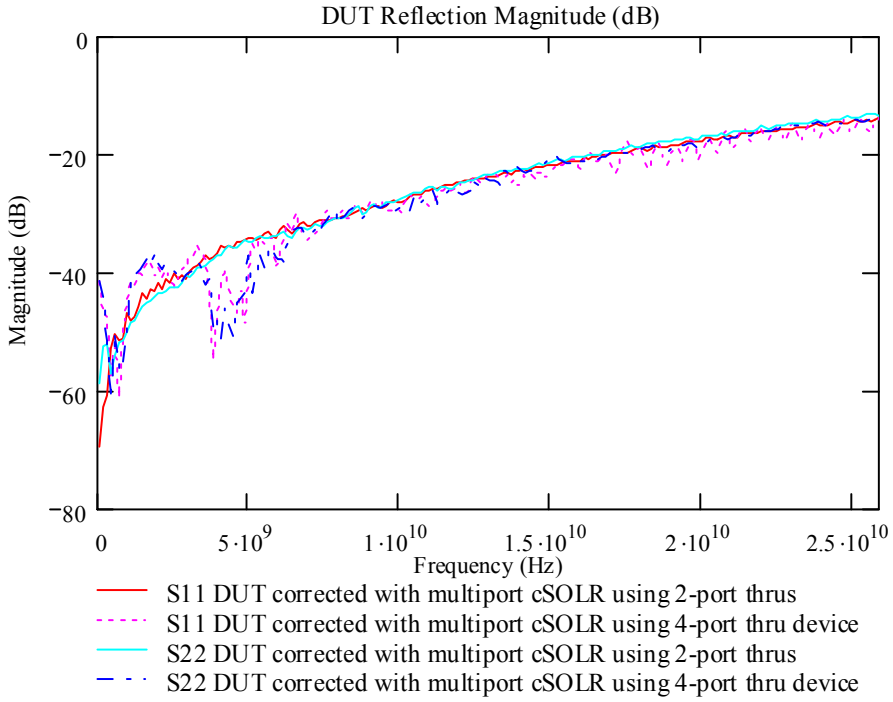

Figure 9.5 – (1,2) Transmission Standard, Reflection Magnitude Measurements Using a 4-Port Transmission Standard in the Multiport cSOLR Calibration.

Figures 9.6 and 9.7 show that this degradation is also present in the transmission measurements. The likely cause for this variance is the differences in the characterization of the auxiliary terminations for the renormalization process. Because the auxiliary terminations are measured through the connection of the transmission standard they are inherently a product of the devices S-parameters. The problem occurs when a device such as the coupled line is connected and for example the port 2 termination is measured by switching to the (1,4) switch configuration.

This measurement will excite port 1 and the desired measured reflection coefficient is only that associated with the transmission line between port 1 and 2 and the termination at port 2. However, because of the coupling what is measured is the desired information plus information of the coupled paths and their terminations as well. The solution to this problem is still being researched however, the problem is minimal and the use of a reciprocal multiport device is shown in these Figures to be feasible concept. More will be discussed on this in Section 9.3.

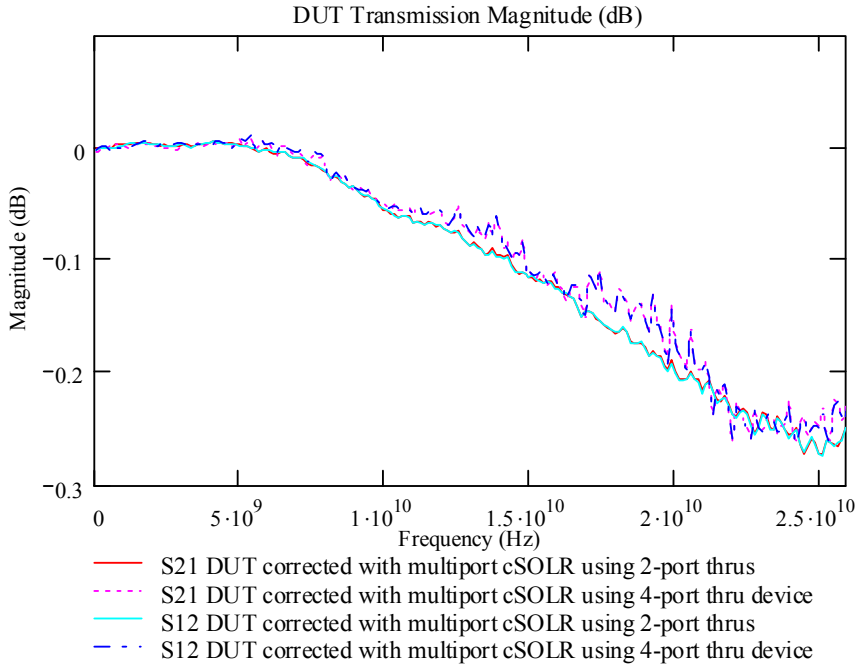

Figure 9.6 – (1,2) Transmission Standard, Transmission Magnitude Measurements Using a 4-Port Transmission Standard in the Multiport cSOLR Calibration.

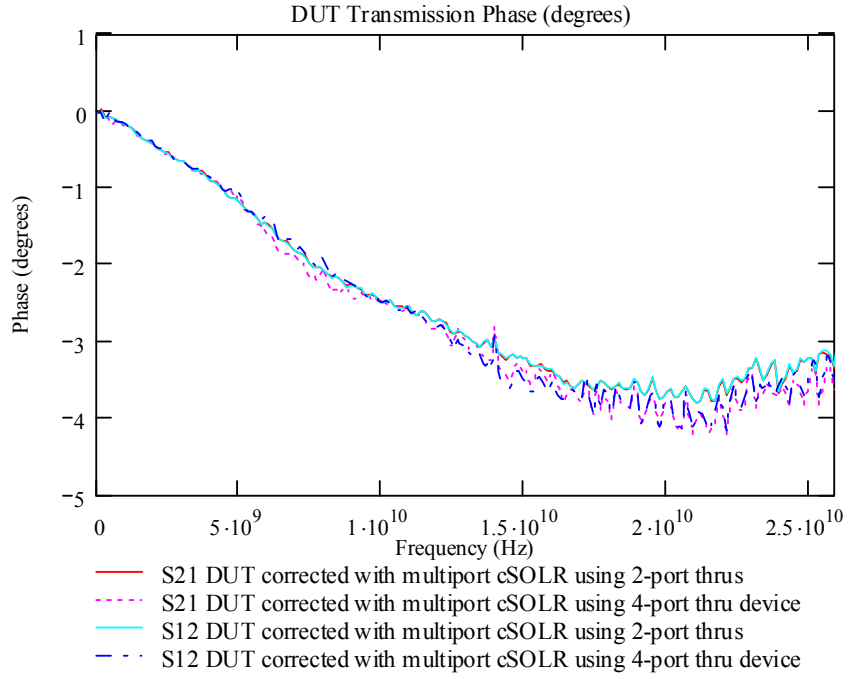

Figure 9.7 – (1,2) Transmission Standard, Transmission Phase Measurements Using a 4-Port Transmission Standard in the Multiport cSOLR Calibration.

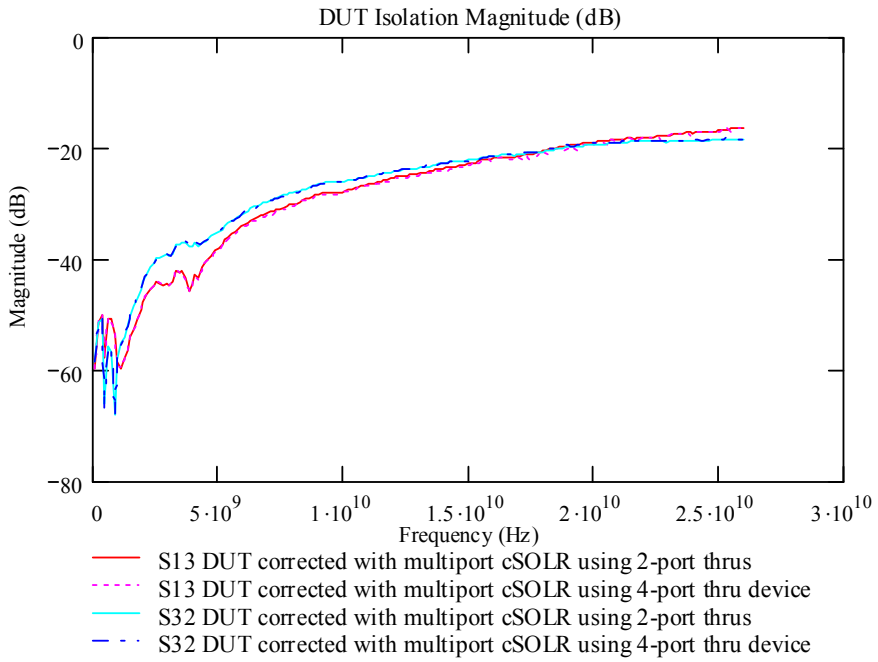

Figure 9.8 – (1,2) Transmission Standard, Isolation Magnitude Measurements Using a 4-Port Transmission Standard in the Multiport cSOLR Calibration.

9.2 The 6600 Parallel Coupled Line Structure

Comparison measurements of the 6600 um coupled line structure, which was used for the cSOLmR calibration, are presented in Figures 9.10 through 9.16. Figure 9.10 shows good agreement between the reflection measurements of the transmission line input ports measured with the multiport cSOLR and cSOLmR. The good agreement between the two calibrations is evident in the transmission measurements of Figures 9.11 through 9.16.

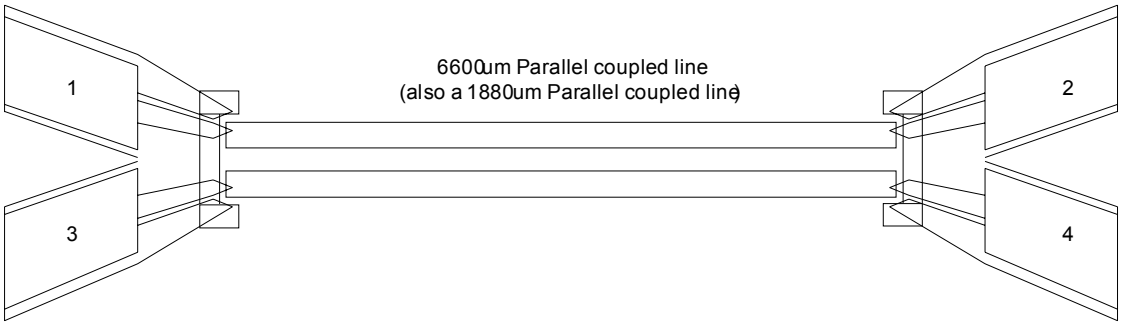

Figure 9.9 – GSSG 6600 um Parallel Line Structure

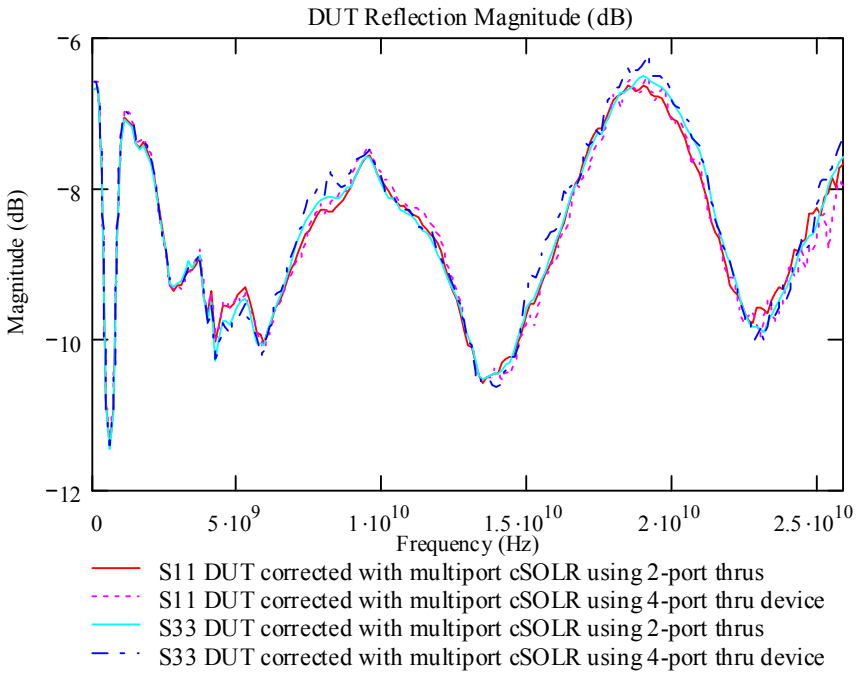

Figure 9.10 – 6600 um Coupled Line Structure (1,2) (3,4), Reflection Magnitude Measurements Using a 4-Port Transmission Standard for Multiport cSOLR Calibration.

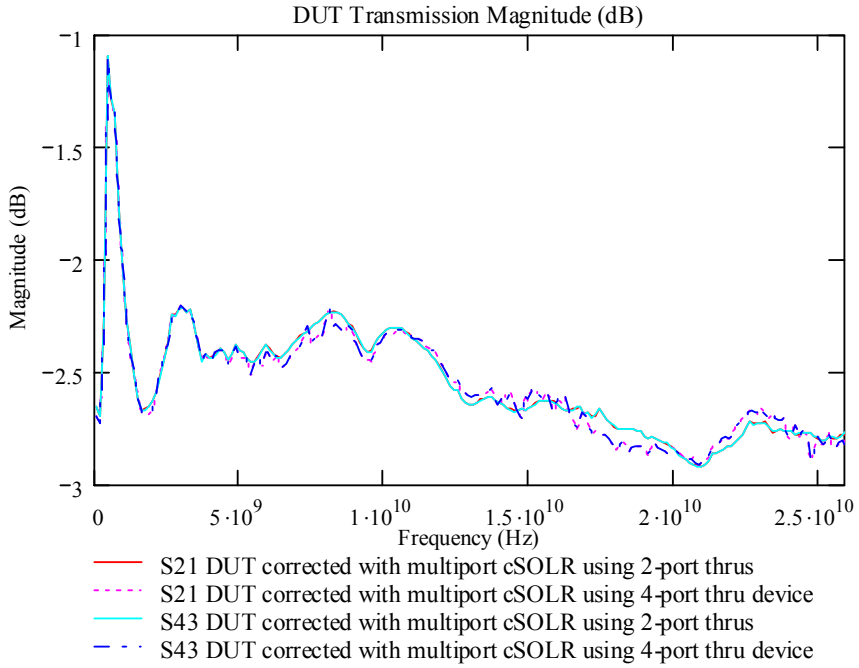

Figure 9.11 – 6600 um Coupled Line Structure (1,2) (3,4), Transmission Magnitude Measurements Using a 4-Port Transmission Standard for Multiport cSOLR Calibration.

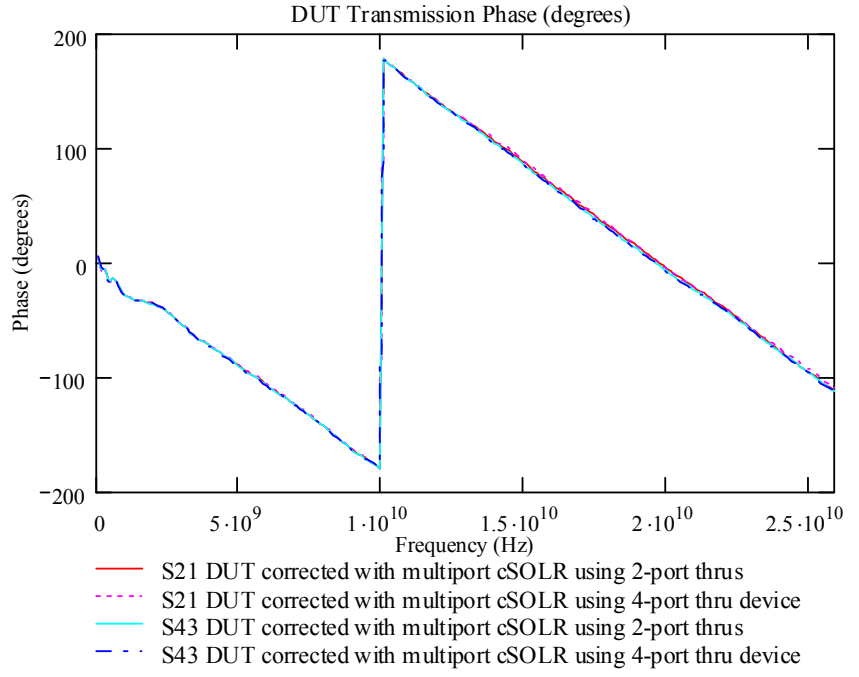

Figure 9.12 – 6600 um Coupled Line Structure (1,2) (3,4), Transmission Phase Measurements Using a 4-Port Transmission Standard for Multiport cSOLR Calibration.

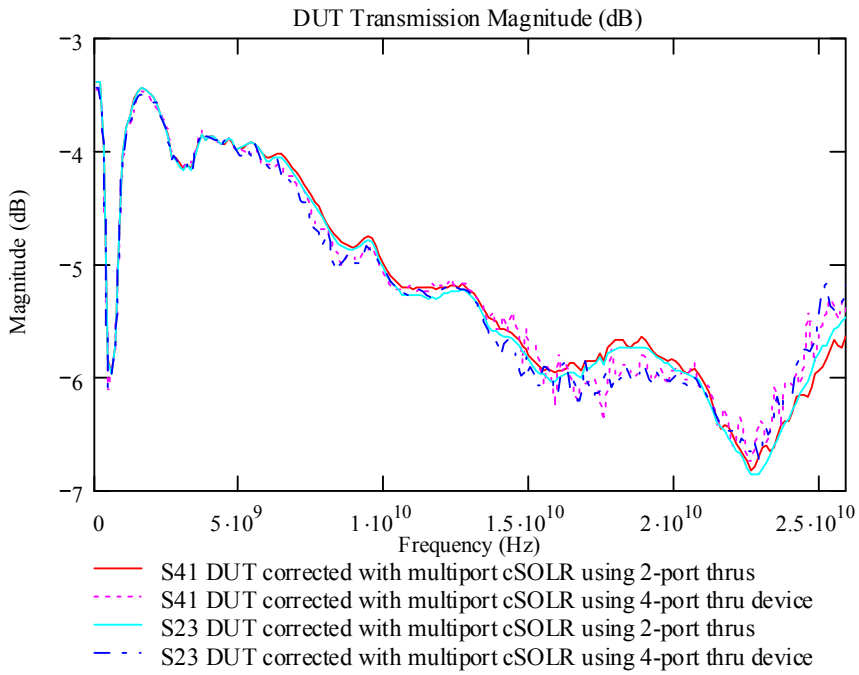

Figure 9.13 – 6600 um Coupled Line Structure (1,4) (3,2), Transmission Magnitude Measurements Using a 4-Port Transmission Standard for Multiport cSOLR Calibration.

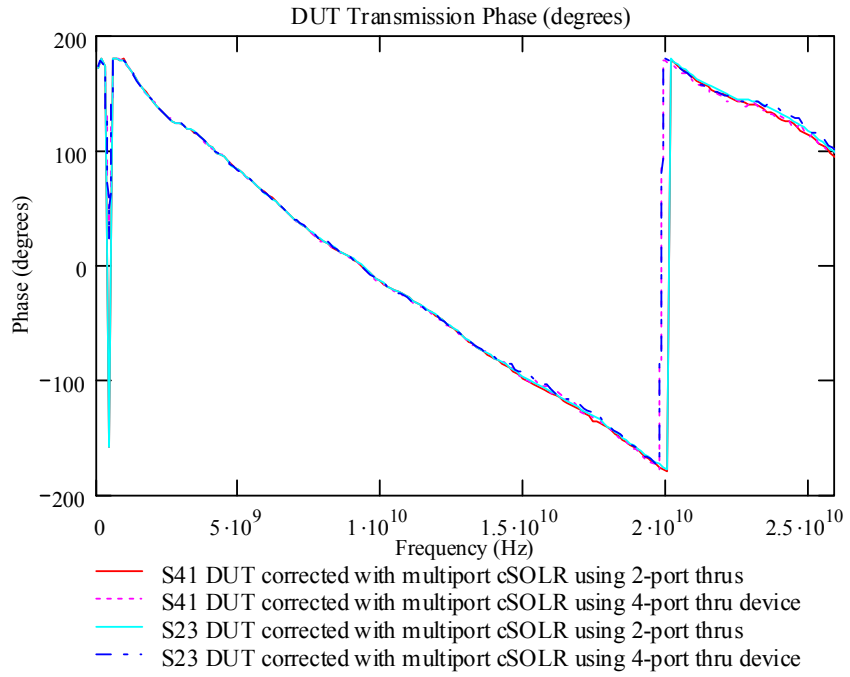

Figure 9.14 – 6600 um Coupled Line Structure (1,4) (3,2), Transmission Phase Measurements Using a 4-Port Transmission Standard for Multiport cSOLR Calibration.

This structure is far from an ideal transmission line. Depending on the measurements that are made the terminating port impedance changes, also, co-planar structures have a tendency to have different propagation velocities for even and odd modes [4].

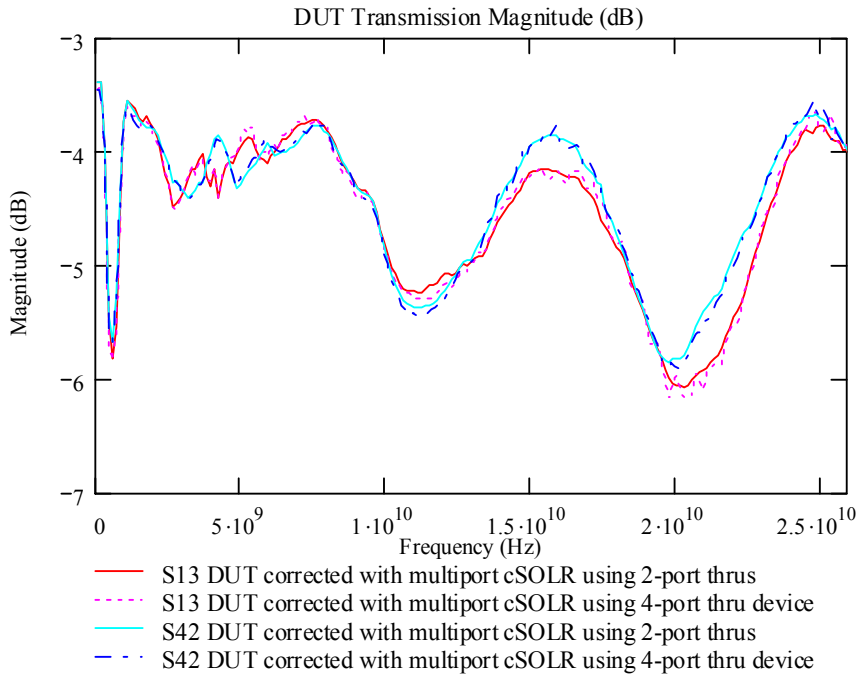

Figure 9.15 – 6600 um Coupled Line Structure (3,1) (2,4), Transmission Magnitude Measurements Using a 4-Port Transmission Standard for Multiport cSOLR Calibration.

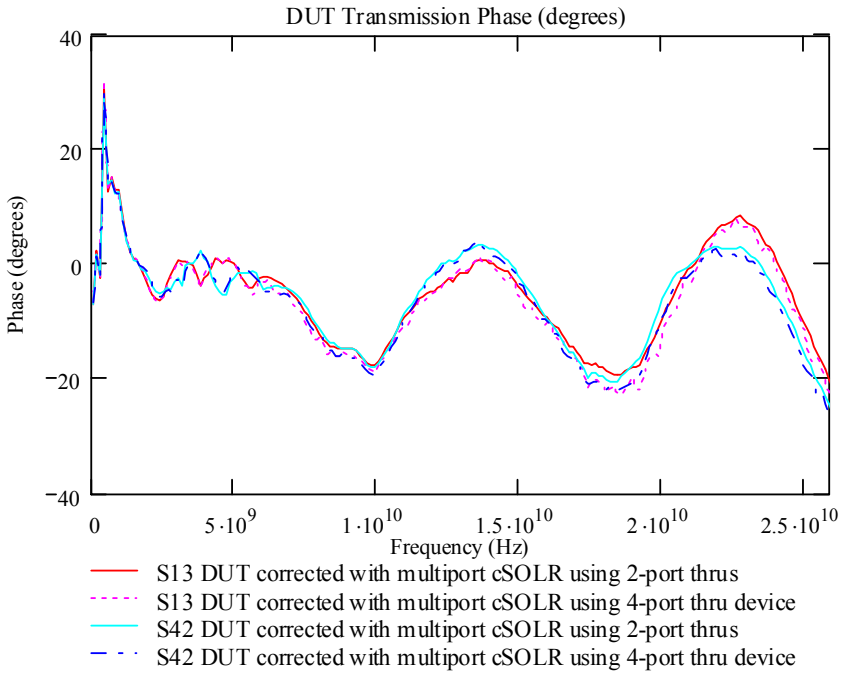

Figure 9.16 – 6600 um Coupled Line Structure (3,1) (2,4), Transmission Phase Measurements Using a 4-Port Transmission Standard for Multiport cSOLR Calibration.

9.3 Problems Measuring Auxiliary Termination on Reciprocal Multiport Devices

On a 2xN system in order to achieve true multiport data the measurements must be renormalized. The renormalization process requires the measurement of the auxiliary terminations used by the switch matrix. The measurement of these terminations usually occurs during two of the transmission standard measurements. The problem with using the reciprocal 4-port standard is that when a reflection coefficient is measured in order to characterize the load what is actually being measured is the reflection coefficient of the entire four-port network which includes the other auxiliary termination as well as the VNA termination. This problem is depicted in Figure 9.17. If the (1,4) two-port correction is applied than the VNA termination can be assumed to be 50 ohms which leaves only Z_1 and Z_3 unknown.

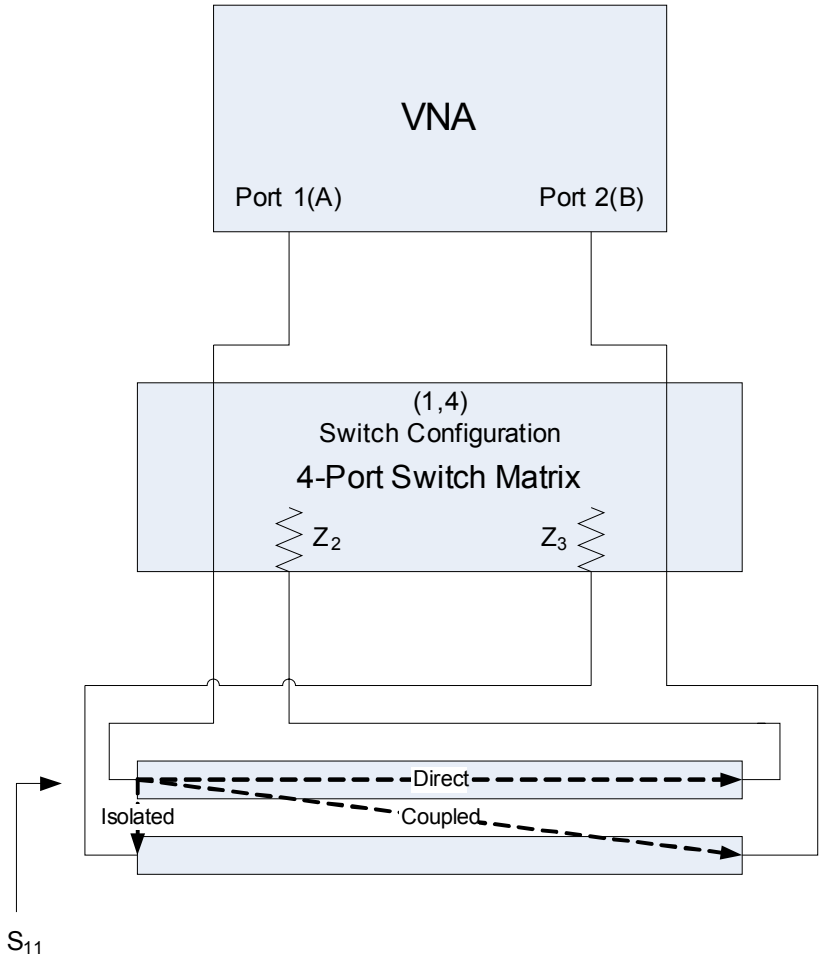

Figure 9.17 – Attempted Measurement of the Z_2 Auxiliary Termination Using a Reciprocal Coupled Line Transmission Standard for Multiport cSOLR.

This problem is shown by comparing the measurements made on the load standards to those of the 6600 um coupled line structure. The data results between the two methods are very similar for the load measurements but are slightly different for the coupled line. This is because the load structure has little to no transmission between the ports and therefore the auxiliary terminations do not greatly affect the measurement. Hence, any problems in the renormalization will not affect the measurements. Therefore the problem must lie in the renormalization otherwise the loads would show the same measurement variation as the coupled lines.

9.4 Chapter Summary

This chapter has demonstrated the use of a 4-port reciprocal device in place of the four required 2-port transmission standards implemented by multiport cSOLR, thereby reducing calibration time and calibration standard real-estate on-wafer. The measurements made with this implementation of a reciprocal multiport calibration standard showed fairly good agreement with the standard characterization using two-port transmission standards in calibration. The problems occurred in measuring the auxiliary terminations for renormalization is believed to be what is causing any of the slight variation between the measurements. Potential solutions will be discussed in Chapter 10.

CHAPTER 10

CONCLUSIONS AND RECOMMENDATIONS

10.1 Conclusions

A relatively thorough theoretical development for network analyzer calibrations has been presented using either the 12-term or 8-term error model. Throughout this theory special care was given so that a single consistent error term convention could be used both in either two port models or the multiport error models. Emphasis was also placed on the use of switch term corrected data many authors tend not to fully address when developing and implementing 8-term algorithms, this can sometimes become confusing and it is clearly defined within this thesis.

After laying the foundation for conventional SOLR theory, in Chapter 4, it was shown in Chapter 5 that by using a more complex model to better characterize the load standard (as compared to the conventional series RL model or perfect load assumption) the high frequency accuracy of SOLR can be improved.

This improved SOLR algorithm, termed cSOLR herein, was the first step toward accomplishing the ultimate goal of the thesis, which was to establish and demonstrate an accurate broadband multiport calibration that can utilize non-ideal transmission structures and be performed on the available 2xN multiport system. This was accomplished by applying the multiport cSOLR algorithm to a 2xN switch matrix calibration method.

The adaptation of the cSOLR algorithm to a 2xN system required the development of a modified redundancy equation to calculate the transmission terms (Section 7.3.3)

Since 2xN systems essentially uses two-port calibrations to achieve a four-port measurements, the accuracy increase that was seen in the two-port case of cSOLR is carried over to the multiport case. Therefore, multiport cSOLR will be more accurate at high frequencies than multiport SOLR for calibration standard sets that include load models that cannot adequately be represented by the conventional load model.

It can be concluded that multiport cSOLR provides for an accurate broadband calibration, comparable in accuracy to a multiport multiline TRL algorithm; if one could be performed. Accurate multi-port TRL calibrations are not a given for many situations of interest, because of the non-ideal nature of typical commercially available transmission line standards for GSGSG and GSSG probe setups.

That said, it was possible to show(in Chapter 8) that the multiport cSOLR calibration has comparable accuracy to NIST's multiport LRM and TRL algorithms when the LRM and TRL algorithms are performed on well behaved line standards. A minimal solution for the number of transmission standard connections needed for calculating the transmission tracking terms was found. Though the number of connections is one more than other multiport calibrations it functions on a 2xN system that the others do not.

Another advantage of multiport cSOLR (or SOLR) that was demonstrated preliminarily is the possibility to use a reciprocal multiport device such as a coupled line structure as the transmission calibration standard.

This attribute allows faster on-wafer calibration times by reducing the number of needed connections. However, more work is needed to fully implement a more rigorous implementation of this idea.

10.2 Recommendations for Future Work

Much work can be built upon the work presented here. One possibility for improvement would be to find a more optimal solution to the calculation of the transmission tracking terms via redundancies than the one presented in Section 7.3.3 in order to allow more flexibility. This has not been published for a 2xN and the optimal solution for a true multiport system is already well developed as discussed in Section 7.2.2.

The proposed conceptual error box model of the 2xN system was shown in Chapter 7. If the errors associated with the VNA from the sampler to the first multiplexing switch could be isolated from the errors from the switch to the DUT, then the error dependence of switch matrix port to the VNA port connection could potentially be eliminated. Essentially the errors associated with the switch matrix could be separated from the errors of the analyzers reflectometers. This would allow the characterization of any transmission standard from redundancy by cascading it with the appropriate VNA port error. This two tier concept is similar to that presented in [36] although the exact solution and the use of a cascade error model may be different.

Further demonstration of the utility of cSOLR versus conventional SOLR could be accomplished through the development and use of on-board (or on-wafer) multi-port calibration structures that used less well-behaved load standards. It is suggested that both 50 ohm and non-50 ohm characteristic impedances and corresponding load standards be utilized. For example it would be interesting to see how well one can do in establishing a broad-band multi-port 10 ohm or say 200 ohm S-parameter calibration. Additional multi-port DUT device validations would be helpful as well including those targeting varying impedance calibrations, as well as passive and active differential mode devices.

The use of a reciprocal 4-port transmission standard in the multiport cSOLR algorithm has great potential to reduce the number of needed calibration standards as well as the calibration time. By reducing the number of needed standards not only is valuable on-wafer real-estate conserved but the number of probe lifts and reconnects is also reduced saving valuable measurement time.

However, there is so far an unsolved problem of measuring the auxiliary terminations through multiport transmission structures that as discussed in Chapter 9. However, if all the transmission paths are measured, not just between those that have a physical connection then it stands to reason that there would be enough measurement redundancy to isolate the individual auxiliary termination reflections. Additional theoretical work may reveal enough information to solve for all the switch terminations from the multiport reciprocal device calibration.

Also, the available reciprocal 4-port device was a pair of parallel strip transmission lines without corresponding ground line paths and future work should explore use of different types of 4-port reciprocal devices.

Another idea for reducing the number of standard connection requirements is to use on-wafer diodes for the reflectometer standards. In prior work, [55] used a varactor diode as the reflection standard to accomplish in-fixture calibrations. By characterizing the diodes at three unique biases one would be able to connect the three needed reflectometer standards use in cSOLR electronically and thus create an on-wafer e-cal. This would greatly speed up calibration time for on-wafer multiport measurement.

In short a complete development of a multiport cSOLR calibration which is able to use non-ideal transmission and load standards and achieve broadband accuracy has been presented The calibration can be perform on a 2xN system using a minimum of 4 two-port transmission or a single 4-port transmission standard by using a modified redundancy relationship.

REFERENCES

[1] Lesher, T.; Hayden, L., A high isolation dual signal probe technology" *ARFTG Microwave Measurements Conference, Fall 2004. 64th* 2-3 Dec. 2004 Page(s):167 – 171.

[2] Kruppa, W.; Sodomsky, K.F., "An Explicit Solution for the Scattering Parameters of a Linear Two-Port Measured with an Imperfect Test Set (Correspondence)" Microwave Theory and Techniques, IEEE Transactions on Volume 19, Issue 1, Jan 1971 Page(s):122 – 123.

[3] H. J. Eul and B. Schiek, "A Generalized Theory and New Calibration Procedures for Network Analyzer Self-Calibration," *IEEE Trans. on Microwave Theory & Techniques,* vol. 39, April 1991, pp 724-731.

[4] A. Davidson. E. Strid. and K. Jones "Achieving greater on-wafer S-parameter accuracy with the LRM calibration technique." *IEEE ARFTG Digest* Dec. 1989.

[5] Engen, G.F.; Hoer, C.A., "Thru-Reflect-Line: An Improved Technique for Calibrating the Dual Six-Port Automatic Network Analyzer" Microwave Theory and Techniques, IEEE Transactions on Volume 27, Issue 12, Dec 1979 Page(s):987 – 993.

[6] Ferrero, U. Pisani, "Two-port Network Analyzer Calibration Using Unknown Thru," *IEEE Microwave and Guided Wave Letters*, Vol.2, No 12, December 1992.

[7] Basu, S.; Hayden, L., "An SOLR calibration for accurate measurement of orthogonal on-wafer DUTs", *Microwave Symposium Digest, 1997*, IEEE MTT-S International Volume 3, 8-13 June 1997 Page(s):1335 - 1338 vol.3.

[8] Roger B. Marks, "A Multiline Method of Network Analyzer Calibration", IEEE Transactions on Microwave Theory and Techniques, Vol. 39, No 7, July 1991.

[9] D. F. Williams and R. B. Marks, "Accurate Transmission Line Characterization," *IEEE Microwave and Guided Wave Letters*, vol. 3, no. 8, pp. 247-249, Aug. 1993.

[10] S. Padmanabhan, "Broad-Band Space Conservative On Wafer Network Analyzer Calibrations With More Complex SOLT Definitions*," Master's Thesis, University of South Florida.*

[11] S. Padmanabhan, P. Kirby, J. Daniel, L. Dunleavy, "Accurate Broadband on-wafer SOLT calibrations with Complex Load and Thru Models," *61st ARFTG Conference Digest*, June 2003.

[12] Andrew Davidson, Keith Jones, Eric Strid, "LRM and LRRM Calibations With Automatic Determination of Load Inductance," Cascade Microtech, Inc.

[13] Doug Rytting, "Network Analyzer Error Models and Calibration Methods," 54th ARFTG Conference short notes, December 2000.

[14] David M. Pozar, Microwave Engineering, 2nd edition, John Wiley & Sons, Inc.

[15] Agilent technologies, "Agilent Technologies and Communications: Six Decades of Measurement Contributions", publication 5980-2090E.

[16] R.A. Hackborn, "An automatic network Analyzer System", *Microwave Journal*, May, 1968.

[17] Agilent Technologies "Network Analyzer Basics" from the Agilent back to basics seminar.

[18] Hoer, C.A, "A Network Analyzer Incorporating Two Six-Port Reflectometers" Microwave Theory and Techniques, IEEE Transactions on Volume 25, Issue 12, Dec 1977 Page(s):1070 – 1074.

[19] Roger B. Marks, "Formulations of the Basic Vector Network Analyzer Error Model Including Switch Terms," *50th ARFTG Conference Digest*, Fall 1997, pp 115-126.

[20] Rehnmark, S., "On the Calibration Process of Automatic Network Analyzer Systems (Short Papers)"Microwave Theory and Techniques, IEEE Transactions on Volume 22, Issue 4, Apr 1974 Page(s):457 – 458.

[21] M. Imparato, T. Weller, and L. Dunleavy, "On-wafer calibration using space conservative (SOLT) standards," *1999 IEEE MTT-S Int'l Microwave Symposium*, June 1999.

[22] P. Kirby, "Improved Vector Network Analyzer Calibrations utilizing Lumped Element Standards," Master's Thesis, *University of South Florida*.

[23] Agilent Technologies, “Specifying Calibration Standards for the Agilent 8510 Network Analyzer”, Application Note 8510-5B.

[24] Donald C. DeGroot, Jeffrey A. Jargon, Roger B. Marks, “Multiline TRL Revealed,” *60th ARFTG Conference Digest*, pp 131-155, December 2002.

[25] Williams, D.F., Marks, R.B., “LRM probe-tip calibrations using non-ideal standards”, Microwave Theory and Techniques, IEEE Transactions on Volume 43, Issue 2, Feb. 1995 Page(s):466 – 469.

[26] Andrea Ferrero and Umberto Pisani, “QSOLT: A new Fast Calibration Algorithm for Two Port S Parameter Measurements,” *38th ARFTG Conference Digest,* Winter 1991, pp 15-24.

[27] Dylan Williams, National Institute of Standards and Technology, StatistiCAL V1.1.39 software.

[28] Dylan Williams, Jack C. M. Wang, Uwe Arz, “An Optimal Vector Network Analyzer Calibration Algorithm”. IEEE transactions December 2003.

[29] Cascade Microtech’s Wincal™ software.

[30] R. B. Marks, J. A. Jargon, John R. Juroshek, “Calibration Comparison Method for Vector Network Analyzers,” *48th ARFTG Conf. Digest*, pp 38-45, Dec 5-6 1996.

[31] GGB Industries, P.O.Box 10958, Naples FL 34101.

[32] Michael Imparato, "Investigation on the Accuracy of Calibration for On-Wafer MM-Wave Measurements," MSEE Master’s Thesis, *University of South Florida.* April 9, 1999.

[33] M/A Com 1011 Pawtucket Blvd.Lowell, MA 01853, www.macom.com.

[34] Agilent application note 1373-2 – Concepts in Balanced Device Measurements.

[35] Tippet, J.C.; Speciale, R.A., “A Rigorous Technique for Measuring the Scattering Matrix of a Multiport Device with a 2-Port Network Analyzer,” Microwave Theory and Techniques, IEEE Transactions on Volume 82, Issue 5, May 1982 Page(s):661 – 666.

[36] Dylan F. Williams, David K. Walker, “In-line Multiport Calibration Algorithm”. *51st ARFTG Conference Digest* , pp. 88-90, June 12, 1998.

[37] Anritsu Technical Data Sheet “Microwave Multiport Balanced VNA.”

[38] N. Bouleifen, A. Ferrero, F.M. Ghannouchi, A.B. Kouki, "An Automated N-port Network Analyzer for Linear and Non-linear Multiport RF and Digital Circuits", *IEEE Instrumentation and Measurement Technology Conference*, May 1997.

[39] A. Ferraro, U. Pisani, K.J. Kerwin, "A new implementation of a multiport automatic network analyzer", IEEE Transactions on Microwave Theory and Techniques, November 1992.

[40] Agilent Physical Layer Test Systems – Data Sheet.

[41] Agilent PNA Series RF Network Analyzer – Data Sheet.

[42] Bockelman,D.E.; Eisenstadt,W.R, "Combined differential and common-mode scattering parameters: theory and simulation"; Microwave Theory and Techniques, IEEE Transactions on Volume 43, Issue 7, Part 1-2, July 1995 Page(s):1530 – 1539.

[43] Maxim Integrated Products, Application Note HFAN-5.1.0, "Single-Ended and Differential S-parameters".

[44] Douglas Brooks, "Differential Signals, the Differential Difference".

[45] D.E. Bockelman, W.R. Eisenstadt, "Pure mode network analyzer for On-wafer measurements of mixed mode S-parameters of differential circuits", IEEE Trans Microwave theory, vol. MTT-45, July 1997.

[46] Joel Dunsmore, "New Methods & Non-Linear Measurements for Active Differential Devices", *IEEE Microwave Symposium Digest*, June 2003.

[47] Seguinot, C.; Kennis, P.; Legier, J.-F.; Huret, F.; Paleczny, E.; Hayden, L., "Multimode TRL. A new concept in microwave measurements: theory and experimental verification," Microwave Theory and Techniques, IEEE Transactions on; Volume 46, Issue 5, Part 1, May 1998 Page(s):536 – 542.

[48] Buber, T.; Rodriguez, A.; Jenkins, A.; Mahon, J.; Liss, C.; Lanteri, J.-P.; Kinayman, N.; Wohlert, R.; Gresham, I.; Khalil, A.; Bennett, J.; Dunleavy, L.P., "Multimode TRL and LRL calibrated measurements of differential devices," *ARFTG Microwave Measurements Conference, Fall 2004. 64th* 2-3 Dec. 2004 Page(s):157 – 166.

[49] Ferrero, A.; Sampietro, F.; Pisani, U., "Multiport vector network analyzer calibration: a general formulation," Microwave Theory and Techniques, IEEE Transactions on Volume 42, Issue 12, Part 1-2, Dec 1994 Page(s):2455 – 2461.

[50] NISTCal Four-Port Measurement software, developed by the NIST/Industrial Measurement Consortium.

[51] Martens, J., "Multiport SOLR calibrations: performance and an analysis of some standards dependencies," *ARFTG Microwave Measurements Conference, 2003*. Fall 2003. 62nd 4-5 Dec. 2003 Page(s):205 – 213.

[52] Wei-Kung Deng; Tah-Hsiung Chu, "A three-port vector network analyzer - measurement system, calibration and results," Microwave *Symposium Digest, 2001 IEEE MTT-S International* Volume 3, 20-25 May 2001 Page(s):1531 - 1534 vol.3.

[53] Cascade Microtech, 2430 NW 206th Avenue Beaverton, OR 97006.

[54] W. L. Gore, 402 Vieve's Way Elkton, MD 21921.

[55] Peck, D.E.; Peterson, D.F.; "A Measurement Method for Accurate Characterization and Modeling of MESFET Chips," *Microwave Symposium Digest, MTT-S International Volume 81*, Issue 1, Jun 1981 Page(s):310 – 312.

APPENDICES

APPENDIX A: MULTIPORT CSOLR METHOD ON A 2XN SYSTEM FLOW DIAGRAM

This appendix will detail a programmatic flow diagram of the multiport cSOLR algorithm for a 2xN System. This diagram can be used in conjunction with the step by step process for performing a multiport cSOLR calibration on a 2x4 system. The flow chart is broken into two parts the first is standard characterization and modeling and the second is multiport cSOLR measurements. Out put variables are given by a trapezoidal shape at the bottom while input variable are in the trapezoidal shapes at the top.

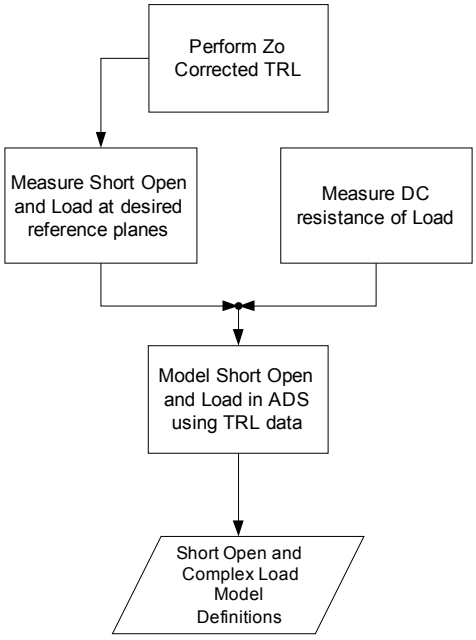

Figure A.1 – SOL Standard Characterization and Modeling Flow Diagram.

Once the short open and load have been modeled over the desired frequency range the multiport cSOLR calibration can be performed. The calibration begins by making measurements of the calibration standards and the DUTs. The flow diagram of the measurement routine for the multiport cSOLR method is shown in Figure A.2.

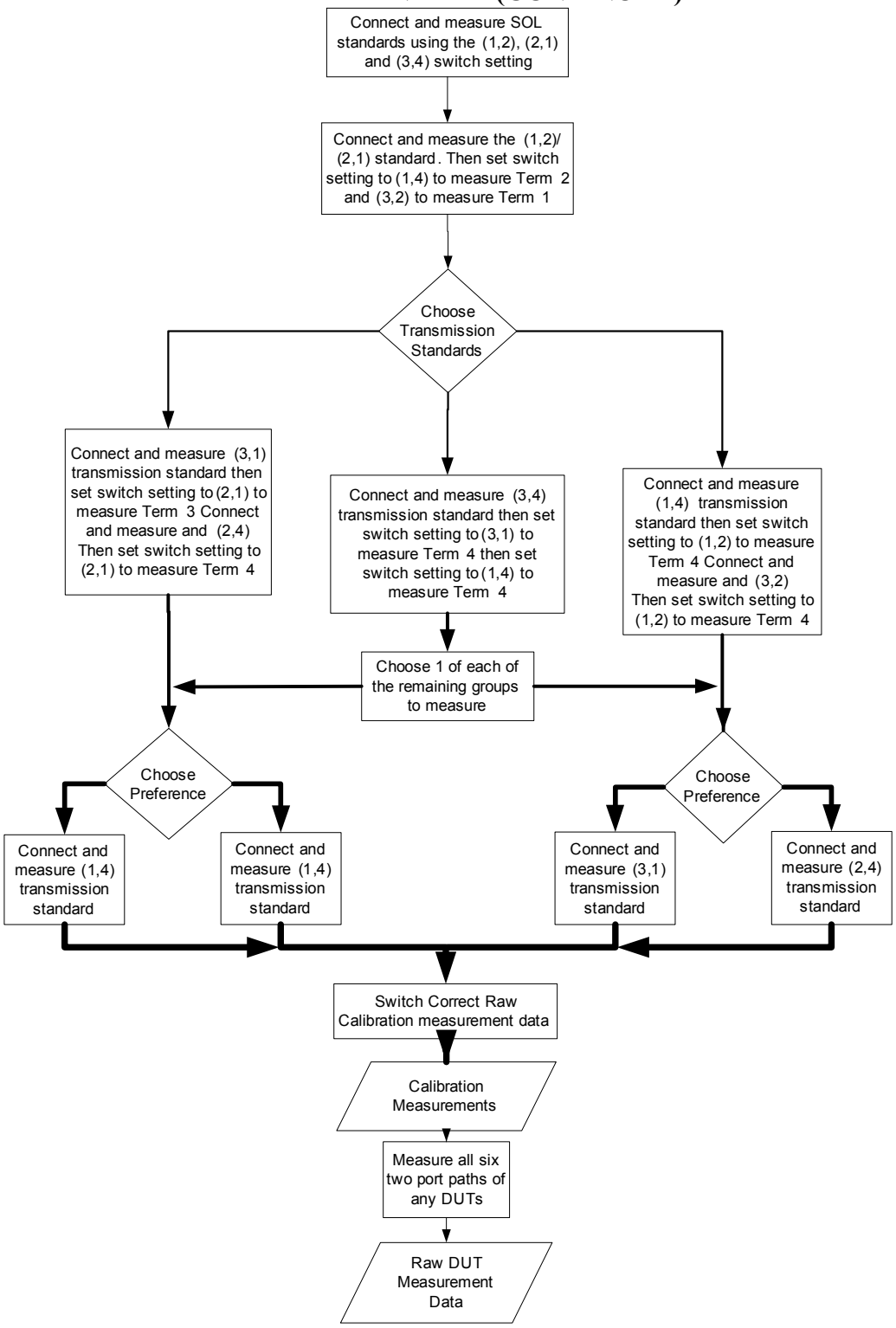

Figure A.2 – Multiport cSOLR Calibration Standard and DUT Measurement Routine Flow Diagram.

Once the measurement and DUT raw data is taken the calibration process can begin. Figure A.3 details this process.

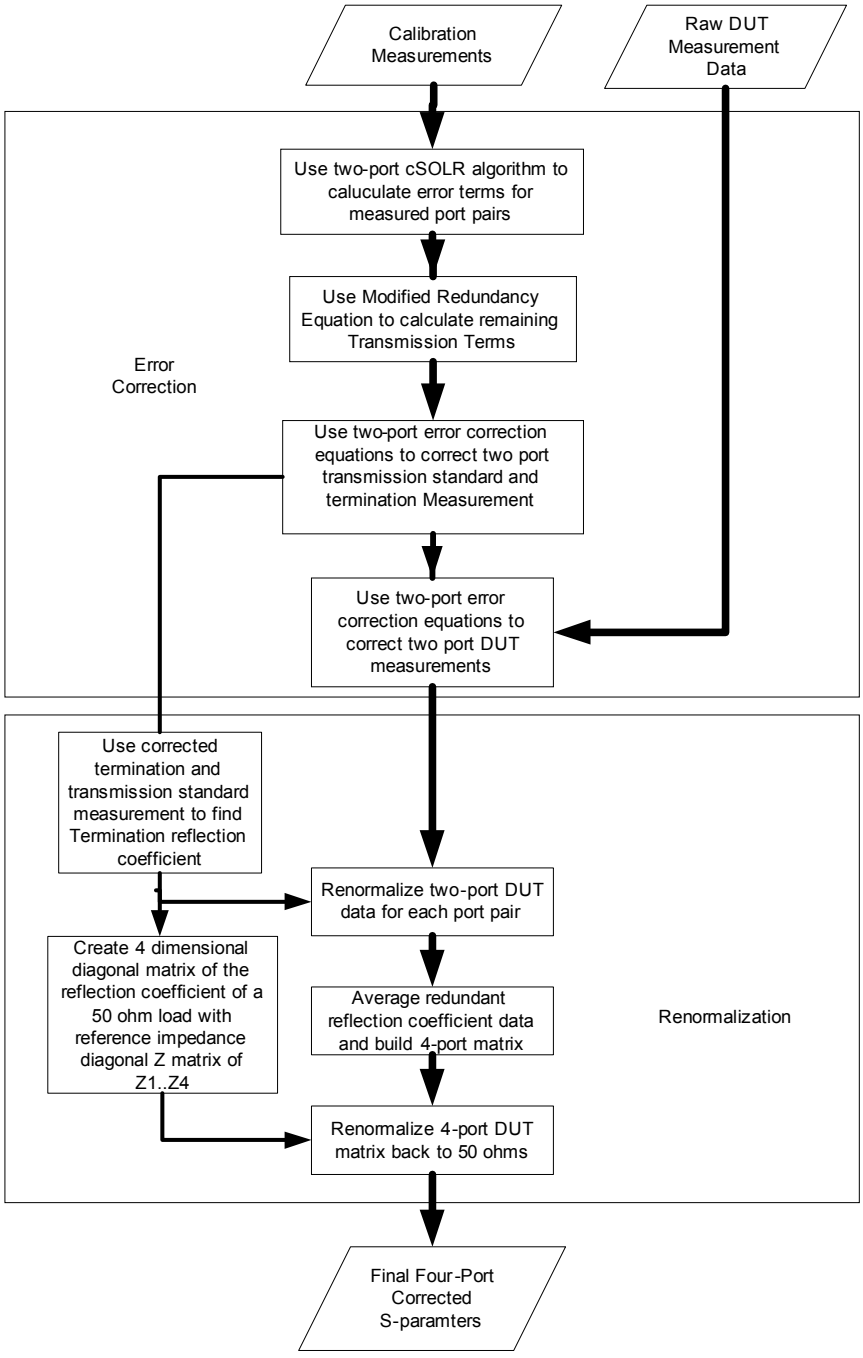

Figure A.3 – 2x4 System Error Correction and Renormalization Flow Diagram.

APPENDIX B: GGB CS-2-150 CALIBRATION SUBSTRATE MEASUREMENTS

This appendix contains the remaining measurements performed on the GGB CS-2-150 substrate. Characterization of the DUTs are shown in Section B.1 and the remaining comparison measurements of multiport cSOLR to NISTcal 4-port TRL are shown in Section B.2

B.1 Additional GGB CS-2-150 Characterization Measurements

The measurements shown in this section are the remaining characterization measurements from Section 8.2.1. The DUTs are from the GGB CS-2-150 and have been characterized using the 6/2 multiport cSOLR method. The open and short reflections standards are presented first and then the parallel, offset and U thru standards are presented. Finally the 1880 um parallel delay line is shown.

Open

It can be seen in figure B.1 that the port 4 reflection magnitude has a larger ripple than the rest. This is most likely do to the less than ideal K female to female adapter which was used on this port. This adapter was almost out of spec with respect to its pin depth and was slightly worn. This mismatch may have cause the raw directivity of the system to be reduced for the port four connection and thereby causing a little more ripple. However, this ripple is small and not of concern for the measurements shown. Figure B.3 shows that the isolation of the open is far less for the inter-probe signal paths.

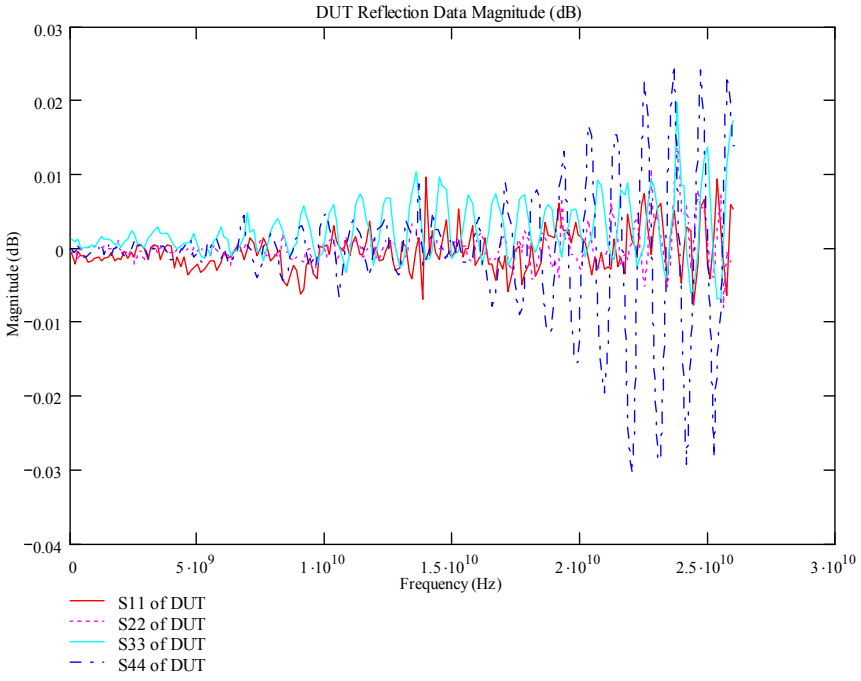

Figure B.1 - Calibrated Open Reflection Magnitude Using the 6/2 Multiport cSOLR Calibration Routine.

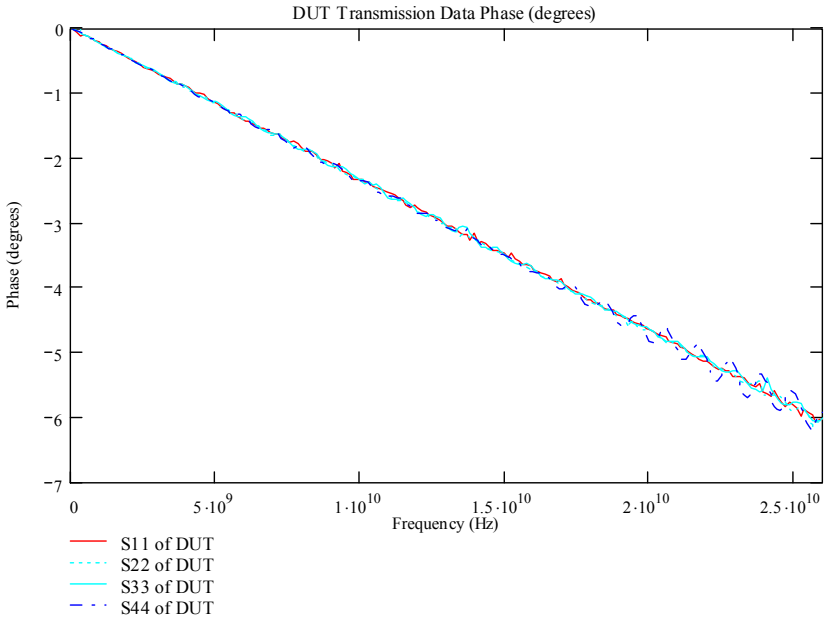

Figure B.2 - Calibrated Open Reflection Phase Using the 6/2 Multiport cSOLR Calibration Routine.

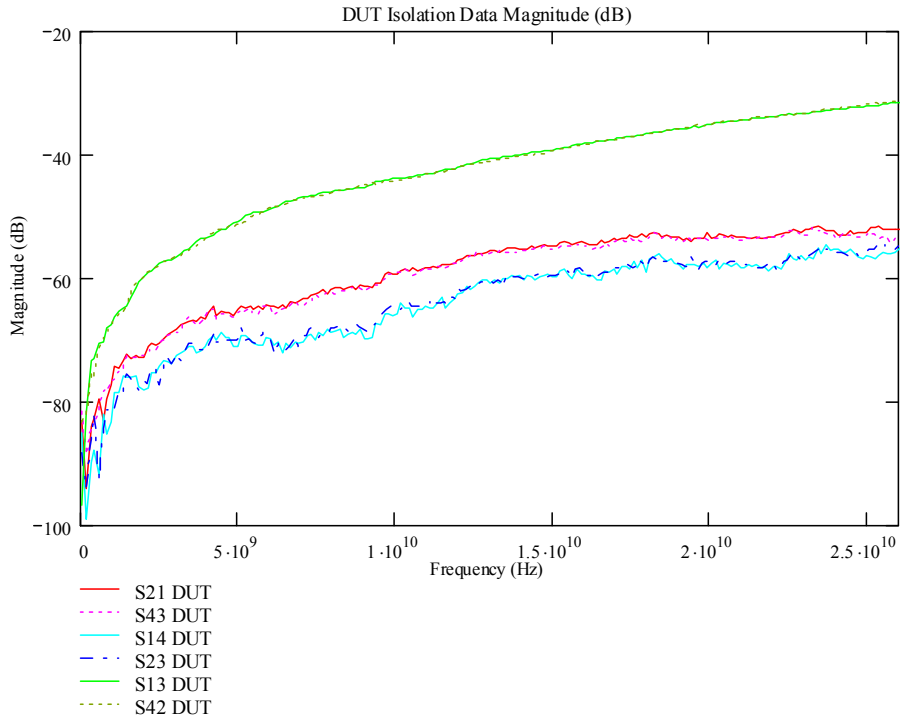

Figure B.3 - Calibrated Open Isolation Data Using the 6/2 Multiport cSOLR Calibration Routine.

Short

Figures B.4 – B.6 show the short standards. The shorting bars connect the GSGSG connections of each probe to a single shorting bar. It makes since that the isolation of the inter-probe signal paths are reduced because of their mutual connection. In comparing the isolation of the short standards shown in Figure B.6 to the isolation of the opens B.3 the fact that the straight transmission paths have more isolation in the short may indicate some radiated coupling in the open standard.

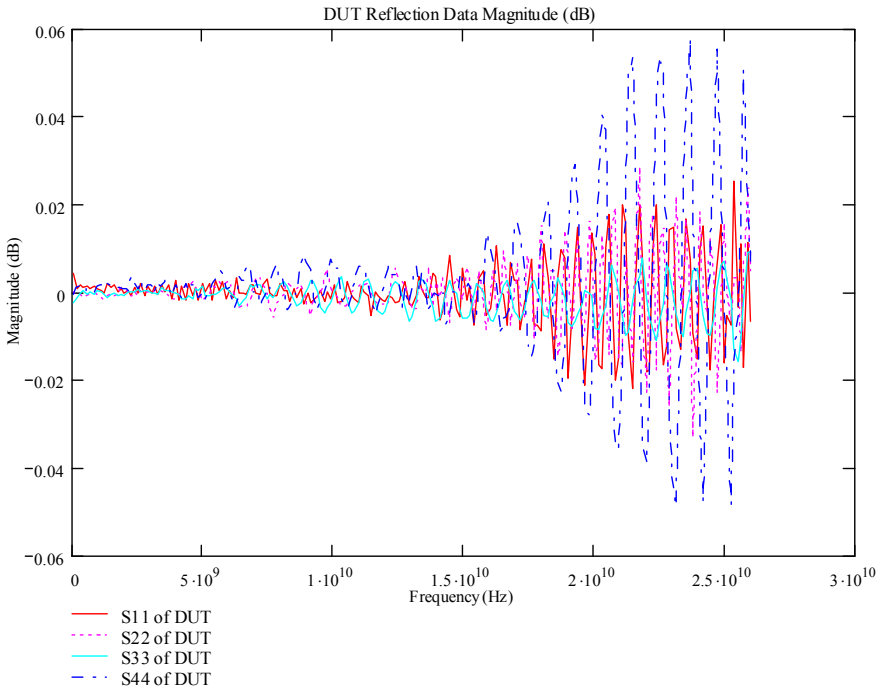

Figure B.4 - Calibrated Short Reflection Magnitude Using the 6/2 Multiport cSOLR Calibration Routine.

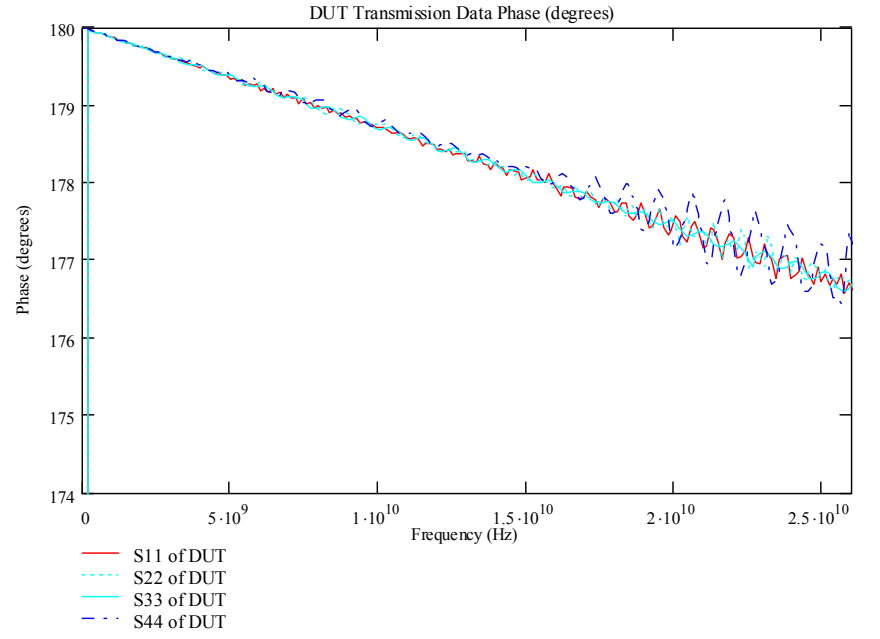

Figure B.5 - Calibrated Short Reflection Phase Using the 6/2 Multiport cSOLR Calibration Routine.

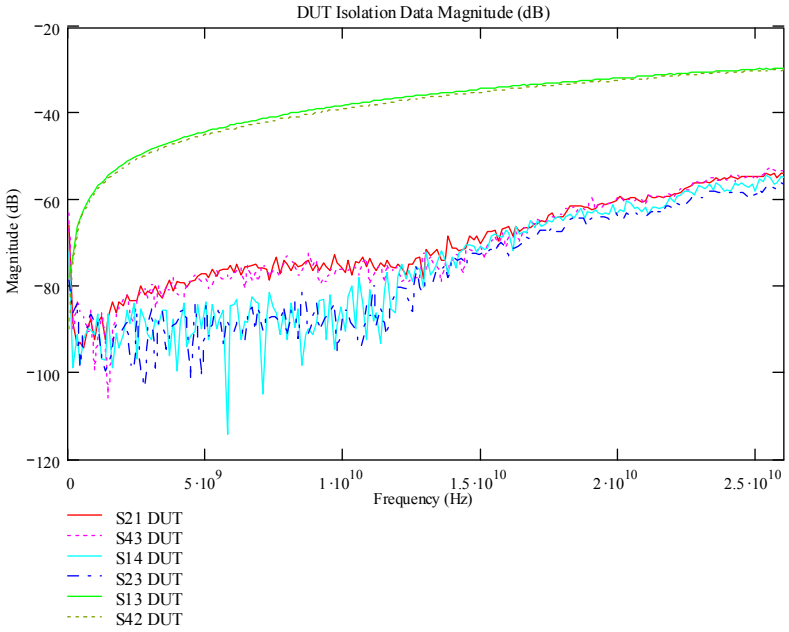

Figure B.6 - Calibrated Short Isolation Magnitude Using the 6/2 Multiport cSOLR Calibration Routine.

Parallel Transmission Standard

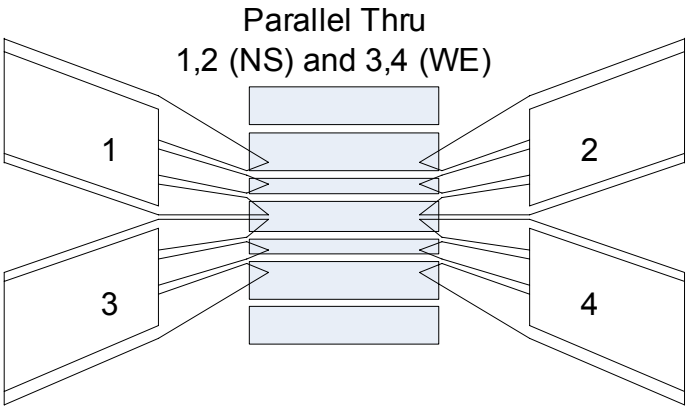

Figure B.7 – GSGSG 580 um Parallel CPW Transmission Standard.

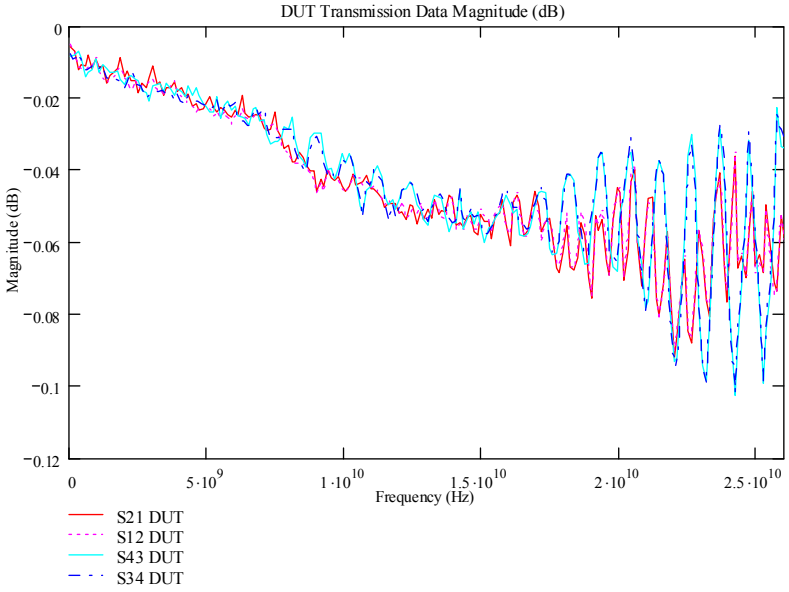

Figure B.8 - Calibrated Parallel CPW Transmission Standard Transmission Magnitude Using the 6/2 Multiport cSOLR Routine.

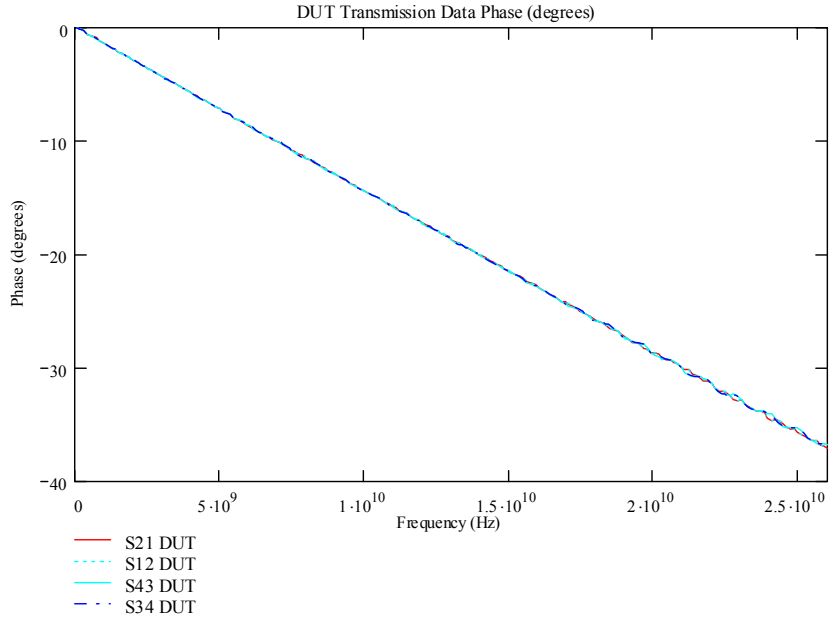

Figure B.9 - Calibrated Parallel CPW Transmission Standard Transmission Phase Using the 6/2 Multiport cSOLR Calibration Routine.

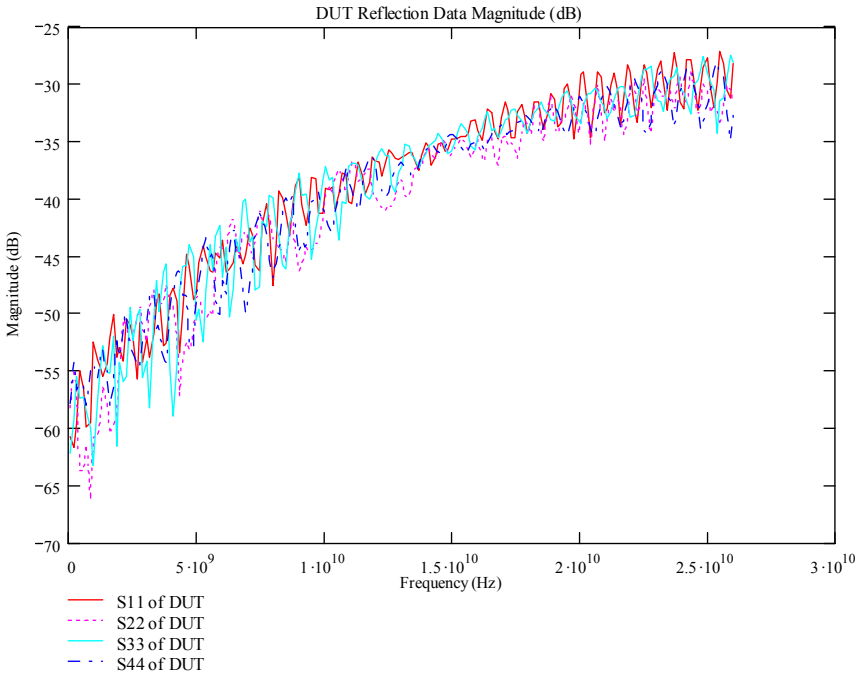

Figure B.10 - Calibrated Parallel CPW Transmission Standard Reflection Magnitude Using the 6/2 Multiport cSOLR Calibration Routine.

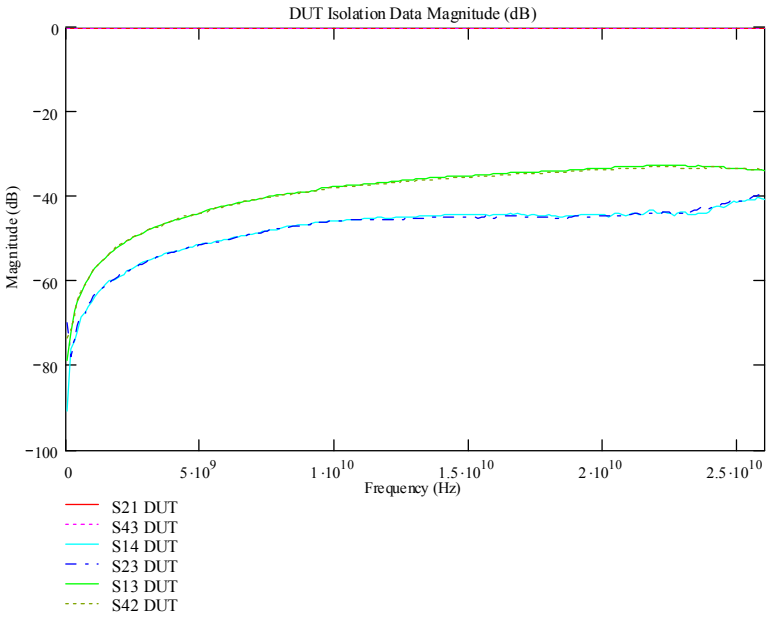

Figure B.11 - Calibrated Parallel CPW Transmission Standard Isolation Data and S21/43 Transmission Using the 6/2 Multiport cSOLR Calibration Routine.

Offset (3,2) Transmission Standard

The offset (3,2) transmission standard data is shown in Figures B.12 to B.15.

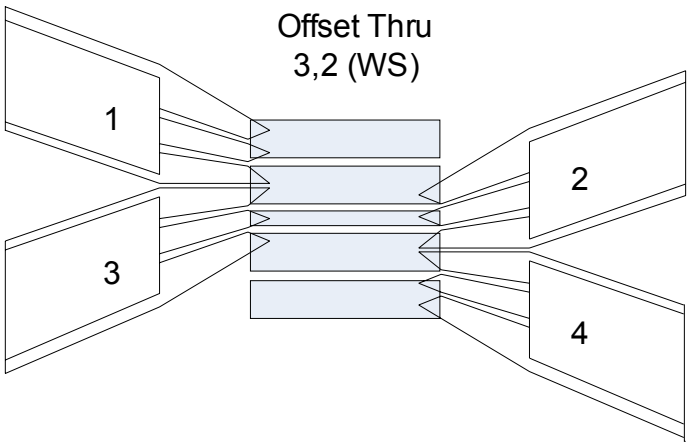

Figure B.12 – Layout of GSGSG (3,2) Offset Transmission Standard.

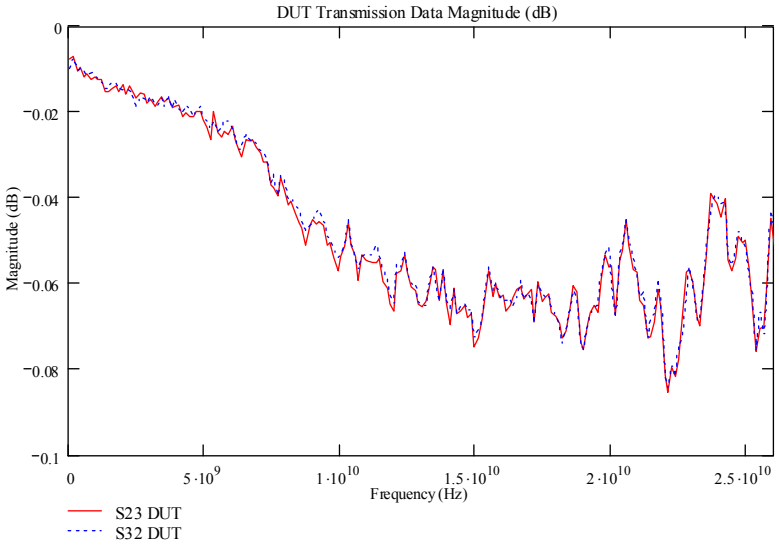

Figure B.13 - Transmission Magnitude Data of 4.0ps CPW (3,2) Transmission Line Using the 6/2 Multiport cSOLR Calibration Routine.

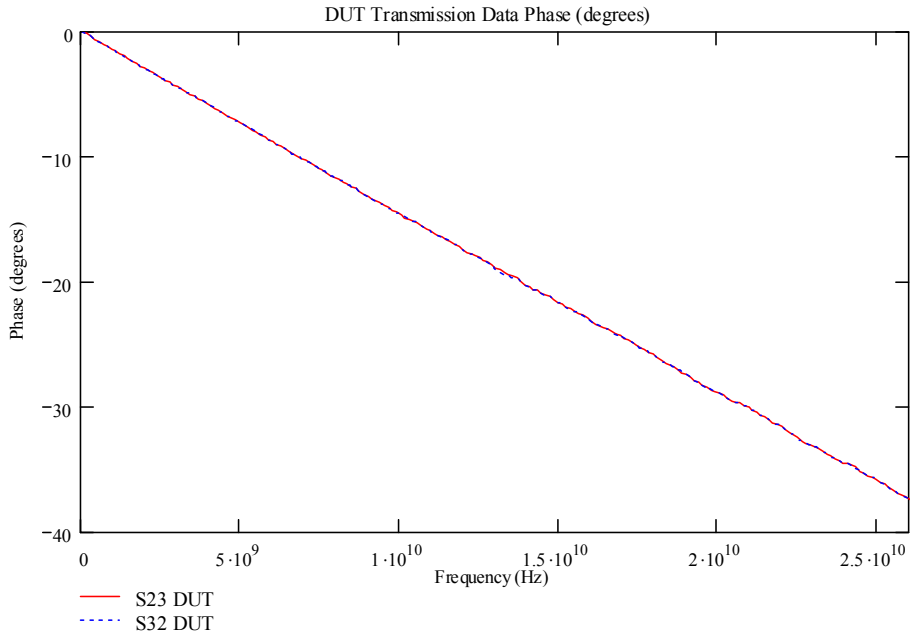

Figure B.14 - Transmission Phase Data of 1.13ps CPW (3,2) Transmission Line Using the 6/2 Multiport cSOLR Calibration Routine.

The unused signal pins are shorted on the ground plane of the CPW. Figure B.15 may indicate some coupling, because it is observed that as frequency increases the reflection coefficient of ports 1 and 4 dramatically decreases from an ideal 0dB. This indicates that some of the signal is propagating elsewhere or radiating and/or transmission is taking place. This can be seen in Figure B.16 as the isolation deviates from the ideal isolation of the 50 ohm load measurements. However the isolation is not that poor this indicates that there is a good deal of radiation loss associated with the coupled signals.

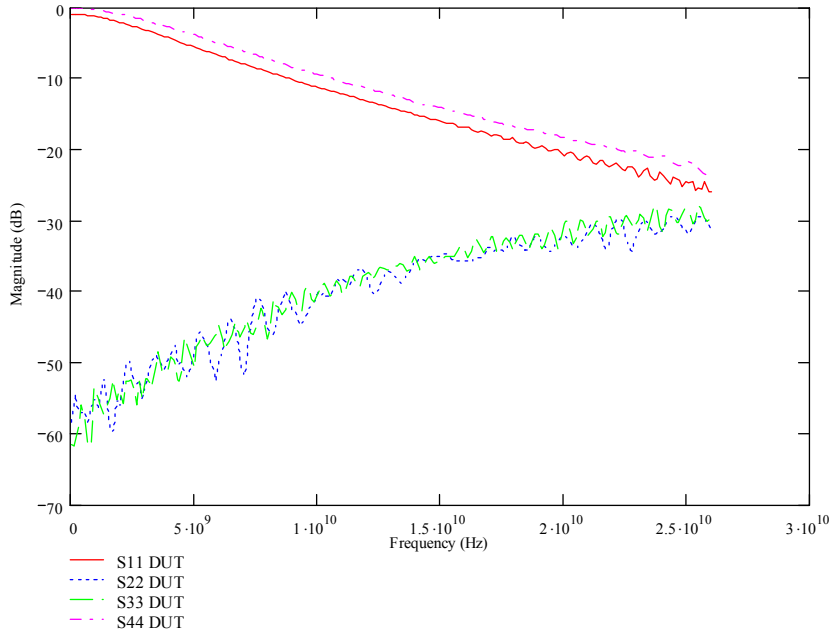

Figure B.15 - Reflection Magnitude Data of 1.13ps CPW (3,2) Transmission Line Using the 6/2 Multiport cSOLR Calibration Routine.

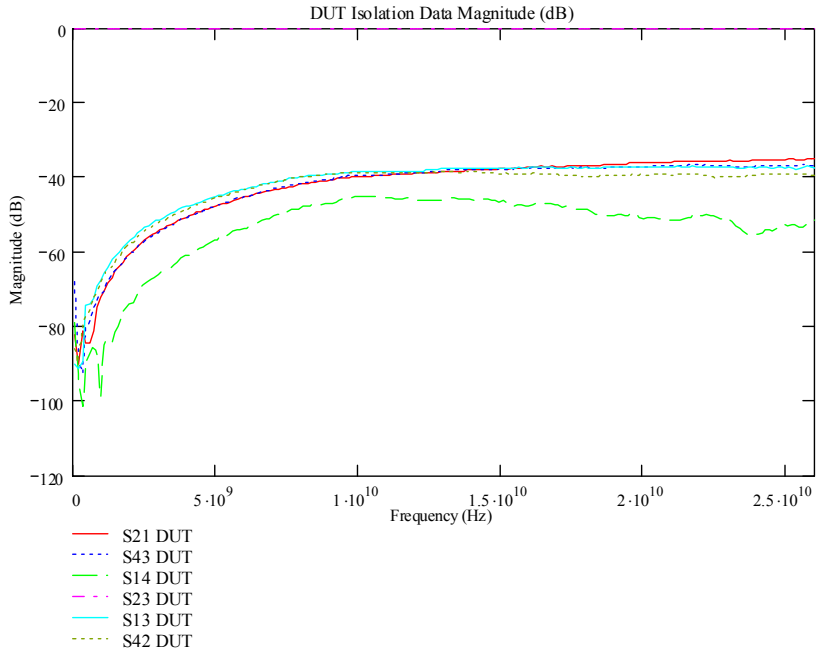

Figure B.16 - Isolation Magnitude Data and S23 Transmission of 1.13ps CPW (3,2) Transmission Line Using the 6/2 Multiport cSOLR Calibration Routine.

Offset (1,4) Transmission Standard

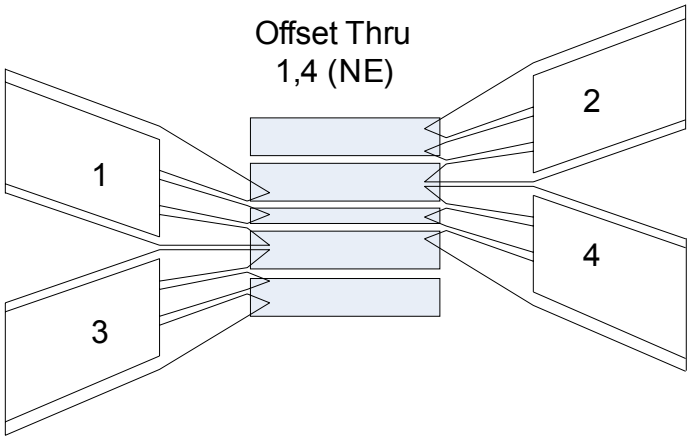

Figure B.17 - Layout of GSGSG (3,2) Offset Transmission Standard.

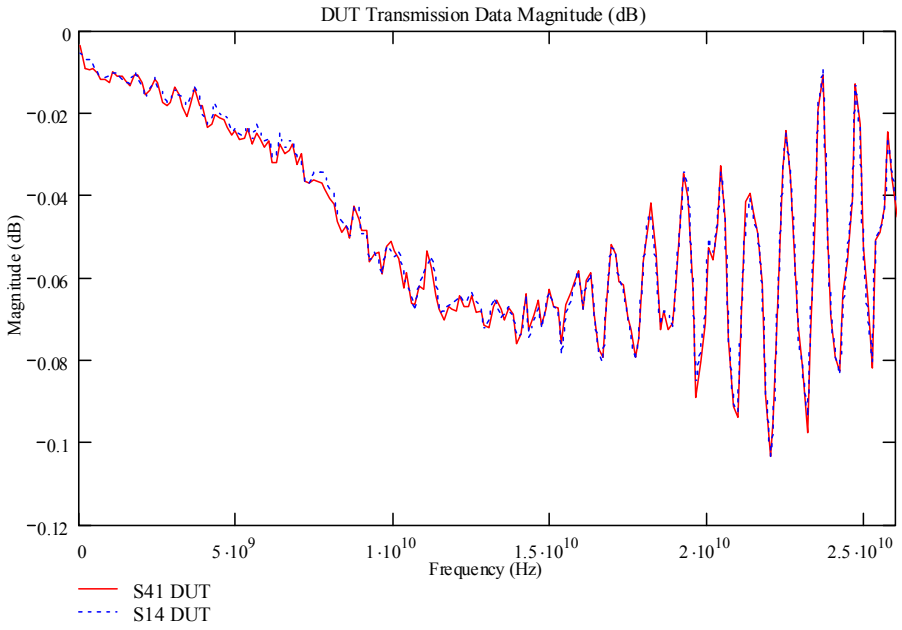

Figure B.18 - Transmission Magnitude Data of 4.0ps CPW (1,4) Transmission Line Using the 6/2 Multiport cSOLR Calibration Routine.

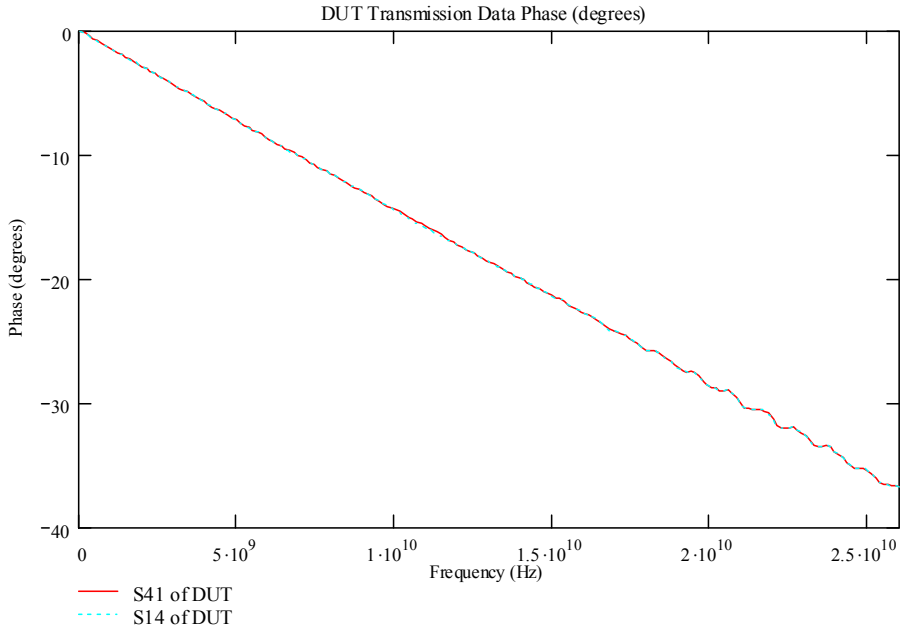

Figure B.19 - Transmission Phase Data of 4.0ps CPW (1,4) Transmission Line Using the 6/2 Multiport cSOLR Calibration Routine.

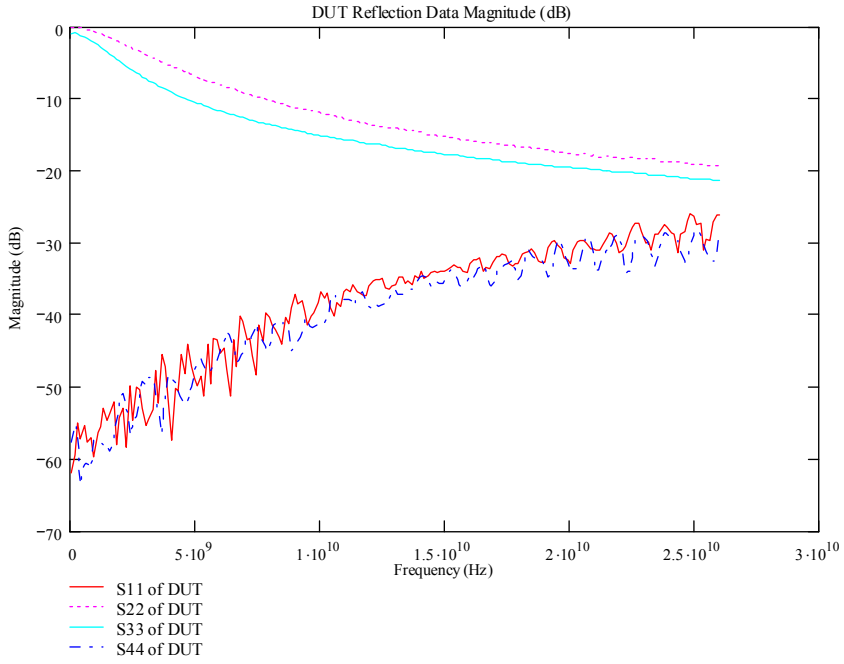

Figure B.20 - Reflection Magnitude Data of 4.0ps CPW (1,4) Transmission Line Using the 6/2 Multiport cSOLR Calibration Routine.

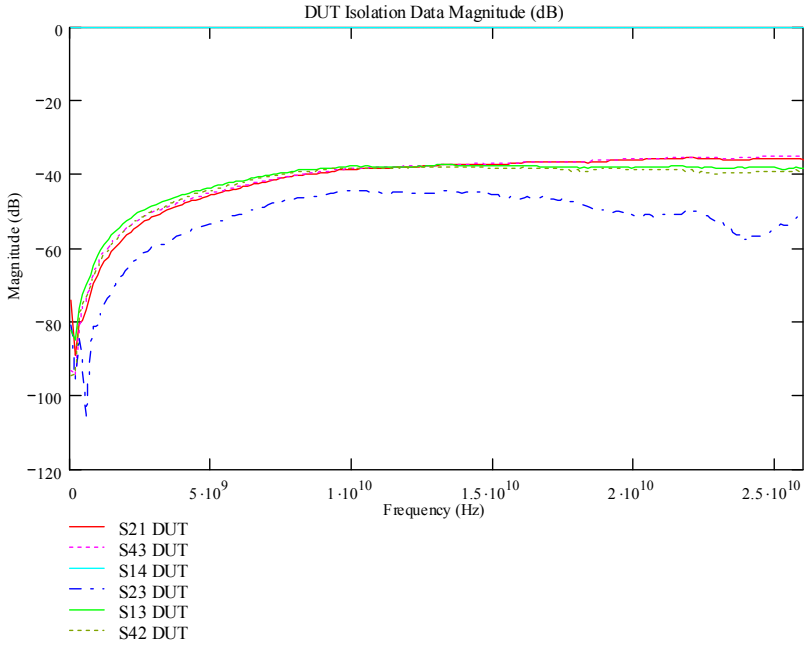

Figure B.21 - Isolation Data and S14 Transmission of 4.0ps CPW (1,4) Transmission Line Using the 6/2 Multiport cSOLR Calibration Routine.

U Thru

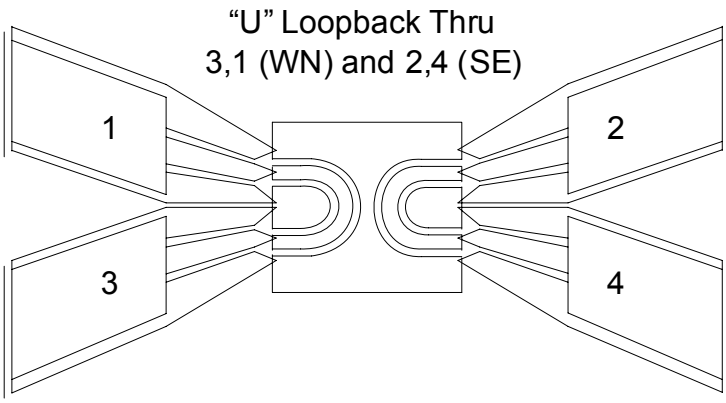

Figure B.22 – Layout of the GSGSG Loopback Transmission Standard.

Figure B.23 shows the transmission magnitude results for the loopback thru. The ripple in the measurement past 16 GHz has a maximum peak to peak magnitude of approximately 0.06 dB. This ripple is seen in the delay 1 transmission measurement as well and maintains the same magnitude therefore, it is not a concern to the accuracy of the measurements. The reflection coefficient data of Figure B.24 reveals that the standard is poorly matched. A fairly simple theoretical concept is demonstrated in Figure B.26. The (1,4) and (3,2) probe signal pins are physically further apart than the (1,2) and (3,4) signal pins; thus, the isolation between the (1,4) and (3,2) pins are higher than the (1,2) and (3,4) pins.

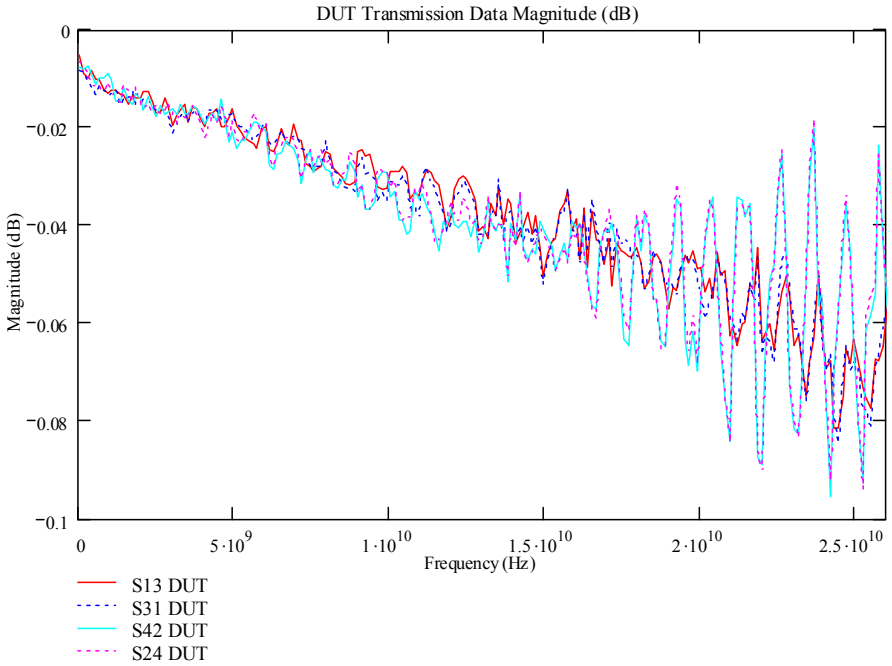

Figure B.23 - Transmission Magnitude Data of the 4.0 ps Loopback "U" Transmission Lines Measured Using the 6/2 Multiport cSOLR Calibration Routine.

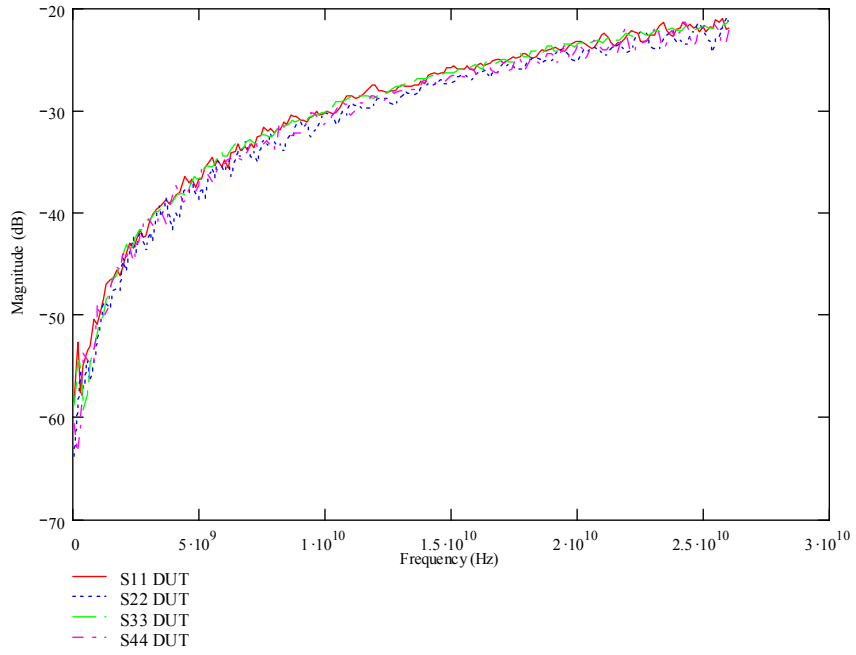

Figure B.24 - Reflection Magnitude Data of the 4.0 ps Loopback "U" Transmission Lines Measured Using the 6/2 Multiport cSOLR Calibration Routine.

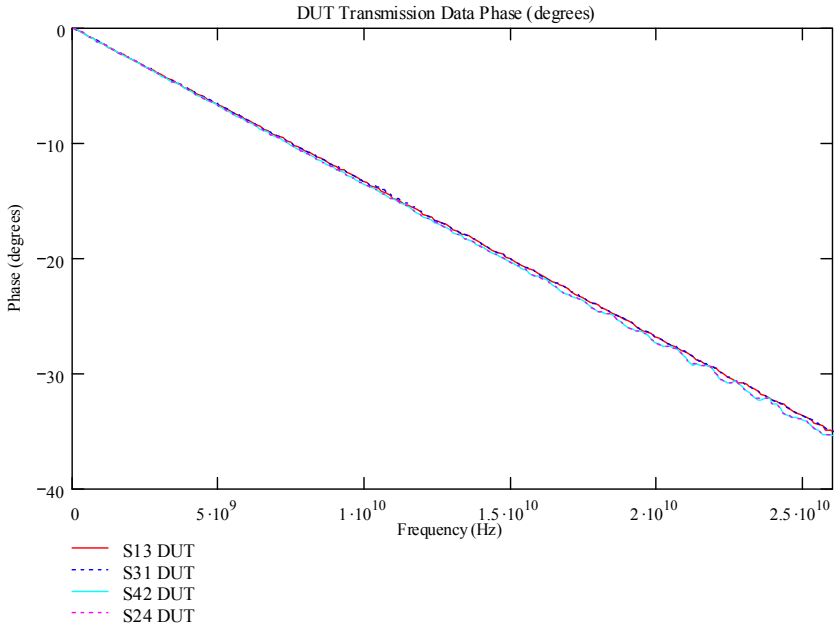

Figure B.25 - Transmission Phase Data of the 4.0 ps Loopback "U" Transmission Lines Measured Using the 6/2 Multiport cSOLR Calibration Routine.

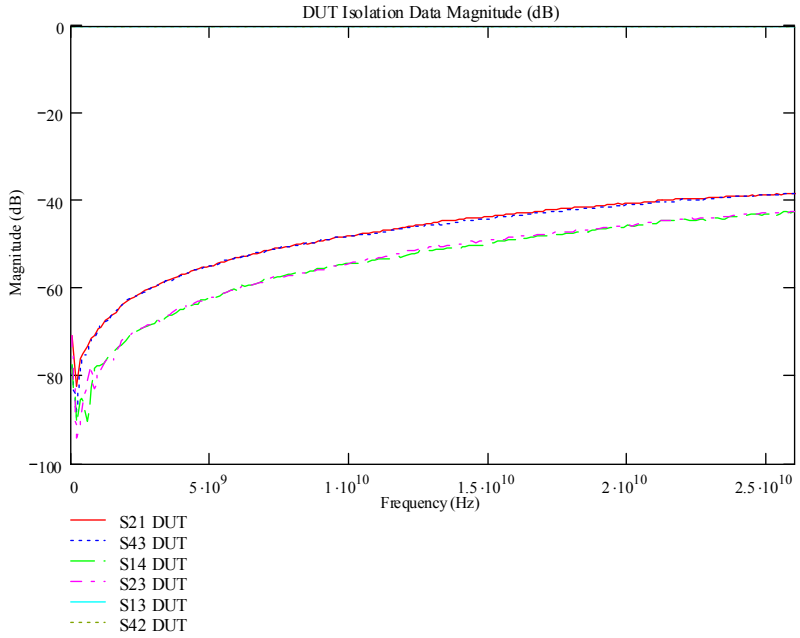

Figure B.26 - Isolation Data and S42/13 Transmission of the 4.0 ps Loopback "U" Transmission Lines Measured Using the 6/2 Multiport cSOLR Calibration Routine.

1880 um Parallel Delay

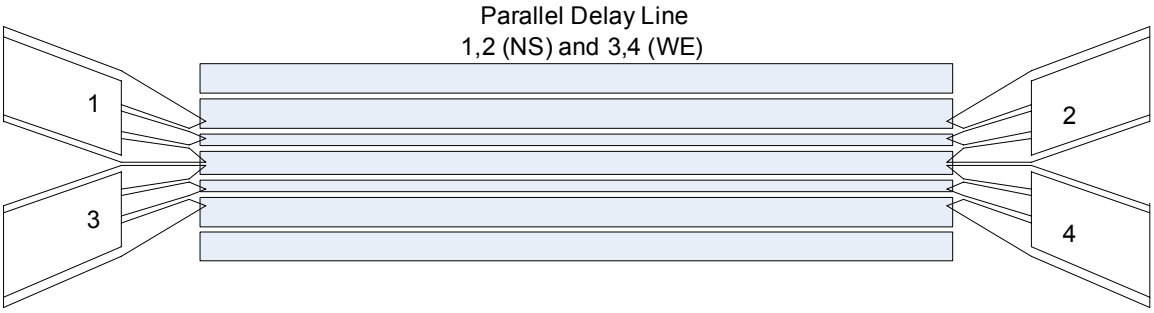

Figure B.27 – GSGSG Layout of1880 um Parallel CPW Transmission Structure.

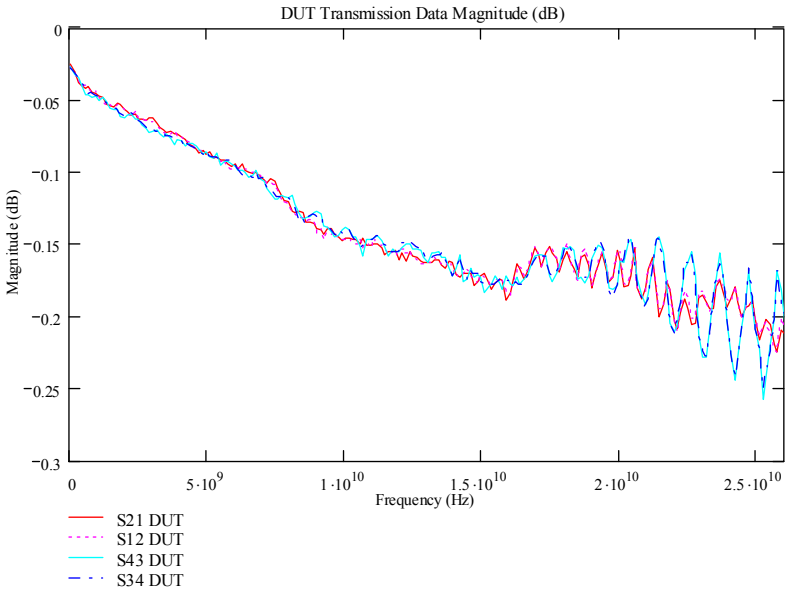

Figure B.28 - Transmission Magnitude Data of 1880 um Parallel CPW Transmission Line Using the 6/2 Multiport cSOLR Calibration Routine.

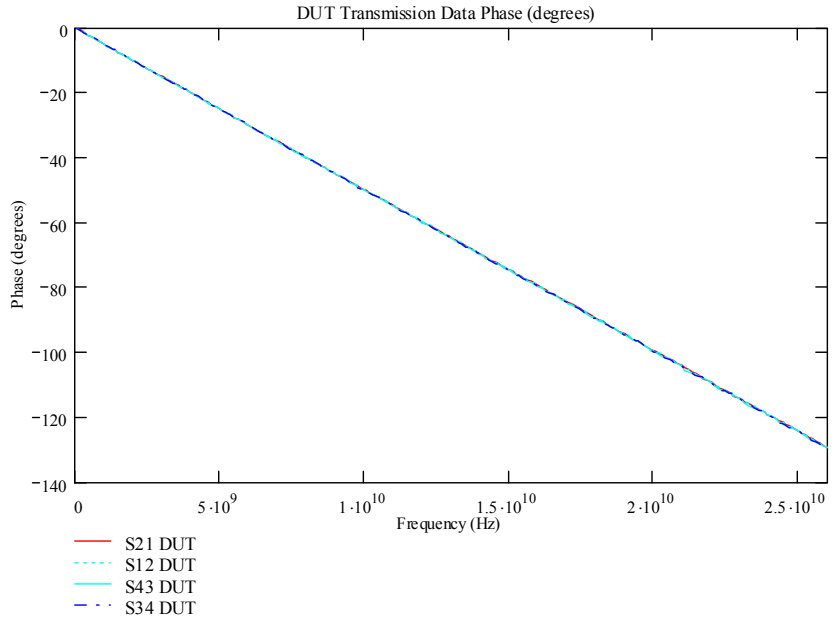

Figure B.29 - Transmission Phase Data of 1880 um Parallel CPW Transmission Line Using the 6/2 Multiport cSOLR Calibration Routine.

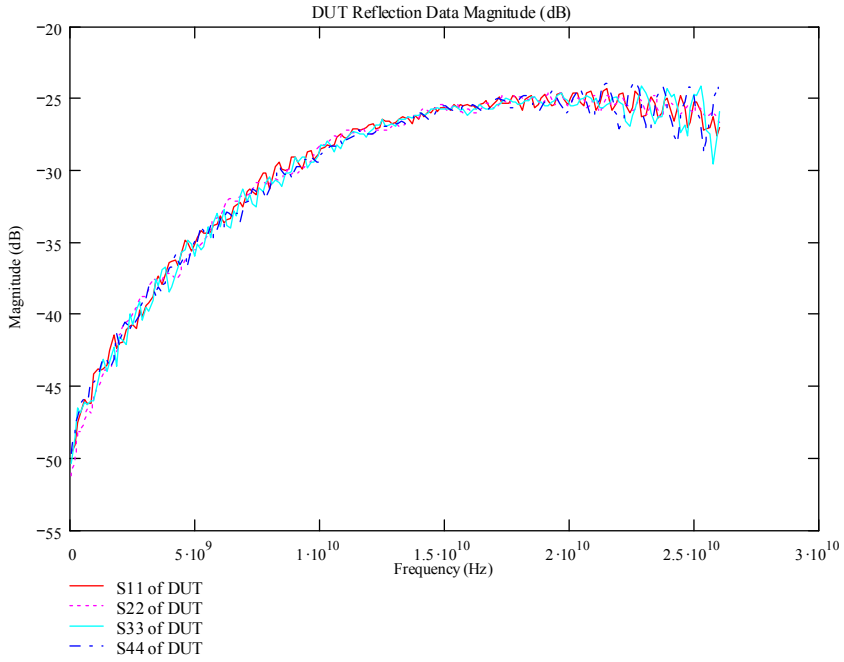

Figure B.30 - Reflection Magnitude Data of 1880 um Parallel CPW Transmission Line Using the 6/2 Multiport cSOLR Calibration Routine.

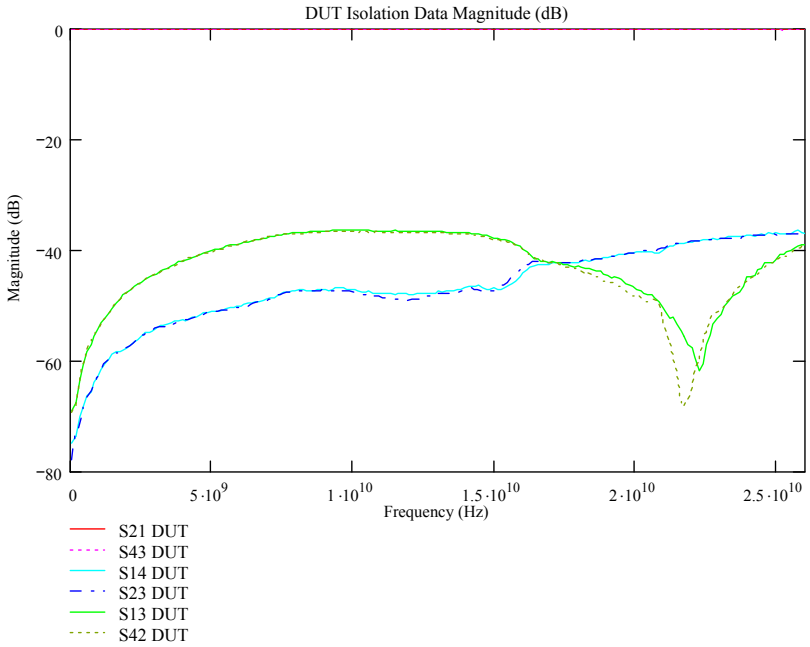

Figure B.31 - Isolation Data and S21/43 Transmission of 1880 um Parallel CPW Transmission Line Using the 6/2 Multiport cSOLR Calibration Routine.

B.2 Additional Measurements of Multiport cSOLR vs. NISTcal 4-Port TRL

The measurements presented in this section are the additional comparison measurements made on the GGB CS-2-150 between multiport cSOLR and NISTcal 4-port TRL that were not shown in Section 8.2.2. The NISTcal data still becomes erratic after around 17 GHz as was observed in Chapter 8. However the reflection magnitude of the 580 um and 1880 um parallel structures show better agreement than the 6600 um structure shown in Chapter 8.

580 um Parallel Transmission Standard

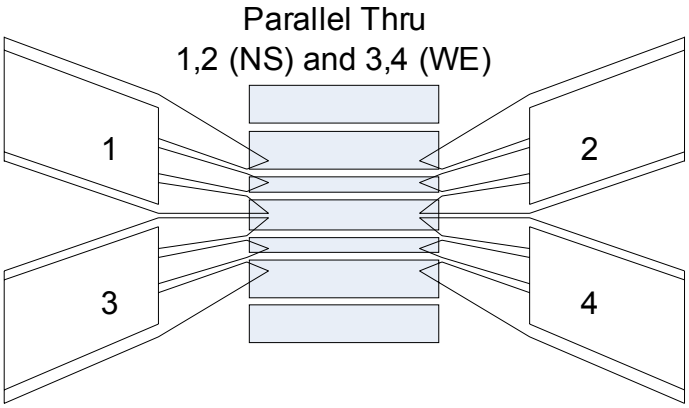

Figure B.32 – Layout of the GSGSG 580 um Parallel CPW Structure.

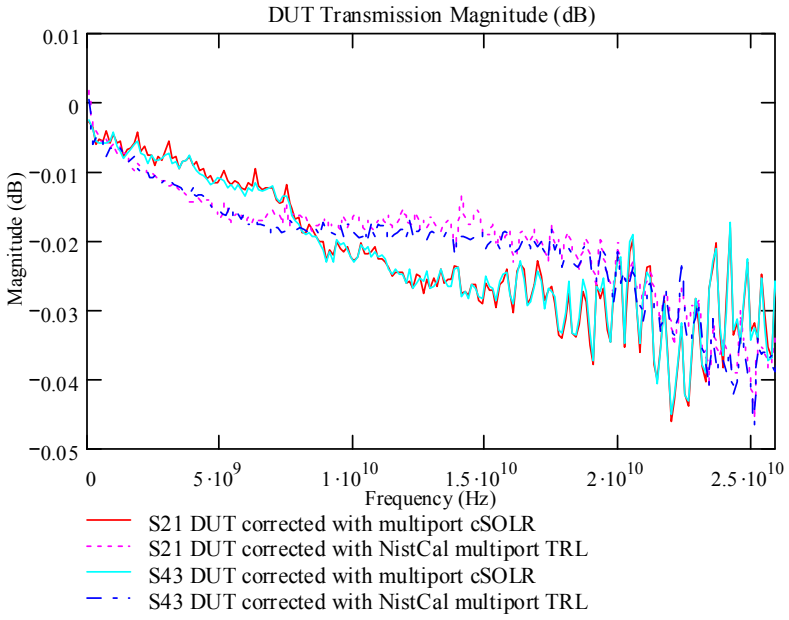

Figure B.33 – Transmission Magnitude Measurements of 580 um Parallel CPW Transmission Line Corrected with NIST 4-port TRL vs. Multiport cSOLR.

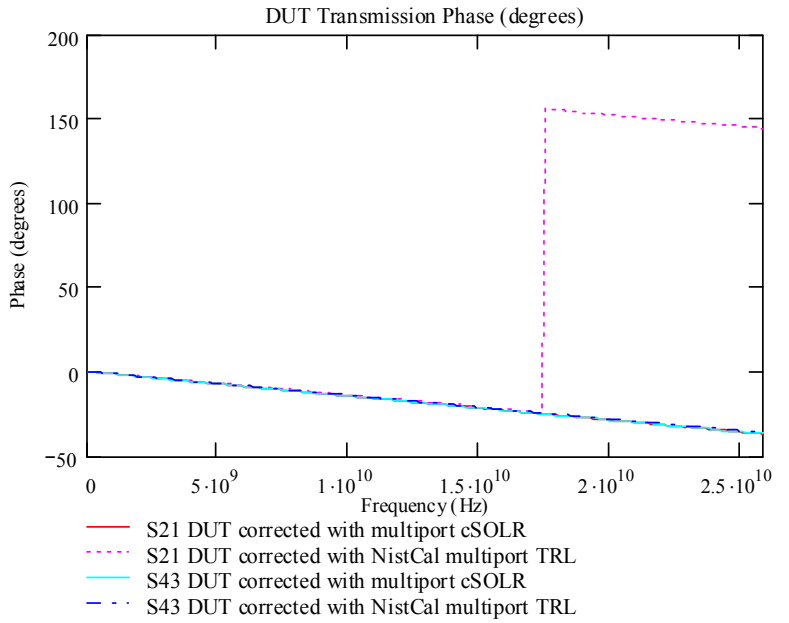

Figure B.34 – Transmission Phase Measurements of 580 um Parallel CPW Transmission Line Corrected with NIST 4-port TRL vs. Multiport cSOLR.

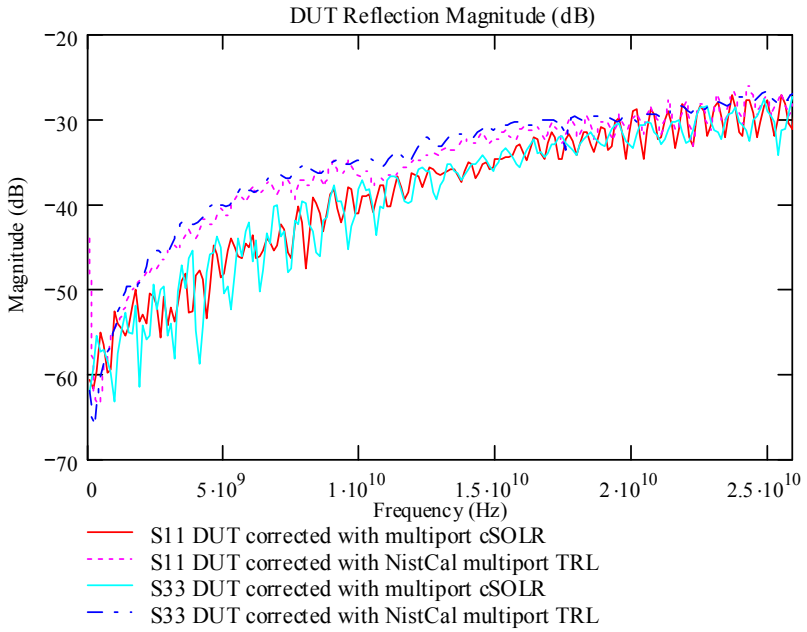

Figure B.35 – Reflection Magnitude Measurements of 580 um Parallel CPW Transmission Line Corrected with NIST 4-port TRL vs. Multiport cSOLR.

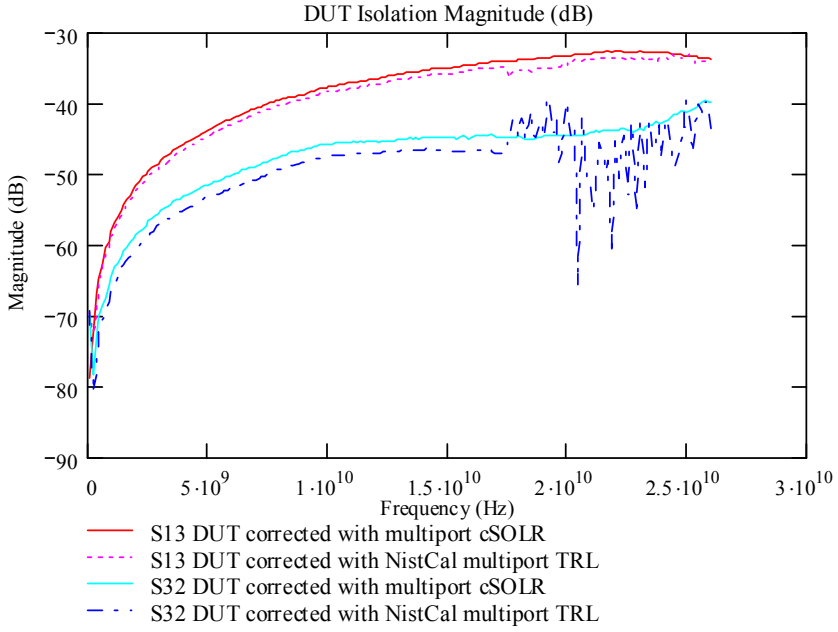

Figure B.36 – Isolation Measurements of 580 um Parallel CPW Transmission Line Corrected with NIST 4-port TRL vs. Multiport cSOLR.

1880 um Parallel Transmission Standard

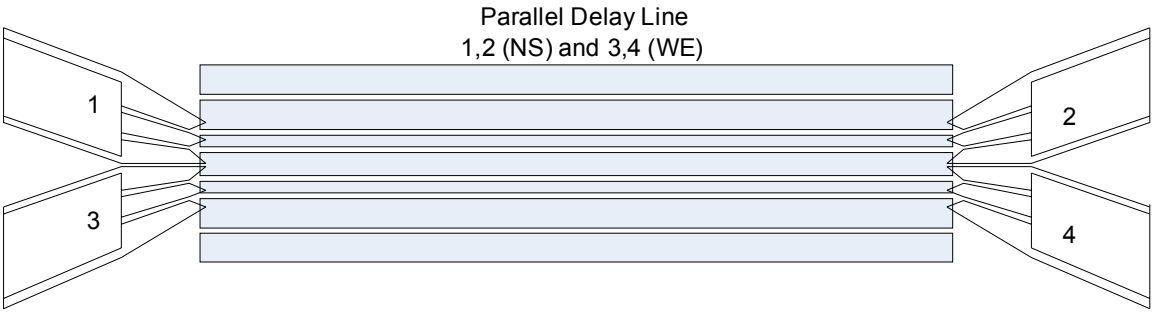

Figure B.37 – GSGSG Layout of 1880 um Parallel Transmission Standard.

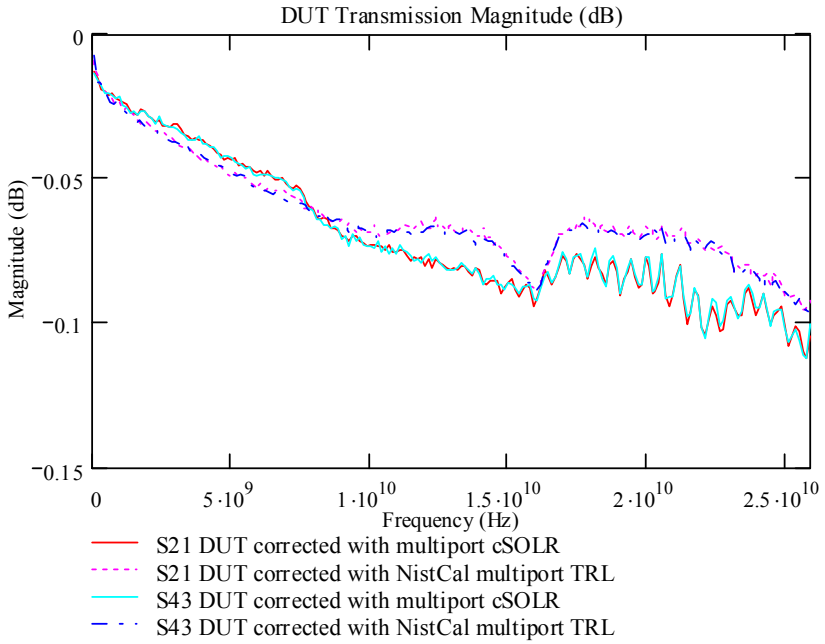

Figure B.38 – Transmission Magnitude Measurements of 1880 um Parallel CPW Transmission Line Corrected with NIST 4-port TRL vs. Multiport cSOLR.

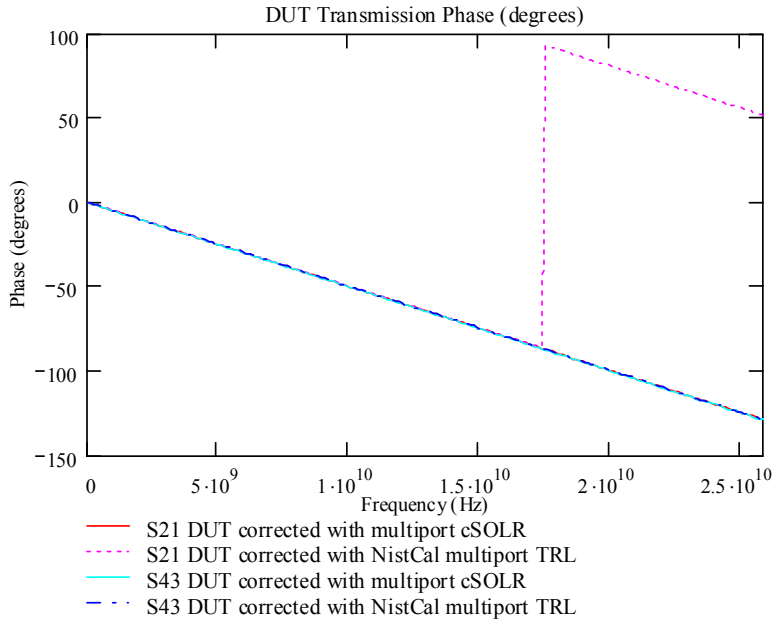

Figure B.39 – Transmission Phase Measurements of 1880 um Parallel CPW Transmission Line Corrected with NIST 4-port TRL vs. Multiport cSOLR.

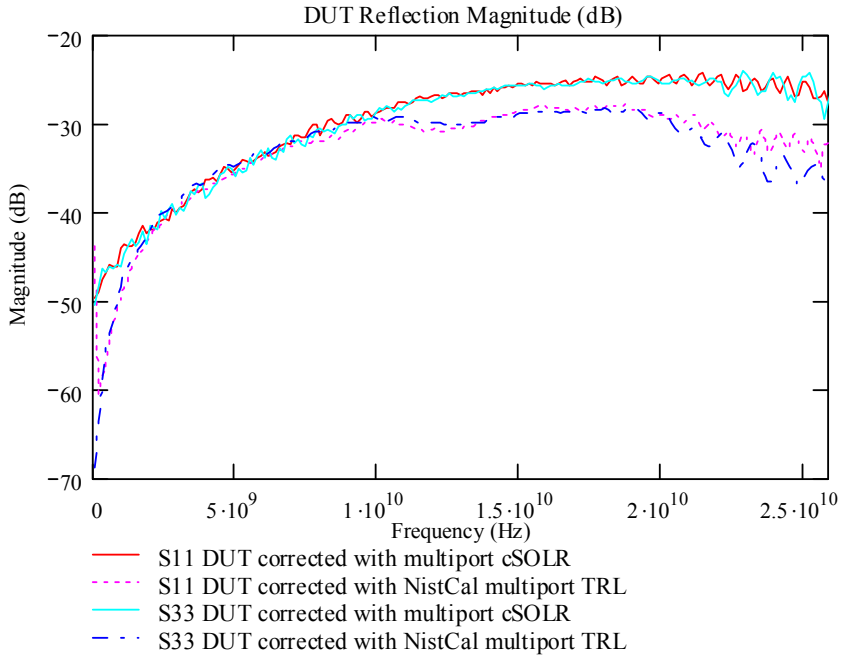

Figure B.40 – Reflection Magnitude Measurements of 1880 um Parallel CPW Transmission Line Corrected with NIST 4-port TRL vs. Multiport cSOLR.

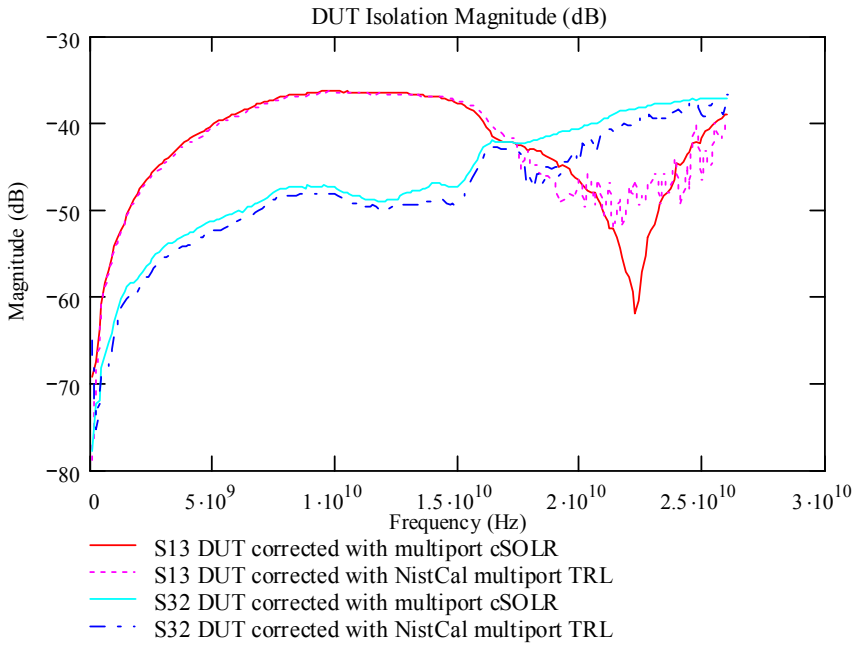

Figure B.41 – Isolation Measurements of 1880 um Parallel CPW Transmission Line Corrected with NIST 4-port TRL vs. Multiport cSOLR.

APPENDIX C: COAXIAL VERIFICATION OF MULTIPORT CSOLR METHOD

A triplexer is a device which takes an incoming RF signal into its common port and divides is into its fundamental frequency and its second and third harmonics. Triplexers are designed for a given fundamental center frequency. The Maury Microwave triplexer which was measured has a fundamental frequency of 5.35 GHz. Figure 8.32 shows the test setup of the Maury triplexer. The numbers represent the port numbers that correspond to the measurement port of the NISTcal software and the letters correspond to the connection ports of the USF 4-port system. These can be used to help identify measurements in graphs below.

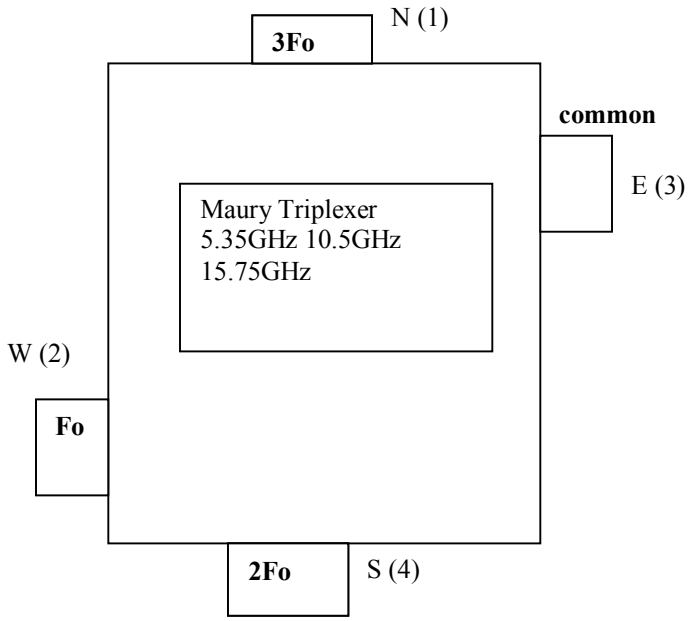

Figure C.1 - Connection Setup of the Four-Port Measurement of the Maury Microwave Triplexer.

Ideally what is seen is that the common port is well matched throughout the entire measurement bandwidth and the fundamental and harmonic ports will be well matched only within their designed bandwidth.

The harmonic ports will reject frequencies outside of their bandwidths. Essentially, a triplexer is a network of filters designed to separate fundamental and harmonic frequencies. There should be good isolation between the output ports at the ports frequencies of operation.

Three sets of measurements were made on the triplexer. All three sets were made from 40 MHz to 18 GHz with 101 data points and an averaging factor of 64 using the Anritsu 37xxx series VNA. Calibrations were made using the Anritsu K calibration kit. Anritsu k to 7mm adapters were added after the calibration on order to mate with the triplexer. Hence the actual triplexer performance has to it the response of a k-to-7mm adapters connected to each port. Two sets were measured on the USF four-port system using the USF 4-port switch matrix. The first was measured by performing a 4-port LRM calibration in the NISTcal software and then measuring the triplexer. The second set measured with the switch matrix was made by measuring the raw calibration SOL and thru line standards the switch terms and internal switch matrix terminations as well as the raw triplexer measurement data for use in the multiport cSOLR algorithm. The final set of measurements was made using a front panel 2-port SOLT calibration and then measuring the triplexer 2 ports at a time by terminating the unused ports with 7mm loads. The measurements of the triplexer are shown in the following figures. Problems in cable movement during the cSOLR affected the measurements and thus the larger ripples should be ignored

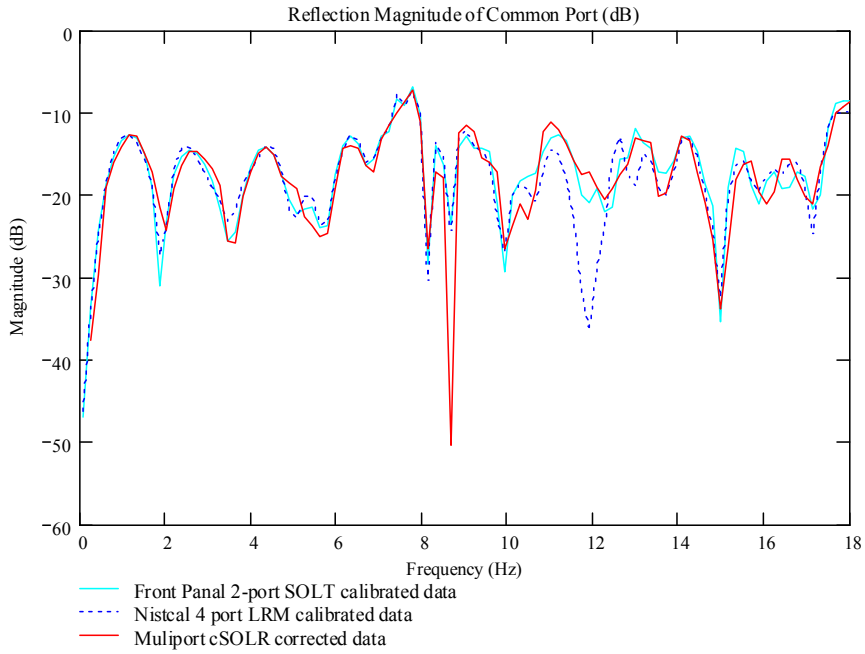

Figure C.2 – Reflection Magnitude of the 5.25 GHz Triplexer at the Common Port Measured with Various Multiport Calibration Methods.

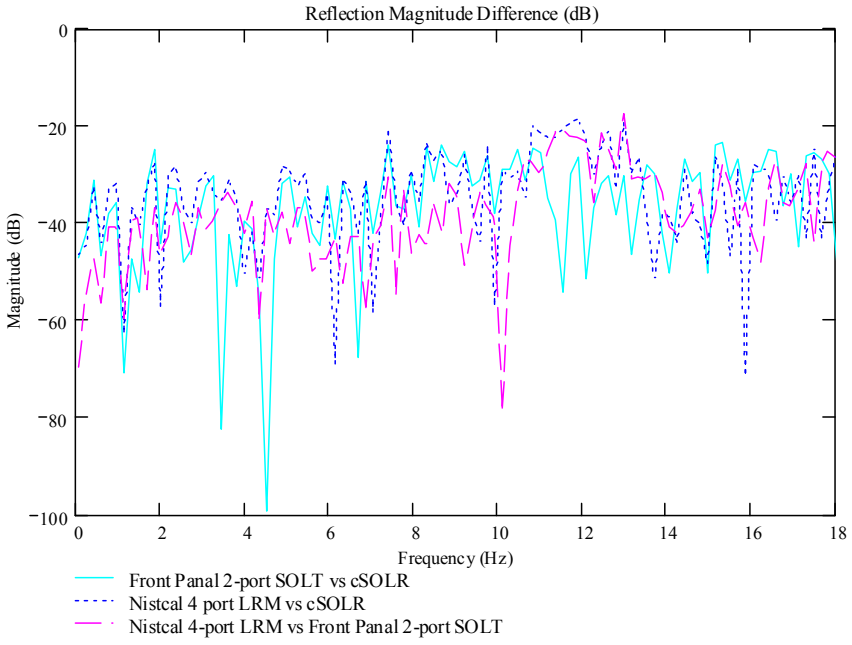

Figure C.3 – Reflection Magnitude Difference of the 5.25 GHz Triplexer at the Common Port Measured Between cSOLR and Various Calibrations.

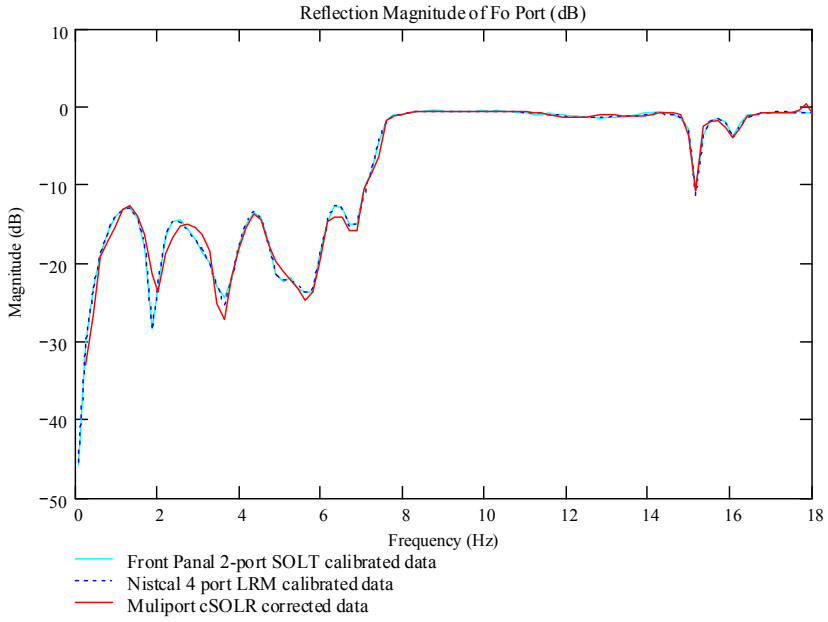

Figure C.4 – Reflection Magnitude of the 5.25 GHz Triplexer at the Fo Port Measured with Various Multiport Calibration Methods.

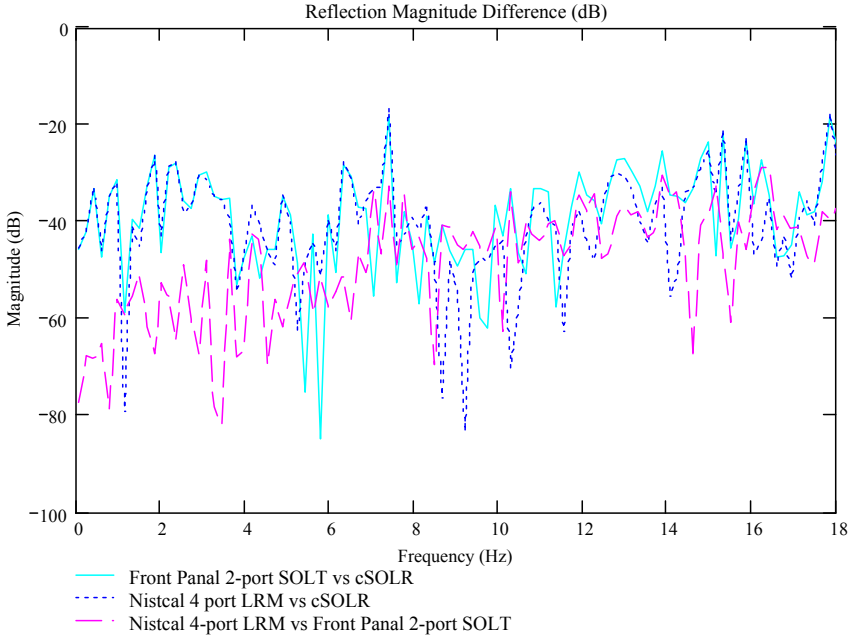

Figure C.5 – Reflection Magnitude Difference of the 5.25 GHz Triplexer at the Fo Port Measured with Various Multiport Calibration Methods.

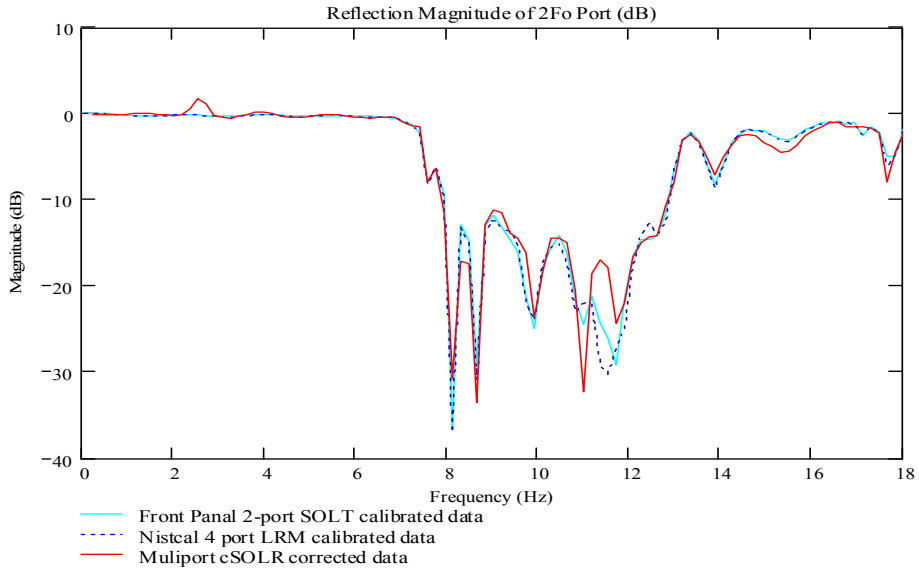

Figure C.6 – Reflection Magnitude of the 5.25 GHz Triplexer at the 2Fo Port Measured with Various Multiport Calibration Methods.

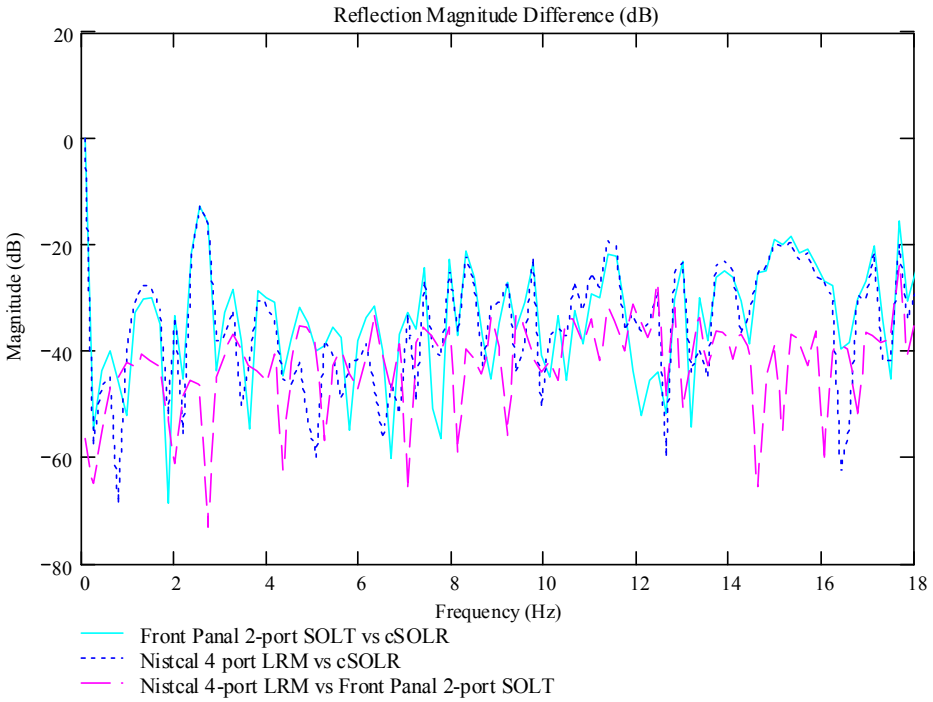

Figure C.7 – Reflection Magnitude Difference of the 5.25 GHz Triplexer at the 2Fo Port Measured Between cSOLR and Various Calibrations.

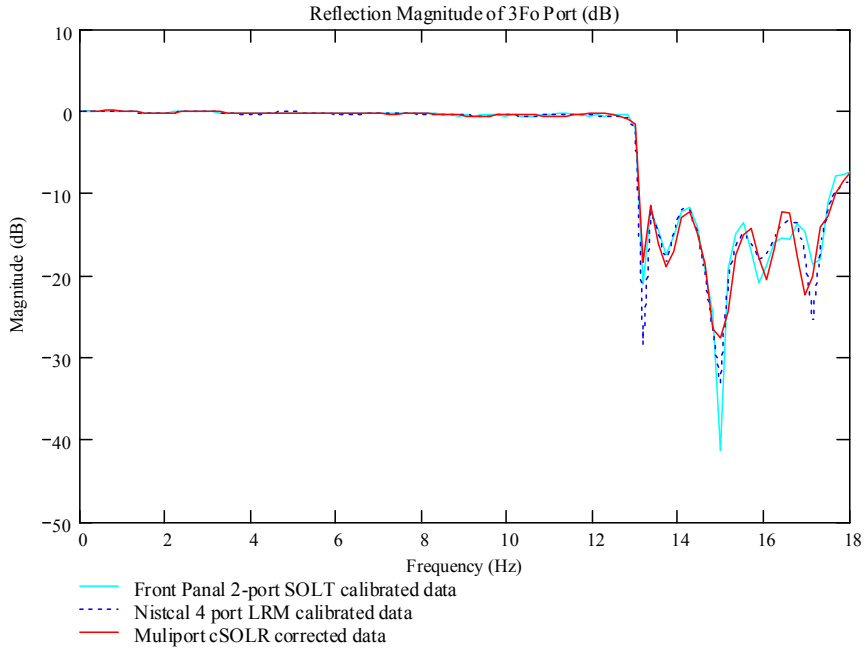

Figure C.8 – Reflection Magnitude of the 5.25 GHz Triplexer at the 3Fo Port Measured with Various Multiport Calibration Methods.

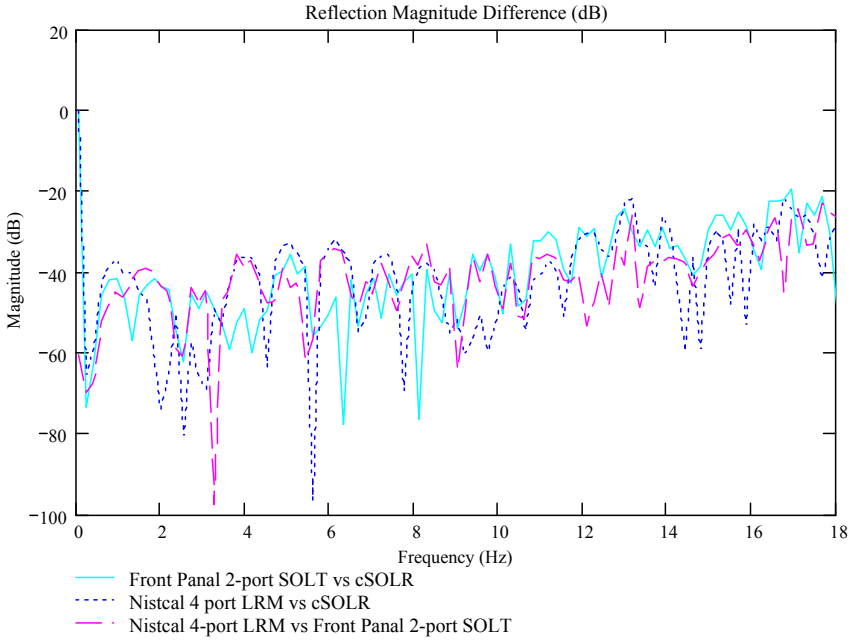

Figure C.9 – Reflection Magnitude Difference of the 5.25 GHz Triplexer at the 3Fo Port Measured Between cSOLR and Various Calibrations.

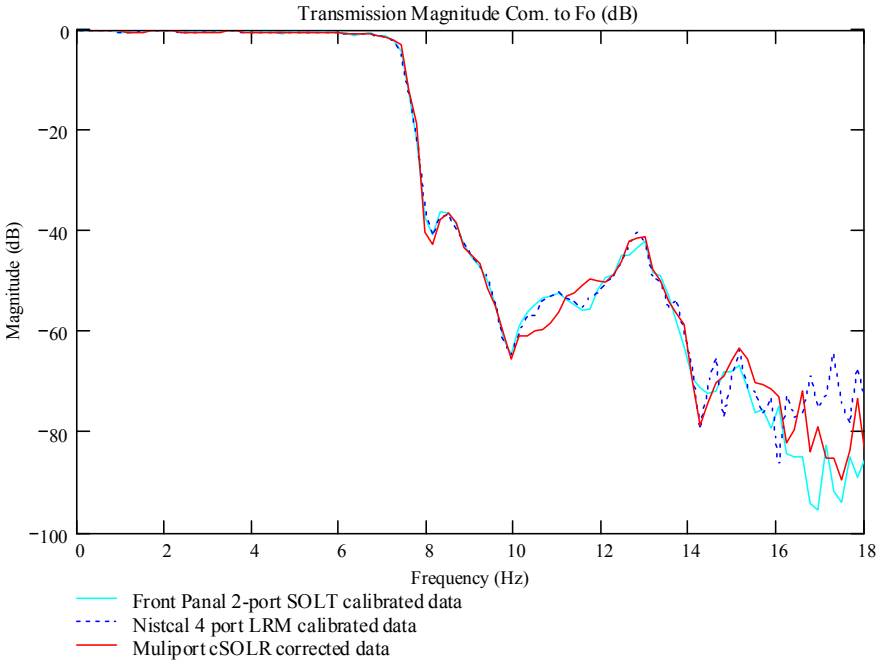

Figure C.10 – Transmission Magnitude of the 5.25 GHz Triplexer from the Common Port to the Fo Port Measured with Various Multiport Calibration Methods.

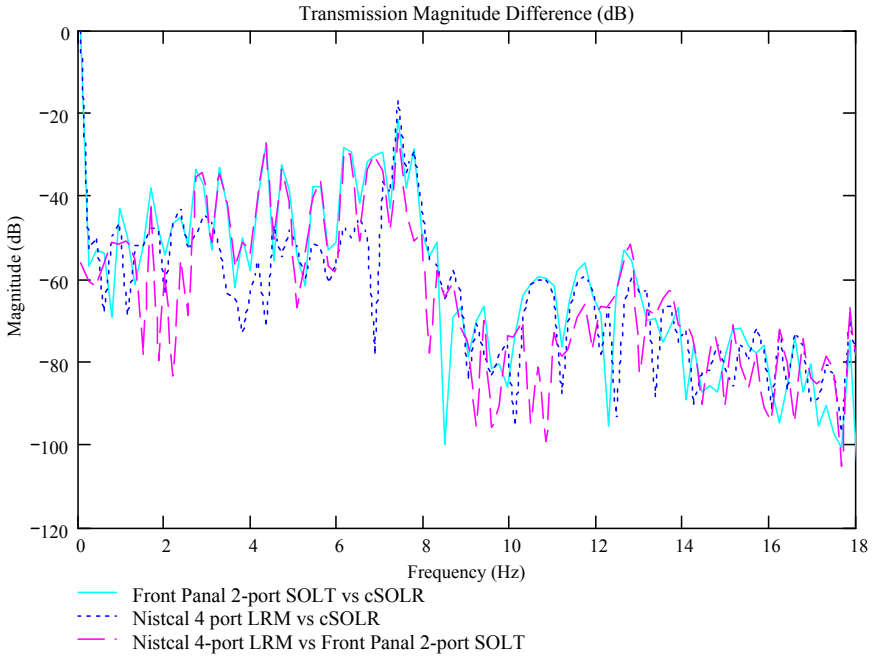

Figure C.11 – Transmission Magnitude Difference of the 5.25 GHz Triplexer From the Common Port to the 2Fo Port Measured Between cSOLR and Various Calibrations.

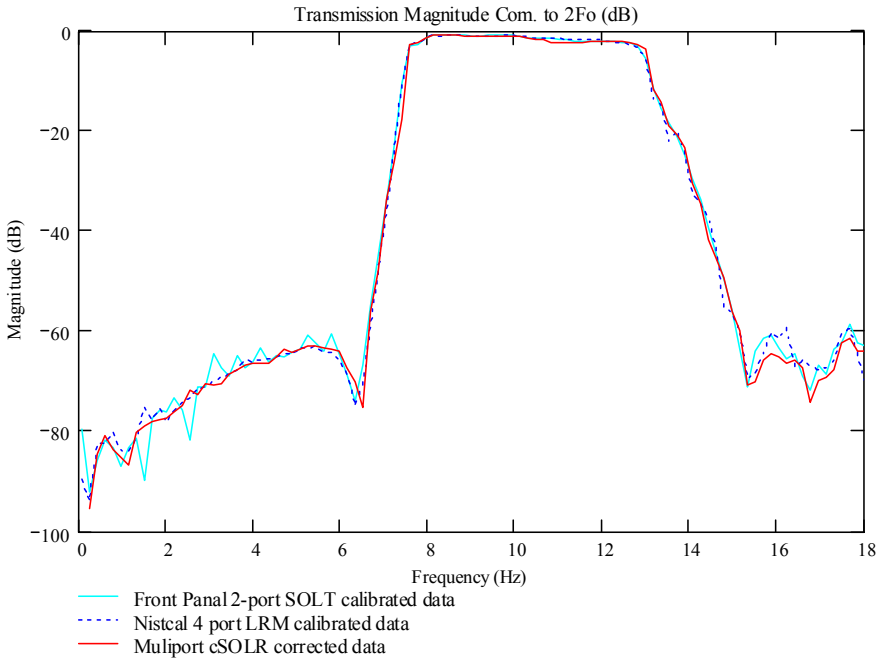

Figure C.12 – Transmission Magnitude of the 5.25 GHz Triplexer From the Common Port to the 2Fo Port Measured with Various Multiport Calibration Methods.

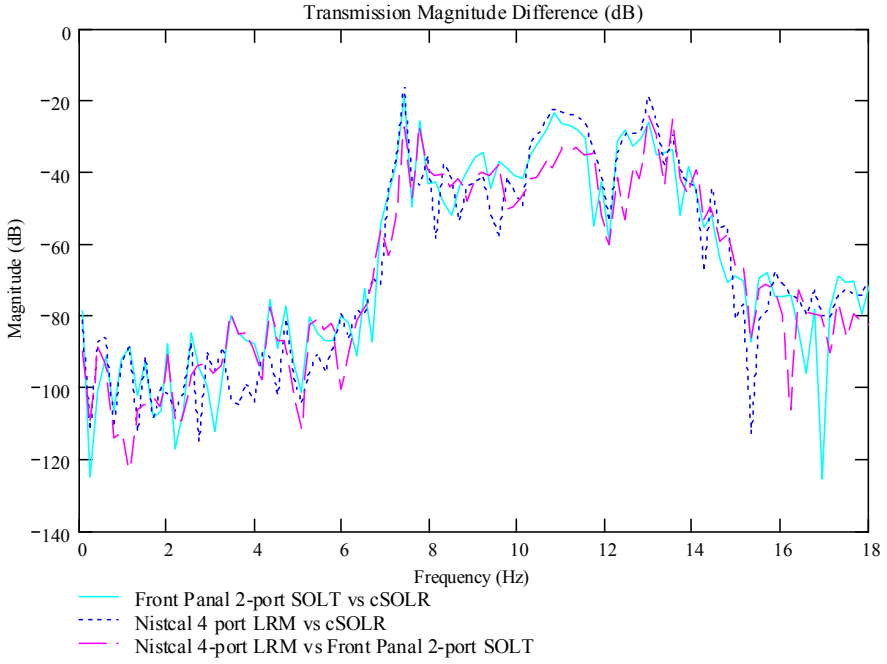

Figure C.13 – Transmission Magnitude Difference of the 5.25 GHz Triplexer from the Common Port to the 2Fo Port Measured Between cSOLR and Various Calibrations.

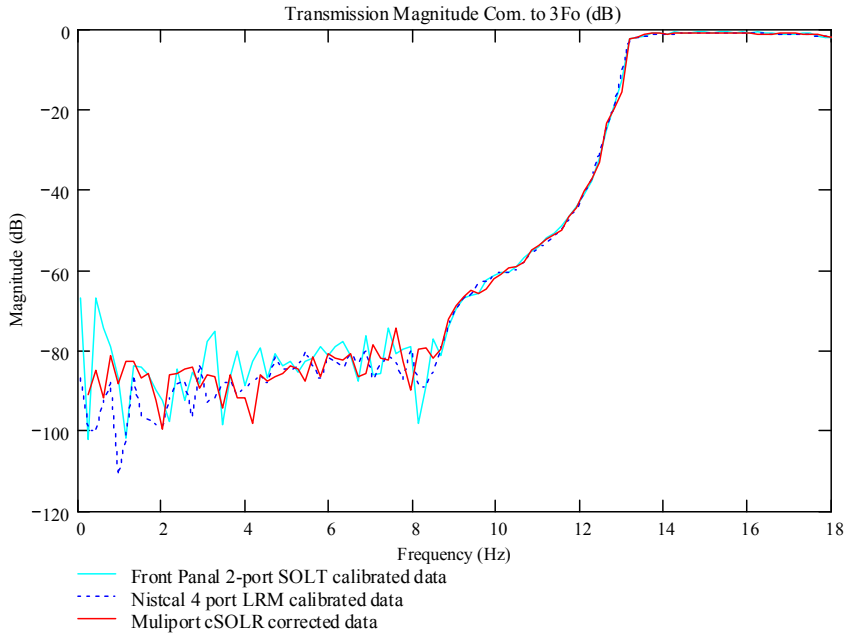

Figure C.14 – Transmission Magnitude of the 5.25 GHz Triplexer from the common Port to the 3Fo Port Measured with Various Multiport Calibration Methods.

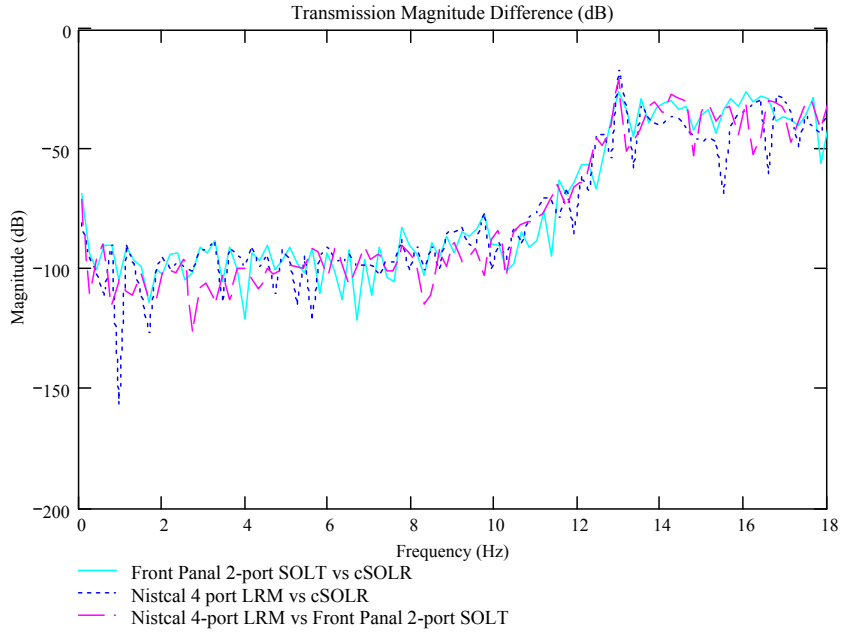

Figure C.15 – Transmission Magnitude Difference of the 5.25 GHz Triplexer from the common Port to the 3Fo Port Measured with Various Multiport Calibration Methods.

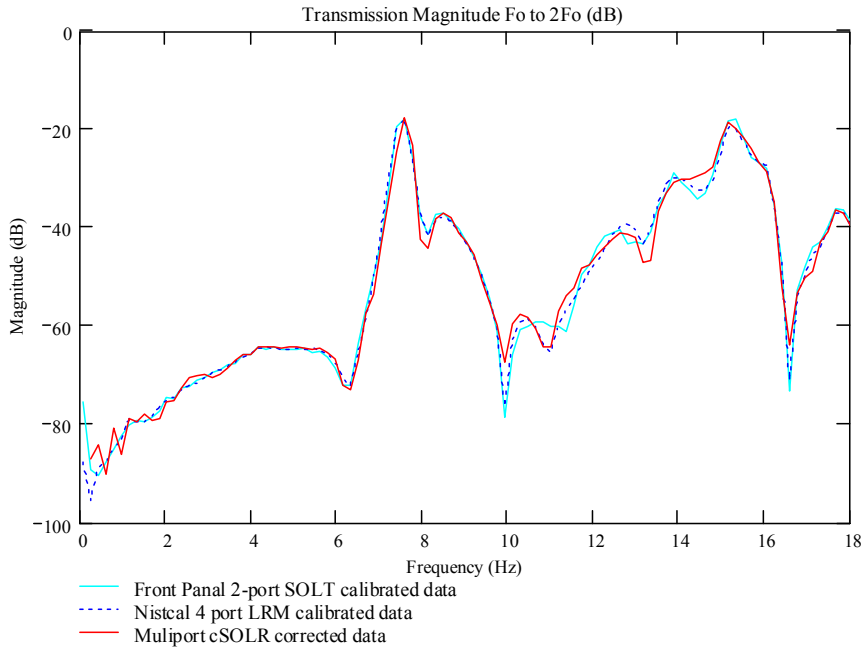

Figure C.16 – Transmission Magnitude of the 5.25 GHz Triplexer from the Fo Port to the 2Fo Port Measured with Various Multiport Calibration Methods.

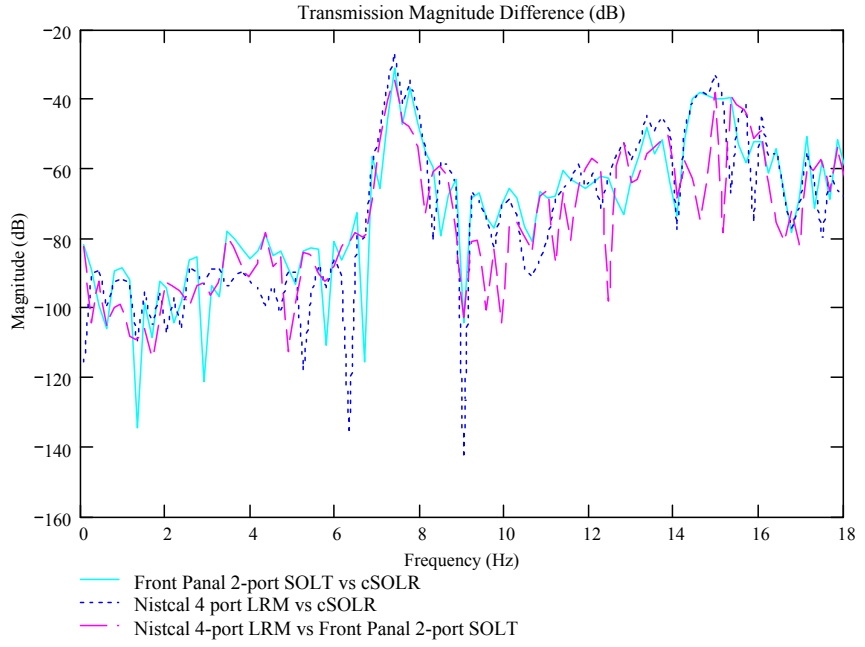

Figure C.17 – Transmission Magnitude Difference of the 5.25 GHz Triplexer from the Fo Port to the 2Fo Port Measured with Various Multiport Calibration Methods.

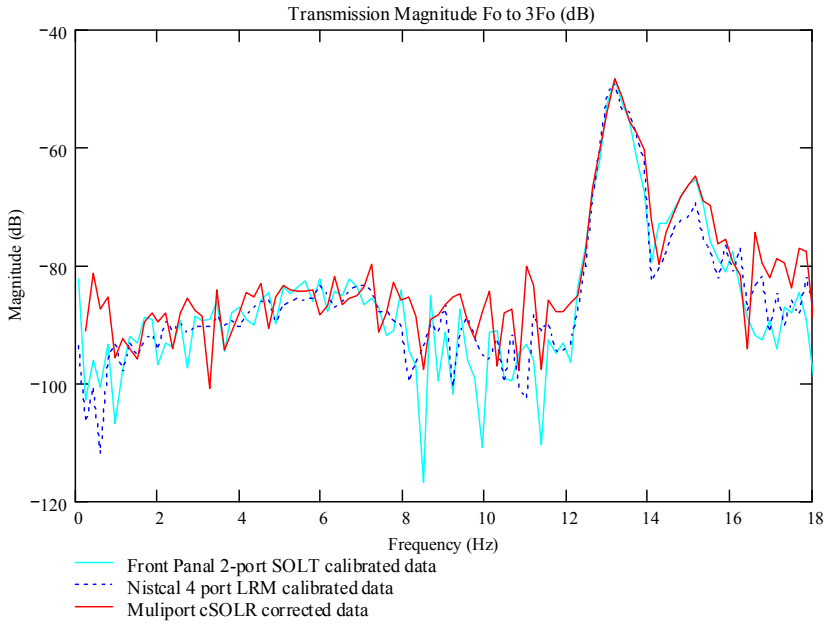

Figure C.18 – Transmission Magnitude Difference of the 5.25 GHz Triplexer from the Fo Port to the 2Fo Port Measured with Various Multiport Calibration Methods.

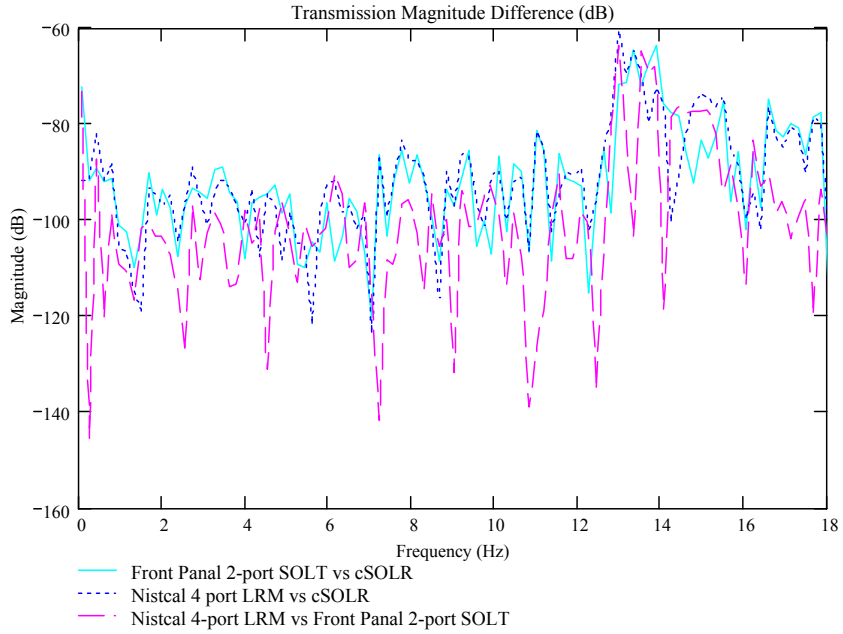

Figure C.19 – Transmission Magnitude Difference of the 5.25 GHz Triplexer from the Fo Port to the 3Fo Port Measured with Various Multiport Calibration Methods.

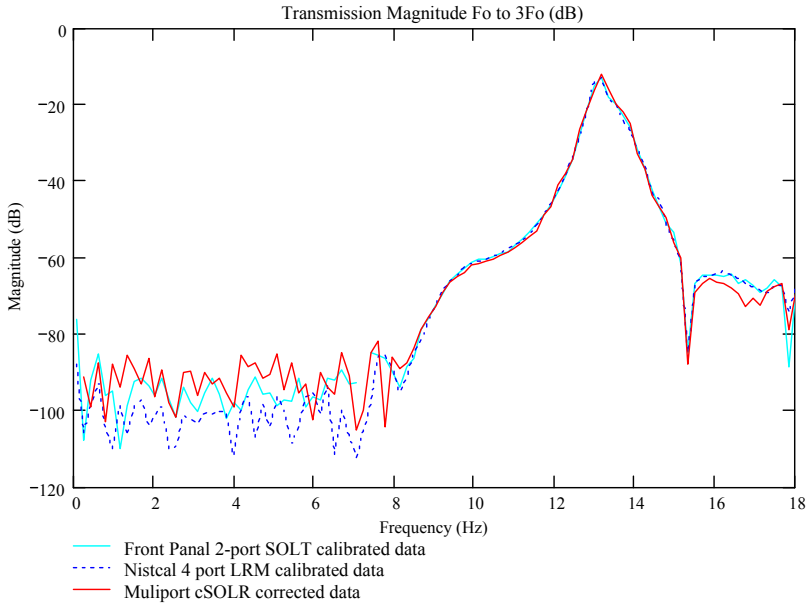

Figure C.20 – Transmission Magnitude of the 5.25 GHz Triplexer from the 2Fo Port to the 3Fo Port Measured with Various Multiport Calibration Methods.

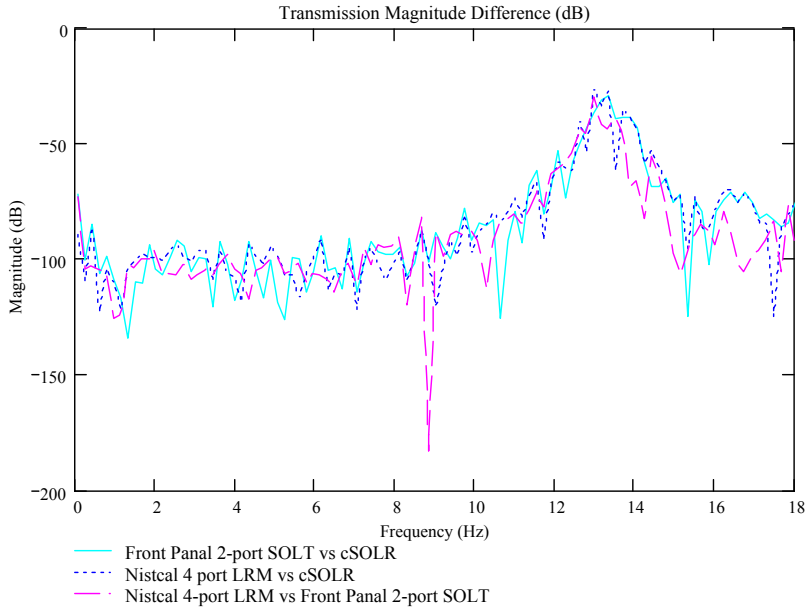

Figure C.21 – Transmission Magnitude Difference of the 5.25 GHz Triplexer from the 2Fo Port to the 3Fo Port Measured with Various Multiport Calibration Methods.

APPENDIX D: GGB CS-13-4130 CALIBRATION SUBSTRATE MEASUREMENTS

In this Appendix the additional measurements of the structures on the GGB CS-13-4130 substrate are presented that were not shown in Chapter 9. The measurements of the structures are shown calibrated with two variations of the multiport cSOLR method; one using four reciprocal two-port transmission standards, the other using a single reciprocal 4-port transmission standard.

D.1 One-Port Standards

Once again as with the load standards the one-port DUTs measured using the cSOLmR calibration is almost identical to the multiport cSOLR calibration using the two-port standards because the renormalization does not have a great affect on the data.

Open

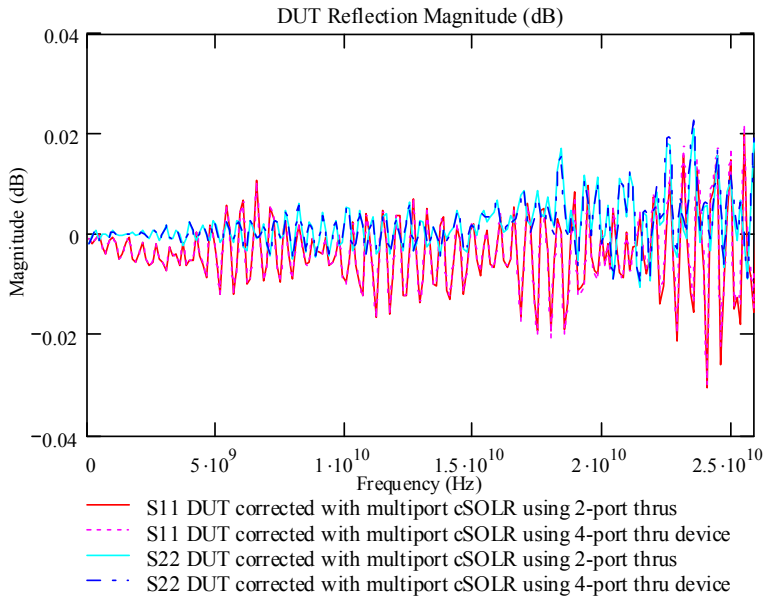

Figure D.1 – Open Reflection Magnitude Measurements Using a 4-port Transmission Standard in the Multiport cSOLR Calibration.

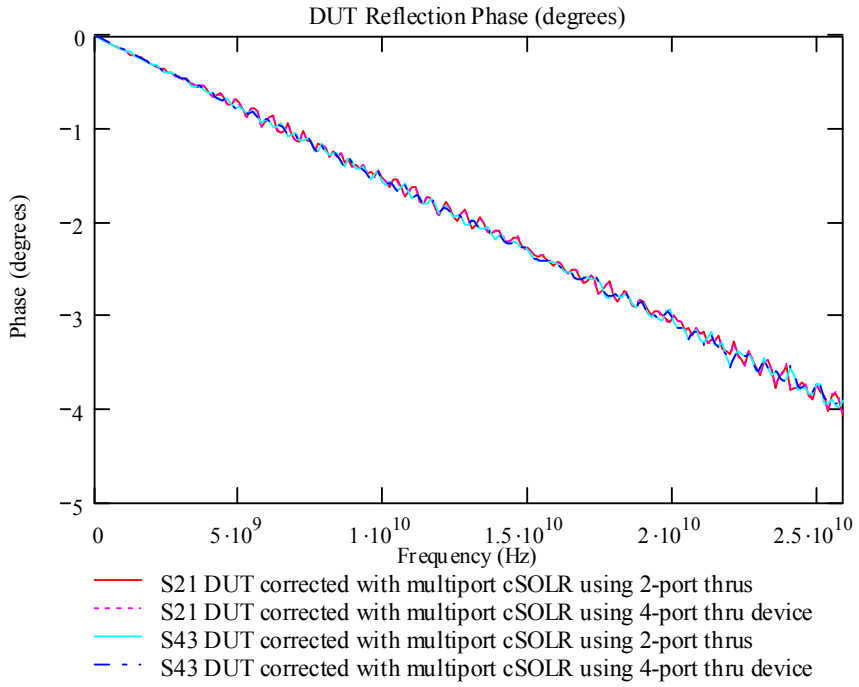

Figure D.2 – Open Reflection Phase Measurements Using a 4-port Transmission Standard in the Multiport cSOLR Calibration.

The isolation data of the open standards shown in Figure 9.2 indicates that once again that the inter-port signal paths (3,1) and (2,4) produce the lowest isolation levels nearing approximately -23 dB.

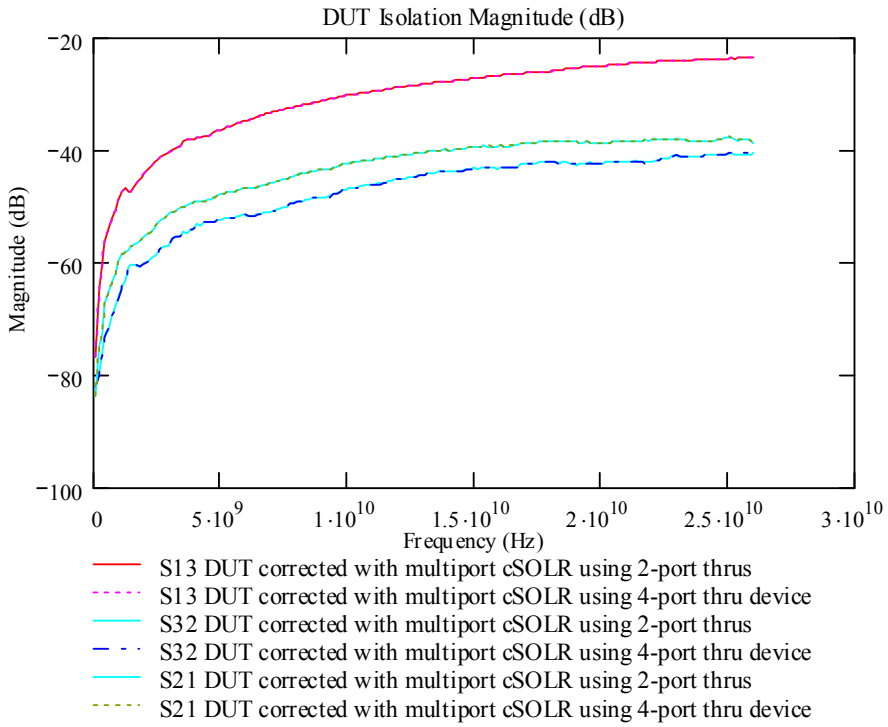

Figure D.3 – Open Isolation Measurements Using a 4-port Transmission Standard in the Multiport cSOLR Calibration.

Short

Perhaps the most interesting results for the shorts standard is the isolation graph. The isolation of the (3,1) paths begins at the same level as the (1,2) path and the drops out smoothly only to rise again and end up at around -20 dB. Unlike with GSGSG probe short standards the GSSG short is not a common shorting bar which connects all pins of the probes together. The GSSG shorts are separate shorting bars for each GS pair.

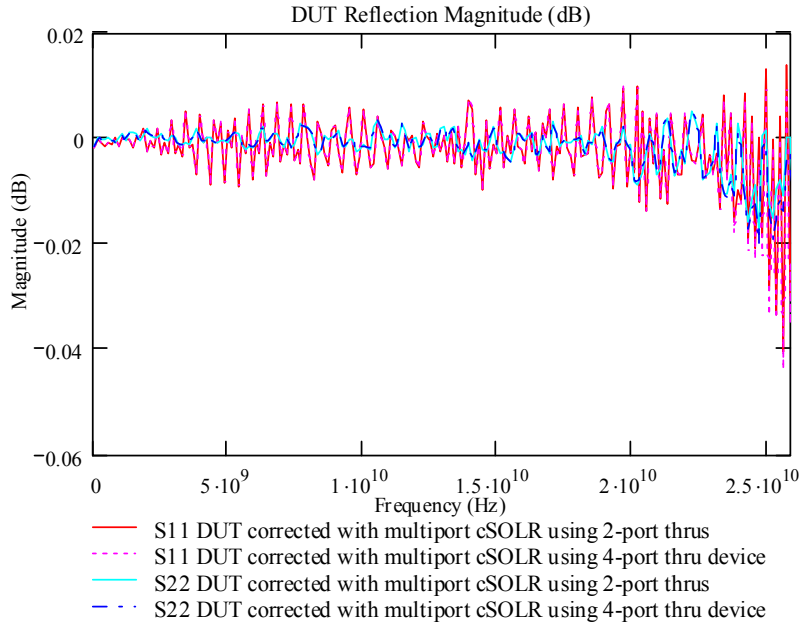

Figure D.4 – Short Reflection Magnitude Measurements Using a 4-port Transmission Standard in the Multiport cSOLR Calibration.

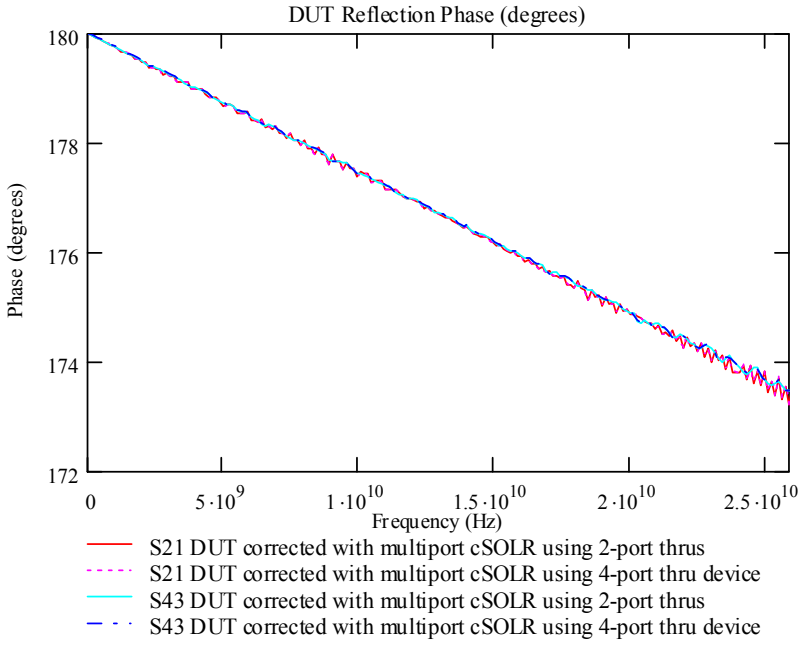

Figure D.5 – Short Reflection Phase Measurements Using a 4-port Transmission Standard in the Multiport cSOLR Calibration.

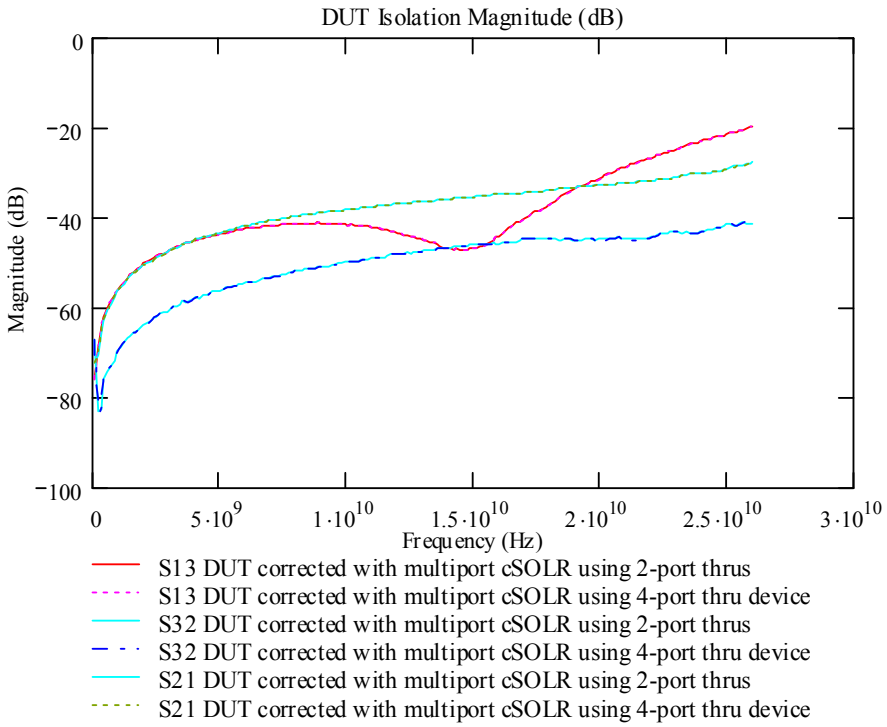

Figure D.6 – Short Isolation Measurements Using a 4-port Transmission Standard in the Multiport cSOLR Calibration.

D.2 Two-Port DUTs

(3,1) Transmission Standard

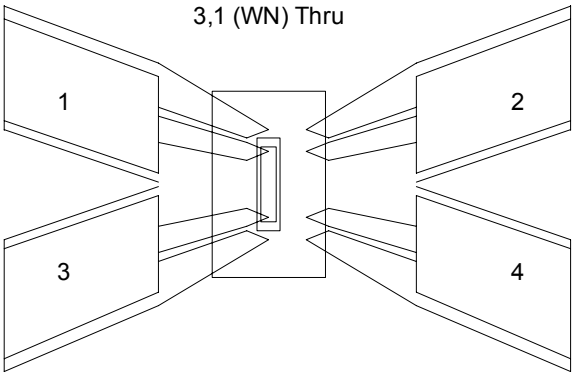

Figure D.7 - GSSG Layout of the (3,1) Transmission Standard.

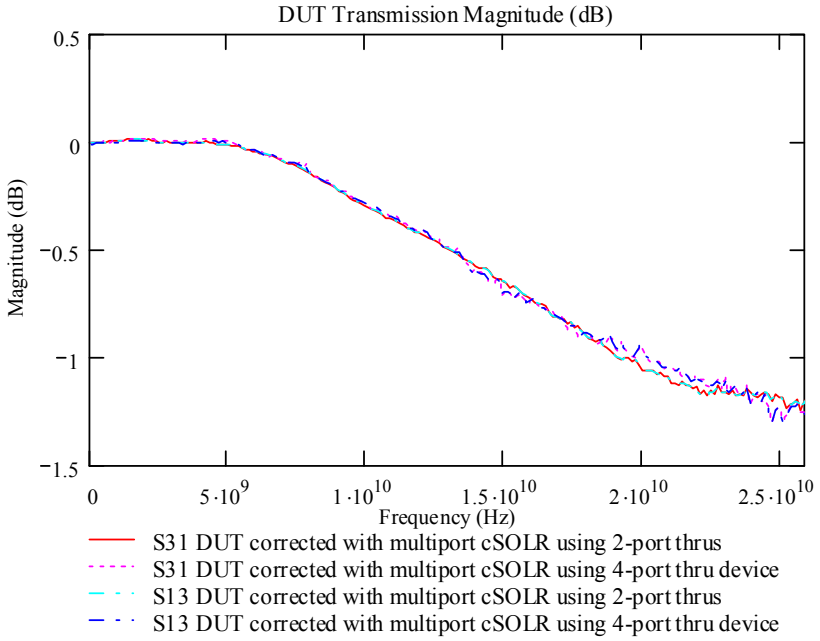

Figure D.8 – (3,1) Transmission Standard, Transmission Magnitude Measurements Using a 4-Port Transmission Standard in the Multiport cSOLR Calibration.

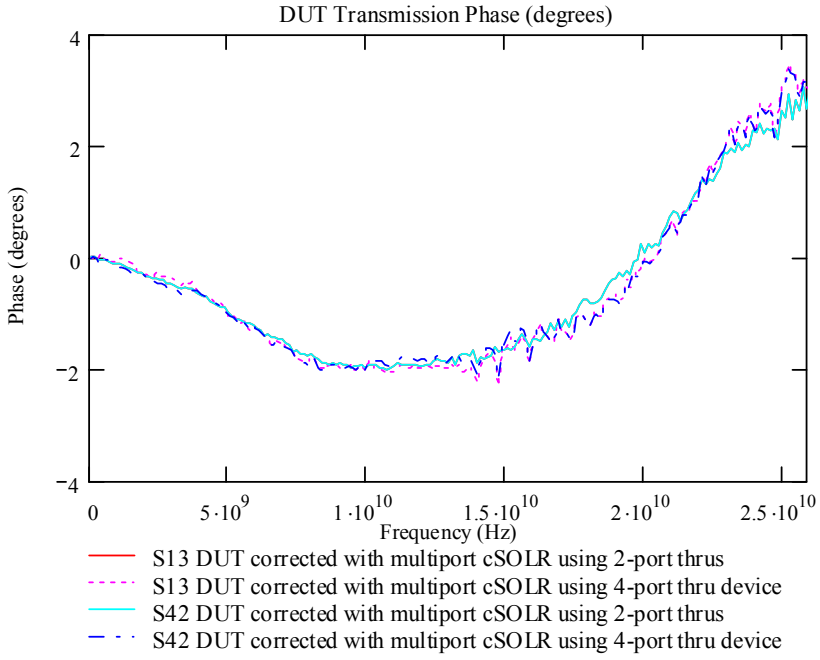

Figure D.9 – (3,1) Transmission Standard, Transmission Phase Measurements Using a 4-Port Transmission Standard in the Multiport cSOLR Calibration.

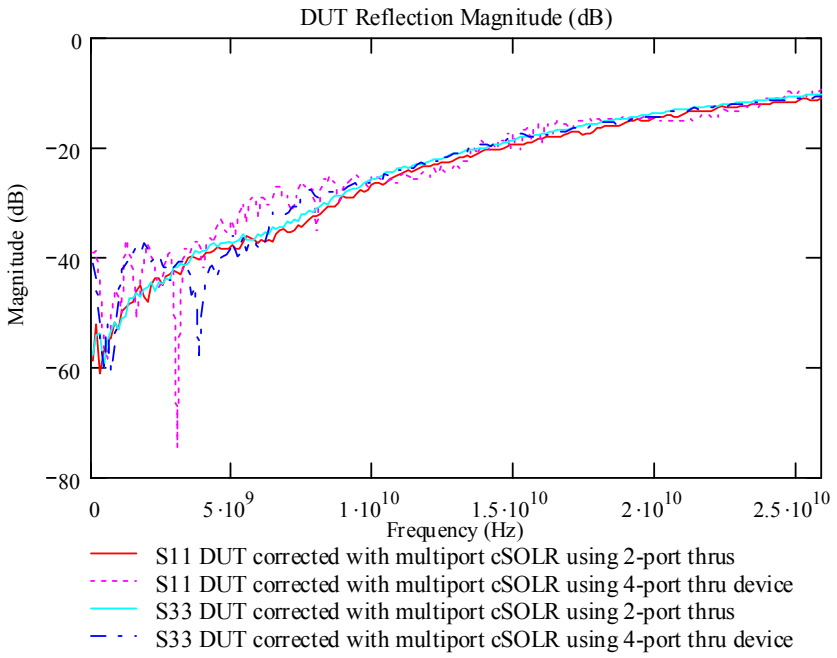

Figure D.10 – (3,1) Transmission Standard, Reflection Magnitude Measurements Using a 4-Port Transmission Standard in the Multiport cSOLR Calibration.

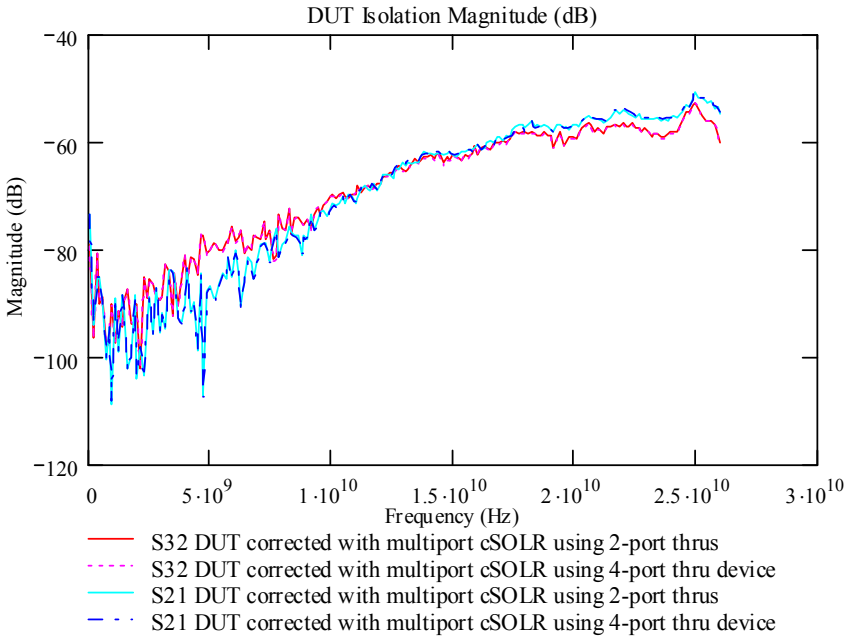

Figure D.11 – (3,1) Transmission Standard, Isolation Magnitude Measurements Using a 4-Port Transmission Standard in the Multiport cSOLR Calibration.

(3,2) Transmission Standard

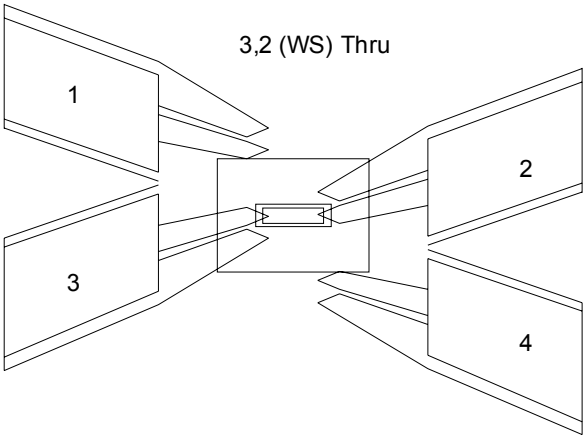

Figure D.12 – GSSG Layout of the (3,2) Transmission Standard.

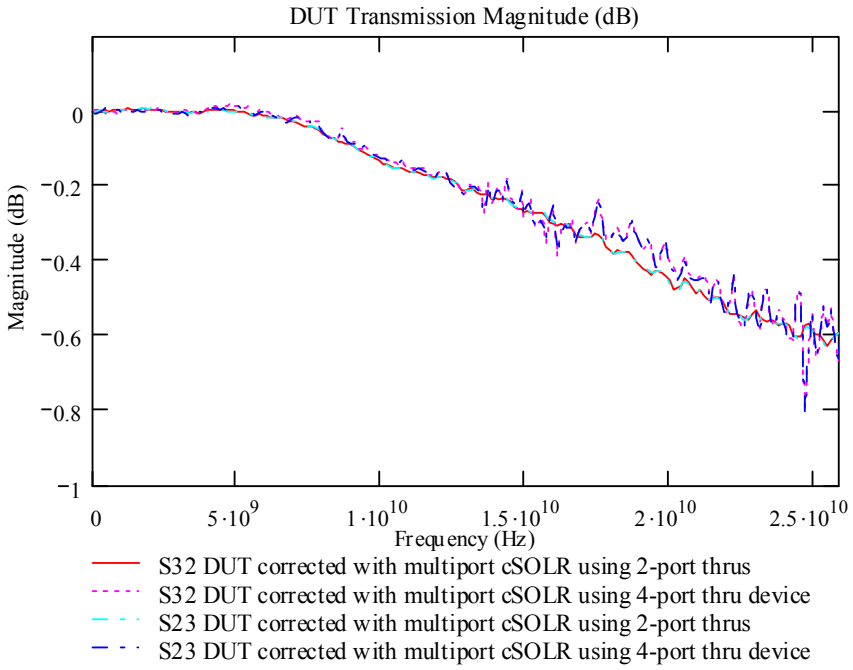

Figure D.13 – (3,2) Transmission Standard, Transmission Magnitude Measurements Using a 4-Port Transmission Standard in the Multiport cSOLR Calibration.

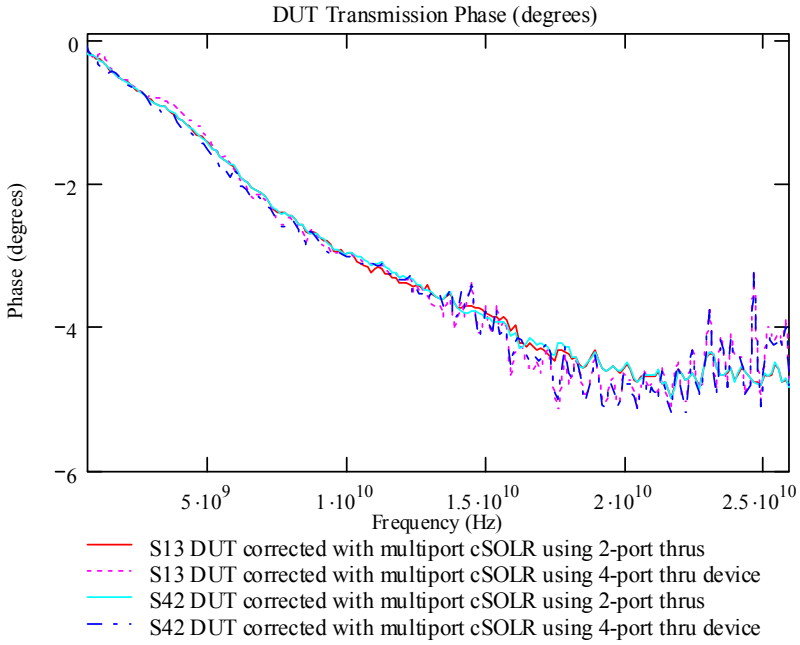

Figure D.14 – (3,2) Transmission Standard, Transmission Phase Measurements Using a 4-Port Transmission Standard in the Multiport cSOLR Calibration.

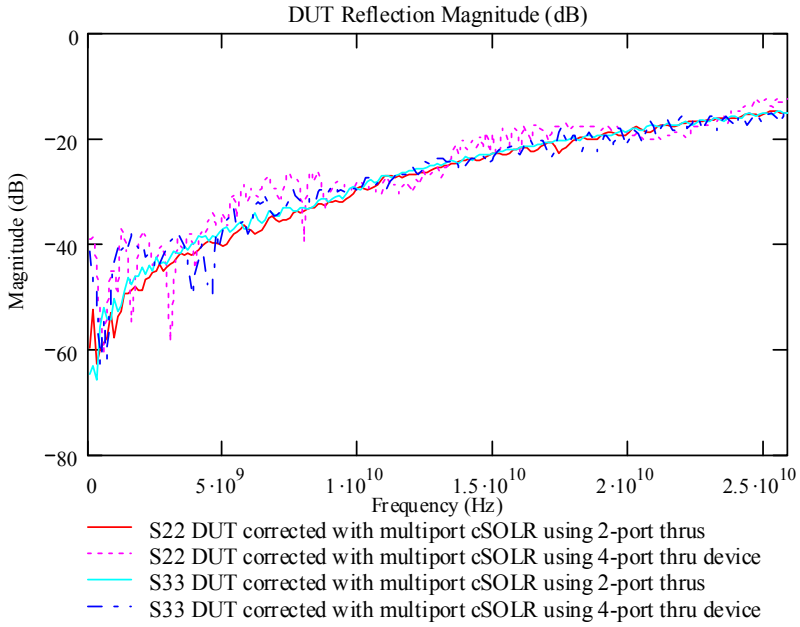

Figure D.15 – (3,2) Transmission Standard, Reflection Magnitude Measurements Using a 4-Port Transmission Standard in the Multiport cSOLR Calibration.

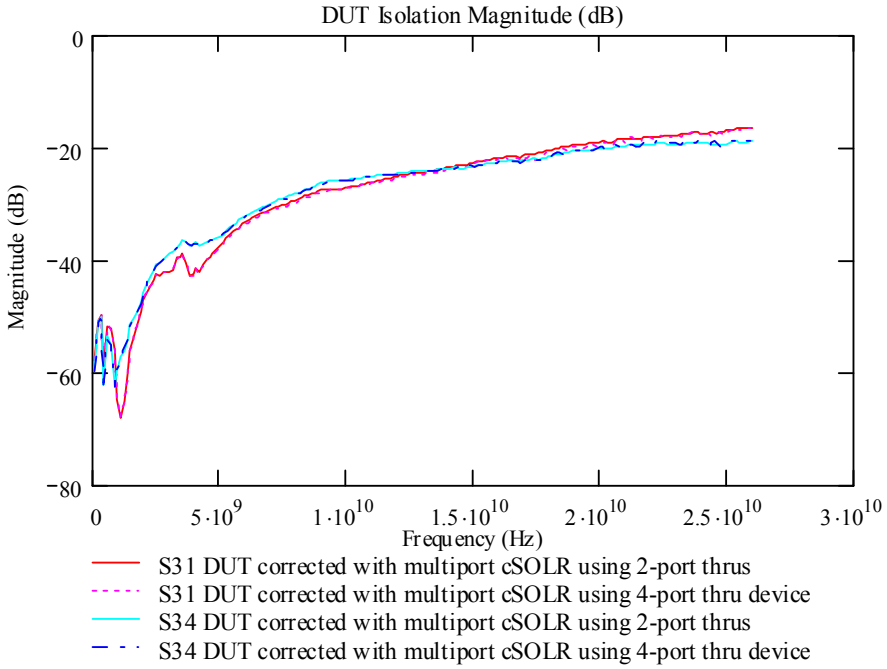

Figure D.16 – (3,2) Transmission Standard, Isolation Magnitude Measurements Using a 4-Port Transmission Standard in the Multiport cSOLR Calibration.

100 Ohm Series Load

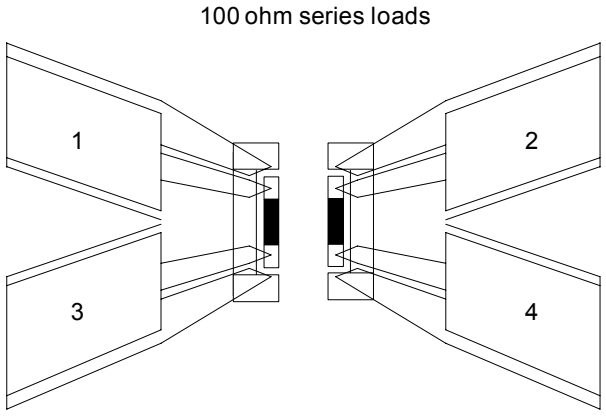

Figure D.17 – GSSG Layout of 100 Ohm Series Load Pair.

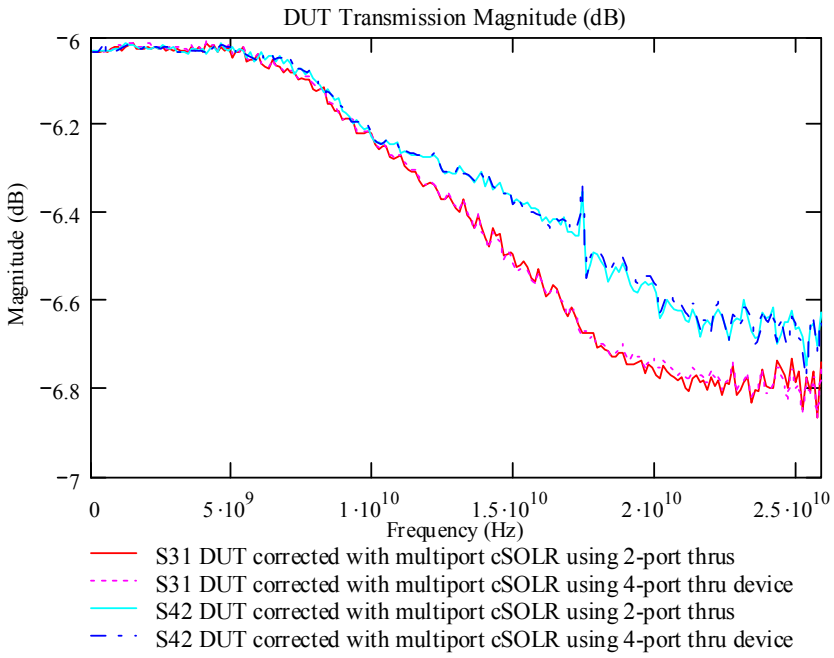

Figure D.18 – 100 Ohm Series Load, Transmission Magnitude Measurements Using a 4-Port Transmission Standard in the Multiport cSOLR Calibration.

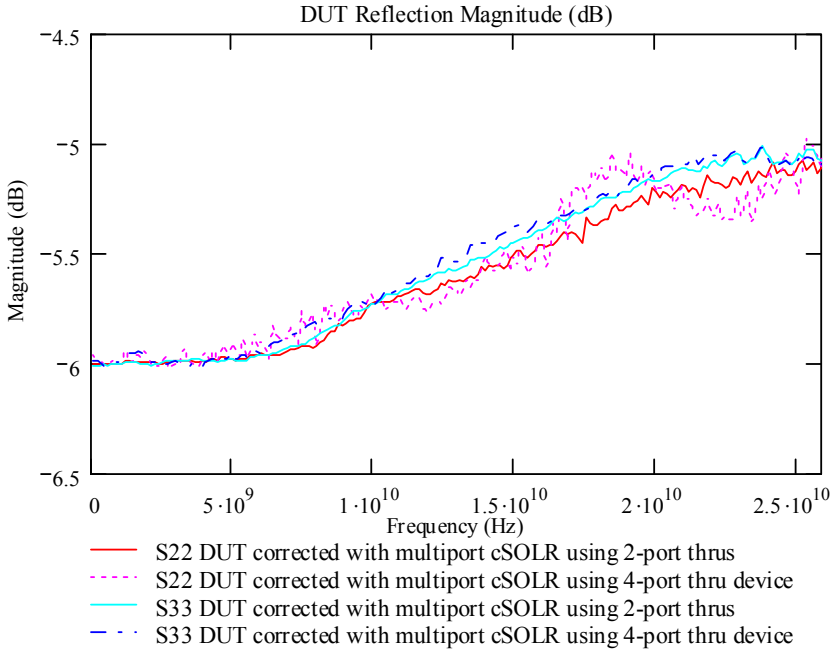

Figure D.19 – 100 Ohm Series Load, Reflection Magnitude Measurements Using a 4-Port Transmission Standard in the Multiport cSOLR Calibration.

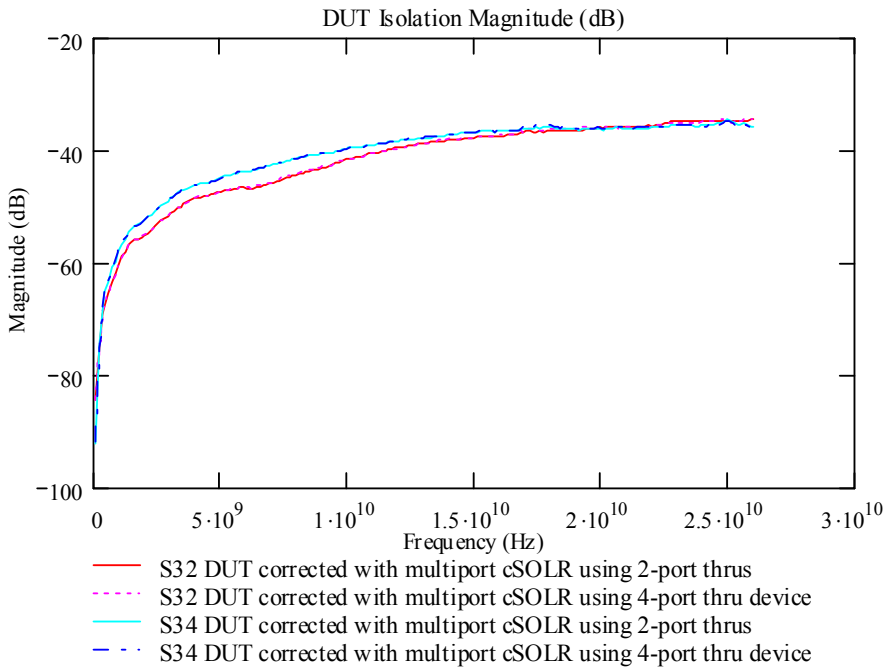

Figure D.20 – 100 Ohm Series Load, Isolation Magnitude Measurements Using a 4-Port Transmission Standard in the Multiport cSOLR Calibration.

200 Ohm Series Loads

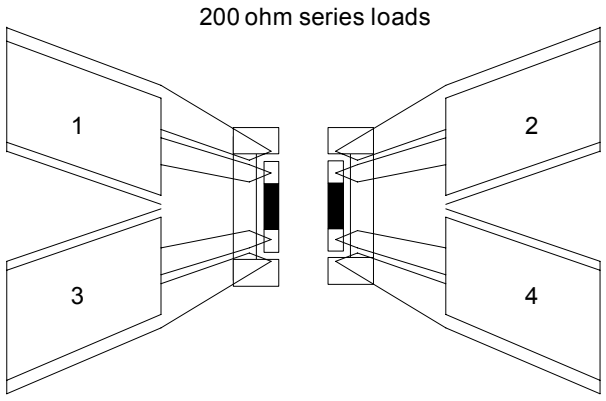

Figure D.21 – GSSG Layout of 200 Ohm Series Load Pair.

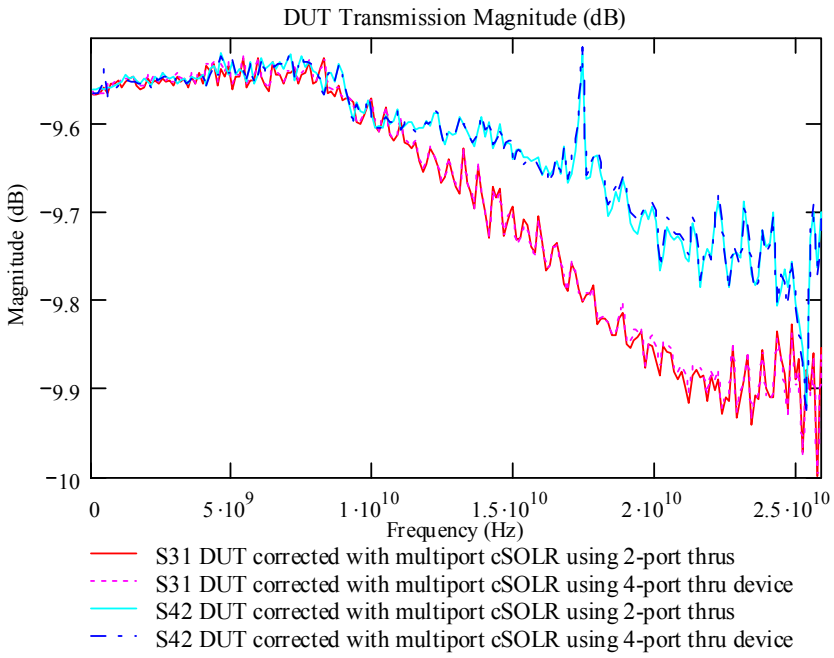

Figure D.22 – 200 Ohm Series Load, Transmission Magnitude Measurements Using a 4-Port Transmission Standard in the Multiport cSOLR Calibration.

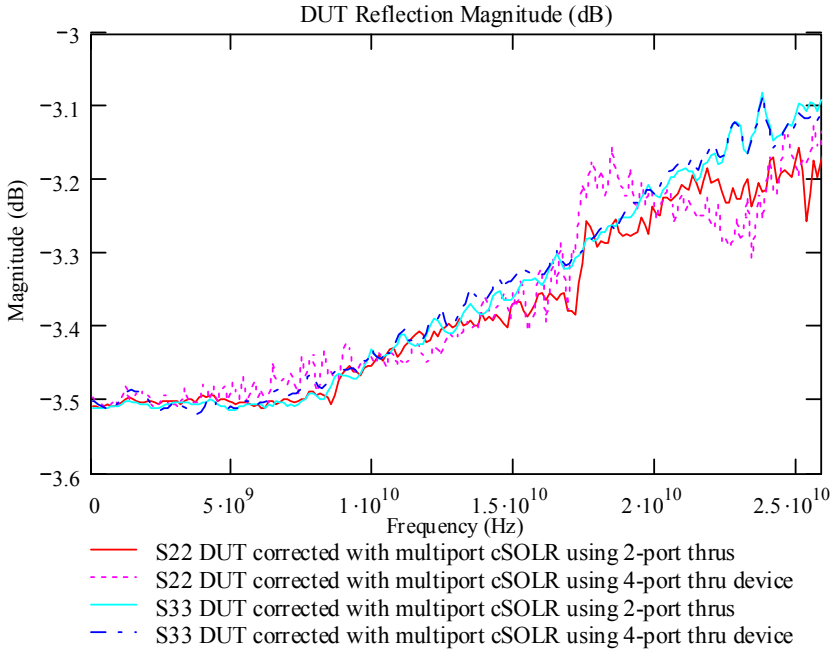

Figure D.23 – 200 Ohm Series Load, Reflection Magnitude Measurements Using a 4-Port Transmission Standard in the Multiport cSOLR Calibration.

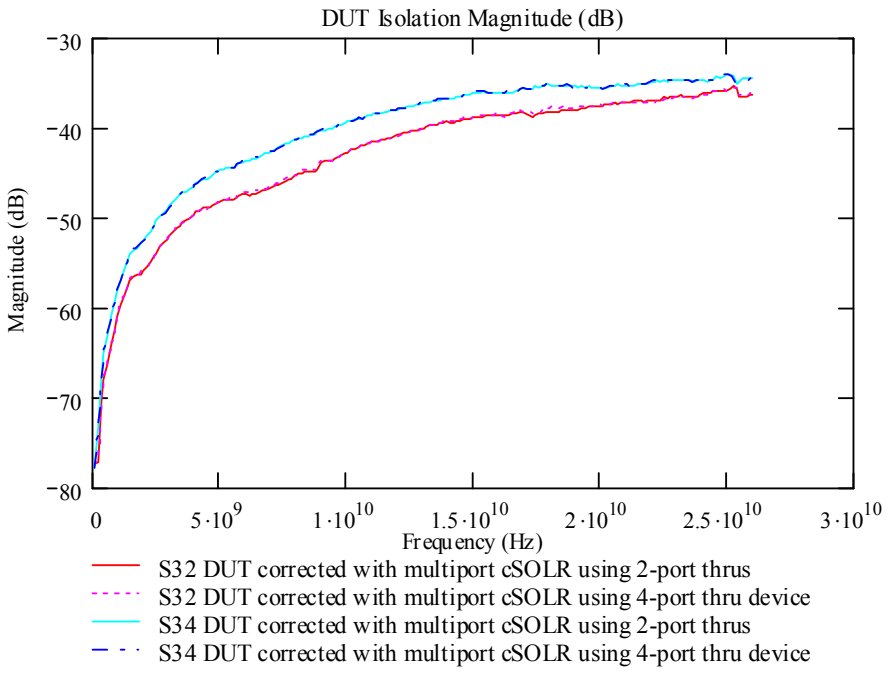

Figure D.24 – 200 Ohm Series Load, Isolation Magnitude Measurements Using a 4-Port Transmission Standard in the Multiport cSOLR Calibration.

D.3 Four-Port DUTs

1880 um Parallel Line

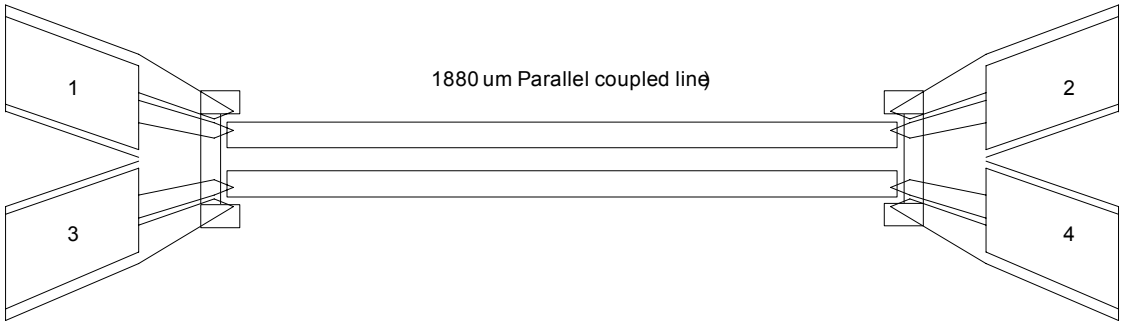

Figure D.25 – GSSG Layout of 1880 um Parallel Coupled Line Structure.

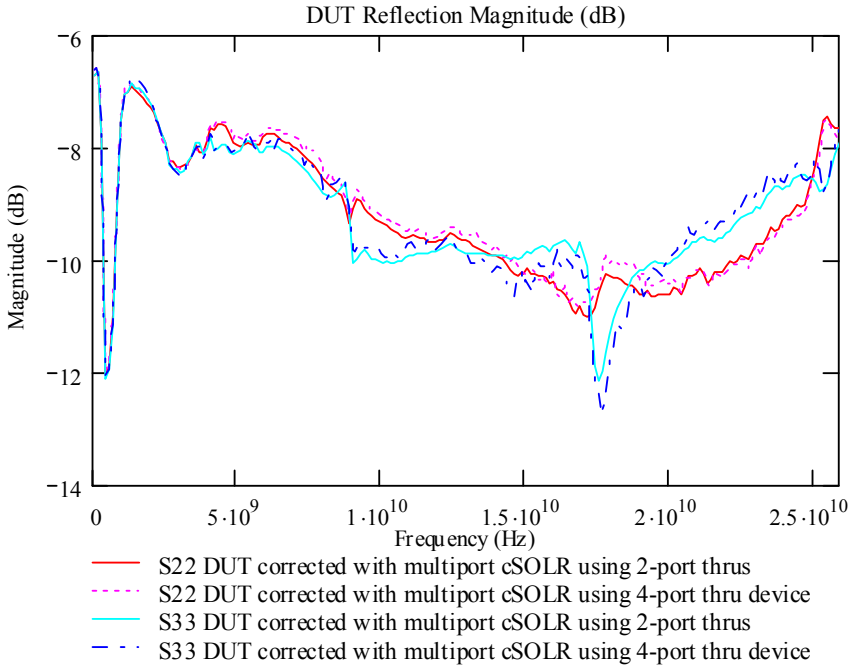

Figure D.26 – 1880 um Parallel Line, Reflection Magnitude Measurements Using a 4-Port Transmission Standard in the Multiport cSOLR Calibration.

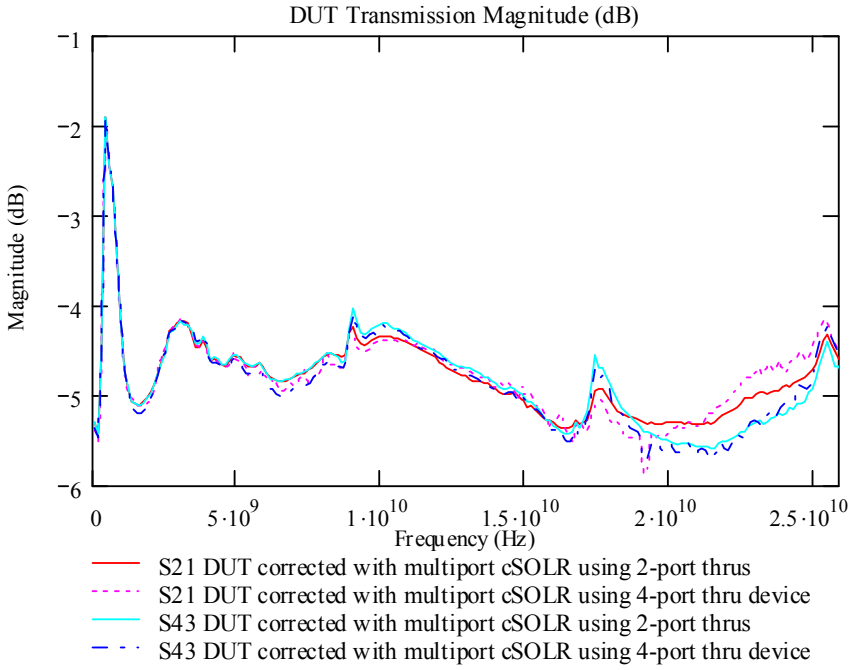

Figure D.27 – 1880 um Parallel Line, Transmission Magnitude Measurements Using a 4-Port Transmission Standard in the Multiport cSOLR Calibration.

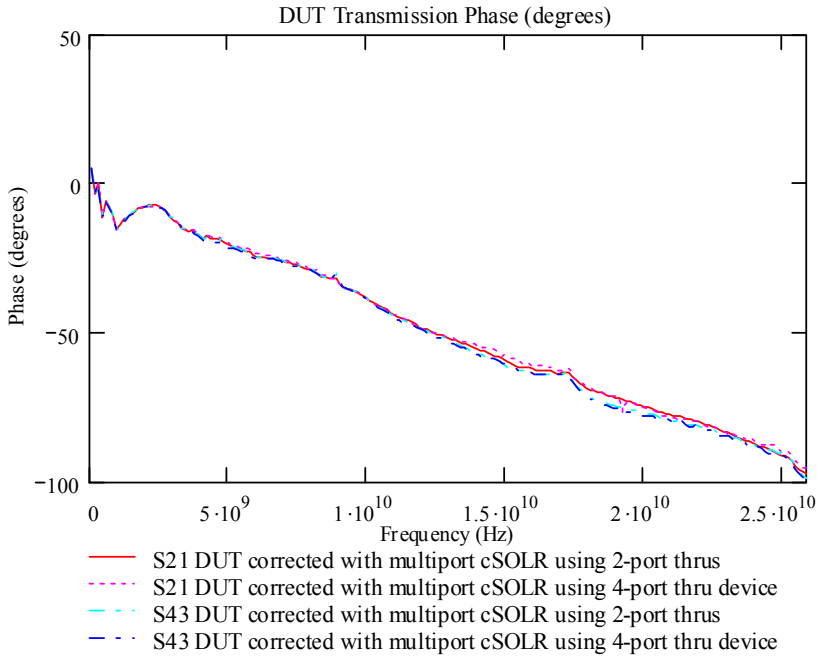

Figure D.28 – 1880 um Parallel Line, Transmission Phase Measurements Using a 4-Port Transmission Standard in the Multiport cSOLR Calibration.

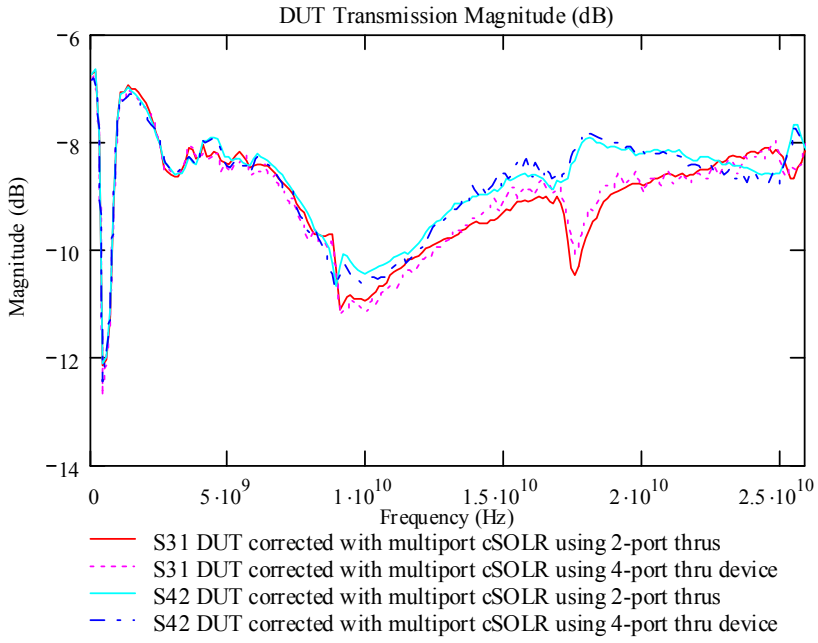

Figure D.29 – 1880 um Parallel Line, Transmission Magnitude Measurements Using a 4-Port Transmission Standard in the Multiport cSOLR Calibration.

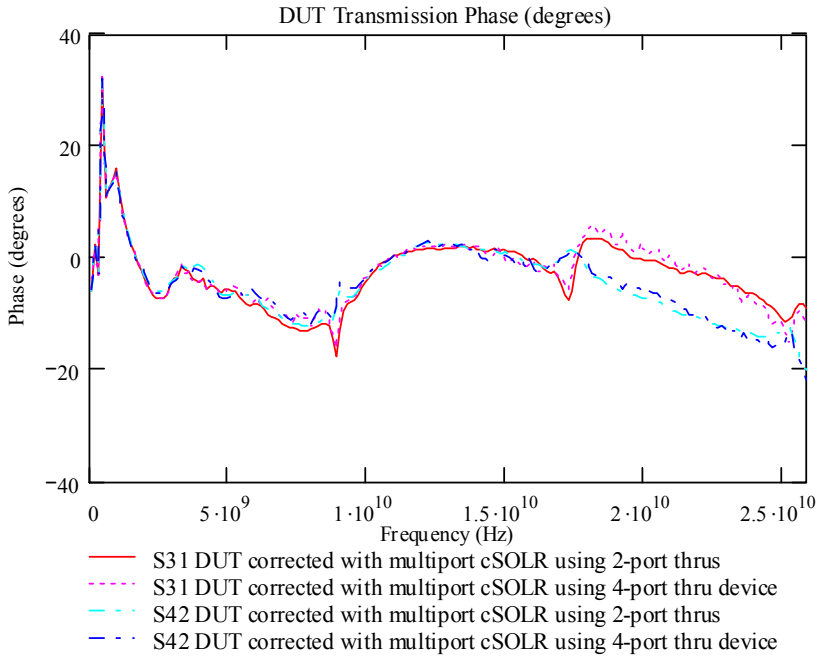

Figure D.30 – 1880 um Parallel Line, Transmission Phase Measurements Using a 4-Port Transmission Standard in the Multiport cSOLR Calibration.

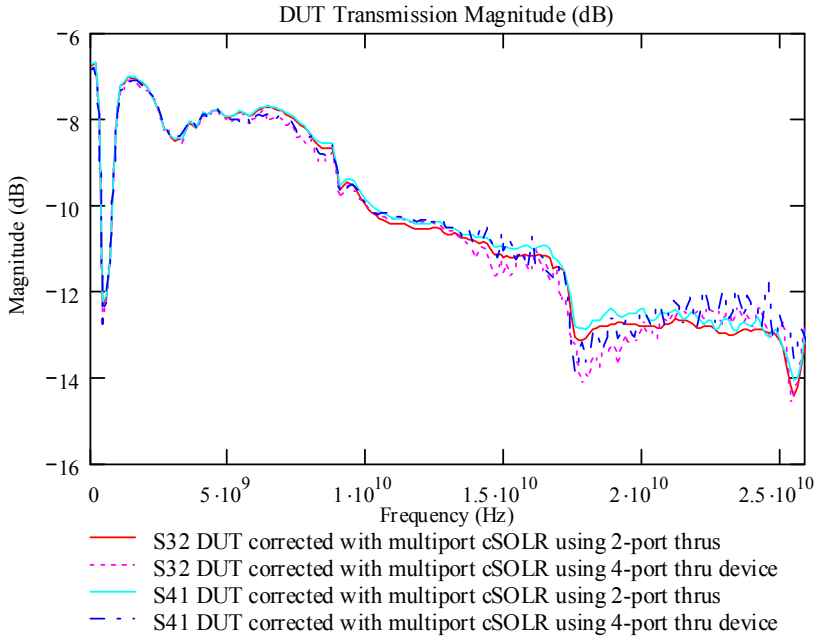

Figure D.31 – 1880 um Parallel Line, Transmission Magnitude Measurements Using a 4-Port Transmission Standard in the Multiport cSOLR Calibration.

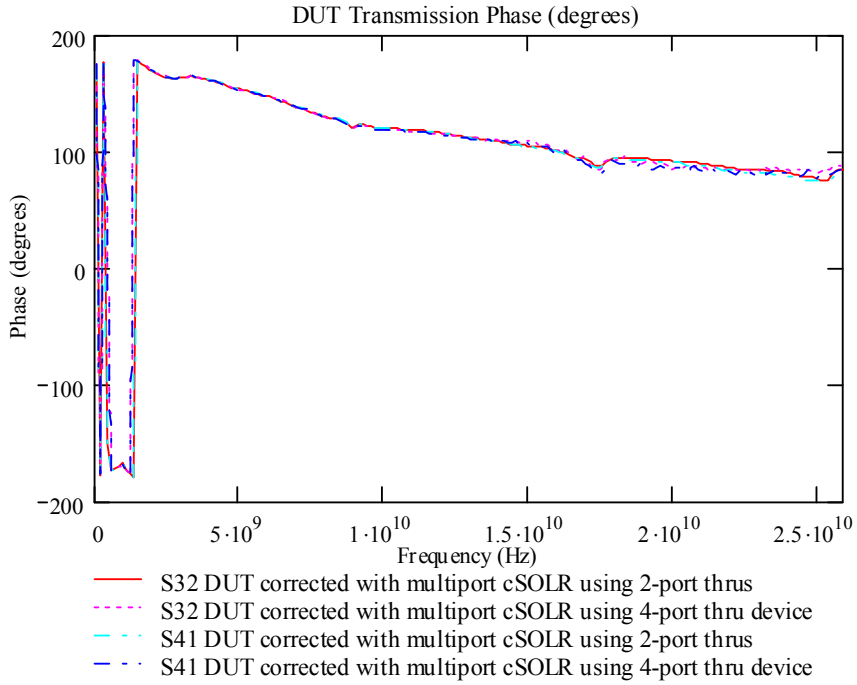

Figure D.32 – 1880 um Parallel Line, Transmission Phase Measurements Using a 4-Port Transmission Standard in the Multiport cSOLR Calibration.